On the conditioning of process-based channelized meandering reservoir models on well data

Anna Bubnova

PSL UNIVERSITÉ PARIS

THÈSE DE DOCTORAT
DE L'UNIVERSITÉ PSL

Préparée à MINES ParisTech

Sur le conditionnement des modèles génétiques de réservoirs chenalisés méandriformes à des données de puits

On the conditioning of process-based channelized meandering reservoir models on well data

Soutenue par
Anna BUBNOVA
Le 11 décembre 2018

Ecole doctorale n° 398
Géosciences, Ressources Naturelles et Environnement (GRNE)

Spécialité
Géosciences et géoingénierie

Composition du jury :

Peter HUGGENBERGER Professeur, Université de Bâle (Suisse)	*Président*
Daniel GARCIA Maître de Recherche, Ecole des Mines de Saint-Etienne	*Rapporteur*
Pauline COLLON Maître de Conférence, HDR, ENSG-Université de Lorraine	*Rapporteur*
Bernard GUY Docteur d'Etat, Ecole des Mines de Saint-Etienne	*Examinateur*
Simon LOPEZ Ingénieur, PhD, BRGM	*Examinateur*
Jacques RIVOIRARD Directeur de Recherche, MINES ParisTech, Université PSL	*Directeur de thèse*
Isabelle COJAN Directrice de Recherche, MINES ParisTech, Université PSL	*Co-directeur de thèse*
Fabien ORS Ingénieur, ARMINES	*Co-encadrant de thèse*

MINES ParisTech | PSL

Sur le conditionnement des
modèles génétiques de réservoirs chenalisés méandriformes à des données de puits

par Anna Bubnova

Résumé

Les modèles génétiques de réservoirs sont construits par la simulation des principaux processus de sédimentation dans le temps. En particulier, les modèles tridimensionnels de systèmes chenalisés méandriformes peuvent être construits à partir de trois processus principaux : la migration du chenal, l'aggradation du système et les avulsions, comme c'est réalisé dans le logiciel Flumy pour les environnements fluviatiles. Pour une utilisation opérationnelle, par exemple la simulation d'écoulements, ces simulations doivent être conditionnées aux données d'exploration disponibles (diagraphie de puits, sismique, …). Le travail présenté ici, basé largement sur des développements antérieurs, se concentre sur le conditionnement du modèle Flumy aux données de puits.

Deux questions principales ont été examinées au cours de cette thèse. La première concerne la reproduction des données connues aux emplacements des puits. Cela se fait actuellement par une procédure de "conditionnement dynamique" qui consiste à adapter les processus du modèle pendant le déroulement de la simulation. Par exemple, le dépôt de sable aux emplacements de puits est favorisé, lorsque cela est souhaité, par une adaptation des processus de migration ou d'avulsion. Cependant, la manière dont les processus sont adaptés peut générer des effets indésirables et réduire le réalisme du modèle. Une étude approfondie a été réalisée afin d'identifier et d'analyser les impacts indésirables du conditionnement dynamique. Les impacts ont été observés à la fois à l'emplacement des puits et dans tout le modèle de blocs. Des développements ont été réalisés pour améliorer les algorithmes existants.

La deuxième question concerne la détermination des paramètres d'entrée du modèle, qui doivent être cohérents avec les données de puits. Un outil spécial est intégré à Flumy - le "Non-Expert User Calculator" (Nexus) - qui permet de définir les paramètres de simulation à partir de trois paramètres clés : la proportion de sable, la profondeur maximale du chenal et l'extension latérale des corps sableux. Cependant, les réservoirs naturels comprennent souvent plusieurs unités stratigraphiques ayant leurs propres caractéristiques géologiques. L'identification de telles unités dans le domaine étudié est d'une importance primordiale avant de lancer une simulation conditionnelle avec des paramètres cohérents pour chaque unité. Une nouvelle méthode de détermination des unités stratigraphiques optimales à partir des données de puits est proposée. Elle est basée sur la Classification géostatistique hiérarchique appliquée à la courbe de proportion verticale (VPC) globale des puits. Les unités stratigraphiques ont pu être détectées à partir d'exemples de données synthétiques et de données de terrain, même lorsque la VPC globale des puits n'était pas visuellement représentative.

Mots-clés de la thèse :

Classification hiérarchique, géostatistique, modèles génétiques, réservoirs, simulations conditionnelles

On the conditioning of
process-based channelized meandering reservoir models on well data

by Anna Bubnova

Abstract

Process-based reservoir models are generated by the simulation of the main sedimentation processes in time. In particular, three-dimensional models of meandering channelized systems can be constructed from three main processes: migration of the channel, aggradation of the system and avulsions, as it is performed in Flumy software for fluvial environments. For an operational use, for instance flow simulation, these simulations need to be conditioned to available exploration data (well logging, seismic, …). The work presented here, largely based on previous developments, focuses on the conditioning of the Flumy model to well data.

Two main questions have been considered during this thesis. The major one concerns the reproduction of known data at well locations. This is currently done by a "dynamic conditioning" procedure which consists in adapting the model processes while the simulation is running. For instance, the deposition of sand at well locations is favored, when desired, by an adaptation of migration or avulsion processes. However, the way the processes are adapted may generate undesirable effects and could reduce the model realism. A thorough study has been conducted in order to identify and analyze undesirable impacts of the dynamic conditioning. Such impacts were observed to be present both at the location of wells and throughout the block model. Developments have been made in order to improve the existing algorithms.

The second question is related to the determination of the input model parameters, which should be consistent with the well data. A special tool is integrated in Flumy – the Non Expert User calculator (Nexus) – which permits to define the simulation parameters set from three key parameters: the sand proportion, the channel maximum depth and the sandbodies lateral extension. However, natural reservoirs often consist in several stratigraphic units with their own geological characteristics. The identification of such units within the studied domain is of prime importance before running a conditional simulation, with consistent parameters for each unit. A new method for determining optimal stratigraphic units from well data is proposed. It is based on the Hierarchical Geostatistical Clustering applied to the well global Vertical Proportion Curve (VPC). Stratigraphic units could be detected from synthetic and field data cases, even when the global well VPC was not visually representative.

Thesis key words:

Hierarchical Clustering, Geostatistics, Process-based models, reservoirs, conditional simulations

Acknowledgments

Firstly, I would like to express my sincere gratitude to my thesis advisors: Jacques Rivoirard and Isabelle Cojan. Thanks to you, I have acquired the skills that will help me during my professional life. I am also grateful to Flumy team: Martin, Jean-Louis and especially to Fabien Ors – for your help during the years of my work.

I would like to thank the members of my thesis committee – Peter Huggenberger, Daniel Garcia, Pauline Collon, Bernard Guy and Simon Lopez.

I would also like to acknowledge our Flumy consortium partners: ENI and ENGIE.

My sincere thanks go to my dear colleagues from the Center of Geosciences MINES ParisTech: Helene, Christian, Laure, Jihane, Ricardo, Marine, Jean, Emilie, Xavier, Marine, Robin, Nathalie, Isabelle et Sylvie, Didier, Gaelle, Chantal, Nicolas and Thomas. It was great to have an opportunity to work in your team.

A very special gratitude goes out to POE Big Data team: Dinh, Avish, Razan, Catalina, Maria Angelica, Sara, Tristan, Zishan and Theo. Thanks to you all for your support during the last months.

And finally, last but no means least, I would like to thank my friends and family. Спасибо моей семье и друзьям – любимым маме и бабушке, Маше, Саше, Сереже, Оле, Аленке, Ксюше и Маше. Я всегда чувствую вашу поддержку, даже на расстоянии.

Summary

Abbreviations

Flumy facies and colorscales

FLUMY™

ARMINES MINES ParisTech PSL

Lithofacies				Grain
Id	Abr.	Full name		ϕ
0	UDF	Undefined		-
1	CL	Channel Lag		-8:-1
2	PB	Point Bar / LAPs		-1:3
3	SP	Sand Plug		0:3
4	CSI	Crevasse Splay I		0:3
5	CCh	Crev. Splay II Chan.		1:4
6	CSII	Crevasse Splay II		3:6
7	LV	Levee		3:6
8	OB	Overbank		7:14
9	MP	Mud Plug	(flu)	11:12
10	CF	Channel Fill	(tur)	11:12
11	WL	Wetland	(flu)	13:14
12	DR	Draping	(flu)	13:14
13	PL	Pelagic	(tur)	13:14

Grain size ϕ class	
-6:-8	Cobble
-3:-5	Pebble
-2	Gravel
-1	Very Coarse Sand
0	Coarse Sand
1	Medium Sand
2	Fine Sand
3	Very Fine Sand
4	Silt
5	Silt
6	Silt
7	Silt
8	Clay
9:10	Clay
11:12	Clay
13:14	Clay

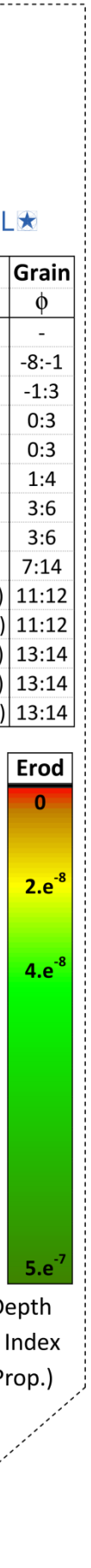

H_{max}: Channel Maximum Depth

I_{sbx}: Sandbodies Extension Index

NG: Net-to-Gross (Sand Prop.)

Hint: Copy this page, cut the image and use it as a bookmark

Abbreviations used for dynamic conditioning:

AB Active Brick;

AL Active Level;

botab active brick bottom elevation;

topab active brick top elevation;

twat top water elevation (top elevation of the channel in a Wet Well);

zb well bottom elevation;

zt well top elevation;

zdep bottom elevation of the last deposit remaining part to be validated;

zdom top elevation of the last deposit (corresponds to the floodplain elevation at the well);

Other abbreviations:

GHC Geostatistical Hierarchical Clustering;

MPS Multiple Point Statistics;

NEXUS Non Expert User Calculator;

PGS Plurigaussian Simulations;

SIS Sequential Indicator Simulations;

TIN Triangulated Irregular Networks;

VPC Vertical Proportion Curve;

List of figures

List of tables

Introduction

The need of models for heterogeneous reservoirs has stimulated the development of stochastic models that are relatively flexible and easy to condition: geostatistical Plurigaussian models (Galli and al., 1994; Le Loc'h and al., 1994; Armstrong, 2011), MPS simulations (Mariethoz and Caers, 2015), Boolean models (Lantuejoul, 2002; Chilès and Delfiner, 2012). However, the geometry and arrangement of sedimentary bodies reproduced by all these models may lack realism. Another solution to produce realistic reservoir models is to combine a stochastic and a process-based approach, providing that the geological processes are well enough known. The increasing performance of computer modeling techniques now allows simulating such process-based, or forward, models relatively easily.

Flumy is a forward model developed at MINES ParisTech, Geosciences research center, for meandering channelized systems. Initially dedicated to fluvial reservoirs (Lopez, 2003; Lopez and al., 2008), it is currently extended to turbiditic ones (Lemay et al., 2016). Simulations are performed based on channel migration, aggradation processes such as overbank floods and avulsion processes. Combination of these three different processes produces realistic and contrasted three dimensional architectures of meandering fluvial sequences.

Flumy simulations need a set of entry parameters. In order to create more realistic simulation, these parameters should be coherent with data (e.g., the wells). The determination of consistent simulation parameters has been a large subject in the development of Flumy model. In particular, if a modeled reservoir shows various stratigraphic units, the simulation parameters should be determined for each unit.

Soft and hard conditioning are proposed to the user: they are based on seismic and well input data, respectively. We will focus here on the well conditioning. The conditioning issue is a challenge for the process-based models because it requires not only to reproduce the known data at the well locations, but also to preserve at the same time the realism of the modeled sedimentary processes. In Flumy, the conditioning algorithm is a straightforward procedure (no trial/error, deposits at wells are to be reproduced during the simulation). It is based on the adaptation of the main fluvial processes (migration, aggradation and avulsion) during simulation for the lithofacies deposition required at the well location. This adaptation allows honoring the data, although not at 100%, but is also responsible for artifacts or distortions of bodies, which may alter the realism.

The first main objective of this thesis is to analyze and reduce the undesirable impact of the well conditioning by developing solutions to improve the conditioning procedures.

As said above, the parameters may change from one sedimentary unit to another one. The distinction of different units is a previous step in the modeling of reservoirs. However, it is not always straightforward. Thus, a second objective of this thesis is to propose an automatic way to assist the identification of sedimentary units from well data.

The manuscript is divided into 5 chapters:

- the first chapter presents an overview of the principal characteristics, and associated processes of the meandering fluvial systems. Then, the implementation of the processes in Flumy is discussed.
- the second chapter is dedicated to the conditioning. First, we present a review of the conditioning methods developed for process-based models. Then, we focus on the

conditioning in Flumy. The main principles of conditioning are presented, with a further detailed description of initial conditioning techniques.

- the third chapter concerns the evaluation of initial conditioning procedures in Flumy. Two aspects are tested and illustrated: well data exact reproduction and sand spatial distribution in conditional simulations. Then, new algorithms are proposed to improve the conditioning in terms of a more uniform sand distribution over the domain and a better sand matching at well while respecting the lithofacies deposition characteristic for non-conditional simulations. At last, the new results are presented and discussed.
- the fourth chapter deals with a crucial point in reservoir modeling, the determination of the stratigraphic units from the well data. A new method based on geostatistical hierarchical clustering applied to the global well vertical sand proportion curve is presented and illustrated with some synthetic cases and a field case study.
- the fifth chapter presents the conclusions of this work with some perspectives.

1 Flumy model for meandering fluvial systems

Résumé français : Ce chapitre introduit le modèle Flumy pour les systèmes fluviatiles méandriformes. Il commence par une description des principaux processus et dépôts liés aux systèmes méandriformes fluviaux, basée sur des exemples actuels et fossiles. Il présente ensuite la manière dont ces processus et dépôts sont simulés par Flumy. Il décrit enfin un outil, le Nexus (Non-Expert User Calculator), permettant le calcul automatique des paramètres du modèle à partir de trois d'entre eux.

In this chapter, we present a brief description of the main processes and depositional elements of the meandering fluvial systems based on modern and fossil examples. Then we present how these processes and associated depositional elements are simulated by Flumy. The automatic inference of the main simulation parameters by the Non-Expert User Calculator (Nexus) is presented at last.

1.1 Meandering Fluvial Systems

1.1.1 Modern systems

Modern meandering systems are dynamic fluvial systems (Figure 1, a). They are generally associated with sandy-clay loads, although there exist meandering systems with gravel and/or pebbles. The meandering channels are characterized by high migration potential, which results in the construction of sandy deposits on the inner banks of the meander loops – the meander point bars. These bars have lenticular to sigmoidal form and migrate transversely to the flow (Figure 1, c-d).

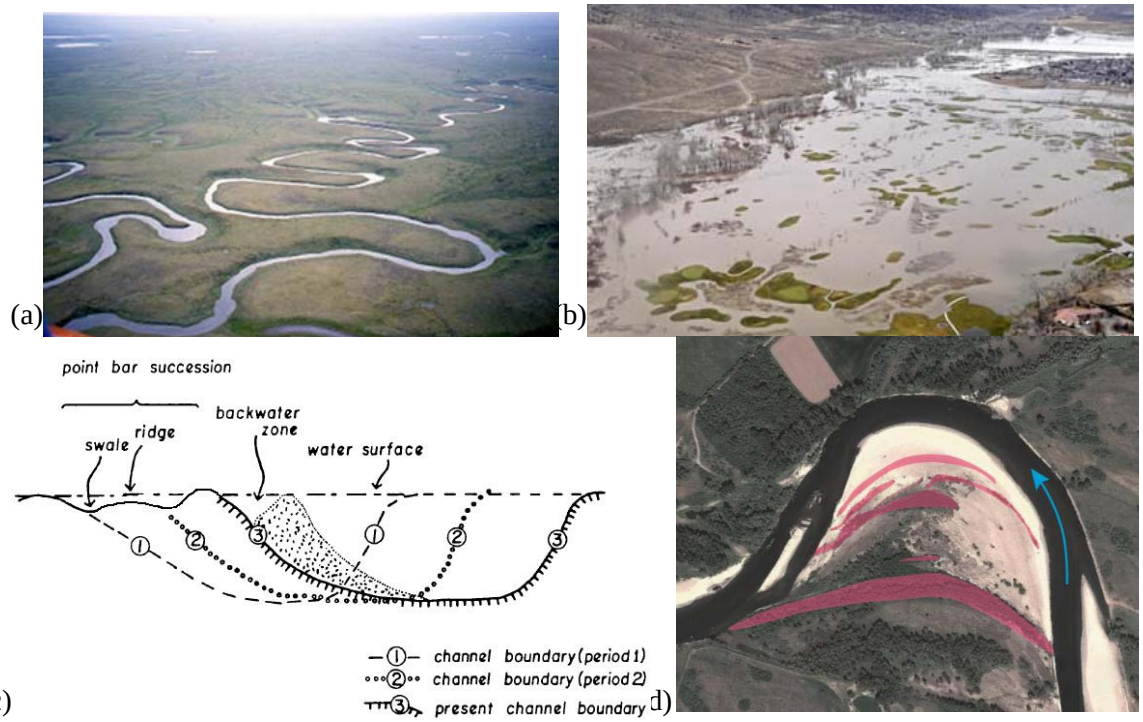

Figure 1. (a) A meandering river in Siberia. Image Credit: Ólafur Ingólfsson, http://www3.hi.is/~oi/; (b) Carson River (USA) during an overbank flood (https://nevada.usgs.gov/crfld/floodtypes.htm) (c) Lateral accreting sand bars in a meander loop (from Hickin, 1974); (d) aerial view of a point bar (Allier river, France), pink shaded area corresponds to the crest height that are quickly colonized by vegetation (from Deleplancque, 2016)

During overbank floods, silty material deposits near the channel forming levees, and fined grained sediments in the floodplain contributing to the floodplain aggradation (Figure 1, b).

1.1.1.1 Meandering channel geometry

In modern hydraulic studies, the **channel geometry** is defined by the bankfull geometry that corresponds to the water elevation before an overbank flood (Leopold and Wolman, 1957; Bridge, 2003). This channel bankfull geometry is characterized by the channel bankfull width and the mean bankfull depth:

- The bankfull width corresponds to the channel width at the bankfull stage elevation, defined at the top of the point bar (Williams, 1978; Sweet and Geratz, 2003). The channel bankfull width is relatively stable along the channel path.
- The mean bankfull depth is obtained by dividing the channel cross section area by the bankfull width.

The maximum channel depth (difference in elevation between the deepest and the highest one in the surveyed section) is dependent of the channel curvature, the occurrence of riffles and pools. It is maximum at the apex of the bend and corresponds to 1.7 the mean bankfull depth (Bridge, 2003).

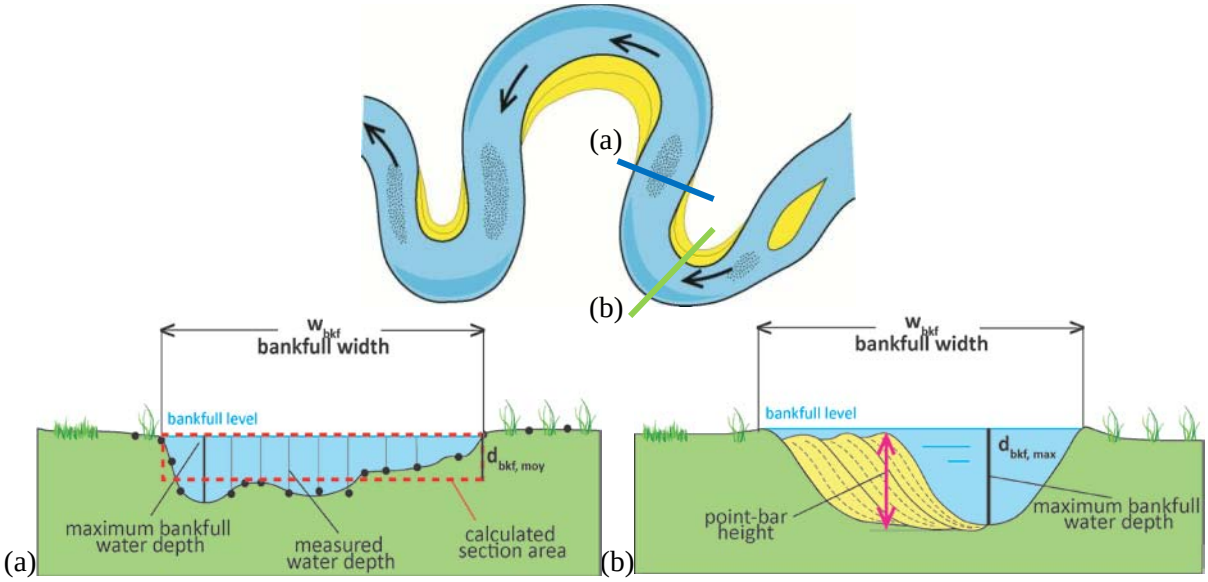

Figure 2. (a) Cross-section in a straight reach mean bankfull depth; (b) cross-section at the bend apex max bankfull depth (From Held, 2011).

This bankfull geometry proved to show good relationship with the channel forming discharge in fluvial systems in humid climates (Bridge, 2003 and references therein). It is used in the restoration of man-managed meandering fluvial system towards natural courses or for paleohydrologic studies (Williams, 1986). In Flumy, the classical power relationship between channel geometry and discharge (Leopold et al., 1964) are used for the channel width/maximum depth ratio. This ratio is taken as 10, based on a power coefficient close to 1:

$$w = 10 * h^1,$$

where w – the channel width, h – the channel maximum depth.

1.1.1.2 Evolution of the meander loops

During migration, the meander loops extend, resulting in a narrowing of the distance between the upstream and downstream channel reaches of the meander bend that can result in a neck or chute cutoff when they are very close (Figure 3, a-b). Thus, the course of the river is modified and eventually an abandoned meander loop is created (*oxbow*) which creates a more or less efficient junction between the floodplain and the channel. These abandoned meanders are then progressively

filled up by the fine grained sediments transported during the successive floods and form sand and clay plugs. In relatively humid climates, the floodplain is never completely drained, the depressions left by these abandoned meanders are occupied by marshy lake systems (*oxbow lake*) and may be filled with peat.

With time, the channel migrates across the floodplain, building a **channel belt**. The channel belt corresponds to the area where the channel paths have been mainly confined (Figure 3, c-d). Many oxbow deposits are preserved on the edges of the channel belt. Their fine grained filling limits migration further away in the floodplain.

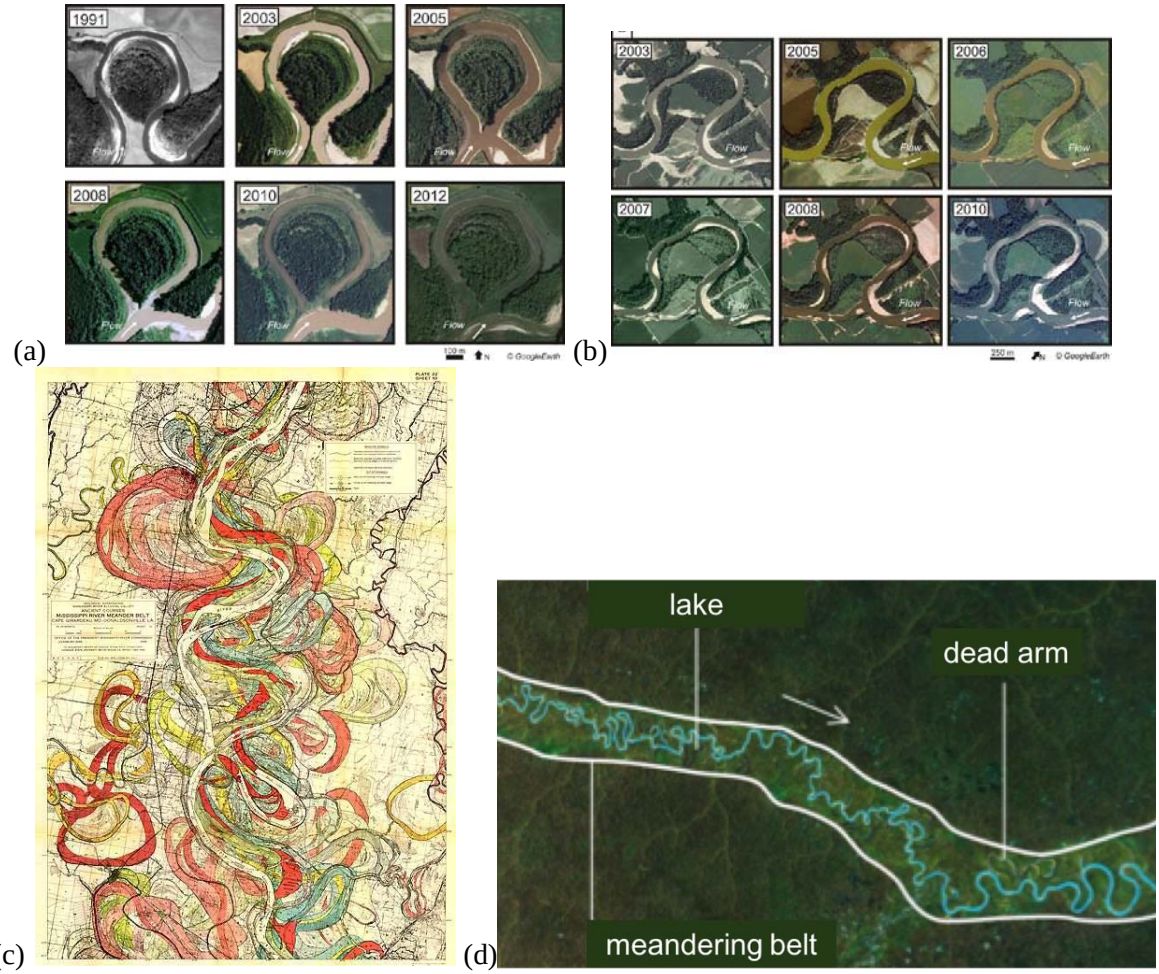

Figure 3. Illustration of a meander loop by neck cutoff (a) and chute cutoff (b) (Dieras, 2013); (c) map of the Mississippi channel belt built over some ten thousand years (Fisk, 1944); (d) satellite photo of the Jutaï River (Amazon, North Brazil) extracted from Google Earth. This picture shows the meandering belt formed by a high sinuosity river, within which meander intersections also cause the formation of lakes and dead arms.

1.1.1.3 Overbank flow sediments

During overbank floods, the area that is submerged corresponds to the floodplain. It is flooded regularly and fine grained sediments accumulate. This is also called the **aggradation**.

As a result, the proximal overbank flow deposits (sandy to silty) build levees, and distal deposits (silty-clayey = silts) cover large areas in the floodplain.

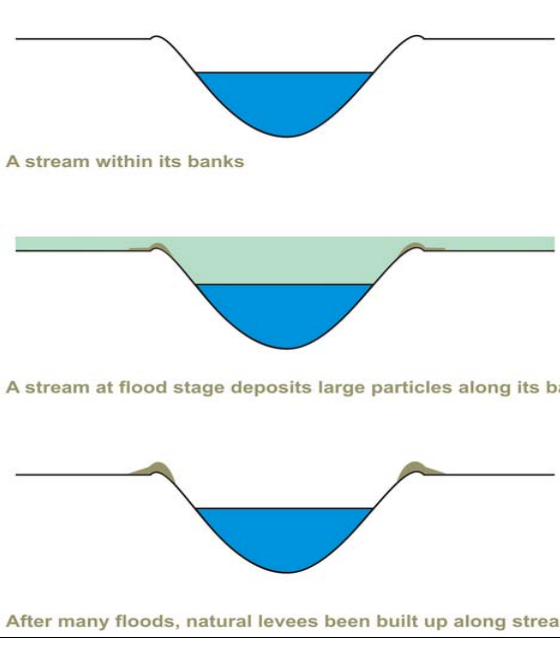

(a)

(b)

Figure 4. (a) Scheme of overflow sediments formation; (b) the Red River during the 1997 flood, viewed southwards from near St. Norbert, Manitoba (Canada). Courtesy Geological Survey of Canada (up), and Missouri River flood (2018 Scripps Media, Inc.) (below)

This results in a transition between the channel and the floodplain marked by a system of **levees**, elongated sandy to silty bodies that lie along the channel (Figure 4, b). Although present on both banks, they are more developed on the outer bank. Thus, the levees are formed during flood episodes (*overbank*) and therefore have a low potential for preservation because they can be eroded during channel migration (Reading, 1978; Brierley et al., 1997). The sedimentation rates of the floodplain are low and decrease with the distance to the channel due to the loss of velocity of the flow which is no longer channelized. It results in the deposition of the fine grained sediments away from the channel, leaving thin layers of silty to shaly alluvium.

The floodplain lowlands are often occupied by wetlands, swamps or lakes depending on the water table level. Areas of higher elevation are the site of pedogenesis in relation with the type of vegetation cover and climate.

1.1.1.4 Levee breaches

The violent floods sometimes cause a sudden rupture of the banks (a levee breach) which can go up to the abandonment of the initial channel path to a new one, resulting in a complete **avulsion** of the channel. In less severe cases, the levee breach may cause diversion of part of the flow into the floodplain, with deposition of **crevasse splays** (Figure 5). The levee breach may heal, and the channel keeps its initial path. The water flowing through the levee breach is loaded with coarser sedimentary load than the overbank flow, resulting in crevasse splays composed of relatively coarse sandy to silty material.

(a)  (b) 

Figure 5. (a) Levee breach along the Mississippi River (source: http://www.20min.ch/ro/news/monde/story/14925437); (b) Crevasse splay, Columbia River, Canada (source: http://www.seddepseq.co.uk/)

1.1.2 Fossil systems

In fossil systems, meandering channel elements can be easily identified based on the geometry of the sedimentary beds, their mineralogical composition and the grain size. Here is a list of principal elements characteristics, illustrated by photos from the Miocene Loranca fluvial deposits (Spain, La Mancha):

- sandy point bar deposits are represented by low angle inclined sandy sets that correspond to migration periods (Figure 6)

Figure 6. Point bar of around 3m height, showing the lateral extension of 18-20m

- levee deposits are characterized by thin units (less than 0.2 m thick) and silty facies (Figure 7)

Figure 7. Levee deposits interrupted by a crevasse splay (thicker bed with a coarser grain size) in relief in the section. Hammer, 0.4m for scale

- overbank alluvial correspond to shaly to clayey facies. Some of them show pedogenic features that led to the oxidation of the facies (reddish colors) and the development of calcisoils characterized by carbonate nodule horizons (Figure 8)

Figure 8. Paleosol

- crevasse splay deposits show very often an erosive contact with the underlying deposits, and are always coarser than the levee or overbank deposits (Figure 7)
- oxbow lakes are filled by clay rich deposits overlaid by a limestone bed (Figure 9)

Figure 9. Oxbow lake with orange clayey deposits and white facies limestone bed. The person is standing on the toe of the last point bar set before the loop abandonment

- low land deposits, depending on the climate, can be represented by organic rich deposits or carbonate-rich ones.

Figure 10. Incision at the base of the sandstone cliff, corresponding to an avulsion

The preservation of these architectural elements in fossil systems depends on the balance between the aggradation and migration rates. Low aggradation rates result in cannibalization of the point bar deposits, numerous mud plugs and well developed soils in the stable floodplain. On the other hand, high aggradation rates favor preservation of the various facies associated to the fluvial meandering systems (Figure 11).

Figure 11. Isolated sandbodies in the alluvium deposits during a period of high aggradation rate; on top – amalgamated sandbodies during a period of low aggradation rate.

The following scheme (Figure 12) contains a summary of main depositional facies presented in modern and fossil meandering systems, illustrated by the Miocene deposits photos of the Loranca basin (Spain).

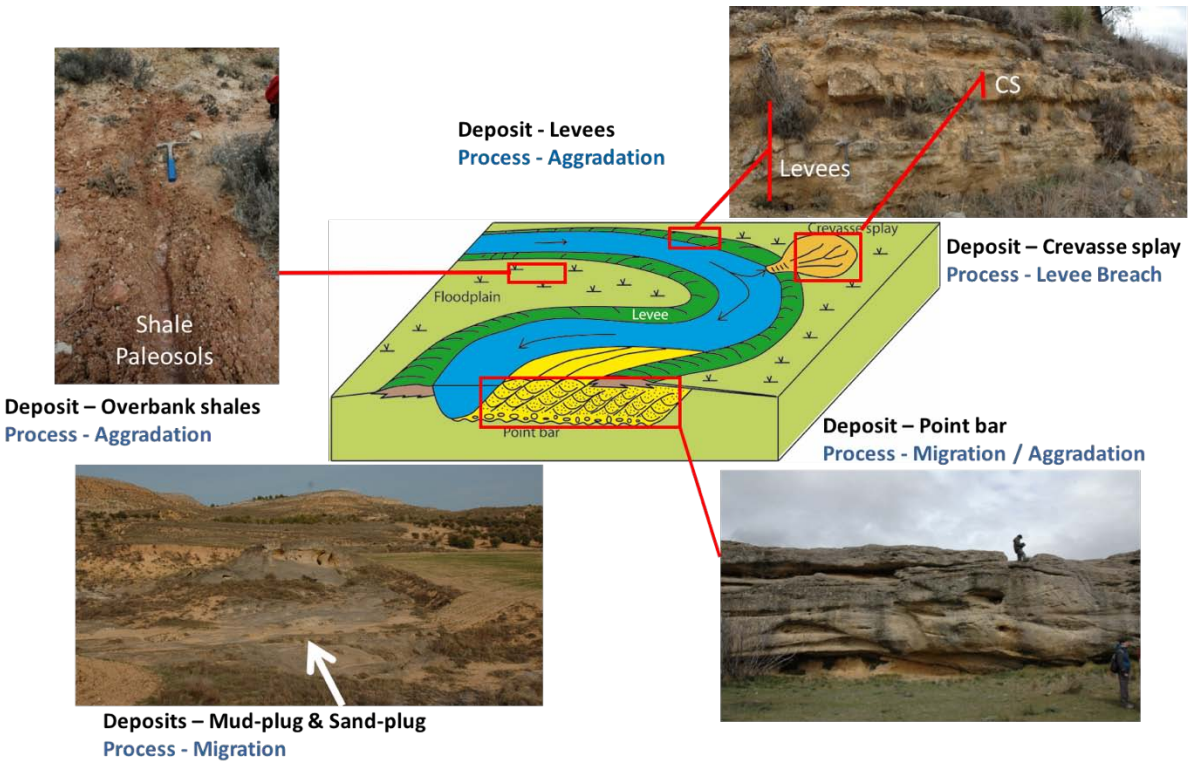

Figure 12. Schematic illustration of principal elements of a Meandering Fluvial System illustrated from outcrops of the Loranca Basin

1.2 Flumy model

Starting from the 1950s, meandering fluvial systems became an object of active field and theoretical studies (Leopold and Wolman, 1957, 1960). These observations, combined with laboratory experiments (Friedkin, 1945), allows now predicting the evolution of meandering rivers quite well (Bridge, 2003; Castro and Jackson, 2001; Mulvihill and Baldigo, 2007). Several generations of models have been developed, that relate the migration rate of river centerline to the integrated effect of velocity asymmetry in meander bends (Howard and Knutson, 1984; Ikeda et al., 1981; Ikeda and Parker, 1989; Johannesson and Parker, 2013; Perucca et al., 2007; Sun et al., 2001). All these lead to 2D reproduction of the long-time behavior of meandering channels, including the dynamic of channel flow and the resulting deposition patterns.

The Flumy software is a modeling tool, both process-based and stochastic, which aims to provide accurate and realistic 3D representations of the simulated sandbodies and their associated deposits at the scale of the reservoir (Lopez, 2003; Lopez et al., 2001, 2008; Lemay et al., 2016).

The model construction is based on **three main processes**:

1) **the channel migration** with the deposition of sandy point bars in the interior part of meander loops, and sand and mud plugs in abandoned channels;
2) **the aggradation process** caused by overbank floods, with the construction of silty levees and fine-grained alluvium deposition on the floodplain;
3) **the channel wandering** thanks to the avulsions – results of the levee breaches, which possibly lead to the creation of new channel paths.

The combination of these three processes enables simulating the depositional facies mentioned above; resulting simulation is illustrated in Figure 13 and explained in details in the following subchapters.

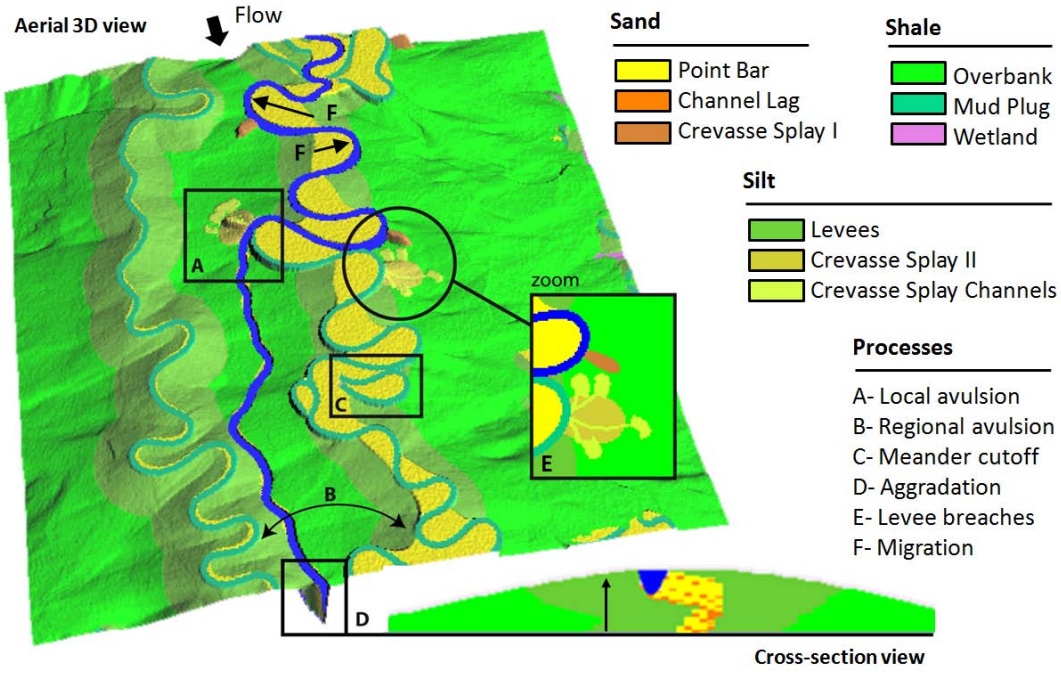

Figure 13. Illustration of the main Flumy processes (Flumy aerial 3D and cross-section views)

During simulation deposits are saved at each node of the 2D grid corresponding to the simulation domain. Information regarding the simulated deposits comprises: X, Y, Z coordinates and thickness; lithofacies, grain size and age (Figure 14):

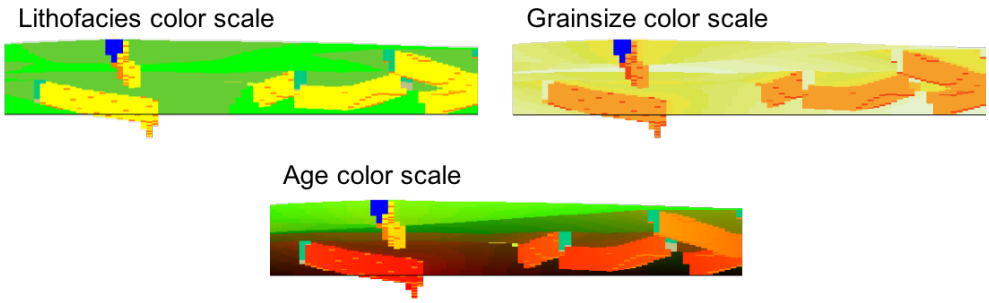

Figure 14. Different color scales in Flumy

The next Table 1 contains the information about the lithofacies types deposited during different processes (as well as their visualization colors):

Related process	Facies	Litho-facies	
Migration	Point bar Channel lag	Sand Gravel	PB CL
Cutoff	Abandoned meander (plug and loop)	Sand Shale	SP MP
Aggradation	Levees Overbank flood	Silt Shale Wetland	LV OB WL
Levee breaches	Crevasse splay 1 Crevasse splay 2 Crevasse channels	Sand Silt Sand	CS1 CS2 CCH
Avulsion	Abandoned channel	Sand Shale	SP MP
Marine incursion	Draping	Shale	DR

Table 1. Eleven Flumy lithofacies deposited during fluvial simulations

The Table 2 shows, sorted in increasing grain size order, the relation between the 11 possible fluvial lithofacies and their grain size. In the rest of this manuscript, Flumy lithofacies could be named "facies" only.

Facies	DR	WL	MP	OB	LV	CS2	CCH	CS1	SP	PB	CL
Classes	Shale				Silt		Sand				

Table 2. Flumy lithofacies sorted in increasing grain size order

1.2.1 Migration

The model is based on the evolution of the channel centerline in time and on the deposition of the associated sedimentary bodies. The 2D river hydraulic equations proposed by Ikeda and collaborators (Ikeda et al., 1981) proved to produce realistic shapes (Lopez, 2003, PhD thesis; Lopez et al., IAS 2008).

Linearization of the main hydraulic equations in the 1980s made possible to propose theoretical equations that replaced the empiric formulae deduced from observations (Ikeda et al., 1981, Johannesson and Parker 1989b, c; Sun et al, 2001). The main hypothesis underlying these models of the geometrical evolution in space and time of meandering rivers is a linear relationship between the lateral migration of the channel and the flow velocity close to the river bank. These linear theories proved to give stable algorithms to model long-term evolution of meandering rivers.

The channel centerline is discretized into several channel points with Cartesian coordinates. The flow velocity *U* depends from the global valley slope I and the mean channel wavelength λ. It is considered constant along the channel. At every channel point, the following properties are calculated: the curvature *k*, the Cartesian distance from the previous upstream point *Δs*, the normal vector *n* and the velocity perturbation *U'* collinear to the normal vector.

In Flumy, the classical model created by Ikeda et al. (1981) is used, with an adaptation made by Johannesson and Parker (1989) and Lopez (2003):

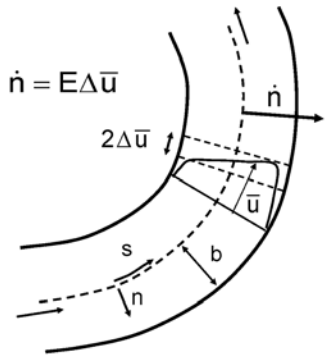

Figure 15. Channel centerline scheme (Parker and al., 2011)

Erosion and migration at the outer bank linearly related to the **velocity perturbation** (U'_b) are presented as following:

$$\overrightarrow{mig} = \vec{n}\, U'_b\, E,$$

where *E* is the bank erodibility coefficient. The smaller this coefficient is, the lower bank erodibility, the slower migration of the meander.

So, for each channel point, the local velocity perturbation U'_{bi+1} is calculated according to:

$$U'_{bi+1} = U'_{bi}\left(1 - 2\,\Delta s_i\,\frac{C_F}{H}\right) + k_{i+1}BU - k_iBU\left(1 + \Delta s_i\,\frac{C_f}{H}\left(\frac{U^2}{gH} + A_{aff} + A_{sec} - 1\right)\right),$$

where U'_{bi+1} – local velocity perturbation (m/s);
U'_{bi} – upstream velocity perturbation (m/s);
Δs_i – distance between upstream node *i* and local node *i+1* (m);
k_{i+1} - local curvature (const);

k_i – upstream curvature (const);
B – bankfull half-width of channel (m);
H – bankfull mean depth (m);
U – mean velocity longitudinal component (m/s);
g – gravitational acceleration (m/s^2);
C_f – friction coefficient (const);
A_{aff} – vortex coefficient (const);
A_{sec} – secondary current coefficient.

These equations are used to simulate the channel centerline migration, accompanied by deposition of sand point bars, and mud plugs in the oxbow lakes created by cutoffs (Lopez, 2003; Lopez et al., 2004 EAGE).

Based on these equations, the meander loops develop a stable pattern from an initial straight centerline with small perturbations. Migration is performed at each iteration (1 year for fluvial systems). Amplitude of the migration is driven by the curvature of the centerline and the erodibility of the substratum. By default, the erodibility is constant over the domain. The erodibility can be defined locally, thus favoring migration in the areas of higher erodibility. After several iterations, some cutoffs occur and meander loops are abandoned. Figure 16 shows the meanders development:

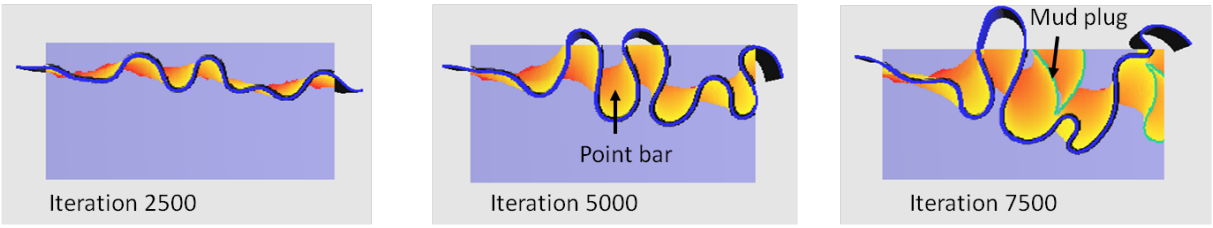

Figure 16. An illustration of meanders development in Flumy

Channel cross-section (Figure 17): geometry of each depositional unit depends on the local curvature of the channel.

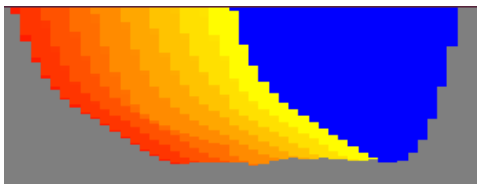

Figure 17. Flumy channel cross-section example. In blue – the channel with the water inside, from red to yellow color – deposited sandy Point Bars from the old to new deposits

Principal parameters associated to the migration are: **erodibility coefficient E**, channel bankfull **width w**, channel bankfull mean **depth H** global valley **slope I** (along flow direction) and mean **wavelength** λ. In the following, channel width and depth are always considered "bankfull".

1.2.2 Aggradation

The frequency and intensity of the overbank flows control the aggradation (the intensity corresponds to the thickness of the deposited Channel Lag). Thickness and grain size of the non-channelized material deposited decrease following a negative exponential law away from the channel (Figure 18, Figure 19). Levee width corresponds to the grain size transition from silt to shale. The period and intensity of the overbank flows greatly influence the aggradation rate and the sand proportion of the resulted modeled reservoir:

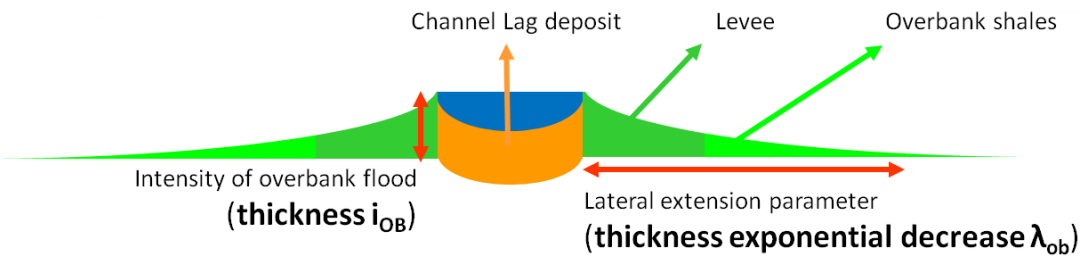

Figure 18. Flumy valley cross-section scheme (vertical scale exaggeration)

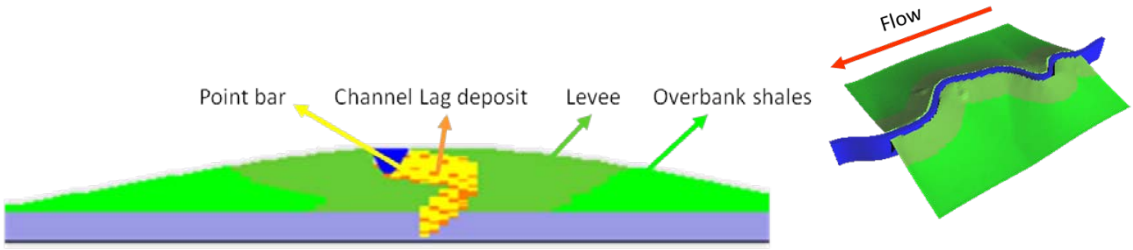

Figure 19. Overbank Flood in Flumy (cross-section and 3D view)

In the fluvial systems, peat (or any wetland deposits) may be deposited in the lowlands as illustrated on Figure 20.

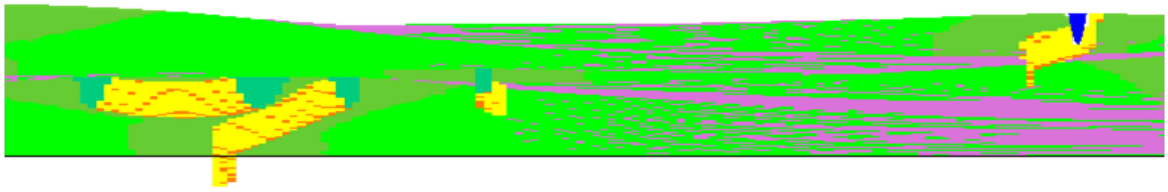

Figure 20. Flumy cross-section with wetland depositions on the floodplain

Principal characterization parameters for aggradation are: **overbank flood thickness i_{ob}** (constant, or defined by Uniform/Normal/Log-normal distribution) **and period T_{ob}** (constant or defined by Poisson distribution), thickness **exponential decrease λ_{ob},** and **levee width L_{LV}**.

1.2.3 Levee breaches and avulsions

From time to time, a levee breach may occur, preferentially where the velocity perturbation is locally maximal. This results either in a chute cutoff, or in the deposition of a crevasse splay possibly followed by an avulsion (the new channel finds a new path downstream using a stochastic steepest path algorithm) (Figure 21).

There exist two types of avulsions in the model: **local**, when a new path is tossed from a levee breach point within the domain, and **regional**, in order to simulate a levee breach upstream of the domain (Figure 22). The regional avulsions, ensure a uniform spatial distribution of the channel paths over the modeled domain through time.

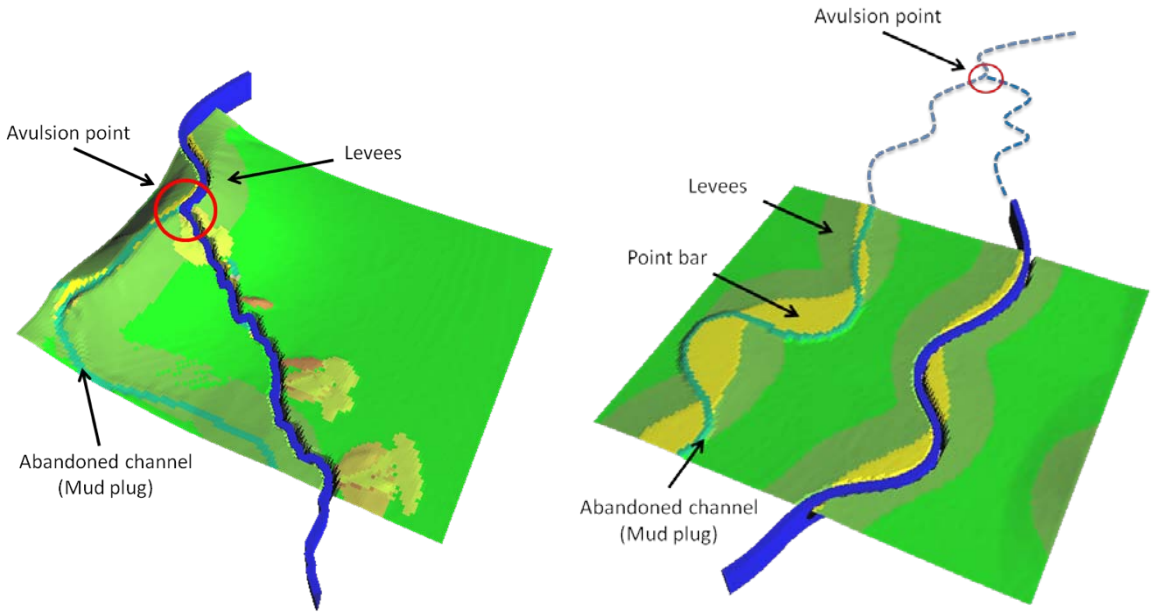

Figure 21. A local (left) and a regional (right) avulsion in Flumy, 3D view

Note: after a successful regional avulsion, the channel may lie outside the simulated domain, and reenter the domain from the lateral sides by migration or avulsions (Figure 22):

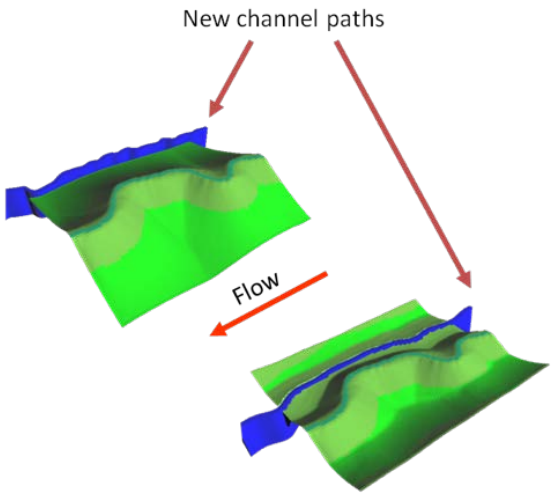

Figure 22. New channel path examples (resulting from a regional avulsions)

Principal characterization parameters for avulsions are: **local avulsion period T_{LAV}** and **regional avulsion period T_{RAV}.** The avulsions periods can be constant or distributed according to Poisson law.

1.2.4 Conclusion

Flumy is a process-based and stochastic model for channelized fluvial meandering reservoirs. The simulations are performed forward. The output is a three-dimensional numerical blocks, informed with lithofacies, grain size and age for each deposition unit.

Time is discretized into iterations, or time steps. At every time step, migration is performed, with deposition of sandy point bars in outer part of meanders. When overbank flow occurs, fine grain material is deposited on the domain, with thickness and grain size decreasing exponentially from the channel. Avulsions, generated during levee breaches within the domain or upstream of the domain allow a uniform distribution of the sandy sediments over the domain thanks to new channel paths formation.

The model is finally ruled by eleven main parameters (Table 3).

Parameter	**Symbol**	**Processes**
Channel maximum depth	H_{max} (*m*)	Migration
Channel width	w (*m*)	
Mean wavelength	λ (*m*)	
Erodibility coefficient	E (*m/s*)	
Global slope along flow direction	I (*const*)	
Overbank flood thickness	i_{ob} (*m*)	Aggradation
Overbank flood period	T_{ob} (number of iterations)	
Thickness exponential decrease	λ_{ob} (*m*)	
Levee width	L_{LV} (multiple of *w*)	
Local avulsions period	T_{LAV} (number of iterations)	Avulsions
Regional avulsions period	T_{RAV} (number of iterations)	

Table 3. List of 11 main Flumy simulation parameters

These allow simulating contrasted reservoir architectures by just varying the migration, the aggradation and the avulsion parameters. Thanks to the stochastic aspect, multiple realizations of the model can also be produced using the same set of parameters. One of the Flumy objectives is the possibility to create blocks with various sandbodies distribution. Figure 23 illustrates the simulation results variability: Sixteen cross-sections of different models are sorted in function of two main characteristics: aggradation rate and avulsion period.

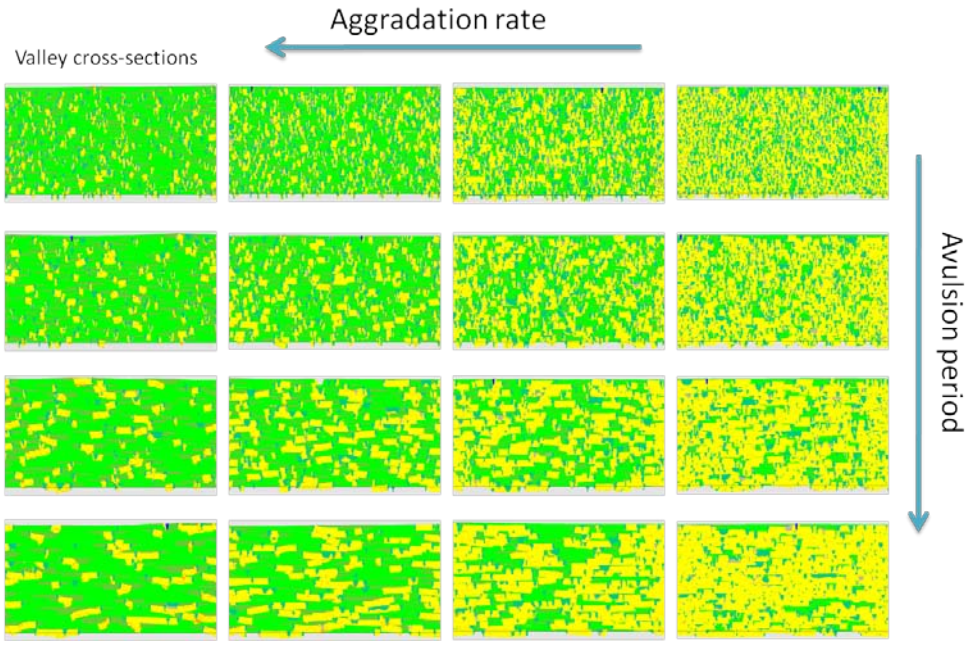

Figure 23. Variability of Flumy results in function of aggradation rate and avulsions period (Flumy cross-section view of 16 different scenarios)

For an easy use of the software, a tool to deduce all main parameters from a reduced number of parameters has been developed and is presented in the next chapter.

1.3 Flumy – Non-Expert User Calculator (Nexus)

It may be difficult for a non-expert Flumy user to determine all the simulation parameters. In order to simplify this task, a special tool is proposed: The Non-Expert User Calculator (Nexus). It is based on some heuristic formulas coming from the Boolean model (Rivoirard et al., 2008) applied to the sedimentary objects generated by Flumy. The Nexus only gives orders of magnitude for the main parameters. At last, the user can choose to adjust the proposed parameters.

The three key Nexus parameters are the following:

- The **Channel Maximum Depth** (H_{max}),
- The **Required Net-to-Gross** (N_G, or sand proportion).
- The **Sandbodies Extension Index** (I_{sbx})

1.3.1 Key Nexus parameters

- **Channel Maximum Depth**

The channel maximum depth (H_{max} in meters) corresponds to the channel maximum bankfull depth. Due to the simplified parabolic shape of the channel cross-section in Flumy, the channel mean bankfull depth used by the migration process is calculated by dividing the maximum depth by 1.5. The channel maximum depth gives information related to the scale of the resulted reservoir.

- **Sand Proportion**

This key parameter is the desired sand proportion in the resulted simulation (N_G in percentage). It can be either given from well data, field sections or chosen by the user. Four Flumy lithofacies are considered as sand: Point Bar (PB), Channel Lag (CL), Sand Plug (SP) and Crevasse Splay I (CSI).

- **Sandbody Extension Index**

The I_{sbx} refers to the horizontal Sandbody Extension Index (from 20 to 160, no-unit). It is a parameter characterizing the lateral amplitude of the channel meanders (maximum distance from meander centerline to the line joining the two inflexion points delimiting the bend. It characterizes the type of sandbodies:

- I_{sbx} from 20 to 80 corresponds to ribbon-type sandbodies;
- I_{sbx} from 80 to 100 is for standard sandbodies; meander loops are well developed but not at their maximum;
- $I_{sbx} > 100$ is for sheet-type sandbodies; the largest amplitude is reached during neck cutoff.

The tests conducted with different Flumy scenarios show that the ratio between the mean sandbody extension (L, in m) and the wavelength (λ, in m) stabilizes after the occurrence of the first cutoff. So, small values of L/λ (0.2) correspond to the less developed ribbon-type sandbodies. Then, the channel curvature starts to increase, and the values of L/λ from 0.2 to 0.4 indicate a standard type sandbodies (until the first meander cutoff). The tests showed that the first cutoff corresponds to $L/\lambda \approx 0.4$, with a further stabilization of this relationship value, so starting from 0.4 the sheet sandbodies are modeled. The next scheme (Figure 24) illustrates the choice of I_{sbx} value thresholds from the L/λ graph.

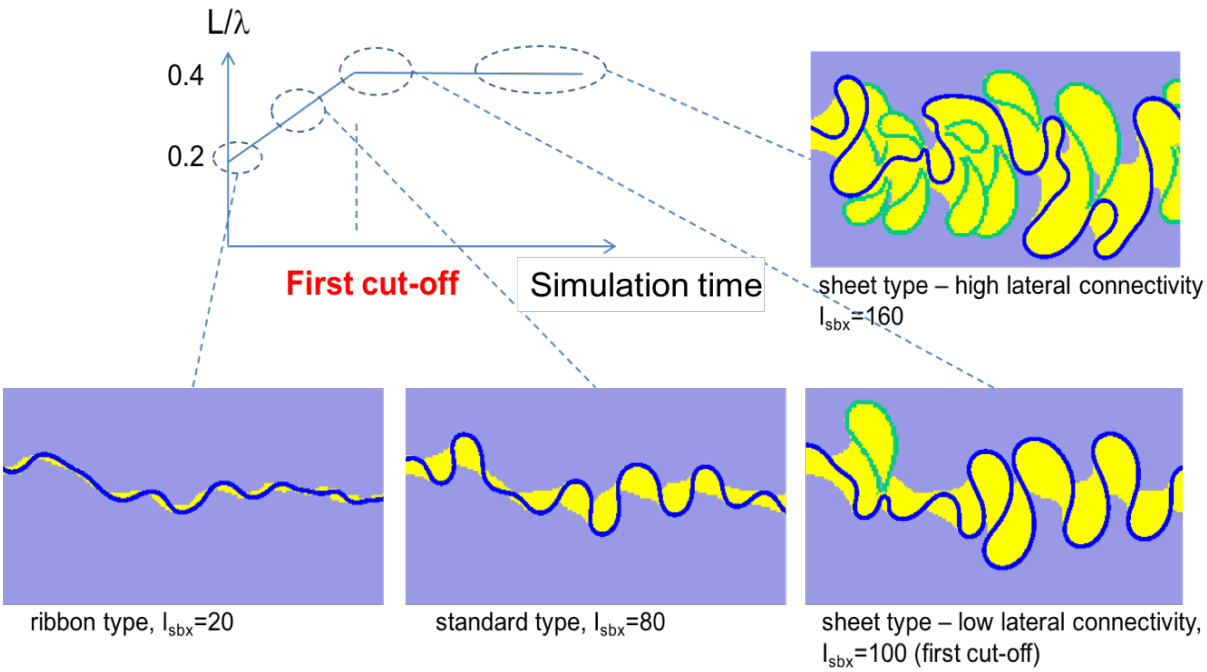

Figure 24. Illustration of I_{sbx} possible values and its influence on the simulation results (Flumy aerial 2D view)

1.3.2 Use of the Nexus

When applying the Nexus from the three key parameters, all other parameters are computed automatically. It should be mentioned that even after the determination of the parameters by the Nexus, the user keeps the access to all parameters and can change their proposed value. The Nexus can be considered as a tool that provides "a first guess" of the simulation parameters from the three key parameters.

The determination of the parameters by the Nexus is performed following these steps (Figure 25):

- The first step calculates all scaled parameters (the channel geometry, the overbank flood thickness and the erodibility coefficient) from H_{max}. As a consequence, the grid parameters (size, mesh) can be adjusted to have a good display of the channel (mesh size ≤ w/2).
- The second step defines the overbank flood period by combining channel geometry with the required N_G.
- The third step defines the local and regional avulsions periods using the I_{sbx} parameter.

Apart from that, the Nexus permits to determine the forecasts resulting sand proportion and aggradation rate which are displayed during the simulation.

When running a Flumy simulation, some other channel and block model statistics are calculated and displayed like the mean topography or the current channel sinuosity.

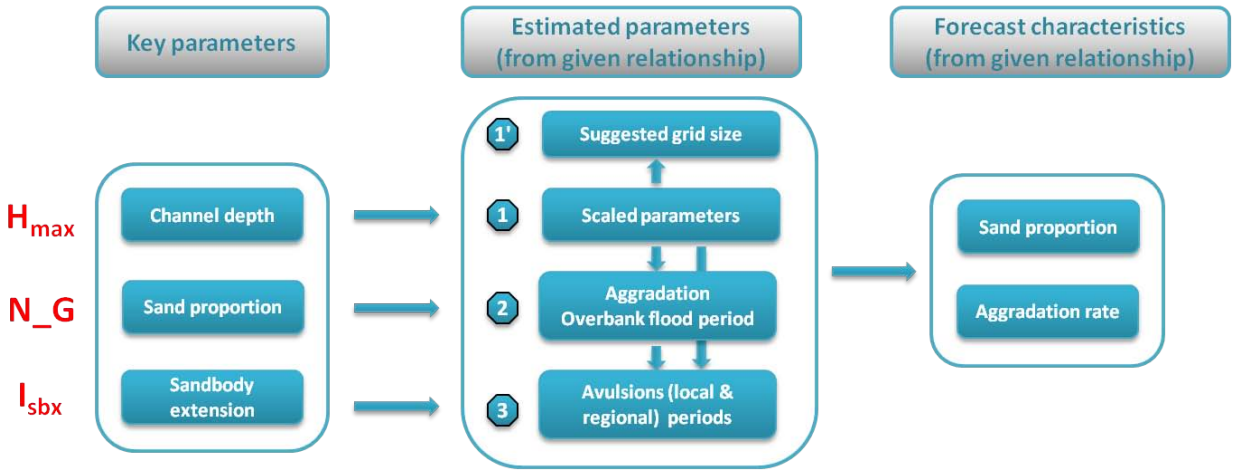

Figure 25. Schematic illustration of Non-Expert User Calculator

Combination of the I_{sbx} and N_G key parameters for a given channel size offers the possibility to generate reservoir simulations with contrasted sandbody geometries as illustrated on Figure 26. Here, only simulated sandbodies are presented in 3D model view (scorched view); three different N_G values (20%, 40% and 60%) are simulated with various sets of I_{sbx} for a constant value of H_{max}.

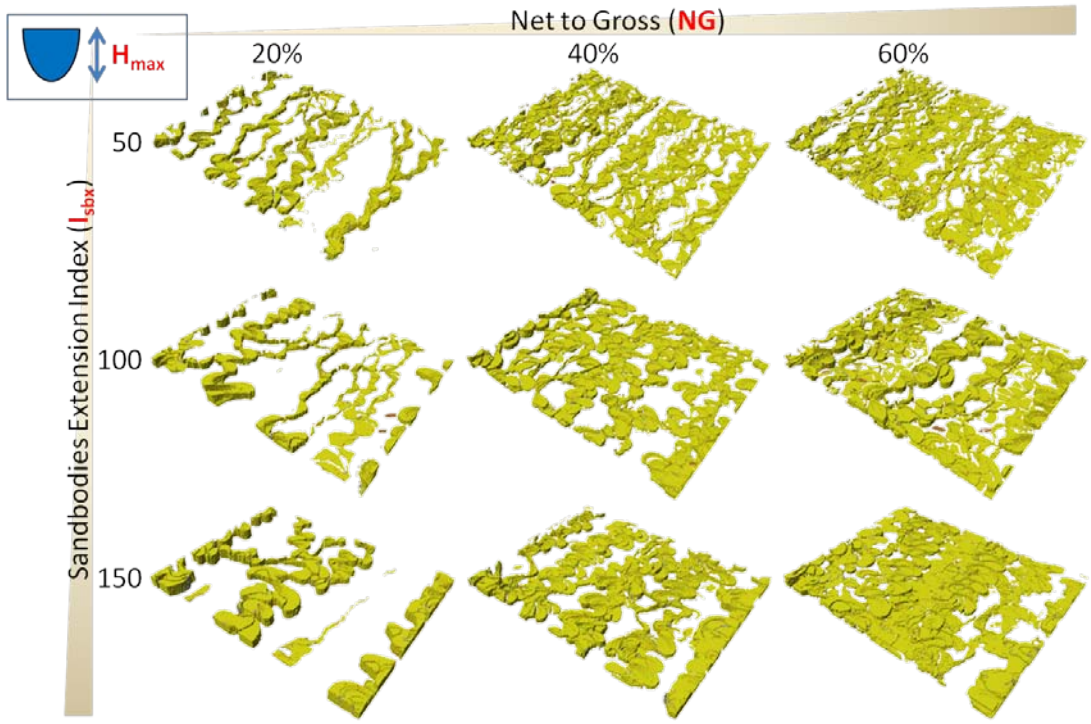

Figure 26. Variability of simulation sandbodies results in function of different I_{sbx} and N_G values

2 Conditioning meandering systems

Résumé français: Ce chapitre traite du conditionnement des systèmes méandriformes. Il commence par une revue des techniques de conditionnement utilisées pour de tels systèmes, qu'elles se fassent à une, deux ou trois dimensions. Sont ensuite présentés les principes généraux du conditionnement dynamique utilisé par Flumy, avant de rentrer dans le détail des algorithmes développés avant ce travail de thèse.

The main objective of reservoir model conditioning is a reproduction of field data in simulation, thus allowing a further fluid flow simulation (useful for a reservoir productivity estimation), history matching, etc. Well data contain the local information about sedimentary body locations. Reproduction of such data in the simulation can improve the realism of model images and make the predictions more robust.

Conditioning algorithms, as well as the level complexity, vary depending on the modelling technique. For example, Plurigaussian models (PGS) or Sequential Indicator Simulations (SIS) are easy to condition whatever the number of wells. Boolean models are more difficult to condition, especially when the number of wells increases. Multi-Points Statistics (MPS) simulations which are easy to use for limited number of facies, becomes less efficient with complex facies description and 3D non-stationary data. Conditioning techniques in process-based models are complex, because it needs to preserve the realistic shapes of the sedimentary bodies while honoring data at the well locations, or data from 2D or 3D seismic.

In this chapter, we focus on techniques that could be applied to process-based simulations. We firstly present a review of existing conditioning techniques for 1D models, mainly based on the meandering channel centerline; 2D conditional simulation of channels, and 3D conditional model examples. Then, we present the main principles of conditioning in Flumy. Finally, these principles are presented in details.

2.1 Review of conditioning techniques

Several remarkable meandering channel models with associated conditioning techniques are considered here. Conditioning of 1D models are divided into two parts: static (Mariethoz et al., 2014) and dynamic (Parquer et al., 2017). A 2D conditional channel model is illustrated by the works of Wang et al., 2009. 3D conditional reservoir models of different types are then presented: geomorphological surface model (Clevis et al., 2006), Boolean model (Hauge et al., 2007), event-based model (Pyrcz and Deutsch, 2005).

2.1.1 1D conditioning

1D conditional simulation concerns the conditioning of **the channel centerline**. It is very useful in the reservoir characterization, by offering the possibility to condition the simulation to a horizontal seismic time slice (Figure 27) using modern data acquisition techniques (satellite images, maps, etc.).

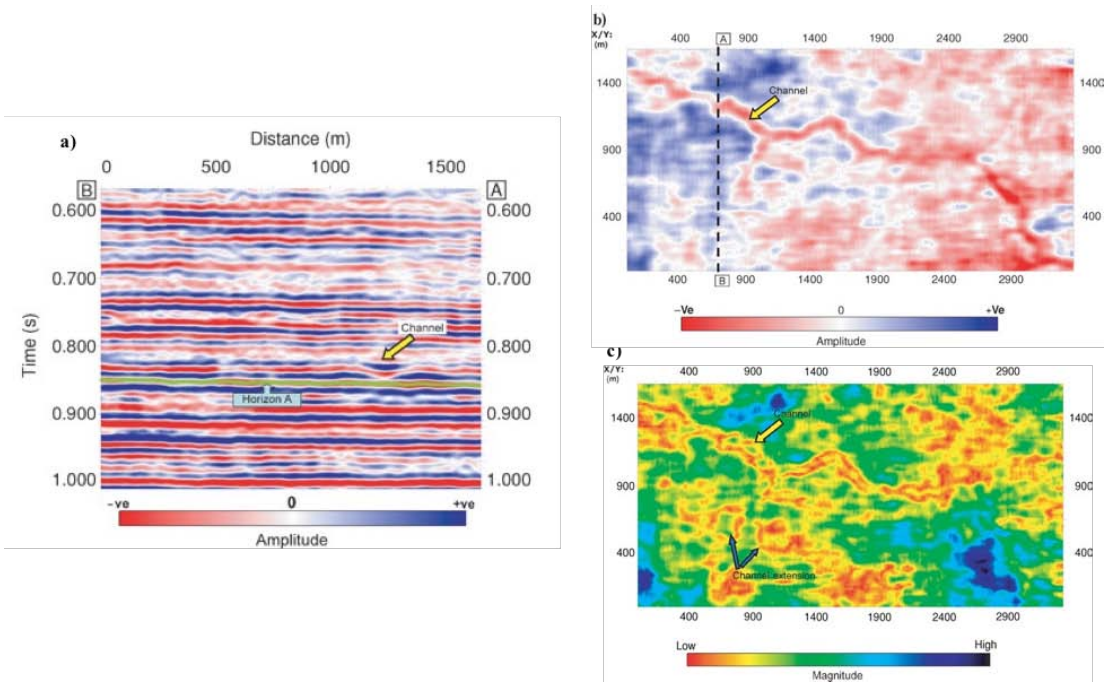

Figure 27. (a) A vertical seismic section through the 3D data set corresponding to line *AB* shown in (b). (b) A horizon slice through the seismic amplitude volume shown in (a). A fluvial channel (yellow arrow) shows up as a negative-amplitude trough on the horizon slice and corresponds to the channel shown in (a). (c) A horizon slice corresponding to the seismic-amplitude map shown in (b). (From Sinha and al., 2005)

2.1.1.1 Static conditioning

There exist several static methods of conditioning of the channel centerline models to well data. Usually, in this case, a well corresponds to 1D point indicating either sandy or clayey deposit. Conditioning to sandy well means that the channel should pass through the well; otherwise the channel should avoid the well location.

Good examples of such conditioning are presented in the works of **Mariethoz and al., 2014**. This model deals with the reconstruction of meandering channel centerline from the training image and local observations (wells) using MPS approach – simulation of succession of directions as a 1D random process. Resulting simulations are stochastic and geologically realistic.

Model creation consists in several steps:

- Analog channel is initially manually digitized (blue dots) from a satellite image and interpolated at regularly spaced steps (Figure 28, Figure 29a). The digitized points are interpolated at equidistant locations along the channel using a spline (red crosses).
  The training image should be large enough to contain a statistically significant number of spatial patterns to inform the generation model, and should also be stationary (similar processes are taking place).

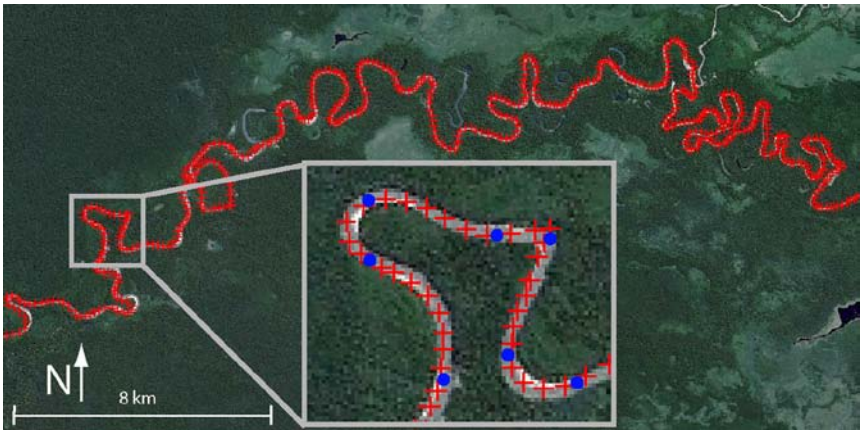

Figure 28. Digitization procedure. Blue dots: original digitized points. Red crosses: spline interpolated points (Mariethoz and al., 2014)

- The succession of directions along the channel from one step to the subsequent is computed (Figure 29b). This model (1D training image in terms of MPS) is used in the Direct Sampling (DS) algorithm for the simulation of another sequence of directions (Figure 29c and e). Directions are a continuous variable in the interval $[-\pi, +\pi]$.
- The simulated sequence has the same statistical properties as the training image (Figure 29d and f). The new channel is drawn with the same morphological characteristics, but with a different centerline. Simulation is a stochastic process; various new channels can be obtained from the same training image (characterization of the uncertainty).

The morphometric attributes used for evaluating the results are the following: sinuosity, half-meander length and straight-line distance (between two inflexion points), wavelength and asymmetry coefficient.

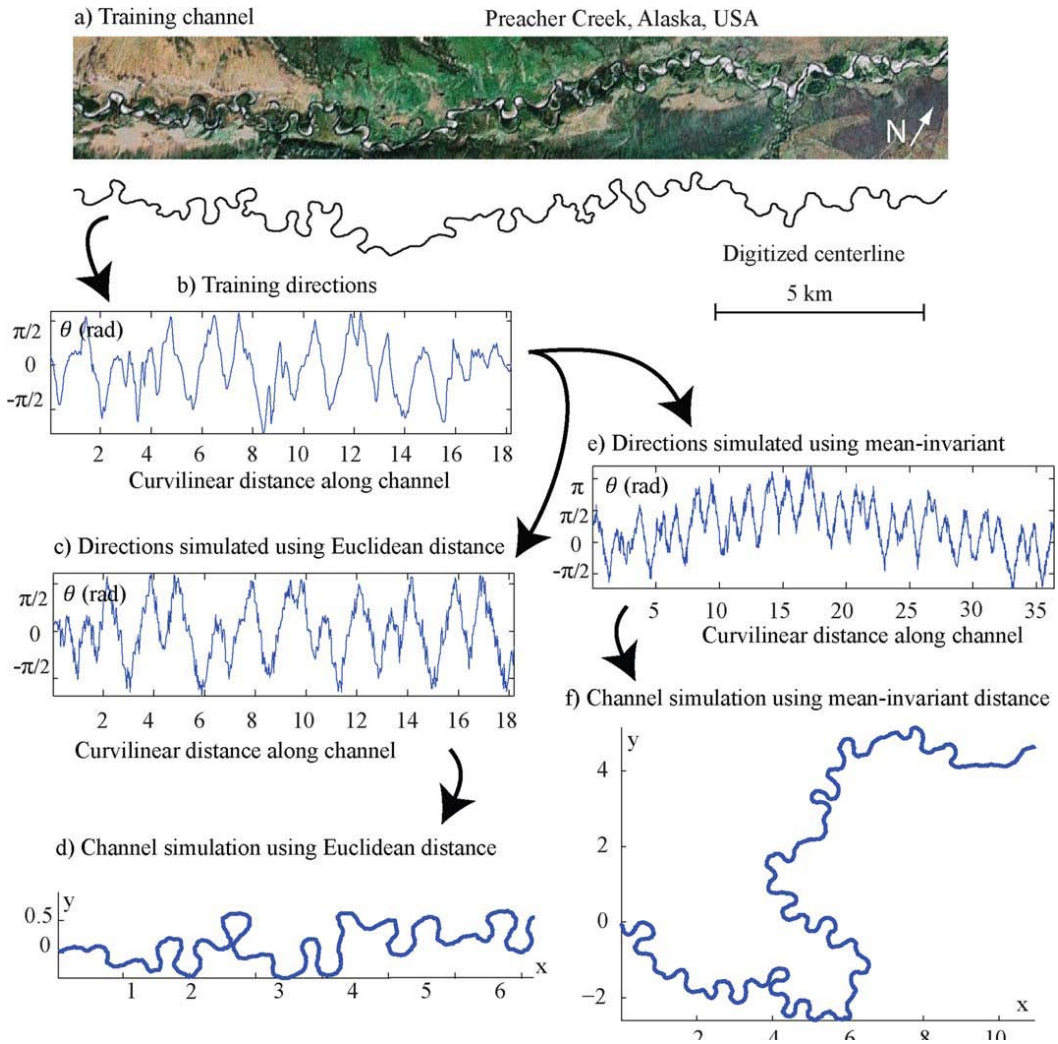

Figure 29. Illustration of channel centerline simulation using MPS applied to the succession of directions as a 1D random-walk process (Mariethoz and al., 2014)

Two methods of conditioning to well data are proposed here. In both, the well data is limited to the occurrence of sand; the conditioning procedure considers that the channel passes through the well location – a hypothesis that assimilates the sand deposits to the channel shape, and that does not consider sand associated to point bars and crevasse splays.

1. Trend-based conditioning (Figure 30)

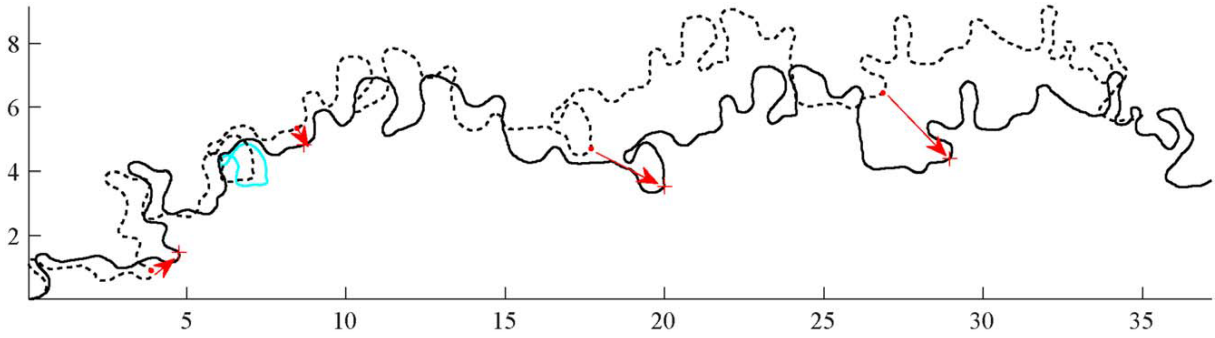

Figure 30. Dotted line: unconditional simulation. Solid line: conditional channel. Red crosses: conditioning data. Blue line: meander shut close because of the conditioning

This method was firstly proposed by Oliver (2002) in context of Gaussian-based channels. The main idea is to add a trend on an unconditional channel, such that the trend helps in reducing the errors to the conditioning points. The points of the channel, closest to the data points, are selected and the trend is applied to adjust the channel to pass through the observed locations. But, in this case nothing ensures the physical consistency of such an additive trend, so the results may present artifacts, and the morphological properties of the channel can be modified. This method is good in cases where the known data is close to the channel.

2. Conditioning by ISR (Iterative Spatial Resampling)

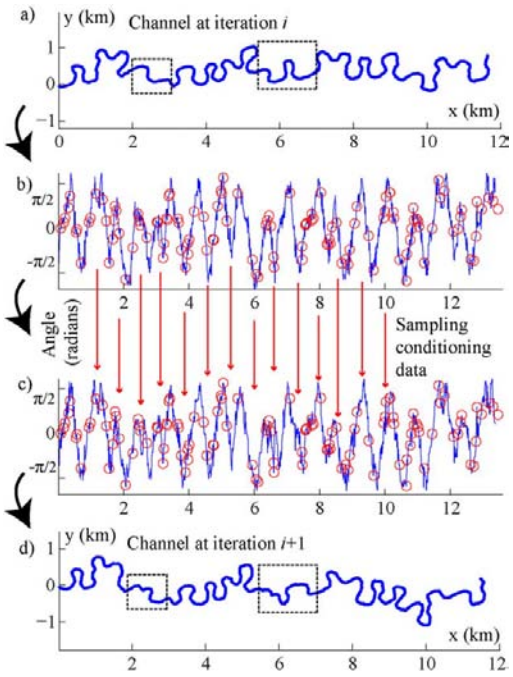

Figure 31. Illustration of the ISR. (a) Initial channel. (b) Corresponding directions, resampled to obtain a new realization. (c)-(d) Perturbed channel

Here, the principle is to iteratively perturb a channel until it honors the conditioning locations (so that the channel remains realistic, to respect the statistics of the training image). After a simulation of an unconditional realization (Figure 31a), a number of points are randomly selected and are imposed as conditioning data for a new simulation (Figure 31b) – using the same training image. The resulting model can be resampled again. The resampling and simulation steps are iterated, yielding a chain of models that all have similar characteristics as the training channel, but vary locally from one iteration to the next one (Figure 31c-d).

Using this method, channels can be conditioned to local data by using an acceptation/rejection criterion that preferentially accepts channels improving the match to the data (Figure 32). The method is illustrated with the unconditional (a) and conditional realizations with small (b) and large (c) error tolerance.

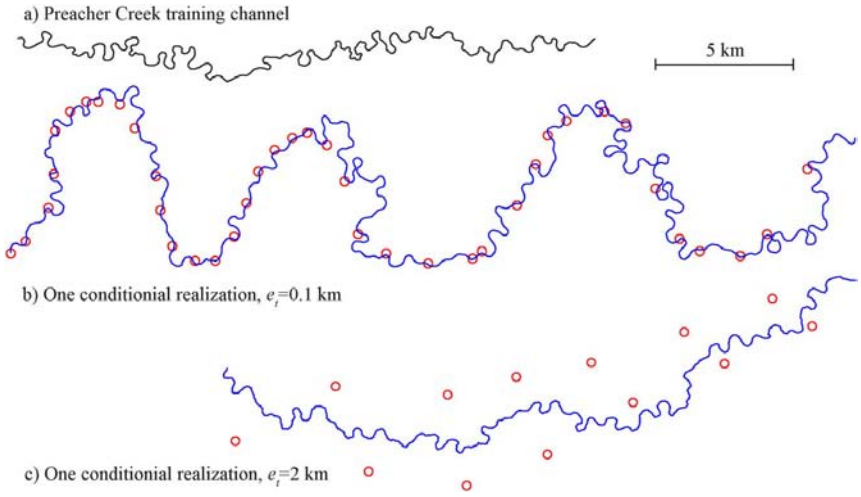

Figure 32. (a) Digitized channel. (b)-(c) Two conditional simulations performed with different values of error tolerance. Red circles represent well data.

2.1.1.2 Dynamic conditioning

Parquer et al. (2017, 2018) propose a stochastic method of channelized systems simulation using an algorithm of reverse channel migration. It permits to reconstruct the plausible past channel and abandoned meander locations from the last observations: the recent trajectories (satellite images or seismic data). That is, the simulation starts from the last observed channel path, and then the channel migrates reversely (going back at time) to match previous observations. Besides that, abandoned meanders are ordered chronologically to permit their successive integration into a simulation process.

Model details:

- the simulations are one-dimensional and stochastic;
- the main objectives are to reproduce the channel migration, and to diversify data conditioning;
- firstly, the last observed channel path is digitalized. Then, the three-dimensional migration vector is defined (three components: vertical, lateral, downstream). After that, the correlation trends between channel curvature and its lateral and downstream migration are determined and translated into model in probabilistic form. Finally, the reverse channel migration can be performed, iteratively: digitalized channel paths are represented as parametric objects in software (Piegl and Tiller, 1997), which permits to perform the continuously connected migration images.
- two points at minimum are required between two successive inflexion points to define a half-meander. Inside each half-meander, the directions of reverse downstream and lateral migration are defined according to the geometry of segments connecting the inflexion points;
- conditioning to data is performed through the integration of observed abandoned meanders and cutoffs into the simulation in defined chronological order;
- the next Figure 33 illustrates the reverse migration process:

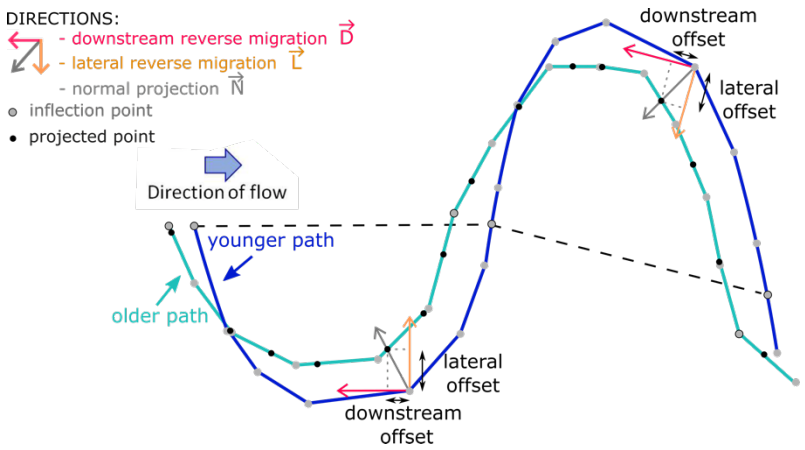

Figure 33. Illustration of reverse migration method. Lateral and downstream reverse migration offsets are deduced by projection of the normal vector on the lateral or downstream one

Chronology of cutoff integration:

- each observed cutoff in a data set can be integrated into simulation – all the observed data is used for conditioning;
- chronology of integration is based on spatial and statistical criteria (distance between the abandoned meander and the current channel path, channel orientation, abandonment probability distribution). Statistical criteria are derived from observations on sedimentary analogues (e.g., the Mississippi river);
- intersections of observations are determined automatically;
- the analysis of the local chronologies is performed before the first step of reverse migration of the main channel;
- the groups of abandoned meanders and the "lonely" cutoffs can be integrated. The groups are also chronologically ordered, through the compilation of the two-by-two relative chronologies observed by human eye;
- this chronology simulation tool is combined with the retro-migration simulations (Figure 34).

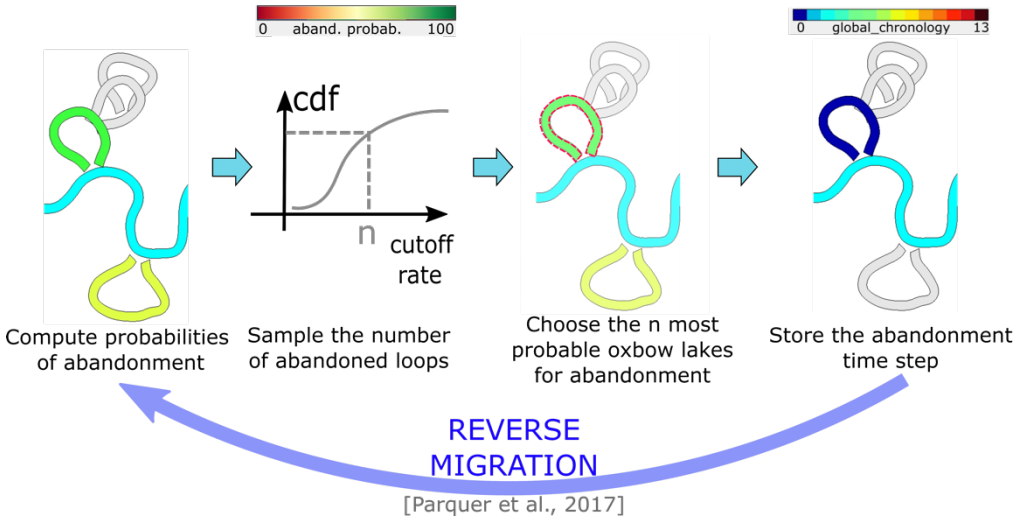

Figure 34. Workflow of abandoned meander draw through probability distribution (image source: Parquer et al., 2017)

2.1.2 2D conditioning

2D conditional simulations are based on the conditioning of centerline but also include the channel width or channel belt. Such method is very useful for a high density of well data or seismic time slices.

Two-dimensional channel conditioning is illustrated in the work of **Wang and al., 2009**. The main principle of this model simulation is tracing the channel through sandy well locations avoiding at the same time the clayey wells. To do that, the random walk approach on graphs of well location is used, in two variants:

- one direction walk model – aims to determine each channel point by the use of a transition probability with a random walk essentially in the main flow direction, for example the N-S;
- two directions walk – simulates different channels that can be oriented in both directions, either N-S or S-N.

In both variants, the channel transition probability through a point is estimated based on two coefficients: one is the correlation coefficient of channel observations (sand presented at wells), the other is the obstacle coefficient of non-channel observations (clay at wells). Random walk approach allows for uncertainty evaluation, by generating many realizations of channel configuration. A widening process is used to determine the channel width (estimation by averaging the space between wells).

The Figure 35 illustrates the results of such simulation. On this figure, the open circles represent the sandy wells (channel observations) and the dots represent clay wells (non-channel observations). Firstly, the one direction random walk is performed (left); then, the two directions random walk deals with the remaining disconnected sand at well locations (right).

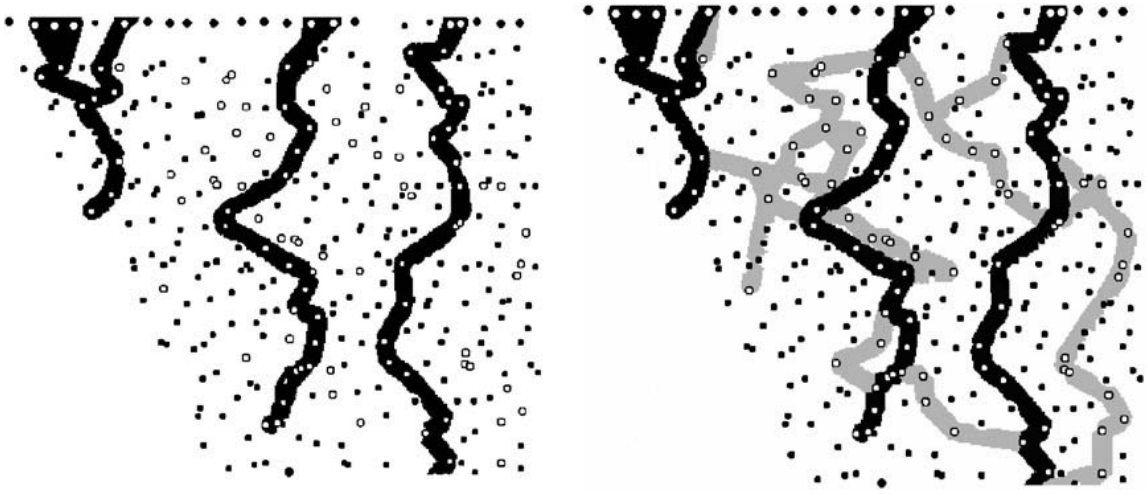

Figure 35. Channels created by one direction walk modeling (black channels, left figure), and by two directions walk modeling (grey channels, right figure) (Wang and al., 2009)

Application of the method on real data showed that simulated channels became more realistic as the number of wells significantly increases – the channel remains linear from one sandy observation to another, and only non-sandy wells aim to increase the channel sinuosity. Only a combination of both data types permits to model the morphologically natural channels.

2.1.3 3D conditioning

2.1.3.1 Geomorphological models

Clevis and al. (2006) present the modeling of landscape evolution (geomorphology) using the Triangulated Irregular Networks (TIN). Such models, due to their adaptive remeshing capability (moving, adding and deleting nodes), have the advantage of representing geological processes that involve a horizontal component, such as faulting and river meandering. However, the accumulation of simulated stratigraphic data is difficult, because it requires 3D subsurface interpolation which may result in a data loss (due to heterogeneity of the subsurface and averaging effects). The authors propose a new algorithm of mapping the changes in the TIN configuration onto static grid, that permits to create a fixed stratigraphic record of TIN surface changes.

TIN generalities:

- this model was created as opposed to the frequently used static rectangular grid, in order to better illustrate changing spatial discretization of the model landscape;
- the nodes representing the surface are connected to each other using Delaunay triangulation. Such models are able to constantly update their landscape representation over geological time by adding, substracting, and/or moving nodes and updating the triangulation accordingly;
- the CHILD software permits to model the meandering channel systems.

Problematic: during the simulation, TIN surface nodes change position according to fixed stratigraphic information. This information is contained in the underlying sedimentary layers: these nodes, representing morphological features (e.g. the channel centerline) can move horizontally relative to already simulated underlying sediments. Such mobility complicates the process of storing/retrieving of stratigraphic information in the resulting simulation.

Method:

- the main idea is to store the stratigraphic information in a fixed subsurface rectangular grid, under the TIN-surface, and successfully map the deposition/erosion events onto this fixed grid,
- in order to minimize the error and information loss, the static grid resolution is defined at least equal or higher than TIN-mesh resolution,
- a new straightforward and fast algorithm is introduced, for communicating and interpolating between a dynamically moving TIN surface and the regular subsurface grid. All changes in elevation due to the shifting meander channel, general erosion and deposition from the TIN landscape are incrementally translated into stratigraphy,
- the meander stratigraphy model is driven by a geologic scenario.

The CHILD software is a model of landscape erosion, sediment sorting and topographic evolution based on TIN-mesh:

- contains modules for stream meandering and stratigraphy,
- the meander module in CHILD uses a process-based approach, in order to operate at geologic time-scales (Lancaster and Bras, 2002; Lancaster, 1998). The time scale is restricted to periods significantly longer than a single storm, to be relevant with sufficiently great topographic evolution, though in the case of rapidly changing landscapes (e.g., gully networks) this can be decades,

- the meander model is based on the concept of 'topographic steering' (Dietrich and Smith, 1983; Smith and McLean, 1984), which goes from the fact that secondary flows over the bed topography translate the erosive high-velocity core in a channel segment laterally. This secondary flow results in transfer of momentum and maximum shear stress towards the outer bank and downstream, causing erosion,
- during the meandering process, the channel centerline nodes are iteratively moved, any obstructing outer bank nodes are deleted, and additional nodes are added behind the former channel position in order to create point bars. The floodplain mesh is continuously updated, its deposition rate decreases exponentially with distance from the channel (Pizzuto, 1987; Howard, 1992, 1996; Mackey and Bridge, 1995). Meander segments that approach one another are able to merge creating cutoffs. The model does not simulate the chute cutoffs or large-scale avulsions.

The next Figure 36 resumes the model features discussed above.

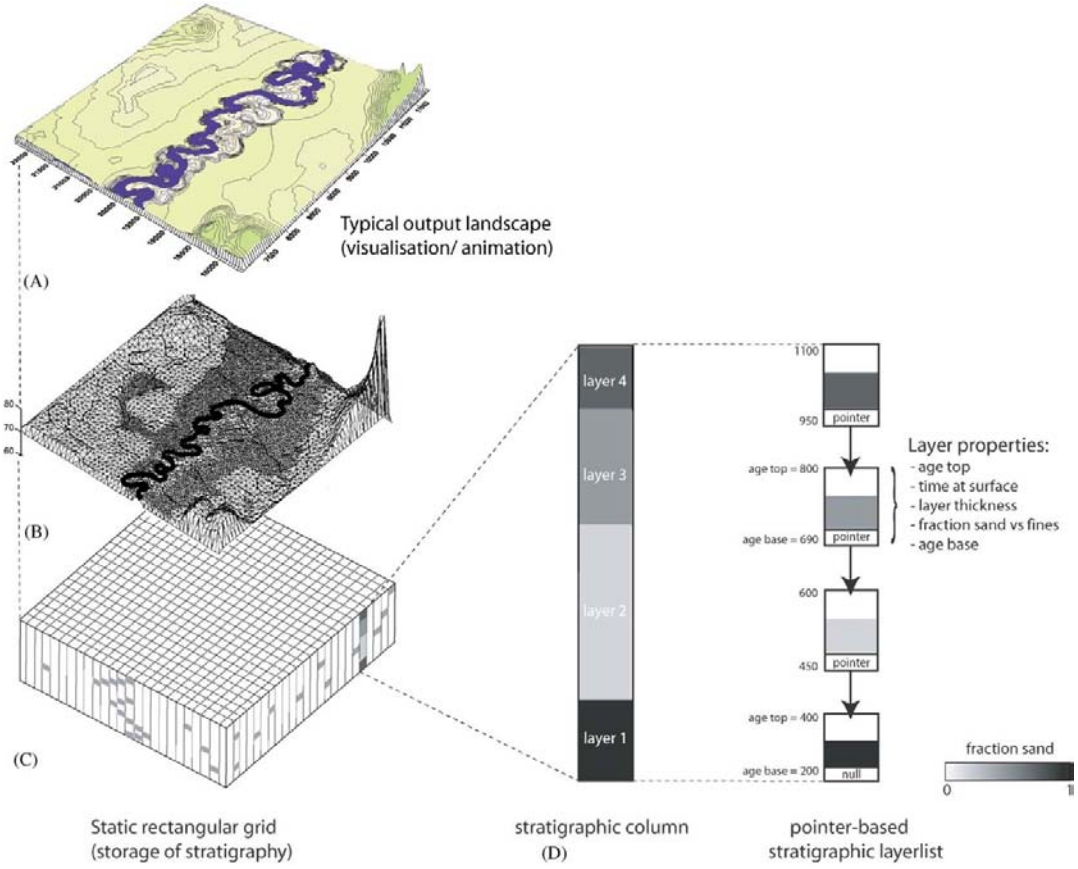

Figure 36. (A) Example of simulation of CHILD meander module. (B) Computational dynamic TIN-mesh used to self-update in result of lateral movement along main channel. (C) Static rectangular grid used for storage of subsurface stratigraphy. (D) Stratigraphic columns are stored as ordered lists of layers coupled to static grid elevations (Oualine, 1997). Layers are informed about age and grain size texture. (Image source: Clevis and al., 2006)

Connection between TIN mobile mesh and static stratigraphic grid:

- at the beginning of a simulation, TIN mesh is created;
- simulations are performed using a time loop during which all surface-process functions are called sequentially. The length of the time steps and the intensity of the associated rainfall (for the floodplain deposition) are randomized using a Poisson probability distribution (Eagleson, 1978);

- the meandering process results in changes in the configuration and elevation of the TIN nodes. These changes are transferred or mapped to the static stratigraphy grid, from several locations within the CHILD main loop;
- after each simulation step, static grid node locations are linked to the closest triangle;
- the new static grid node elevation is the result of remeshing or erosion/deposition. That is, the corresponding static grid node is raised or lowered according to the difference between its old and new elevations, which is defined by linear surface interpolation between the corners of the triangles describing the channel;
- stratigraphic grid module is adapted for two lithofacies. The resulting stratigraphic grid cross-sections are presented on Figure 37.

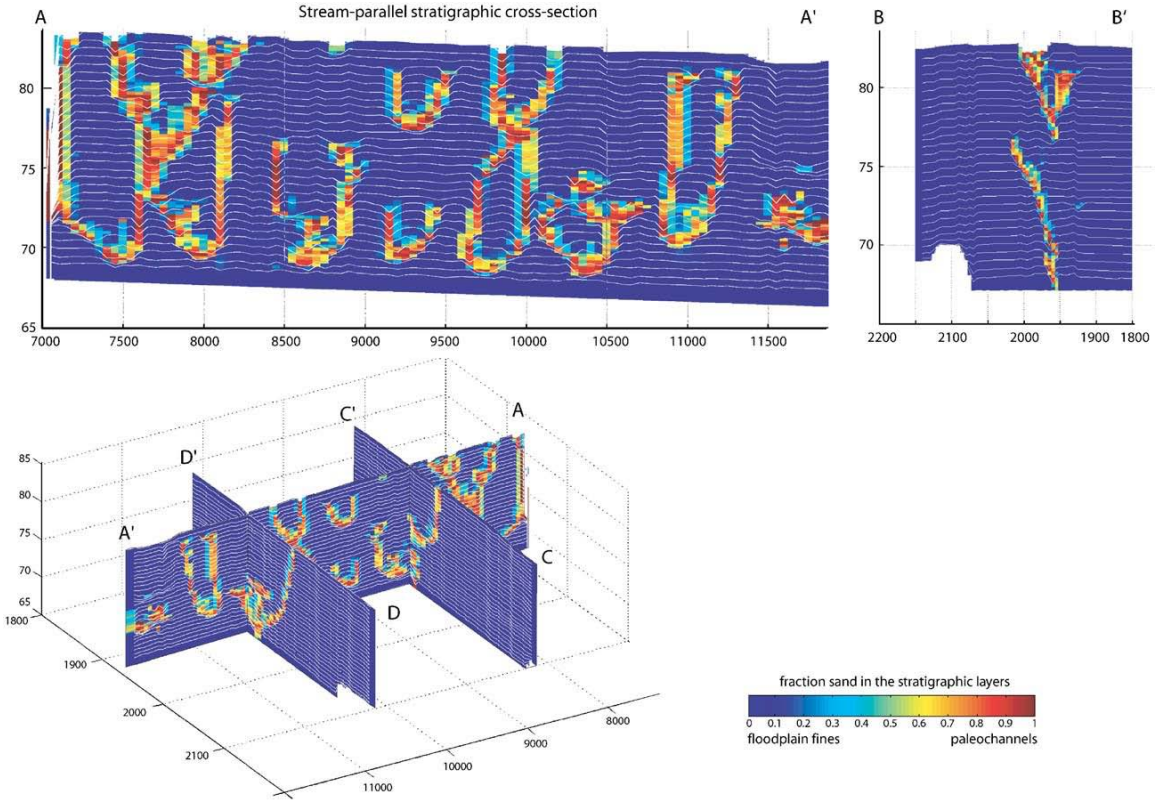

Figure 37. Stratigraphic cross-sections of simulation showing subsurface distribution of paleo-channels (red, sand) and floodplain fines (blue, clay). A-A': longitudinal cross-sections; B-B': transversal cross-sections. Vertical axis represents 500-year time intervals (image source: Clevis and al., 2005)

There is no special conditioning procedure in this method; it was presented as an interesting example of irregular grid used in fluvial channel modeling.

2.1.3.2 Boolean models

Conditioning of Boolean reservoir model is illustrated by **Hauge and al., 2007**. This work presents the object-based model of a fluvial channel with the corresponding conditioning algorithm; the main objective is not only to condition well data correctly, but also to converge in a reasonable time. A method for validating well conditioning algorithms is proposed, to determinate the impact of the conditioning on the models.

In object-based reservoir models, one facies is set as the background facies, and the objects of other facies are added on the top of this one. Here, the background and object facies are clay and sand, respectively. The channel geometry is modeled following the principles:

- Channel is given by a straight line defining the expected channel location and its direction, and four Gaussian fields defining the thickness (VT), width (HW), and vertical and horizontal displacements from the line (VD and HD). Two more 2D Gaussian fields are added, one at the top and one at the bottom of the channel, to take into account the channel slope.
- Between these planes, linear interpolation is used to determine the channel location. The last 2-dimensional Gaussian fields are sampled on finer grids and superimposed on the channel. The resulting channel object is shown on Figure 38.

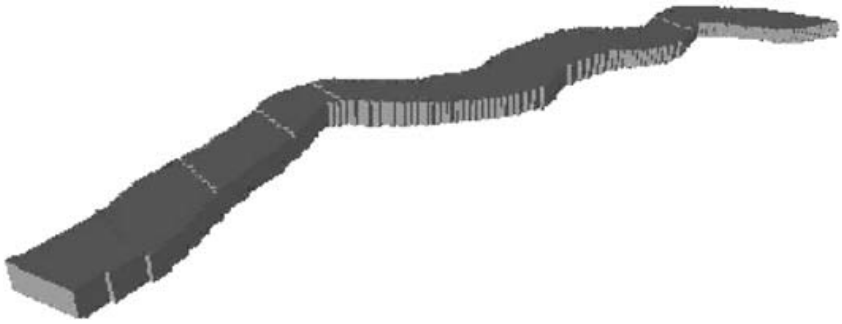

Figure 38. Channel example in object-based model (Hauge and al., 2007)

Metropolis-Hastings (MH) algorithm (Hastings, 1970) is used for conditioning to the well data: the new channel objects are iteratively proposed and then accepted or rejected according to their matching with data, until convergence is reached. A standard MH algorithm is used, with an advanced proposal function heavily influenced by the wells. At each step, either a channel is introduced or removed, or replaced by another one with better parameters.

The test of bias between a conditional and non-conditional realization was performed, with 3 key observators:

- the number of well penetrations of an object (of one Point Bar);
- the mean size of a Point Bar defined as a function of the number of well penetrations (in order to save the flow properties of the reservoir); and
- the global sand distribution comparison in conditional and non-conditional simulations (in order to observe the sand ratio in the wells vicinity).

The method shows good results on the real data. Still, conditional Boolean models remain a difficult computational task because of their long convergence time.

2.1.3.3 Event-based models

Event-based conditional fluvial model is illustrated by the work of **Pyrcz and Deutsch (2005)**. This algorithm may reproduce braided, avulsing, meandering channels and may reproduce realistic geometries and interrelationships of a variety of fluvial reservoir types.

The basic building block of the model is the *streamline* which represents the central axis of a flow event and backbone for architectural elements. Genetically related streamlines may be grouped into *streamline associations* which are interrelated by process (for example, lateral accretion elements within a Point Bar). So, the architectural elements are the streamlines, and its interrelationships are the streamline associations.

The 3D representation of streamlines is modeled as a set of cubic splines. Such splines include the spatial channel characteristics: the channel width, local curvature, relative thalweg location and local azimuth are calculated at the control nodes, and then splines are fit as with the location parameters. Streamline associations are the groupings of interrelated 3D splines.

Several operators are used in modeling:

- The *initialization* operator is applied to generate an initial streamline or to represent channel avulsion proximal of the model area.
- The *avulsion* operator creates a copy of a specific channel streamline, selects a location along the streamline, and generates a new downstream channel segment with same streamline sinuosity and the same geometric parameter distributions.
- *Aggradation* is represented by an incremental increase in the elevation of a streamline (to add a specified constant value to the elevation parameter for all control nodes).
- The streamline migration operator is based on the bank retreat model. Key differences from Sun et al. (1996):
    - standardization of migration steps,
    - integration of 3-D splines for location and properties,
    - application of various architectural elements.

  The meander migration along the streamline is standardized such that the maximum migration matches a user specified value. This removes the parameters such as friction coefficient, scour factor and average flow rate, since only the relative near bank velocity along the streamline is significant (they are replaced by the maximum spacing of accretion surfaces).

The fluvial architectural elements that are modeled (Figure 39) are channel fill (CH), lateral accretion (LA), levee (LV), crevasse splay (CS), abandoned channel fill (FF(CH)) and overbank fines (FF).

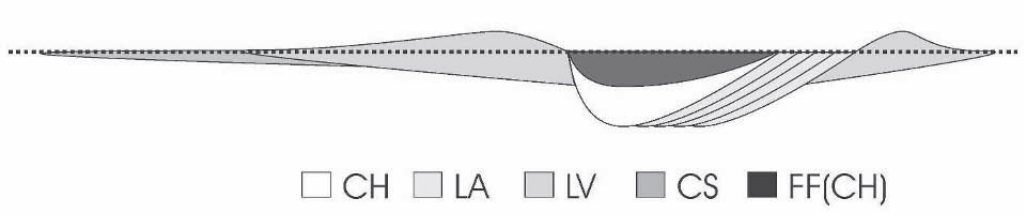

Figure 39. Visual representation of streamline association cross-section (Pyrcz and Deutsch, 2005)

The algorithm is supplied with areal and vertical trends that correspond to seismic data conditioning, as well as distributions of geometric parameters, probabilities of events and architectural elements. The following Figure 40 illustrates an example of the aerial trends in channel density:

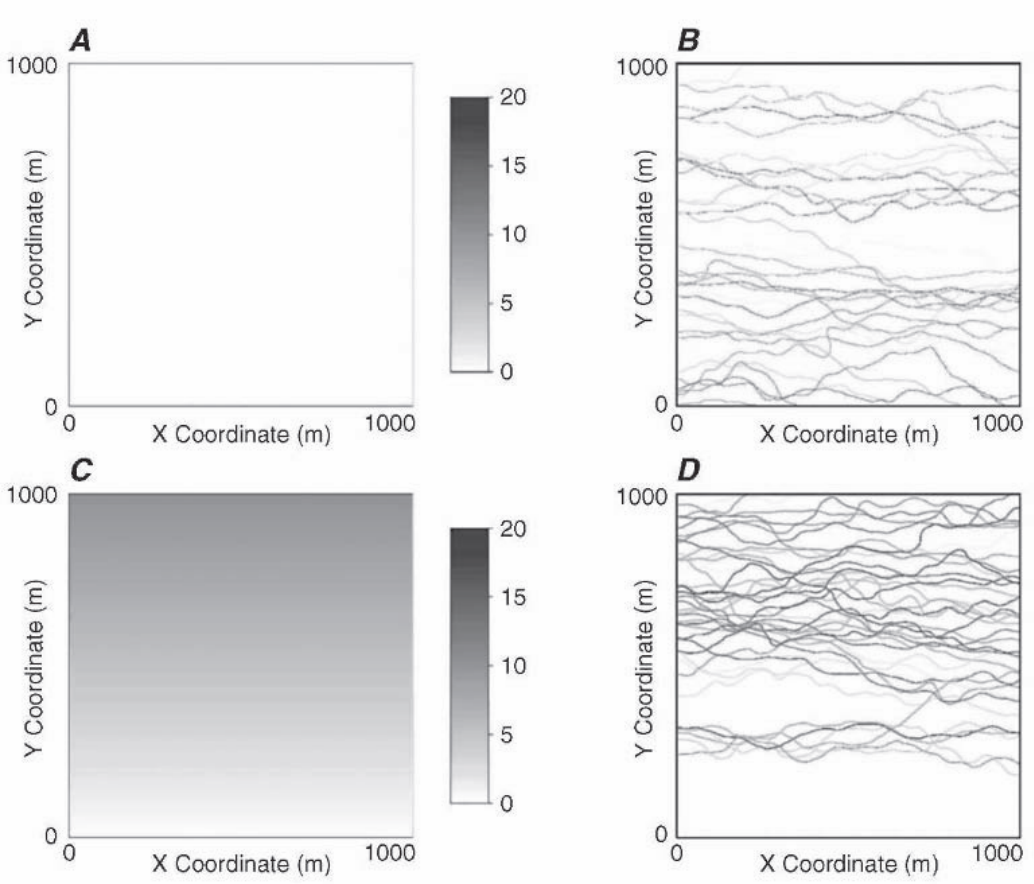

Figure 40. Event-based model simulation conditioned by areal trends (Pyrcz and Deutsch, 2005). (A) – empty areal trend applied to (B) – non-conditional simulation. (C) – areal trend used in conditioning and (D) – conditional simulation

Vertical trends can also be reproduced (levels with a different N_G, for example). They may be honored by constraining the aggradation rate.

In this example, conditioning to the well data is an iterative procedure. It may be described by following steps:

- construct the prior event-based model conditioned by all available seismic information;
- interpret the well data and define all available channel elements (sand);
- update the prior streamline associations to honor channelized well data elements;
- correct for unwarranted channel data intercepts.

Interpretation of the well data includes the location for each well and a list of channel element intervals by their base and original top.

Updating streamline associations to honor the well data is a modification of its position (horizontal and vertical). Entire streamline associations are corrected, to preserve the intern relationships. The correction procedure is illustrated on Figure 41. Channel element intervals are sequentially corrected, according to well data observation; if there is only one well (C on Figure 41A), the correction of channel position is constant for whole streamline association. Figure 41C shows the displacement of channel along OY. If there are several wells, for each one the replacement is performed separately; Figure 41B represents a channel conditioned to the well P, that needs to be conditioned to the well C. In this case, the displacement of channel along OY is shown on Figure 41D.

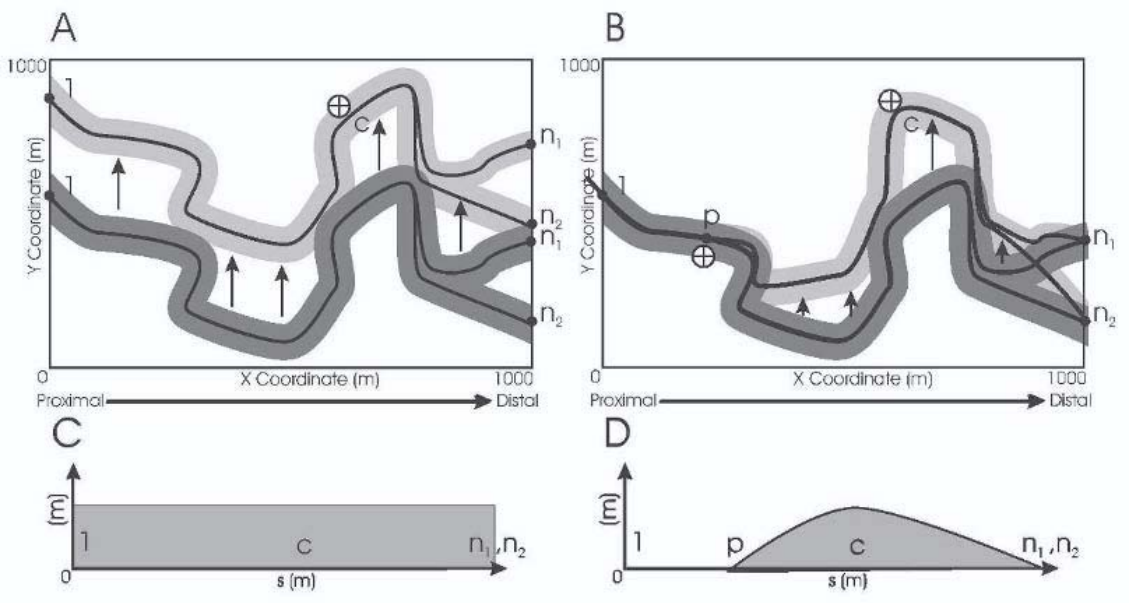

Figure 41. Conditioning to well data in event-based model (Pyrcz and Deutsch, 2005)

The streamline association is then modified until all well data is honored.

The results of the conditioning procedure are presented on Figure 42. A single well with two channel intervals is used for conditioning. The Figure 42A and B illustrate the cross-sections of prior and conditioned models respectively; Figure 42C and D show aerial view.

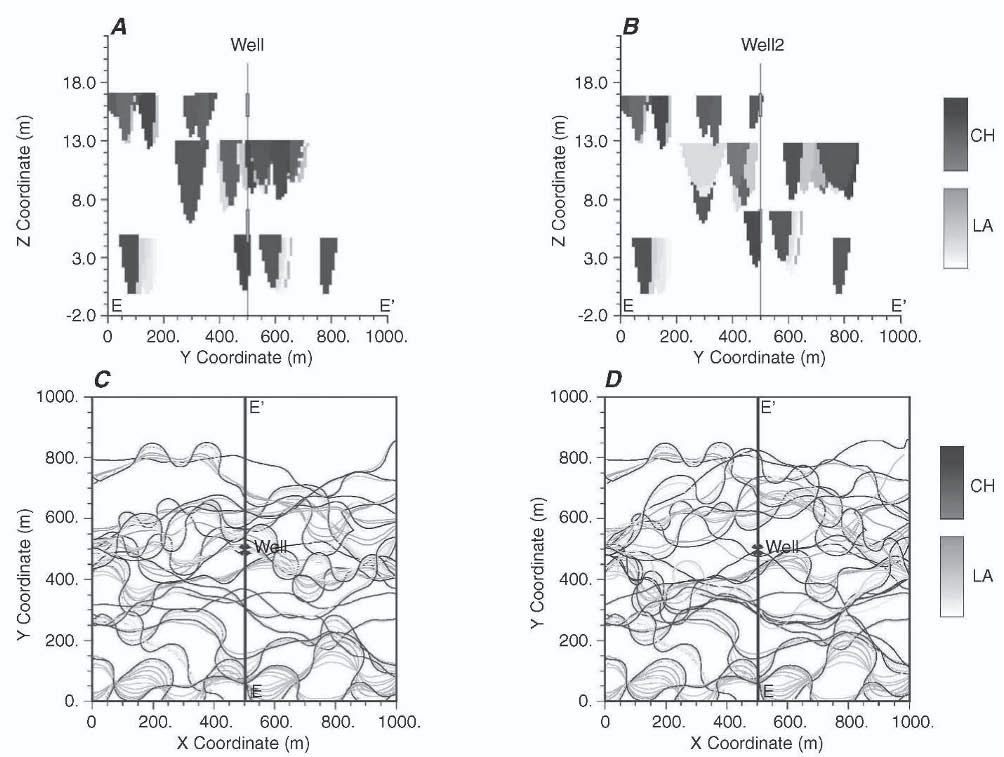

Figure 42. Non-conditional (A, C) and conditional (B, D) event-based simulations (Pyrcz and Deutsch, 2005)

2.1.4 Conclusion

Several methods dedicated to specific issues of fluvial models conditioning were presented above. Various types of conditioning data were noted: wells (Oliver, 2002; Hauge et al., 2007; Pyrcz and Deutsch, 2005; Mariethoz et al., 2014); seismic data (Pyrcz and Deutsch, 2005); ordered past channel states (cutoffs and abandoned channel belts), used in reverse migration simulations (Parquer and al., 2017).

The general idea of conditioning to well data is to move the channel to the well location if the data is sand, and to move it away if the data is overbank sediments (e.g., clay). Multiple-well conditioning can be performed.

Presented fluvial models use a priori choice of fluvial parameters, derived either as initial channel state (digitalized from maps or satellite images), or default simulation parameters.

In order to estimate the influence of conditioning procedure, non-conditional and conditional simulations are compared by their convergence time and spatial sand distribution (Hauge et al., 2007).

2.2 Conditioning in Flumy: principles

The Flumy simulations can be non-conditional or conditional. Even non-conditional simulations, without the dynamic integration of wells into the simulation process, may use the well data analysis to infer the simulation parameters (N_G, channel dimensions, sandbodies extension) (Cojan et al., 2012, 2013). Conditional simulations include not only parameters coherent with wells, but also the dynamic reproduction of known data at the well locations (no trial/error).

2.2.1 From well data to Flumy lithofacies

In a conditional simulation, the first key element is how the well data is interpreted and described to be used in Flumy.

Well data can be represented in various forms, with different degrees of details, from two facies binary wells (sand/no-sand) to detailed well logs (interpreted or not). The next Figure 43 represents three possible data types, derived from one well:

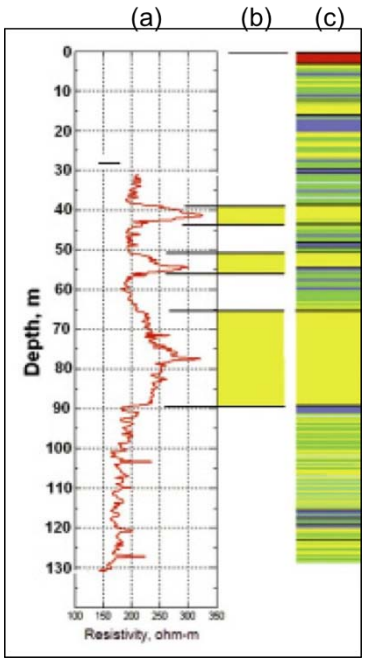

Figure 43. An example of well data. (a) – not interpreted resistivity log; (b) –large sandbodies from large fluctuations of well logging (in yellow); (c) – well-interpreted data log, including smaller sand intervals (yellow), clay (green) and shale (blue). Data source: Wong et al., 2009

In Flumy, well data are loaded from ASCII files (Flumy wells or LAS format); multi-well conditioning is possible. Deviated or vertical wells can be used for conditional simulations. The smallest vertical discretization step of data is 0.01m. All data types (Figure 43) can be used in Flumy conditional simulations; to do that, the input data should be converted into Flumy lithofacies:

- already interpreted well data (discretized data) with different level of discretization and facies variability: a user has the possibility to manually define the relation between data and simulation lithofacies, using an automatic tool provided by Flumy (Figure 44a)
- not interpreted well data logs can also be used in Flumy, by defining simulation facies thresholds (intervals of data values for each Flumy facies, Figure 44b).

(a)

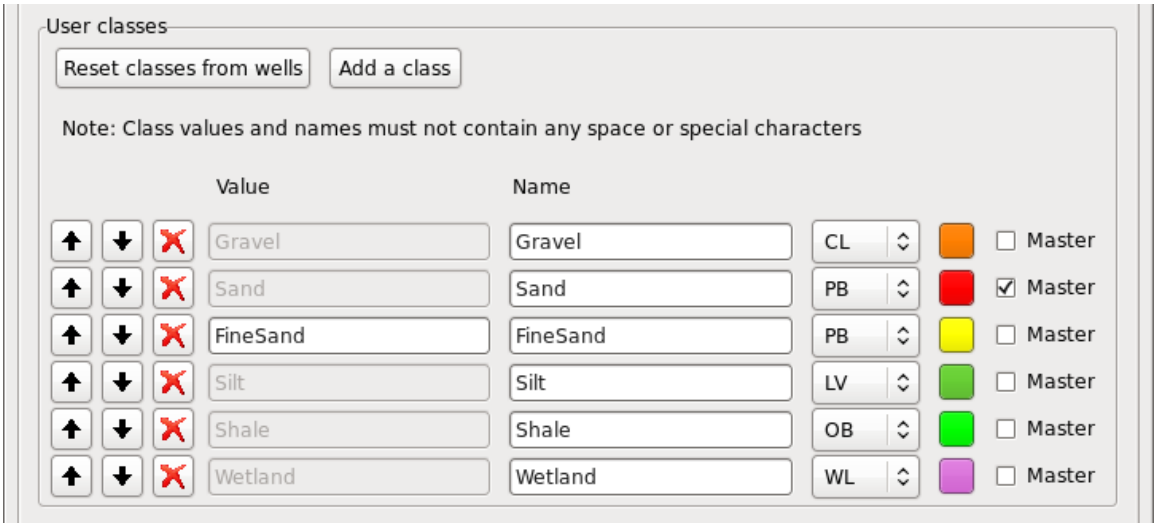

(b)

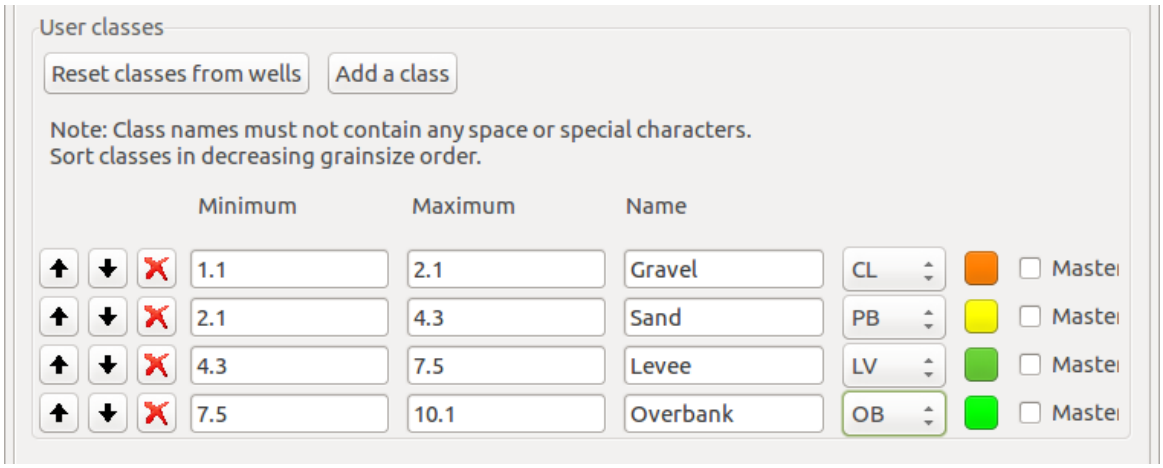

Figure 44. Lithofacies classes definition tool for converting (a) discrete or (b) continous well log data into Flumy facies (here: CL, PB, LV, etc.).

Finally, each well bit is described as a stratigraphic vertical pile of “bricks” of given Flumy facies and thickness.

The wells are loaded before the first iteration of the simulation. As the deposits are simulated from bottom to top during simulation, the “bricks” are ordered in the same manner (Figure 45).

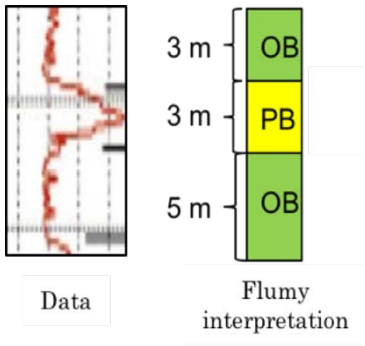

Figure 45. Well data interpretation in Flumy

When running the simulation, wells can be visualized on cross-sections (Figure 46). Each well is visualized within the pillar which contains well 2D coordinates (exact well location is kept internally;

on visualization a well is located at the center of the corresponding cell), one well by pillar. This pillar is represented by two vertical columns; the left one shows the input interpreted data and is shown during the whole simulation time. The right column is the simulated data at the center of the cell. This column is filled during the simulation with the new deposits (Figure 46, right – an Up Arrow indicates the filling of simulated data column during a simulation). Such a representation permits to compare the well data with the simulation results at any moment of the simulation.

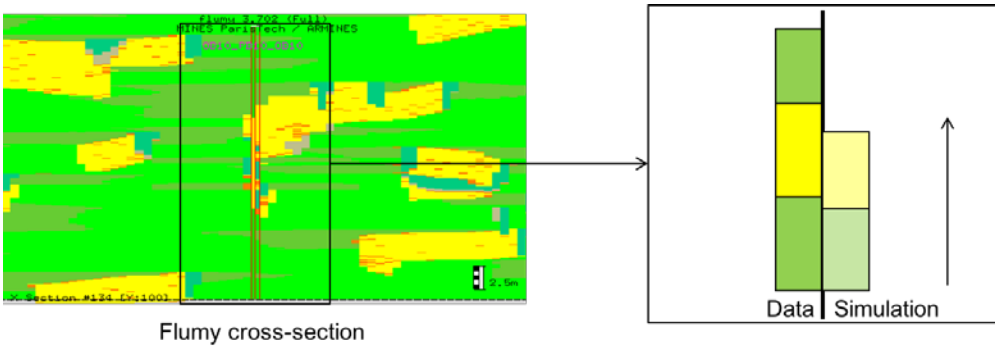

Figure 46. Flumy well view during conditioning simulations: left – Flumy cross-section, right – schematic well illustration

2.2.2 Classifications of lithofacies for conditioning

The conditioning process is based on two facies classifications:

- the first one is based on the channel location relatively to the well location, in order to deposit the desired Flumy facies at the well;
- the second one is based on the Flumy facies potential to be replaced during conditioning.

In the first classification, the 11 different types of Flumy lithofacies are distributed in 3 main classes each one corresponding in a specific depositional context plus one neutral class. This simplifies the conditioning procedure by acting on the channel location according to the following scenarios:

- **Channelized facies**: Point Bar (PB), Channel Lag (CL), Sand Plug (SP) and Mud Plug (MP)
  These facies can be deposited only when the channel passes through the well site.
- **Levee facies**: Crevasse Splay I (CSI), Crevasse Splay II (CSII), Crevasse Channel (CCh) and Levee (LV)
  In order to deposit these facies at the well location, the channel should pass near the well, within the levee zone (default value is equal to 6 times the channel width).
- **Fine-grained facies**: Overbank Alluvium (OB), Draping (DR) and Wetland Deposit (WL)
  This class of facies is deposited in the floodplain, further away from the levees, the channel should be at least 6 times the channel width away from the well location.
- **Neutral facies**: Undefined (UDF)
  This class is introduced to take into account the undefined intervals in the well data. It has no influence on conditioning

The second classification concerns more the deposit validation procedure:

- **"Erodable" facies**: Point Bar (PB), Channel Lag (CL), Sand Plug (SP) and Mud Plug (MP)
  These facies are the channelized facies. To honor the well data, they can be initially deposited at well or replace some previously deposited facies during the migration or the avulsions (erosion, then deposition). They are replacement facies and even when their deposition matches with well data, they can be eroded and deposited again. This is why they are qualified as "Erodable" facies in the conditioning process.
- **"Not-to-be-eroded" facies**: Overbank Alluvium (OB), Wetland Deposit (WL), Crevasse Splay I (CSI), Crevasse Splay II (CSII), Crevasse Channel (CCh), Draping (DR) and Levee (LV)
  These facies correspond to the non-channelized facies (levee and fine-grained facies), deposited during crevasse splays maturation, marine incursion or overbank sedimentation. These facies are not replacement facies. To honor such well data facies, and because there is no trial/error in Flumy, they need to be the first sediment deposited at such a well location, and are "not-to-be-eroded" later.
- **Neutral facies**: Undefined (UDF) – no influence on conditioning.

So, the "erodable" facies are channelized facies, and "not-to-be-eroded" – overbank deposits (levee and clay) are non-channelized facies.

The next Table 4 establishes the relation between the two different lithofacies classifications in Flumy and summarizes all the information above.

First classification	Position of channel relatively to the well	Lithofacies	Second classification	Possibility of replacement
Channelized Facies	Channel at the well	Point Bar (PB) Channel Lag (CL) Sand Plug (SP) Mud Plug (MP)	Erodable Facies	• Deposits can be eroded and redeposited; • Deposits can replace other facies;
Levee Facies	Channel is near the well (less than 6*channel width)	Crevasse Splay I (CSI) Crevasse Splay II (CSII) Crevasse Channel (CC) Levee (LV)	Not-to-be-eroded Facies	• Deposits can be replaced (e.g. to honor channelized facies), but can't replace; • Data should be honored at the moment of the deposition;
Fine-grained Facies	Channel is far from the well (more than 6*channel width)	Overbank Alluvium (OB) Wetland Deposit (WL)		

Table 4. Relation between the two lithofacies classifications in Flumy

These classes will be widely used in the following techniques and examples. It should also be noted that Mud Plug is the only fine-grained facies which belongs to Channelized Facies class for a conditioning; this issue will be discussed in Chapter 3.2.1.2.

2.2.3 Treatment of thin lithofacies for conditioning

There exist two particular cases of well data interpretation in Flumy. The first one (Figure 47) concerns the channelized facies intervals that are too small in relation to the channel depth. If such a small channelized facies interval is situated between two non-channelized bricks, it is interpreted as a less attractive facies like the Crevasse Splay data (because it would be difficult to deposit a sand thickness smaller than the channel's depth without destroying the OB intervals below and above):

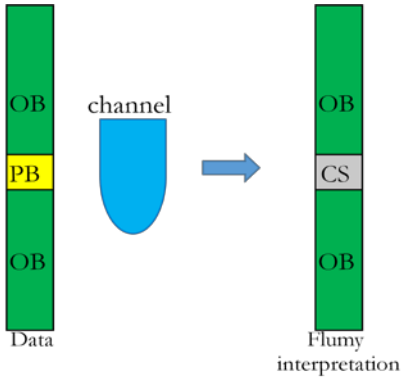

Figure 47. The first case of specific data interpretation in Flumy: a small sand interval situated between two clay bricks is interpreted as Crevasse Splay

Besides that, in the case of an non-sandy interval smaller than 0.1 m (Closure Limit parameter, default value) between two sandy bricks, Flumy replaces it by a small Undefined (UDF) data brick which has no influence on conditioning. Indeed, it's better to ignore too small clay facies than would interrupt the PB honoring algorithm:

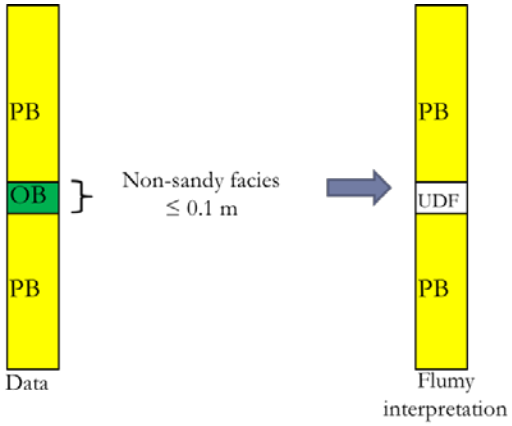

Figure 48. The second case of specific data interpretation in Flumy: a small non-sandy interval between two sandy facies is interpreted as Undefined facies

2.2.4 Concept of Active Level and Active Brick

The aim of the conditioning process is to ensure, if possible, that the sediments that are deposited along the wells when the simulation progresses, match the well data. The validation of sediments deposited at well location is an important part of the conditioning, because of no trial/error in dynamic conditioning procedure. A sediment deposited at a well is validated when it matches the well data. When it does not match the well data, it can be replaced by another sediment, which may itself honor the well data. Sometimes there will be no possibility to honor the well data, and while the deposited

facies does not match the well data, it is however validated. So a sediment deposited at a well location is validated if it matches the well data, or if there is no possibility to match the data. The validation is based on an algorithm that combines facies classification, well description, and the use of two concepts: Active Brick (AB) and Active Level (AL):

- AL is a vertical elevation inside the well, under which all the deposits were considered and validated. During the simulation this indicator varies from well bottom to top, each time the considered new deposit matches the data (AL is lifted up until the top of the new deposit). AL is also updated and new deposits validated when there is no possibility to improve the matching results. AL is never far from the current simulated topography elevation at well location.
- AB is the data brick in which AL is located. If AL is located exactly between two data bricks, the AB is the one above ("looking forward" technique).

The Figure 49 illustrates the concepts presented above:

- First step: AL is in the central of the PB data brick, so AB is channelized facies. All simulated deposits are validated. Now we are waiting for new deposits at well location.
- Second step: New sediments are deposited at the well location: the channel is far from the well, so only clay facies (OB) is deposited. This new deposit is considered and not validated since there is still a possibility to replace it by PB and match the data. So, AL is not updated.
- Third step: The channel passes through the well and replaces non-validated OB deposit by some PB. This new deposit is considered, compared to the well data and validated as it matches the data. AL is updated to the top of the last validated deposit, AB is also switched.

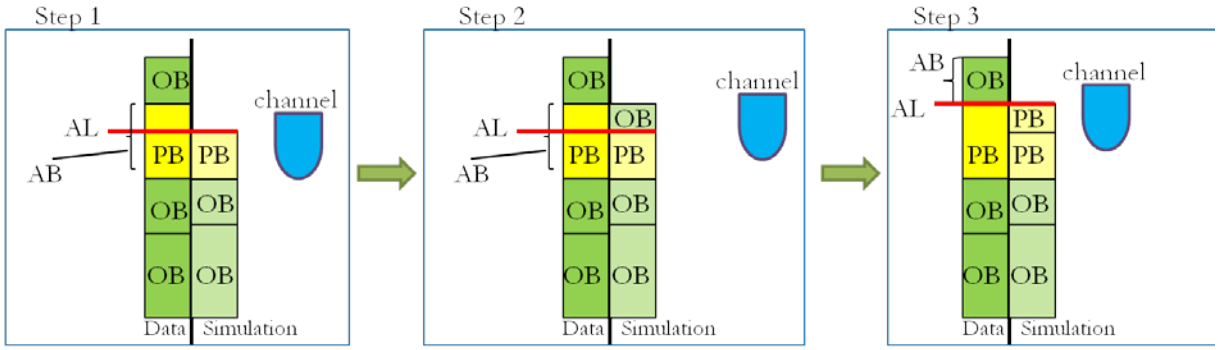

Figure 49. Example of Active Level and Active brick update

In all three steps above, the typical well representation in Flumy is used: on the left – well data, on the right – simulation result.

Now, as the basic concepts of well reproduction, data interpretation and validation process in Flumy have been introduced, the last important thing to present is the principles of Flumy processes adaptation.

2.2.5 Adaptation of migration

Migration of channel is corrected according to the facies class of the Active Brick (coming from the first classification: channelized, levee or fine-grained facies). The main principle is to modify the channel migration rate according to the well facies class (Cojan et al., 2005):

- Channelized facies – channel attraction,
- Levee facies – channel limited attraction,
- Fine-grained facies – channel repulsion.

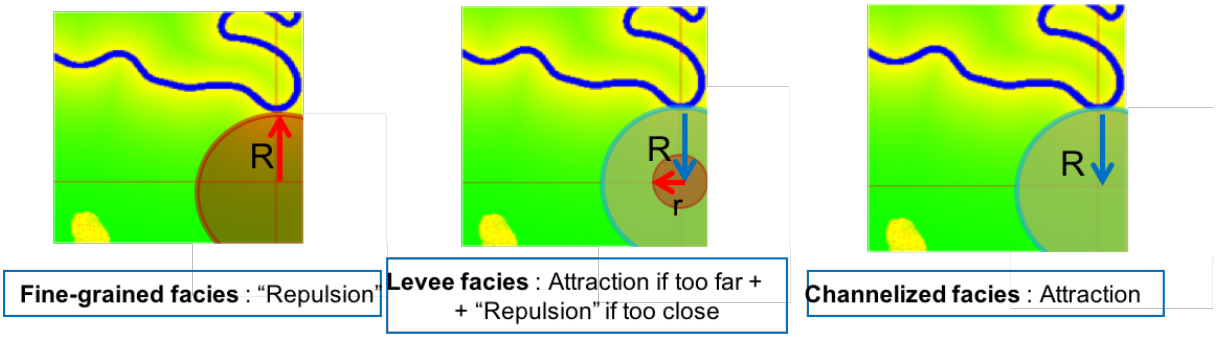

Figure 50. Main principles of migration adaptation in conditioning (R and r are distance parameters)

In the case of **fine-grained facies AB** the channel is not allowed to approach the well, so only floodplain sediments are deposited at the well. In the case of **levee facies AB** the channel is attracted to the well location if it is too far, but still repulsed from the well if it risks passing through the well: the well location should be in the zone of levee deposition. Note that the channel is not really "repulsed". The migration is slowed or stopped. The channel never migrates backward. Finally, in the case of **channelized facies AB** the channel is attracted directly to the well, by increasing the migration velocity in the well direction; so the channelized sediments are deposited at the well location.

2.2.6 Adaptation of avulsions

The new channel path following an avulsion also depends on the facies class of the Active Brick. The objective is to toss the new channel path in the "appropriate" areas of the simulation domain according to the lithofacies class of AB. To do that, before each local or regional avulsion a virtual topography ("pseudo topography") of the simulation domain is created according to the AB facies class (Figure 51):

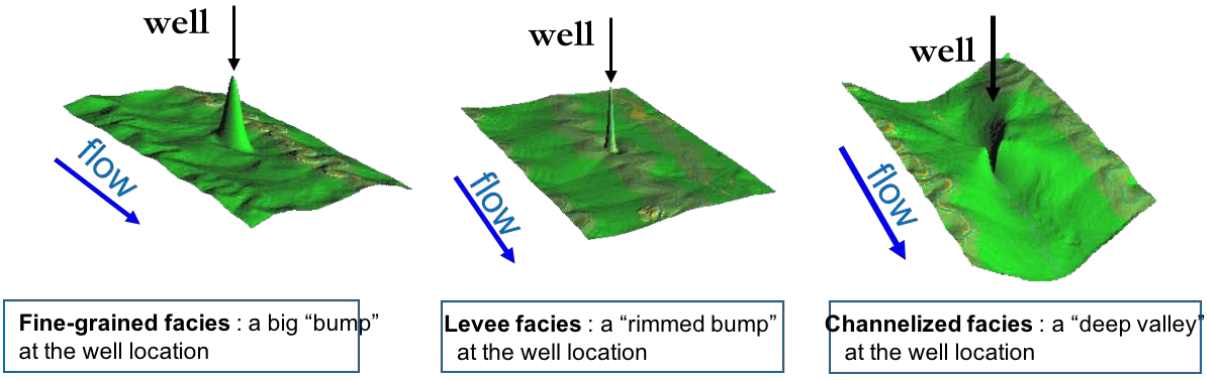

Figure 51. Main principles of avulsion adaptation in conditioning

- In the case of **fine grained facies AB** a big “bump” is created at the well location: so that the new channel path is tossed far from the well (to avoid the levee and channelized deposits at the well).
- If **AB is levee facies**, a “rimmed bump” is formed at the well location: a new channel path will be tossed close to the well, but not too much (zone of levee deposition).
- In the case of **channelized AB**, a “valley” is formed around the well, to attract the new path directly to the well location.

In the case of several wells, the “pseudo topography” corrections for each well are combined.

The next paragraph contains the detailed explications of the three main conditioning procedures: Updating of AL, Migration adaptation and Avulsions adaptation. These are the initial versions of the conditioning dynamic algorithm (before the start of my PhD).

2.3 Conditioning in Flumy: initial algorithms

The conditioning procedures presented in details in this section are functions called at different moments during the program run:

1) Update of the AL in each conditioning well: this function is called each time the topography is changed in the grid cell where a well is located
2) Adaptation of the migration process: this function is called at each iteration of Flumy simulation, before the migration of the channel centerline, in order to calculate the velocity correction due to the influence of the wells (repulsion or attraction)
3) Adaptation of the avulsion process: this function is called just before every local or regional avulsion, in order to calculate the correction to be applied to the real topography in order to create the "pseudo topography".

2.3.1 Update Active Level

The objective is to validate the last deposits and update AL in each well. The list of the internal variable used (each one is calculated at the well location) is the following:

z – floodplain elevation **before** the last deposits (current topography)
th – thickness of the last deposit
wd – water depth in the well (if the channel is inside the well)
z_dep – elevation above which some remaining part of the new deposit must be validated (equal to z at the beginning, then increase while validating new deposits).
zfp = *z* + *th* **–** floodplain elevation **after** the last deposit (new topography)
top_ab – top elevation of the active brick
z_min – the minimal elevation above which existing deposits can be eroded and replaced by new deposits. AL is never lower than *z_min*.

Main algorithm principles to be noted:

- only upwards updates of AL are performed in the updating algorithm. AL can decrease only when the channel passes through the well location. In this case, the AL is set to the channel bottom elevation, in order to consider the erosion of sediments;
- the algorithm can be subdivided into 3 cases, according to the deposits elevation related to AL:
    - New deposit is partially below AL,
    - New deposit is above AL,
    - New deposit bottom elevation is quasi equal to AL (very small gap between *z_dep* and AL).

1) Lower part (base) of deposit is below AL (***z_dep*** < **AL**, cases V and W)

The first variable needed to be introduced is *z_dep*: the bottom elevation of the new deposit. Initially, *z_dep* corresponds to the floodplain elevation at the well before the new deposit.

Case V (Figure 52): deposits are entirely below AL. It's an extreme case that can only happen after a manual change of simulation topography. In this case the AL is not modified:

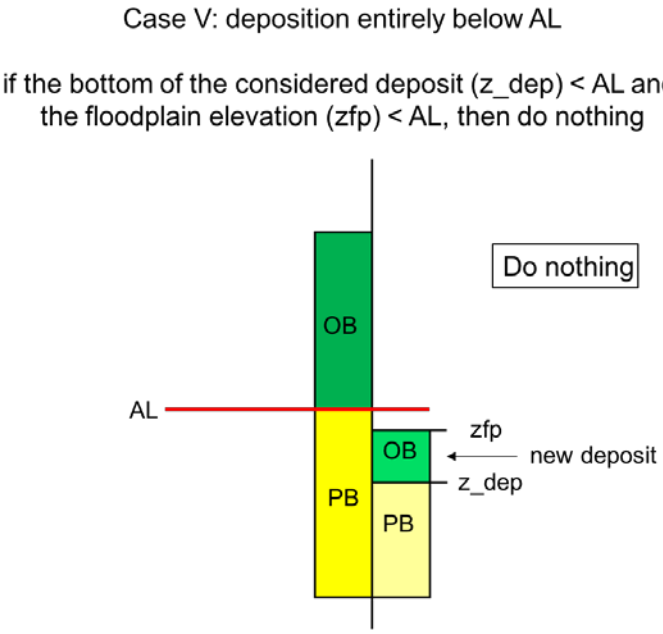

Figure 52. The scheme of case V (update AL algorithm)

Case W (Figure 53): after deposition a floodplain elevation is higher than AL. In this case only the deposited part above AL (and below floodplain elevation) will be considered – the lower part of the deposit is validated:

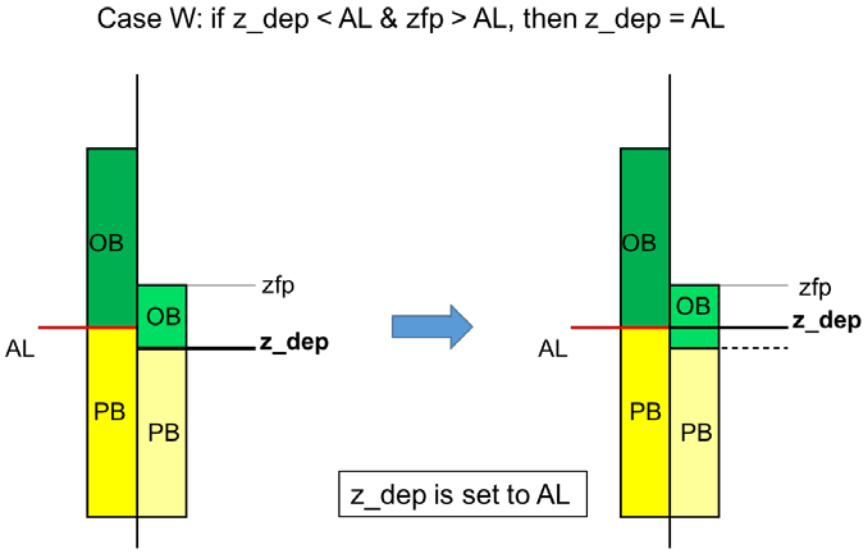

Figure 53. The scheme of case W (update AL algorithm)

2) Deposits above Active Level (cases X and Y)

In this case, another important variable is considered, *z_min* – the minimal vertical elevation above which the sediments can be redeposited due to erosion (for example, a deposited OB that can be replaced by "erodable" facies). In other words, all the deposits already below *z_min* are considered honored (successfully or not) and should be validated. This elevation can be calculated exactly as following:

$$z\_min = zfp + wd - (0.8 * H_{max}).$$

Case X (Figure 54): if the Active Level is lower than *z_min*, it needs to be set up to *z_min* by validating data up to *z_min*. (*Note:* if present *top_ab* is located in [AL; *z_min*] interval, the deposits are validated up to *top_ab*, and, only after, new deposits are validated up to *z_min* – to not skip the change of AB)

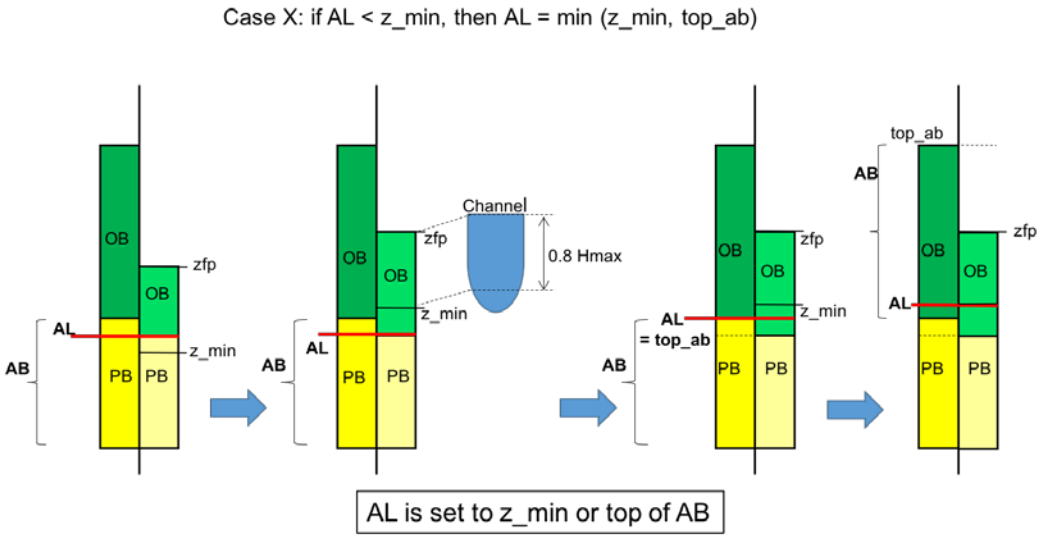

Figure 54. The scheme of case X (update AL algorithm)

Case Y (Figure 55): after data lower than *z_min* have been validated, next data upwards is to be validated, as long as the AB is a "not-to-be-eroded facies" (OB).

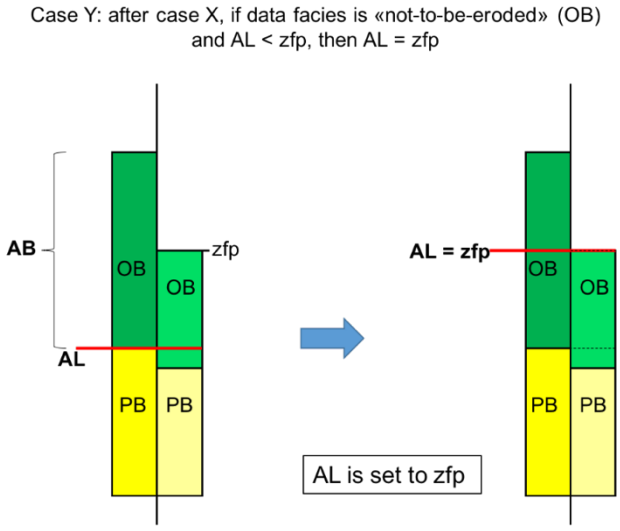

Figure 55. The scheme of case Y (update AL algorithm)

3) Deposits are on Active Level ($|z\_dep - AL| < \varepsilon$, cases Z and ZT)

Case Z (Figure 56): Active Level is updated upwards while deposits either match data facies, or are "not-to-be-eroded" (OB).

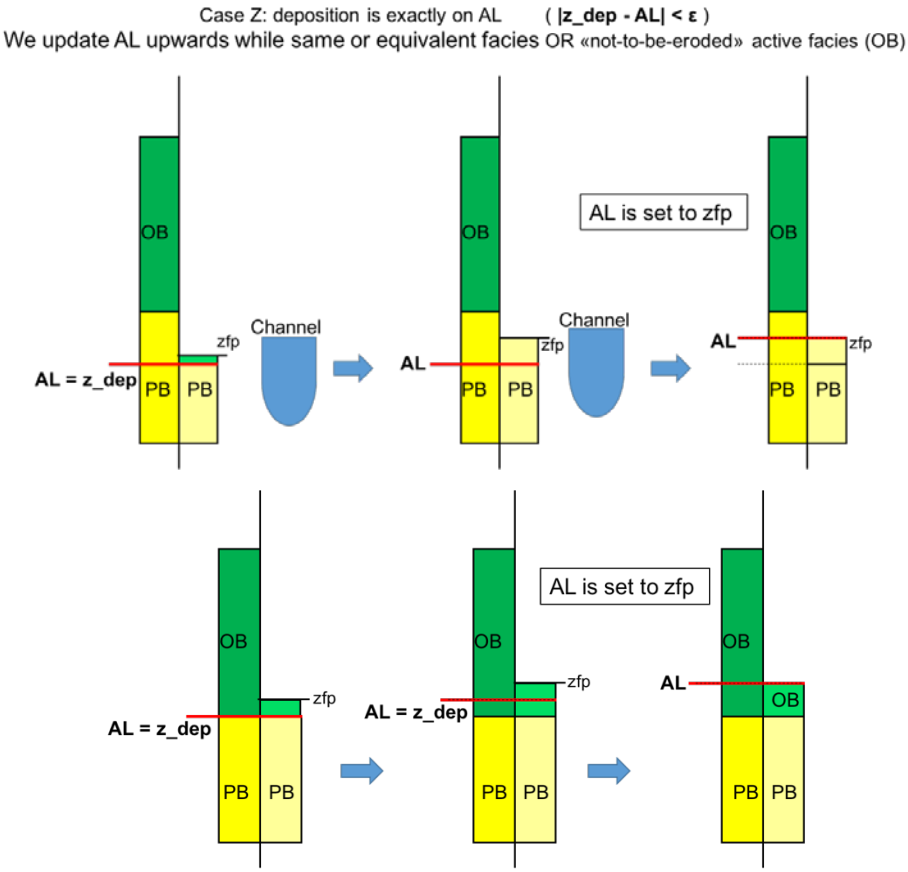

Figure 56. The scheme of case Z (update AL algorithm)

Case ZT (Figure 57): when the Active Brick is close to the final validation (it means that the distance between the AL and the top of AB is less than a tolerance) – we consider AB validated and go further. This tolerance is defined internally (in the source code) to 0.1 m:

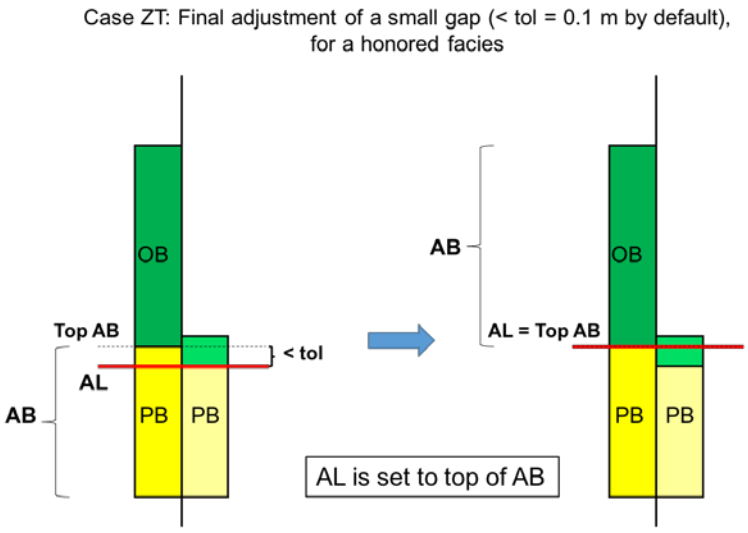

Figure 57. The scheme of case ZT (update AL algorithm)

2.3.2 Adaptation of migration

The function responsible for the correction of migration due to the well influence, aims at changing the velocity of the channel migration according to the lithofacies nature needed to be deposited at the well location. The migration velocity may be increased (in the case of Channelized Facies at the well) or decreased, if the channel is not allowed to go to the well location (Levee and Clay Facies at the well). Correction of migration velocity is performed through the change of the local erodibility values, applied to the channel points closest to the well. This function is called at each iteration before the migration of the channel centerline and uses already updated AL and AB values (previous section).

Three important steps of the algorithm can be distinguished:

1. Identification of the **closest upstream** channel point to the well**,** according to the Von Mises distance formula,
2. Computation of the **multiplicative** factor for correcting the erodibility at the selected channel point,
3. **Extension** of the correction to the points of the same channel meander – the bend between the two inflexion points (where the velocity perturbation is null).

2.3.2.1 Brief algorithm presentation

Step 1. Choice of the closest channel point

In order to preserve as much as possible the already existing Flumy channel migration process, the closest channel point is chosen at the meander which is already moving towards the well. The Von Mises distance formula (Von Mises, 1919, detailed in Mardia and Jupp, 2000) is used to compute the distances between the well and the channel points, because it is non-linear and "favors" the points closest to the well in the flow direction:

$$d^2 = x^2 + y^2;$$

$$\text{Von Mises distance} = \frac{d}{\exp\left(-\frac{x}{d}\right)},$$

where d – the distance between the channel point and the well,

x and y – projections of d on the Ox (or flow direction) and Oy orthogonal axis respectively (Figure 58):

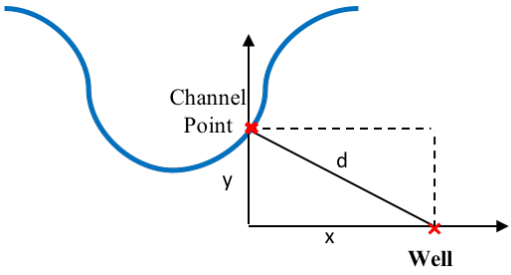

Figure 58. Scheme giving the elements for the computation of Von Mises distance

After calculation of the Von Mises distances between the well location and all the channel points, the smallest distance will indicate the closest channel point of the meander supposed to migrate in the well direction. This channel point is chosen for the following steps of the algorithm.

Example (Figure 59). A graph of the points which are located at the same Von Mises distance from the well, combined with the channel schematic representation. The well is located at origin:

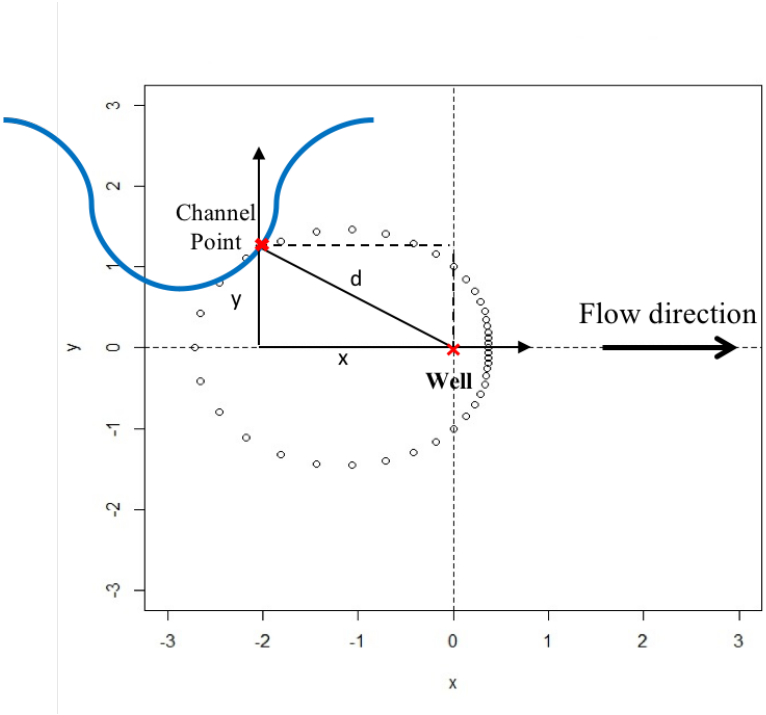

Figure 59. Example of points located at the same Von Mises distance from the well (the Ox axis represents the flow direction)

Step 2. Computation of the multiplicative erodibility correction at the closest channel point

When the closest channel point has been chosen, the **multiplicative** factor is computed, in order to correct the erodibility at the channel point:

1) 1, if the current Active Brick is neutral (e.g. UDF facies),
2) *repulsion_factor*, to reduce migration (a value between 0 and 1), or
3) *attraction_factor*, to favour migration (a value between 1 and 2).

The *repulsion_factor* and *attraction_factor* general formulas are:

$$\text{repulsion\_factor}(radius, lim1, lim2) = \begin{cases} 1, \; if \; radius > lim2 \\ 0, if \; radius < lim2 : \\ \dfrac{radius - lim1}{lim2 - lim1}, else \end{cases}$$

$$\text{attraction\_factor}(radius, lim1, lim2) = \text{repulsion\_factor}(radius, lim1, lim2) + 1,$$

where *radius*, *lim1* and *lim2* are defined separately for each deposit class (see the next section).

The following graph (Figure 59) shows the values of multiplicative factor according to the function used and the *radius* value:

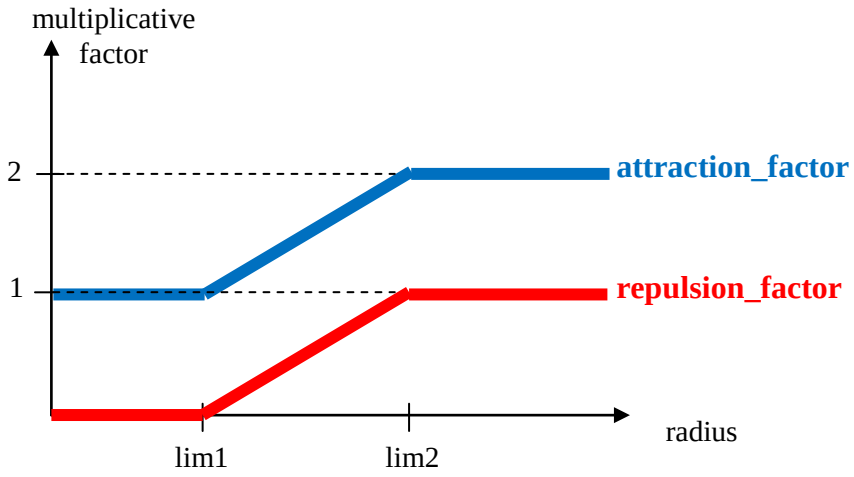

Figure 59. Multiplicative factor values graph, according to the function used and *radius* value

Step 2. Definition of the limits according the required well data facies

This procedure is detailed in the next section after the algorithm presentation.

Step 3. Extension of the erodibility correction to the points of the same channel meander

In order to make the migration adaptation smoother, the multiplicative erodibility correction is extended to all the points of the same channel bend, located between two inflexion points. The following Figure 60 represents the Flumy channel 2D aerial view; the light blue points are the points with the corrected erodibility values, the straight lines are the velocity perturbation vectors:

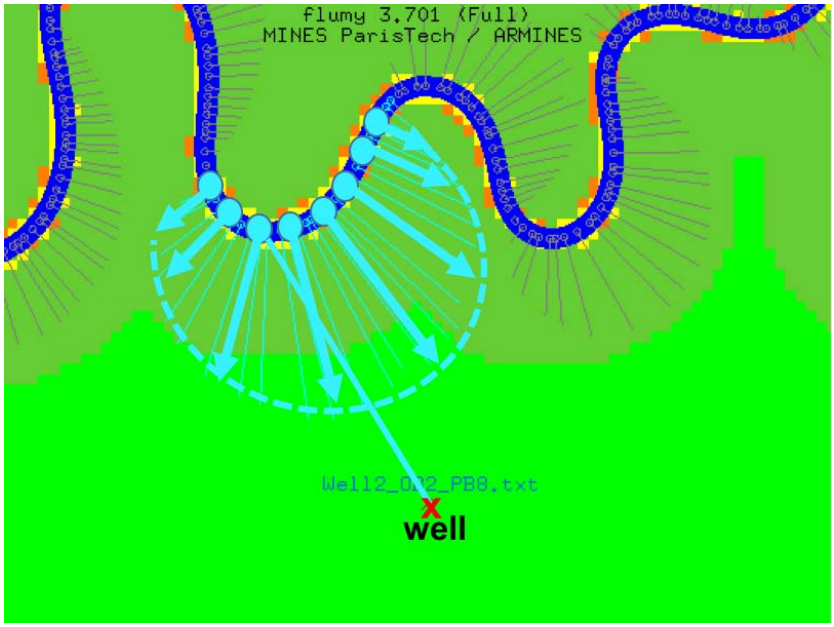

Figure 60. The Flumy channel 2D aerial view; the light blue points are the points with the corrected erodibility values, the straight lines are the velocity perturbation vectors The well (red cross) is linked to the nearest channel point according to the Von Mises distance.

2.3.2.2 Erodibility correction according to the three lithofacies classes

In this section, we detail the calculation of the "attraction" and "repulsion" factors (step 2 in the previous section). Choice of *radius* for each litho class is also indicated.

The multiplicative erodibility correction factor depends on the deposit needed at the well. There exist three different classes of deposits with the different function output and treated in that order:

- **Clay data facies (OB/WL)**

In this case we need to keep channel off the well – it is done by reducing the erodibility down to 0 in the neighborhood of the well ($R = 6 * w$), so a close migration to the well is forbidden.

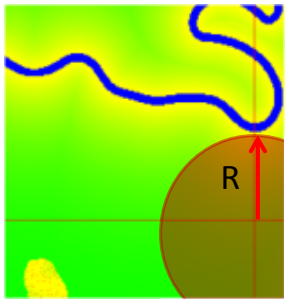

Figure 61. "Repulsion" radius during the OB/WL data facies honoring

The multiplicative erodibility E_{corr} correction in this case is:

$$E_{corr} = \text{repulsion\_factor}\ (radius, 2w, 6w),$$

where $radius = h - 0.5 * w$, *radius* is the distance between the bank point and the well;
h = the distance between the chosen channel point and the well; w = channel width.

- **Levee data facies (LV/CSI/CSII/CCh)**

Here we need to attract channel if it is too far away, and to repulse it if it is coming too close to the well. So we create a "repulsion neighborhood" with a smaller radius $r = 2.5 * w$ than in the case of OB/WL; but if the distance between the channel and the well becomes greater than $R = 0.75 * lv\_w$, the channel is attracted to the well by increasing erodibility up.

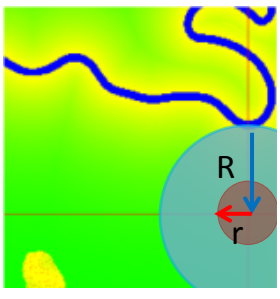

Figure 62. "Repulsion" and "attraction" radius during the LV/CSI/CSII/CCh data facies honoring

The multiplicative erodibility correction in this case is:

- if *radius* < 2.5 * *w* → repulsion_factor (*radius*, 1.5 * *w*, 2.5 * *w*);
- if *radius* > 0.75 * *lv_w* → attraction_factor (*radius*, 0.75 * *lv_w*, *lv_w*).

where *radius* = *h* – 0.5 * *w*,

h = the distance between the chosen channel point and the well,

w = channel width,

lv_w = levee width.

- **Channelized data facies (PB/CL/SP/MP)**

In this case, we attract the channel to the well by increasing erodibility in its neighborhood. Here, *R* is equal to the distance between the well and the closest meander.

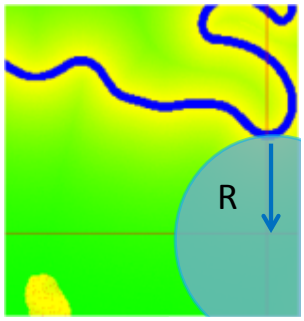

Figure 63. "Attraction" during the PB/CL/SP/MP data facies honoring

The algorithm of PB reproduction is a little bit more complicated, because the channel depth elevation plays an important role. To avoid replacing the lower "not-to-be-eroded" facies and honoring the sand data at the same time, we change the erodibility values by using three new variables: *avoidh*, *gap_up* and *above_al*.

- **Introduction of additional variables: *avoidh, gap_up, above_al***

avoidh computation:

When the "conditioning" channel bottom elevation at well (corresponding to *z_min*) is lower than AL, the channel should not come too close to the well if "not-to-be-eroded" data (OB) is present below. For that reason, we introduce *avoidh* "protection" distance which is calculated as shown in the following figure. When the distance between the channel centerline and the well is less than *avoidh*, we "turn on" a repulsion factor in order to avoid the replacement of OB or LV facies.

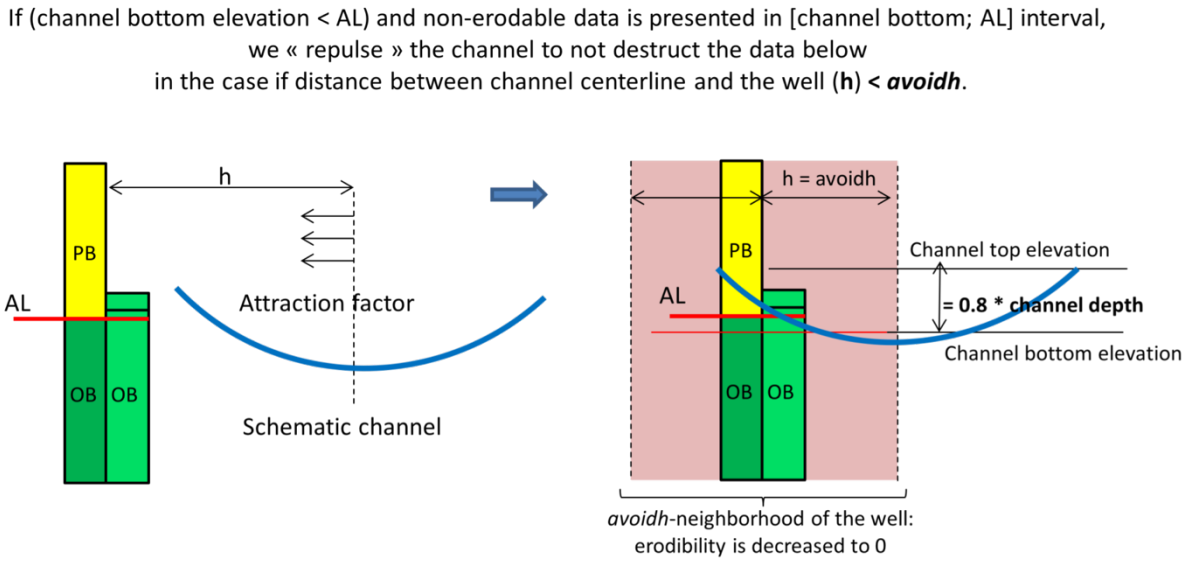

Figure 64. The *avoidh* scheme (migration adaptation)

gap_up computation:

During the construction of PB we also compute *gap_up* value which is the vertical distance between the channel top elevation (*top_ch*) and the top elevation of AB (*gap_up* = *top_ab* – *top_ch*). When *gap_up* becomes too small (less than 0.2 m by default), that means that we should quickly honor the remaining small part of the active brick, the channel is strongly attracted by calculating the erodibility correction as:

$$E_{corr} = 3 - \text{attraction\_factor}\left(gap\_up, 0.1, 0.2\right).$$

Gap_up value – the vertical distance between channel top elevation and the top of AB.

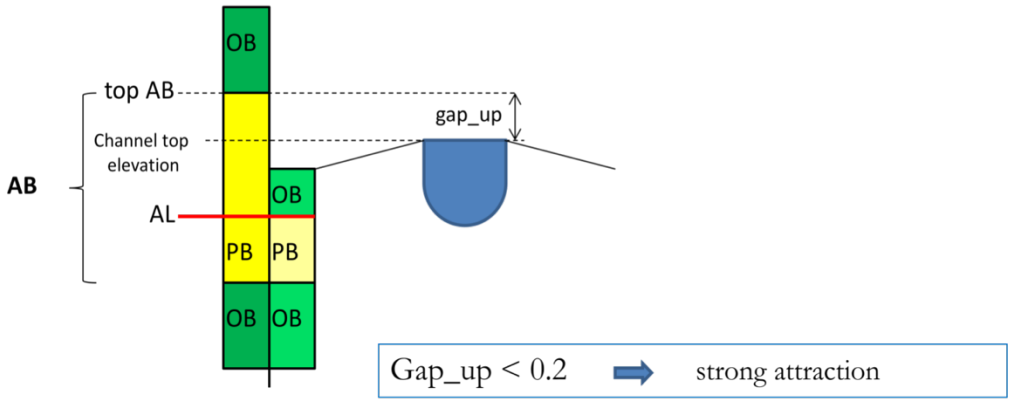

Figure 65. The *gap_up* scheme (migration adaptation)

above_al computation:

Finally, *above_al* variable shows how high is the channel top elevation above AL, relative to channel maximum depth:

$$above\_al = (top\_ch - AL)/H_{max}$$

Recalling the case X of the update AL algorithm, we know that the AL is increasing when the channel top is elevating, so *above_al* aims to avoid the validation of the inappropriate deposits. When *above_al* is more than 0.6 * H_{max}, the attraction of the channel is strongly forced:

$$E_{corr} = attraction\_factor\,(above\_al, 0.6, 0.8).$$

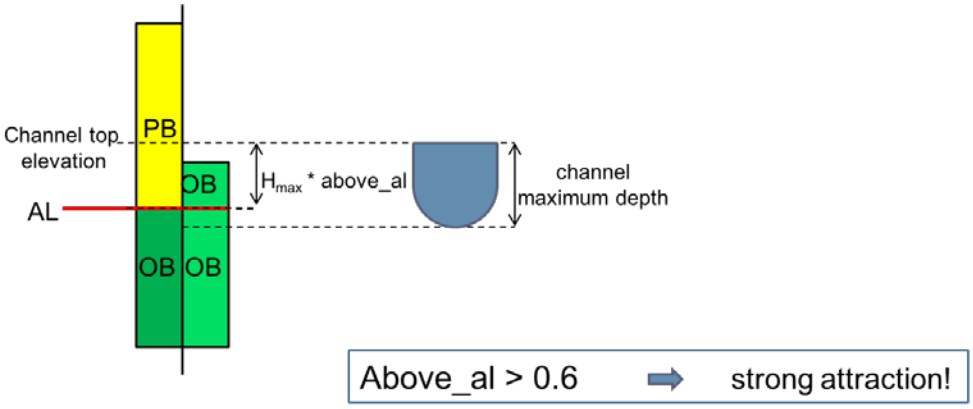

Figure 66. The *above_al* scheme (migration adaptation)

2.3.3 Adaptation of avulsions

The function responsible for the avulsions adaptation is calculated in every cell of the simulation domain just before any local and regional avulsions. It returns an **additive** correction for each cell erodibility and leads to calculate a modified virtual topography ("pseudo" topography). This new relief allows the program to drive the steepest path algorithm used for avulsions in the "right" areas. This virtual topography is only used to toss the new channel path. Then, the channel path is placed on the real floodplain topography, which results in some local adjustments to the real floodplain topography.

In order to compute the erodibility correction, the Gaussian density curve is used. Another important correction of avulsion Flumy processes, is the possibility to force a local avulsion in several "extreme" cases that will be described further.

The output of this function depends on the type of facies which we need to reproduce at the well location – that is, the facies of Active Brick and the position of Active Level within it.

Calculation of erodibility correction

This function indicates how the "pseudo" topography correction is calculated for each type of conditioning data. The erodibility correction value is obtained by "pinching" the real erodibility value in the well cell. A Gaussian density curve is used to extend the correction to other grid cells:

$$\text{gauss\_cov}\,(h, range) = \exp\left[-\left(h\_norm\right)^2\right],$$

where: h – distance between the well and a grid point where we want to calculate the correction;
$range$ – the practical range; theoretical range = range / 1.73,
h_norm = (1.73 * h) / $range$.

Calculation of modified topography

Modified topography *mod_topo* general formula (valid also in the case of several wells and variable erodibility map):

$$mod\_topo = topo + noise - topo\_ampl\left((1 + \lambda_0)\frac{E}{E_{max}} + \sum_{wells}(1 + \lambda_i)E_{corr\_i}\right)$$

where: *topo* – the real topography at the grid point where we want the modified topo;
noise – a topography noise between [-10^{-5} and $+10^{-5}$];
topo_ampl – (maximal topography value – minimal topography value) over the domain;
λ_0 – uniform value between 0 and 1, constant during the whole topography calculation (erodibility impact weight updated at each new modified topography);
$\lambda_1, \ldots, \lambda_i$ – uniform value between 0 and 1 values (i – well index);
E – the erodibility value at the grid point where we want the modified topo;
E_{max} – the maximal erodibility value over the domain;
E_{corr_i} – erodibility correction, influenced by i^{th} well.

Shapes of modified topography for each class of facies:

- **Fine-grained data facies (OB/WL):**

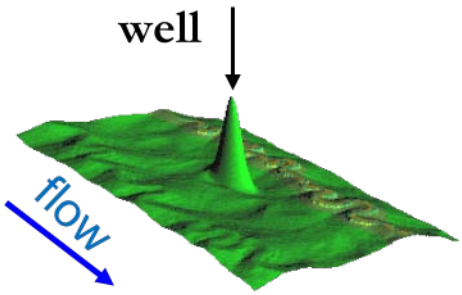

Figure 67. "Pseudo" topography during the OB/WL data facies honoring (3D Flumy view)

In the case of fine-grained data facies, a big cone ("bump" shape) is constructed at the well location; a new avulsion path, can not come too close to that well and deposit LV or PB there.

The formula of the erodibility correction in this case is:

$$E_{corr} = -\,\text{gauss\_cov}\,(hh, 11w),$$

where hh – the anisotropic distance between the well and each grid point, $hh = \sqrt{(dx)^2 + 4(dy)^2}$, the anisotropic distance is used (instead of geometrical one) in order to handle flow direction providing that flow direction is along *Ox* axis;

dx and dy – projections of distance between the well and the grid point on the *Ox* (flow direction) and *Oy* axis respectively;

w – channel width.

- **Levee data facies (LV/CSI/CSII/CCh)**

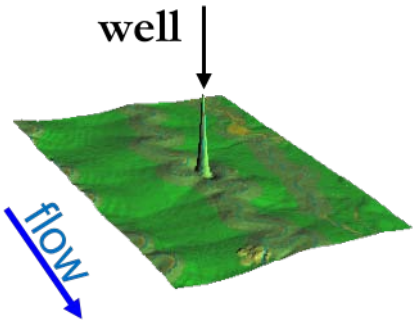

Figure 68. "Pseudo" topography during the LV/CSI/CSII/CCh data facies honoring (3D Flumy view)

To recreate the levee deposits, we construct a "rimmed bump" – more narrow than for OB; so a new channel after avulsion could come close, but not too much (because the migration adaptation function provides us a repulsion of the channel at short distance and an attraction otherwise). The formula of erodibility correction in this case is:

$$E_{corr} = -1.1 * \left(\text{gauss\_cov}\,(hh, 4w)\right) + 0.1 * (\text{gauss\_cov}\,(hh, 12w)),$$

where *hh* – the anisotropic distance between the well and each grid point, $hh = \sqrt{(dx)^2 + 4(dy)^2}$,

dx and *dy* – projections of distance between the well and a grid point on the *Ox* and *Oy* axis respectively;

w – channel width.

- **Channelized data facies (PB/CL/SP/MP)**

Again, in this case we update the pseudo topography of the grid according to the values of *avoidh*, *gap_up* and *above_al*.

avoidh computation:

To avoid the replacement of the inferior OB during the avulsions, we imagine the case of the channel **already at** the well location. We take channel elevation equal to the elevation of the floodplain in the well (*zfp* value in the update AL algorithm).

While channel bottom elevation is less than AL, we compute *avoidh* distance. The only difference with migration adaptation procedure is that we consider *h* as the distances between the well and the grid cell where we need the correction (and not the distance between the channel centerline and the well). In all the grid cells for which *h* < *avoidh* (that is, in the *avoidh*-neighborhood of the well) we construct a big peak (E_{corr} = -2), to not allow the channel « jump » too close to the well location during the avulsions:

To avoid the situation of channel inside of the well after an avulsion, we create a peak of the radius *avoidh* with the center in the well

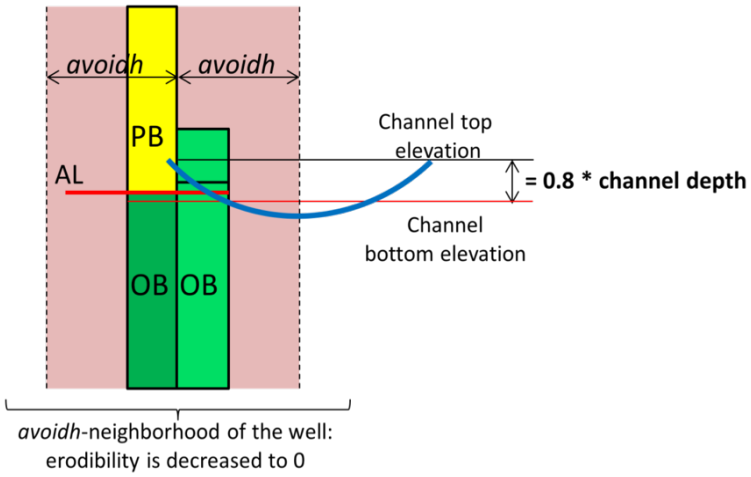

Figure 69. The *avoidh* scheme (avulsions adaptation)

gap_up and *above_al* computations:

Two other variables, *gap_up* and *above_al*, aim to determine the appropriate time to construct a "deep valley" in the "pseudo" topography in order to attract the channel during the avulsions:

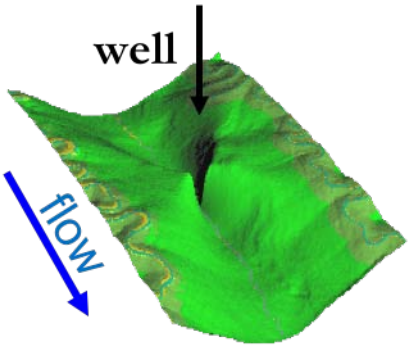

Figure 70. "Pseudo" topography during the PB/CL/CP/MP data facies honoring (3D Flumy view)

During the avulsions correction we use *gap_up* value to determine the moment when we should create a "deep valley" (which is shown on the image above). So, here again we consider the case of the channel at the well location and use the floodplain elevation in the well instead of the real channel top elevation (whatever its location in the domain).

Gap_up value – the vertical distance between floodplain elevation and the top of AB.

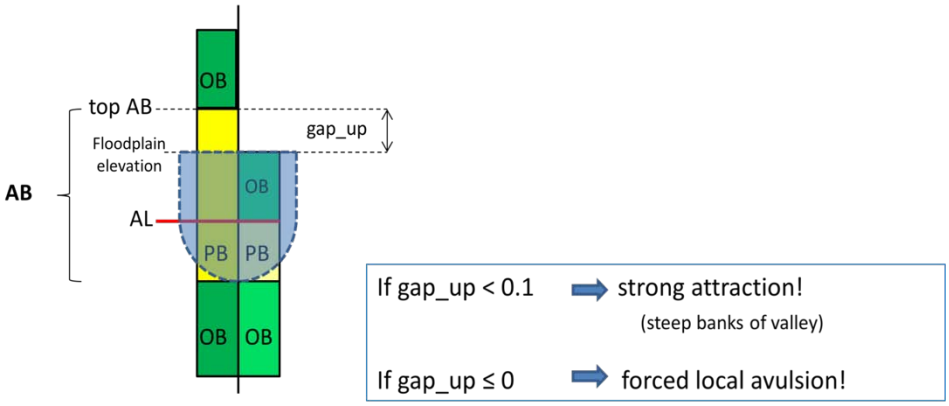

Figure 71. The *gap_up* scheme (avulsions adaptation)

When *gap_up* = 0 (that means that Non-Channelized data have been deposited at the well), the local avulsion is forced. This is the last chance to honor the PB active brick.

above_al variable, as the *gap_up*, aims in constructing the « valley » and in triggering a forced avulsion. Instead of channel top elevation we use the floodplain elevation at the well,

$$above\_al = (zfp - \mathrm{AL}) / H_{max},$$

where *zfp* – floodplain elevation, H_{max} – channel maximum depth.

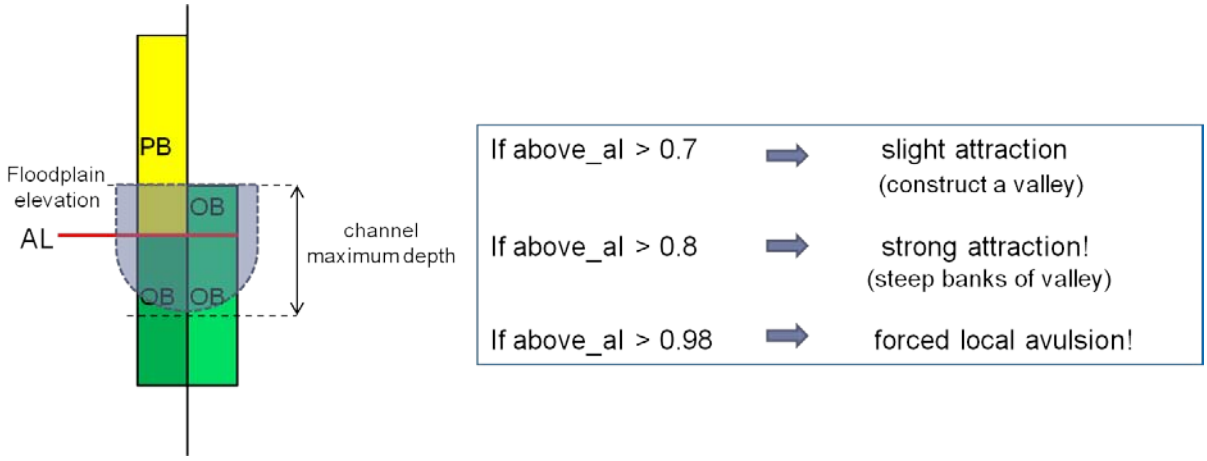

Figure 72. The *above_al* scheme (avulsions adaptation)

If *above_al* > 0.7 and *above_al* ≤ 0.8, the floodplain elevation is (*0.7 * H_{max}*) higher than the AL, we construct a valley to attract the channel. The formula for the erodibility correction in this case is:

$$E_{corr} = 0.5 * above\_al * \text{gauss\_cov}\,(hy, 4w + hx)$$

If *above_al* > 0.8 and *above_al* ≤ 0.98 or if *gap_up* < 0.1, then we make the banks of the valley deeper (strong attraction of the channel). The formula for the erodibility correction in this case is:

$$E_{corr} = \text{gauss\_cov}\,(dy - w + w * \cos\left(\frac{2\,\pi dx}{20w}\right), (4w + hx))$$

where *dx* and *dy* – projections of distance between the well and a grid point on the *Ox* and *Oy* axis respectively, *hx* = | *dx* |, *w* – channel width.

If *above_al* > 0.98 or *gap_up* < 0, a forced local avulsion is required from the closest upstream channel point.

Forced local avulsions:

As it was mentioned above, an additional option offers the possibility to require forced local avulsions. This is useful when sand deposition is strongly and urgently needed in an "attractive" well (due to the aggradation, the channel may not have been attracted at well in time). Exact conditions of forced avulsions are:

- If the *above_al* value becomes more than *0.98* or
- the *gap_up* value becomes negative.

In these cases, a local avulsion is attempted, whatever the avulsion period (but not more often than a half of programmed local avulsions period). In this case, the channel is expected to toss a new path exactly at the well location, because the topography of the grid is already "prepared" for this avulsion by the function of avulsion adaptation.

2.3.4 Conclusion

Compared to other conditioning techniques, Flumy uses the same general principles of sand / no-sand well reproduction: relatively, moving the channel closer / more far from the well location. The simulation processes adaptation is integrated into the simulation.

The difference with some other techniques is that there is no trial/error in Flumy, the conditioning is a dynamic forward procedure. Besides that, Flumy does not perform the conditioning to the potential channel states (for example, abandoned channels belts); only vertical well data and seismic data (not treated in my PhD) are accepted. The combination of facies classes, Active Brick and Active Level concepts, channel migration adaptation and “pseudo topography” are the basic principles of the dynamic conditioning in Flumy.

3 Towards a finer conditioning

Résumé français: Après un bref aperçu des outils d'évaluation utilisés, ce chapitre commence par examiner la performance du conditionnement dynamique tel qu'il avait été développé auparavant, qu'il s'agisse de la reproduction des lithofaciès aux puits ou de la distribution spatiale du sable. L'analyse des effets indésirables du conditionnement conduit ensuite à une modification des algorithmes. La performance de ces nouveaux algorithmes montre une nette amélioration des résultats.

The conditioning method implemented in Flumy aims at reproducing the well data with simulated deposits during the building of the 3D block. In this chapter, we present the tools to be used for evaluating the conditioning results. Then, we investigate the influence of the conditioning procedure and the well layout on the spatial sand distribution and the conditioning results. Finally, we propose a new algorithm for the dynamic conditioning procedures and estimate its impact on the same conditional simulations results.

3.1 Tools for evaluation of conditioning results

In order to estimate the efficiency of the conditioning procedure, as well as its impact on Flumy simulations (e.g. spatial sand distribution), several analysis tools have been developed in addition to the face-to-face display of well and simulated data at well location (Figure 73): this display is very useful during tests for a visual evaluation of the quality of the facies matching.

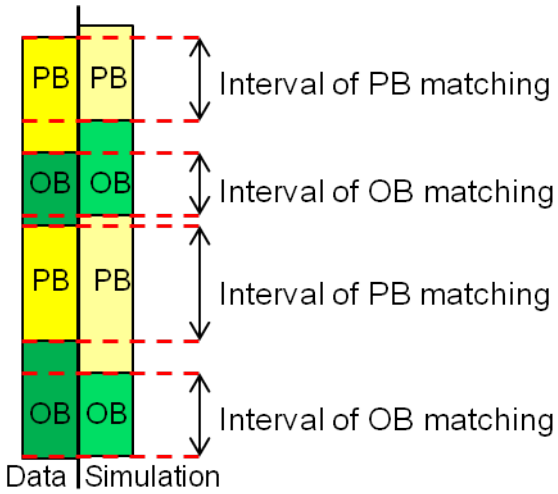

Figure 73. Matching between the well data and simulation results

In the following, other analysis tools are detailed.

3.1.1 Conditioning statistic table

A comprehensive statistic table is available in the Flumy software (Figure 74). This statistic table contains all facies proportion and all facies matching proportion for each well (well data and simulated data at well).

This table makes the distinction between the Sand and the Channelized Facies (to take into account the expected presence of Mud Plug (MP) instead of Sand). The following statistics are proposed:

- Well Sand/Channelized Facies proportion – the sand proportion calculated from the well data;
- Simulation Sand/Channelized Facies proportion – the sand proportion calculated from the simulated well data;
- Matching at Sand/Channelized Facies – the percentage of matching at sand well data.

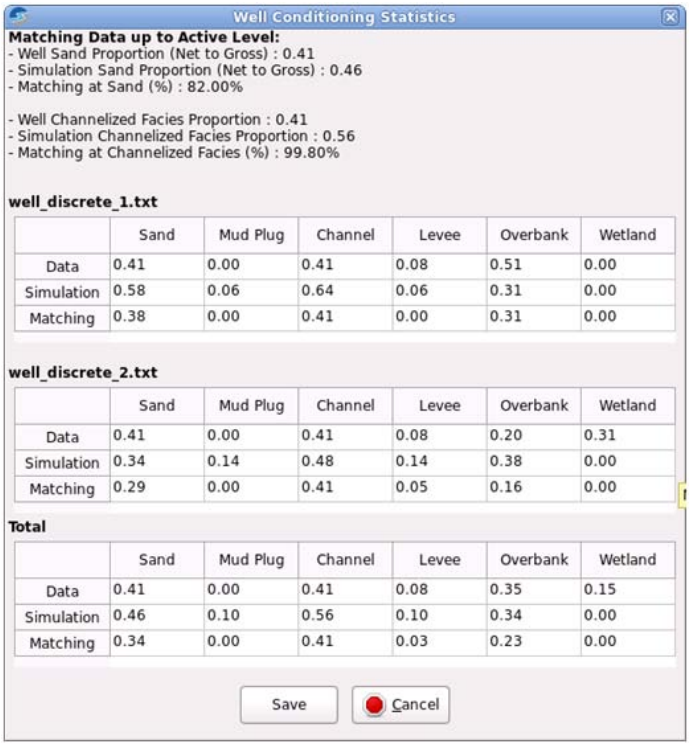

Figure 74. Well conditioning statistics for each wells and for all wells combined

3.1.2 Non-conditional and conditional simulation cross-section comparison

A quantitative visual comparison of facies distribution and proportion on the corresponding cross-sections of a non-conditional and a conditional simulations performed using the same parameter set permits to check the impact of the conditional procedure:

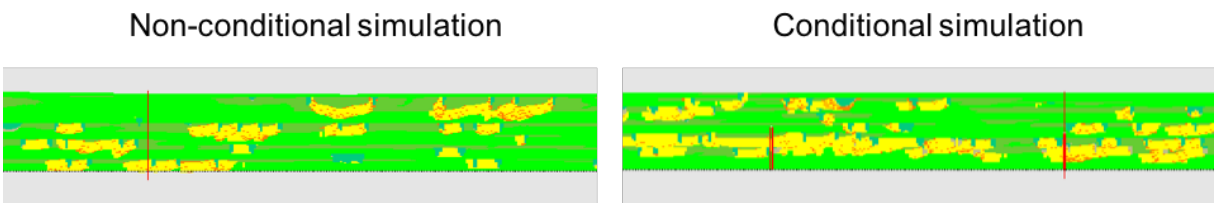

Figure 75. Example of cross-section comparison of non-conditional and conditional simulations

3.1.3 Sand Proportion Map

The Sand Proportion Map (SPM) are built by calculating the average sand proportion in each vertical pile of the simulation block. Such maps (Figure 76) are created in the Isatis® software. After performing a simulation in Flumy, the resulting 3D block is exported as a regular 3D grid and imported into Isatis. Then, the mean sand proportion in each vertical cell of the imported block is computed and displayed on the SPM. Such maps illustrate the homogeneity/heterogeneity of the spatial sand content in the conditional simulation and enables comparison with the non-conditional simulation:

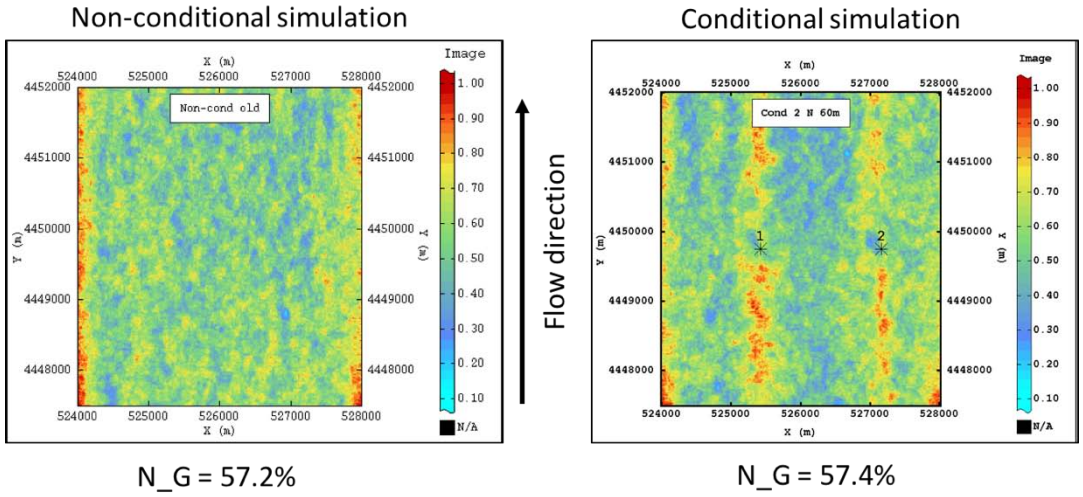

Figure 76. Sand Proportion Maps of non-conditional (left) and conditional by two wells (right) simulations, with the corresponding N_G

3.2 Reproducing lithofacies at wells

The first set of tests is conducted to evaluate the exactness of well reproduction during a conditional simulation. The following tests are performed:

- one well containing one lithofacies (non-channelized or channelized): single-facies wells,
- one well composed of several lithofacies (non-channelized and channelized): multi-facies wells,
- several multi-facies wells.

3.2.1 Single-facies well

In the following, simulations are run over the same domain, with the same channel parameters for one-facies and multi-facies well tests:

Parameters	**Values**
Channel maximum depth	3m
Domain Grid	4000m x 3000m; cell = 15m x 15m
Flow direction	From west to east (90°)
Well location	At the center of the domain

Table 5. General Flumy simulation parameters for one-facies and multi-facies wells tests

- In order to emphasize the results of well reproduction and not to get lost in all parameters values, we only indicate for each test the new modified simulation parameters and the predicted **sand proportion** and **sandbodies extension**.
- The sand proportion predictions within the simulated block from these tests are: Extremely poor (nearly 5%), Poor (17-23%), Average (47-53%) and Extremely Rich (90-95%).
- The sandbodies extensions used for the tests are: Ribbon type, Standard type and Sheet type sandbodies (see Figure 24).

The first lithofacies classification was used for interpreting well data: Non-Channelized and Channelized Facies. In the following, OB is used as Non-Channelized Facies and PB – as a Channelized Facies.

3.2.1.1 Non-channelized facies

We perform several conditional simulations with one well containing 15 m of OB only and for different sand proportions.

3.2.1.1.1 Extremely rich sand proportion

This test uses a Standard sandbodies extension and an Extremely Rich sand proportion (rare aggradation events). The aim is to test the conditioning algorithm with a well containing a thick interval of Non-Channelized deposits in a context of large sand proportion (incompatible parameters with well data).

Parameters	**Values**
Avulsions: - regional - local - sandbodies extension	 Periodical (600) Periodical (400) Standard
Aggradation: - occurrence - thickness - sand proportion	 Poisson (300) Const (0.1) Extremely Rich
Flumy version	3.612

Table 6. Flumy simulation parameters, test of Non-Channelized facies well, large sand proportion

The next Figure 77 contains the entire resulting model cross-section (with the well in the middle) and an enlarged view of this cross-section (for checking the well reproduction):

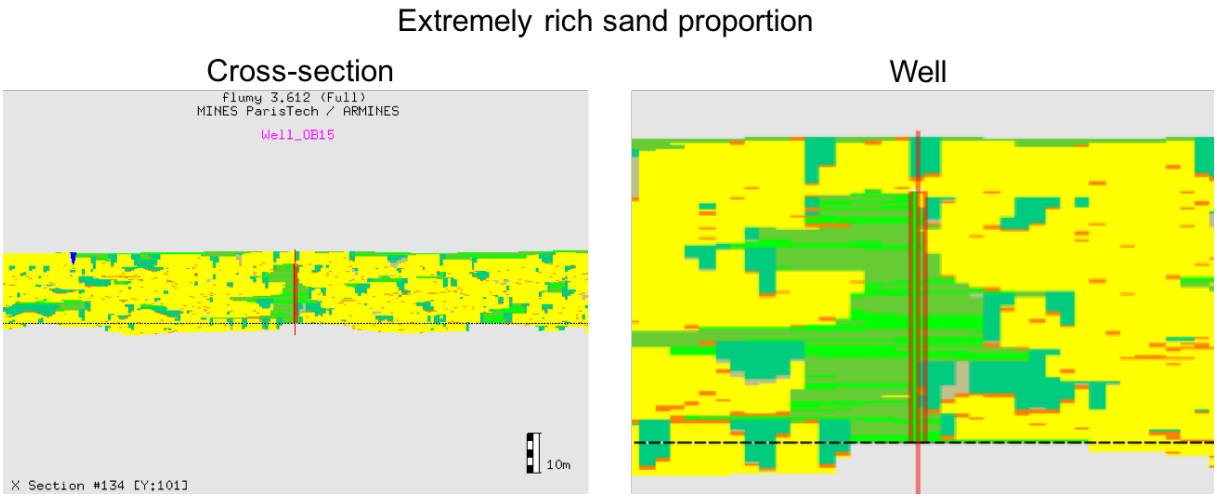

Figure 77. Non-Channelized facies well, with rich sand proportion: transversal cross-section containing well (left) and well reproduction (right)

Analysis of results:

In the simulation, the Non-Channelized facies deposited at well are evenly distributed between OB and LV facies (nearly 30% of OB vs. 70% of LV), both corresponding to Non-Channelized facies. LV deposition at the well is explained by the intense channel migration relatively close to the well location. In terms of facies reproduction, the results are almost perfect: only the small upper part of the well is replaced by Channelized facies (Point Bar). This non matching interval is due to the poor repulsive influence of the already completely honored well (to protect the top of deposits). Indeed, the channel could pass through the well location. This problem is noted for further modifications of the conditioning algorithm.

Besides of this mismatch, this test is a good illustration of the conditioning influence on the simulation. The model cross-section analysis shows that the simulation 3D block is almost completely filled by channelized sediments over the whole domain, except at the well vicinity where Non-channelized sediments have been deposited. It is an obvious result of the conditioning techniques corresponding to: “repulsion” of the channel from the well (adaptation of migration) and “protection” of the well location from the new channel paths (adaptation of avulsions).

3.2.1.1.2 Ribbon sandbodies

In another significant test of one-facies Non-Channelized well, the avulsions are occurring very frequently, resulting in new channel paths so often that the sandbodies cannot be sufficiently developed horizontally due to the limited migration time. This simulation parameter set is also an extreme case for Flumy model, but in terms of conditioning it represents an interesting test of avulsion adaptation: every new channel path should not be tossed at the well location, in order to respect the Non-Channelized well data.

This test uses the following simulation parameters: very frequent avulsions → Extremely Ribbon type of sandbodies. A Poor sand proportion is predicted.

Parameters	Values
Avulsions: - regional - local - sandbodies extension	 Periodical (10) Never Extremely Ribbon
Aggradation: - occurrence - thickness - sand proportion	 Poisson (28) Const (0.1) Poor
Flumy version	3.612

Table 7. Flumy simulation parameters, test of Non-Channelized well, extremely ribbon sandbodies

The next Figure 78 contains the entire resulting model cross-section (with the well in the middle) and an enlarged view of this cross-section (well reproduction):

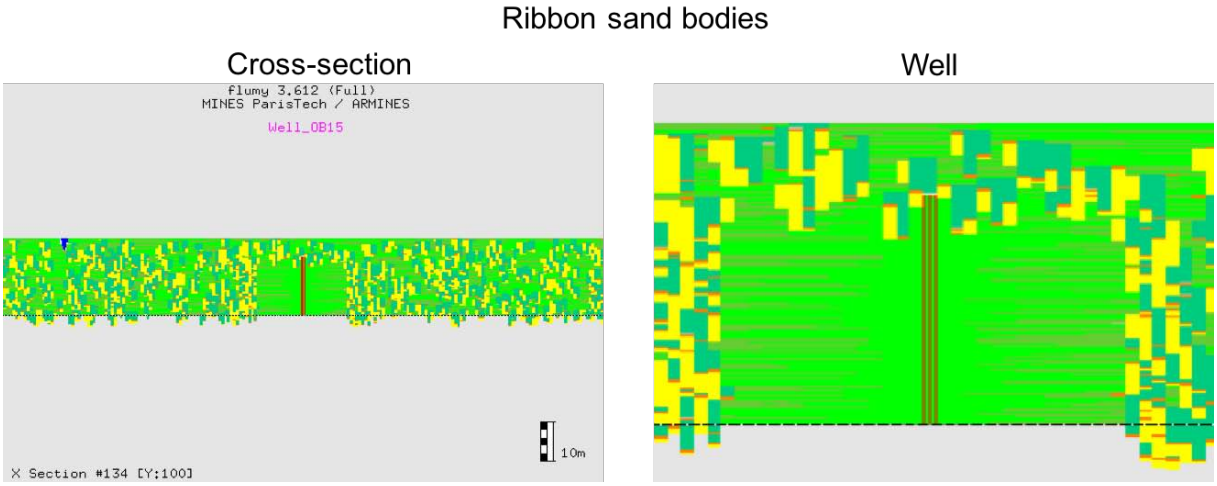

Figure 78. Non-Channelized facies well, result of test with extremely ribbon sandbodies; transversal cross-section containing well (left) and well reproduction (right)

Analysis of results:

In this test the well is 100% honored as Non-Channelized facies well and, more precisely, as an OB facies well. Also, the adaptation of avulsions is well illustrated on the resulting simulation cross-section: the “pseudo topography” created during avulsions adaptation does not permit to toss new channel paths through the well even in the case of extremely frequent avulsions. This effect can be observed on the Figure 78; it can be compared with some sort of “umbrella” located just upon the well.

3.2.1.1.3 Conclusion

The first conclusions to be made from these tests conducted with one facies well (Non-Channelized facies):

- reproduction of OB in the conditional simulation is not 100% exact: some levee facies can be deposed instead of clay sediments;
- reproduction of Non-Channelized facies in the conditional simulations is generally 100% exact: the well is protected from the channel presence by migration and avulsions adaptation techniques;

- a problem has to be noted for future modifications: an additional protection is needed for already completely honored well, in order to prevent from replacing the deposited Non-Channelized Facies at the top of the well by some Channelized facies.

3.2.1.2 Channelized facies

The well used in this part contains 15m of PB only (sand well).

Channelized facies are made of Point Bar sediments (PB) deposited during channel migration and Sand and Mud Plug deposits (SP and MP) following an avulsion or a meander neck-cutoff. It is important to note that abandoned channels are filled with Sand Plug (in the vicinity of the avulsion point) and Mud Plug sediments (further downstream).

The avulsion process is needed during simulations, because it results in a good sweeping of the simulation domain by the channel path which gives a more homogeneous sand distribution in the simulated block. But, on the other hand, Mud Plug is the only Channelized facies that is not made of sand, but of clay. A more accurate filling of the abandoned channel with a specific sand/clay distribution is probably needed. This issue is studied in the framework of another PhD (L. Szewczyk, started in 2018).

Presently, we cannot distinguish the general sandy Channelized facies from the clay Mud Plug. In the following tests Mud Plug will be considered as an appropriate facies type to be deposited instead of sand at the well location. It is interesting to note that both sandy and clay Channelized facies indicate that the channel was at the well location during that period.

3.2.1.2.1 Default simulation parameters

The first test uses the default simulation parameters with a Standard type of sandbodies but with a Poor predicted sand proportion.

Parameters	**Values**
Avulsions: - regional - local - sandbodies extension	 Periodical (600) Periodical (400) Standard
Aggradation: - occurrence - thickness - sand proportion	 Poisson (28) Const (0.1) Poor
Flumy version	3.612

Table 8. Flumy simulation parameters, test of sand well, default parameters, Flumy version 3.612

Two tests with the same input parameters but different seeds are performed in order to test the influence of the channel location with respect to the well location. The results of the well reproduction during the simulation are presented on the Figure 79:

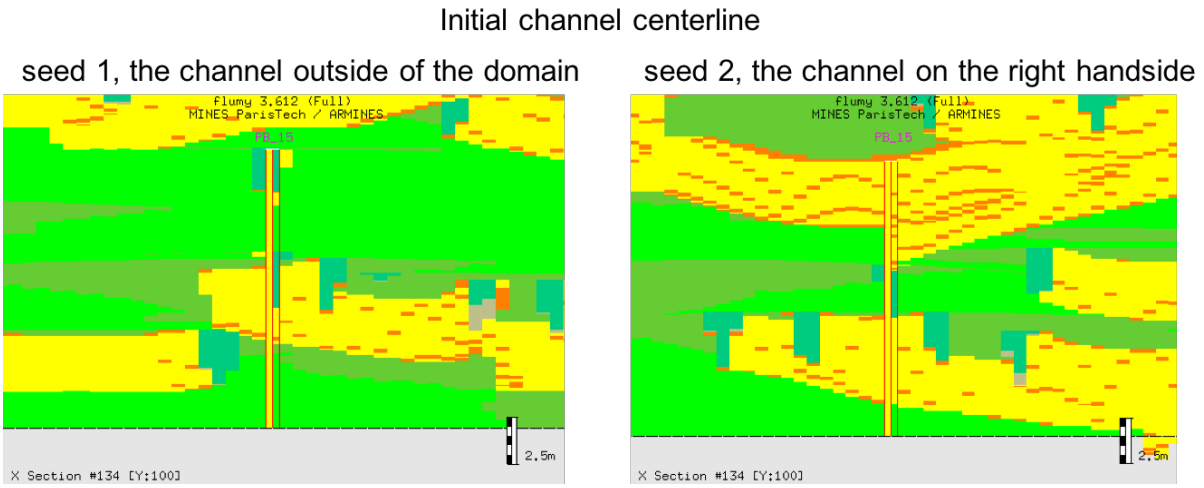

Figure 79. Channelized well reproduction, results of first (left) and second (right) tests with default parameters, Flumy version 3.612

Analysis of results:

The sand matching at well is lower than expected in both cases and the sand distribution is very different from one to the other section. In left case the inclusion of the Mud Plug deposits in the sand calculation gives a higher Channelized facies matching proportion (from 20% to 50%).

This facies succession and in particular the occurrence of OB deposits at the well location result from an incompatibility of the internal coefficients used in "Update Active Level" (section §2.3.1) and "Forced avulsions" (section §2.3.3) algorithms. This setting results in the fact that "the forced avulsion algorithm" is never called in the case of an immediate need of sand at the well bottom. This problem was resolved early during my PhD and that's why the proposed correction is detailed directly in the next section.

3.2.1.2.2 Early resolution of forced avulsions problem

Two aspects of detailed conditioning techniques are used here: firstly, it's the case X of "Update AL" algorithm (chapter 2.3.1):

Firstly, the AL is raised if the vertical elevation between the AL and the current topography at well is more than 0.8 * H_{max}. The thickness of non-validated deposits at the well location can never exceed 80% of input channel maximum depth parameter.

Secondly, the forced avulsions call in "Avulsions adaptation" algorithm depends on two additional parameters: *above_al* and *gap_up* (chapter 2.3.3). The forced avulsions are called when *above_al* value is close to 1 (*above_al* > 0.98), it means that the elevation of non-validated deposits should be more than 98% of the channel depth. But the AL is updated upwards every time this elevation exceeds 80% of the channel depth. That's why the forced local avulsions were never called, and these coefficients should be corrected in order to take into account the AL update algorithm.

An easier way to fix the problem is to change the *z_min* calculation by setting its value to the exact channel bottom elevation (no more 80% factor):

$$z\_min = zdom - H_{max}.$$

This modification was implemented in the version 3.702 of the Flumy software. That's why for the following tests, the version 3.702 is used. There is no need to conduct again the first tests of single-Non-Channelized facies well – all the other conditioning techniques remain the same.

New simulations are run with the same default simulation parameters (Table 8).

The next Figure 80 contains one resulting model cross-section (with the well in the middle of it) and the enlarged well reproduction:

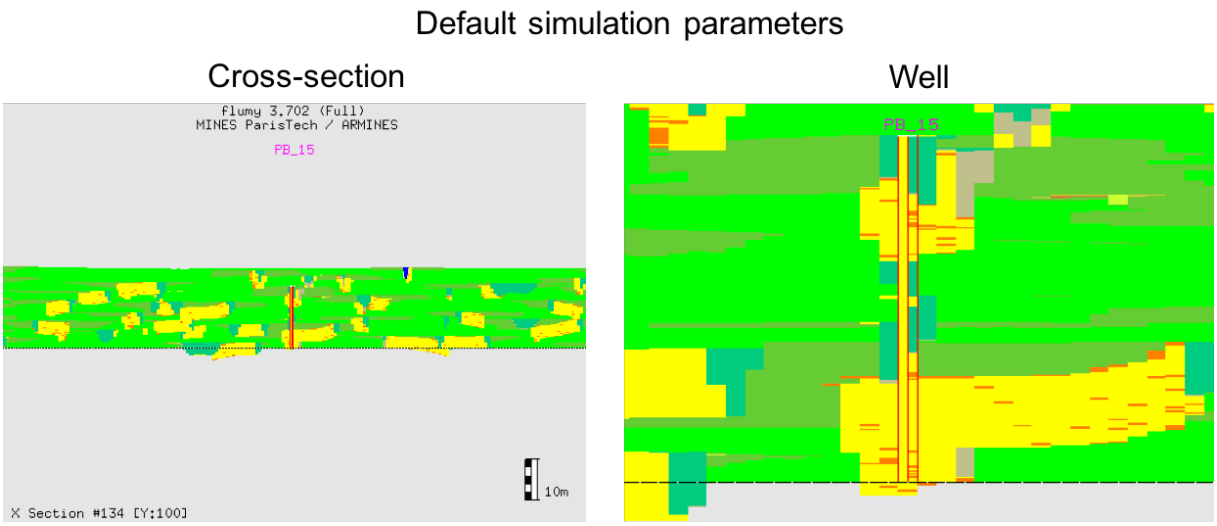

Figure 80. Channelized facies well, result of test with default parameters: transversal cross-section containing well (left) and well reproduction (right), Flumy version 3.702

Analysis of results:

After the correction of the forced avulsions problem, the Channelized facies at well is 100% reproduced (the only observed mismatch is the MP presence at the well during the conditional simulation while 100% Sand is expected). But now, the forced avulsion algorithm plays its role: the channel is always attracted to the well location when needed, in order to deposit the Channelized facies sediments – which results in better facies matching proportion.

3.2.1.2.3 Extremely poor sand proportion

To test the repulsion process during a conditional simulation with Non-Channelized facies well (OB deposits) we use an inverse simulation, i.e. we test whether it is possible or not to reproduce well full of Channelized facies with a very poor resulting sand proportion.

Simulation parameters: Standard type of sandbodies, Extremely Poor sand proportion are predicted.

Parameters	**Values**
Avulsions: - regional - local - Sandbodies extension	 Periodical (600) Periodical (400) Standard
Aggradation: - occurrence - thickness - Sand proportion	 Poisson (10) Const (0.1) Extremely Poor
Flumy version	3.702

Table 9. Flumy simulation parameters, test of sand well, small sand proportion

The next Figure 81 contains one resulting model cross-section and the enlarged well reproduction:

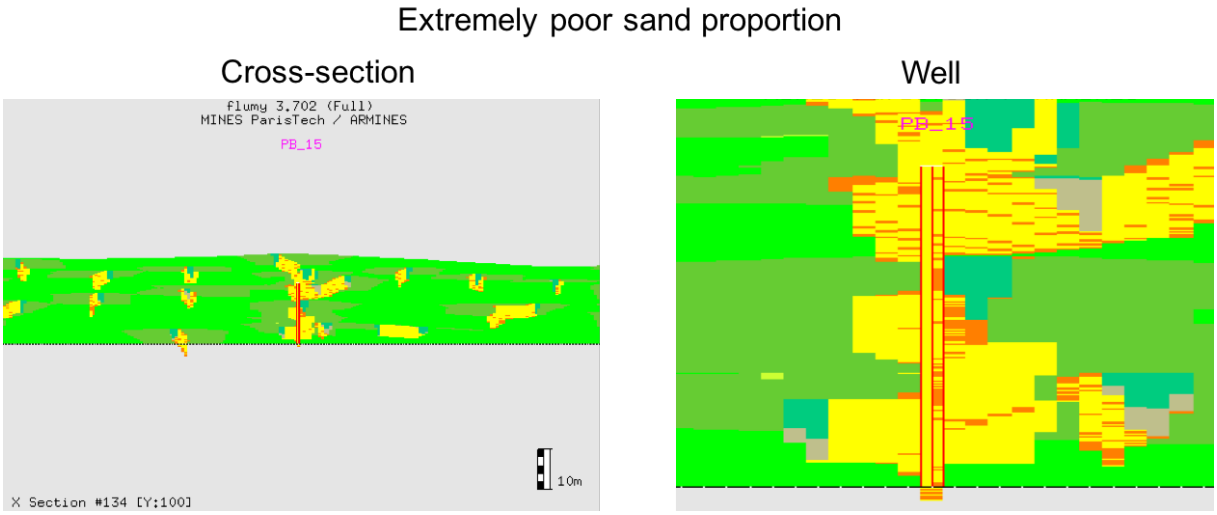

Figure 81. Channelized facies well, result of a test with small sand proportion: transversal cross-section containing well (left) and well reproduction (right), Flumy version 3.702

Analysis of results:

The test is successful – Channelized facies at well is 100% reproduced. However, when considering the entire cross-section of the resulting simulation, we see that the sandbodies are not homogeneously distributed over the simulation domain: sand is concentrated around the well vicinity. This point illustrates another important issue in the conditioning procedure: the simulation parameters have to be compatible with the well data; it will result in more homogeneous and “natural” conditional models. Indeed, it’s not rational to reproduce a completely sandy well with the simulation parameters chosen for this test (poor sand proportion), even if the dynamic conditioning techniques are capable to deal with it.

3.2.1.2.4 Ribbon type sandbodies

This test is conducted to illustrate the influence of the sandbody extension (related to migration time) in a simulation with a predicted low sand proportion.

The following parameters are used for this test: Ribbon type of sandbodies, Poor sand proportion are predicted.

Parameters	Values
Avulsions: - regional - local - Sandbodies extension	 Periodical (220) Periodical (112) Ribbon
Aggradation: - occurrence - thickness - Sand proportion	 Poisson (28) Const (0.1) Poor
Flumy version	3.702

Table 10. Flumy simulation parameters, test of sand well, ribbon sandbodies

One resulting model cross-section containing the well (left) and the enlarged well reproduction (right) are given in the Figure 82:

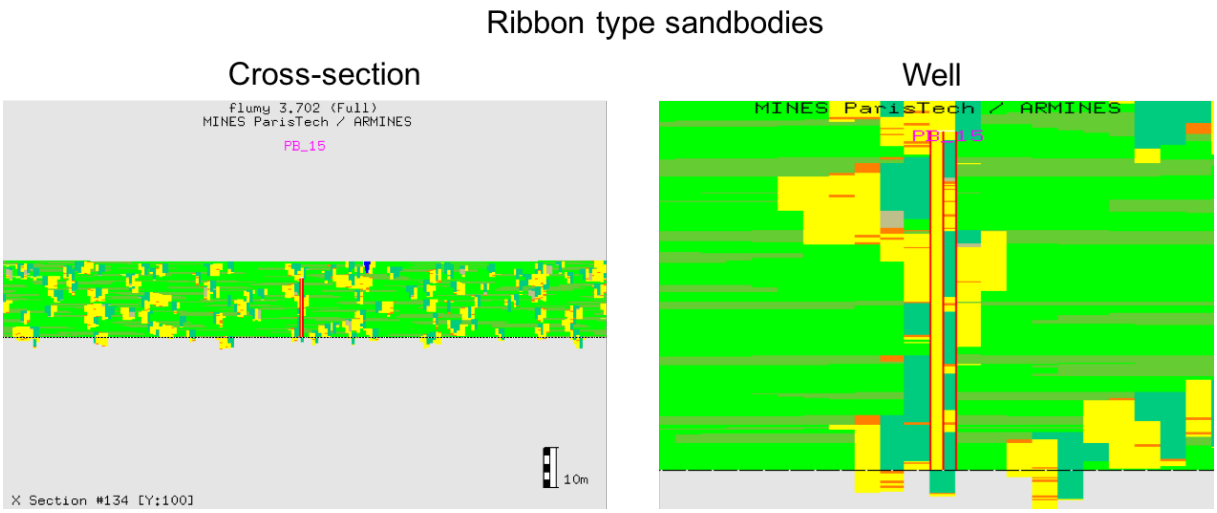

Figure 82. Channelized facies well, result of a ribbon sandbodies: transversal cross-section containing well (left) and well reproduction (right), Flumy version 3.702

Analysis of results:

The channelized facies at well are 100% reproduced, but with a high proportion of MP. The presence of MP at well is the result of the avulsion adaptation algorithm (new channel path is tossed at the well location), and the fact that the channel stays at the well until the next avulsion (abandoned channel is filled by MP).

3.2.1.3 Conclusion

The influence of some key Flumy parameters on the conditioning results shows the following:

- After the correction of the *z_min* calculation in the "update active level" algorithm, it is possible to reproduce a one-facies (Channelized or Non-Channelized) well at 100%. This generalization (Channelized facies instead of Sand, Non-Channelized facies instead of Clay or Silt) includes the following problems detected during the tests: presence of MP in the Sand well, presence of LV in the Clay well.
- In order to create realistic models, the question of the consistency of simulation parameters with the well data should not be under-estimated (because the Dynamic Conditioning alone may be sufficient for reproducing exactly one well, but is not enough for obtaining a realistic model).
- The change of key Flumy parameters does not influence the results of conditioning in the case of one-facies wells.

In the next part we consider a more complicated well test – three-facies well. This example will illustrate how exactly the conditioning techniques can reproduce the transitions between the main facies classes in the well data.

3.2.2 Multi-facies well

The well used in this test corresponds to the following stratigraphic succession: the first data brick is made of 10m of OB, the second data brick – 10m of PB and the last data brick – again, 10m of OB. Such a well is used to test the ability of the Flumy conditioning techniques to switch between different facies during the conditioning process ("repulsion" of channel for the first OB brick, then "attraction" of the channel for PB, and finally, a last "repulsion").

3.2.2.1 Low sand proportion

The default simulation parameters are used: Standard type of sandbodies, Poor sand proportion are predicted.

Parameters	Values
Avulsions: - regional - local - Sandbodies extension	 Periodical (600) Periodical (400) Standard
Aggradation: - occurrence - thickness - Sand proportion	 Poisson (28) Const (0.1) Poor
Flumy version	3.702

Table 11. Flumy simulation parameters, test of three-facies well, default parameters, Flumy vers. 3.702

The Figure 83 represents the well reproduction during the simulation:

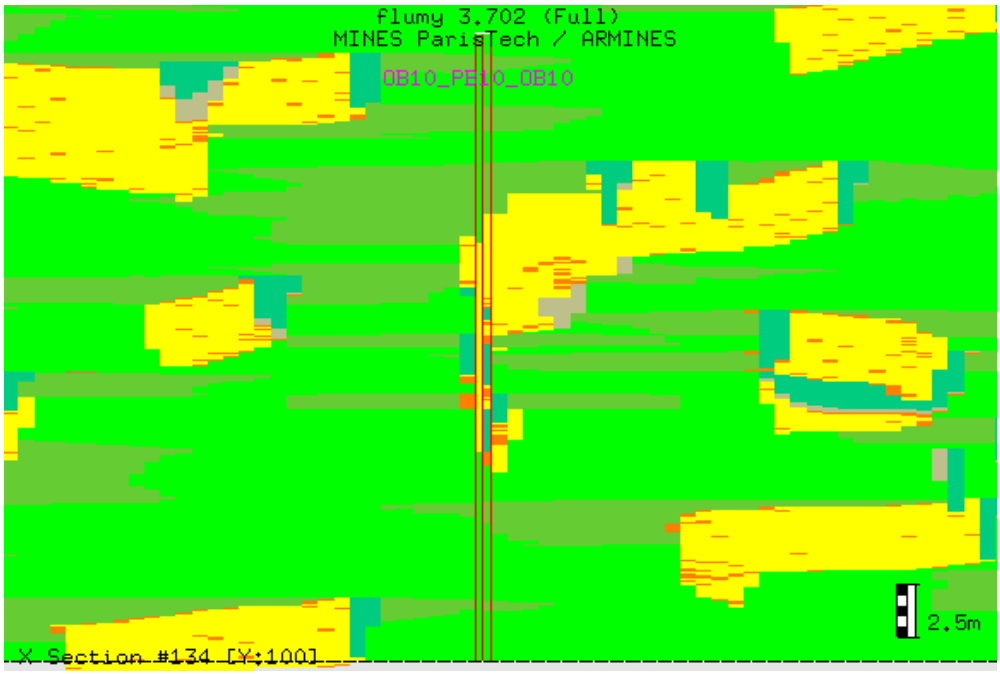

Figure 83. Three-facies well reproduction, result of a test with default parameters, Flumy version 3.702

Here are the conditioning statistics:

Parameters	Results
Well Sand Proportion	0.33
Simulation Sand Proportion at well	0.25
Matching at Sand (%)	54.10%
Well Channelized Facies Proportion	0.33
Simulation Channelized Facies Proportion at well	0.40
Matching at Channelized Facies (%)	100%

Table 12. Resulting conditioning statistics, three-facies well, default simulation parameters, Flumy version 3.702

Analysis of results:

After a successful phase where the first OB data facies has been honored, the channel is attracted to the well location for reproducing the PB facies above. As a result, the channel comes to the well location, but too early, resulting in the replacement of the top of already deposited OB facies by Channelized Facies. Then, the PB facies of the well is properly reproduced (as it was already seen during the channelized facies well test in the previous part). Finally, we observe a second problem – the channel stays in the well too long and deposits PB facies above the top limit of the PB facies brick. As OB facies is a “not-to-be-eroded” facies, a mismatch is created between the simulation and the well data and cannot be fixed later.

This mismatch leads to a higher percentage of Channelized Facies proportion at well (40% simulated instead of 33% from well data), with a 100% matching at Channelized Facies (Table 12). That means that the second data brick (PB) is 100% reproduced, but 7% of the Channelized Facies is deposited instead of OB in the first and the third data bricks.

In conclusion: the channel comes to the well location too early and stays in it too long.

3.2.2.2 High sand proportion

The following simulation parameters are used: Standard type of sandbodies, Extremely Rich sand proportion are predicted.

Parameters	Values
Avulsions: - regional - local - Sandbodies extension	 Periodical (600) Periodical (400) Standard
Aggradation: - occurrence - thickness - Sand proportion	 Poisson (300) Const (0.1) Extremely Rich
Flumy version	3.702

Table 13. Flumy simulation parameters, test of three-facies well, high sand proportion, Flumy vers. 3.702

The well reproduction during the simulation:

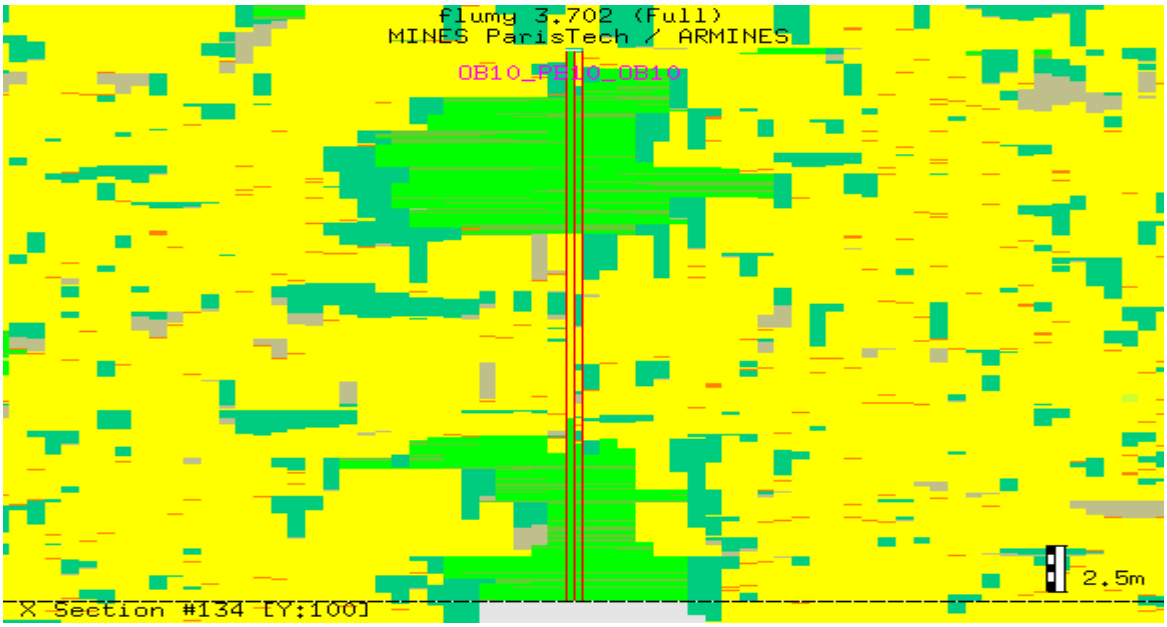

Figure 84. Three-facies well reproduction, result of a test with high sand proportion, Flumy version 3.702

Conditioning statistics:

Parameters	Results
Well Sand Proportion	0.33
Simulation Sand Proportion at well	0.34
Matching at Sand (%)	76.40%
Well Channelized Facies Proportion	0.33
Simulation Channelized Facies Proportion at well	0.46
Matching at Channelized Facies (%)	100%

Table 14. Resulting conditioning statistics, three-facies well, large N_G, Flumy version 3.702

Analysis of results:

The first OB interval is well reproduced, but its upper part is replaced by Channelized Facies because of the too early arrival of the channel at the well location. The second facies (PB) is 100% honored, and in this test the channel succeeds to leave the channel perfectly at time: the bottom of the third facies deposits (OB) is appropriately reproduced. On the contrary, the top of the well (OB facies) was not enough “protected” after the well completion, and some part of top OB was eroded by the channel. This problem was already detected during the one-facies Non-Channelized well tests.

Considering the conditioning statistics, 46% of Channelized Facies were deposited at the well during the simulation, instead of 33% corresponding to the well data. It means that 13% of Channelized Facies were deposited additionally, instead of OB facies, due to the problems indicated above.

3.2.2.3 Sheet type sandbodies

The last test of three-facies well is performed with the following parameters: Sheet type of sandbodies, Poor sand proportion are predicted.

Parameters	Values
Avulsions: - regional - local - Sandbodies extension	 Periodical (1100) Periodical (644) Sheet
Aggradation: - occurrence - thickness - Sand proportion	 Poisson (28) Const (0.1) Poor
Flumy version	3.702

Table 15. Flumy simulation parameters, test of three-facies well, sheet type sandbodies, Flumy vers. 3.702

The well reproduction during the simulation:

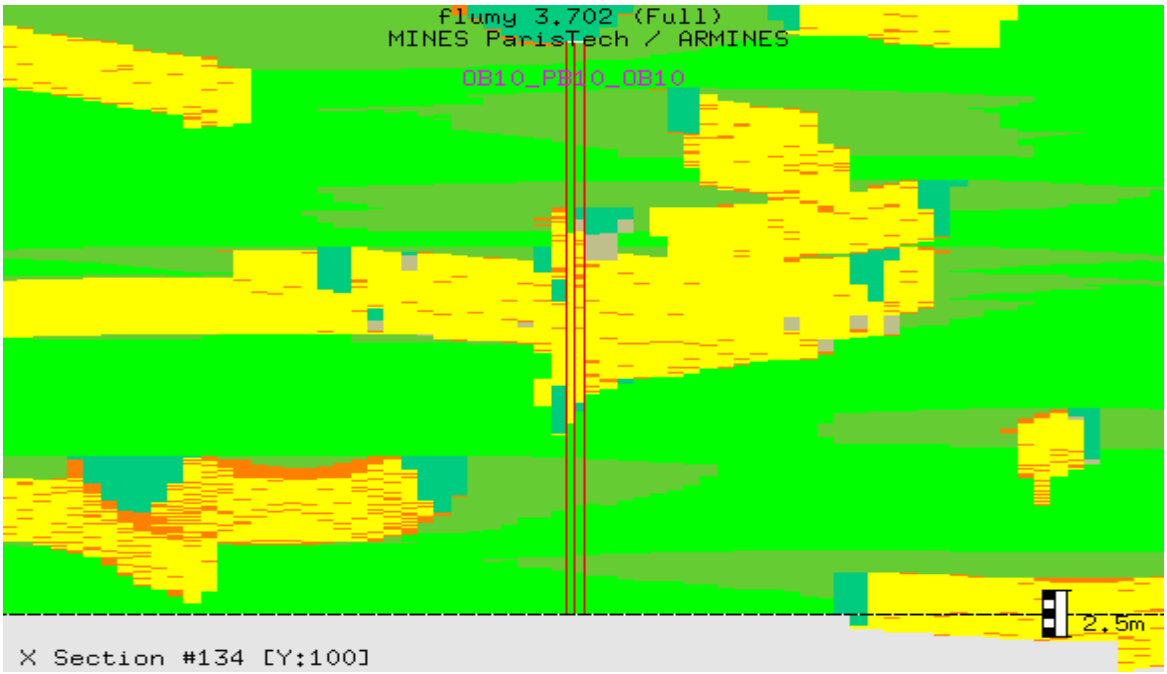

Figure 85. Three-facies well reproduction, result of a test with sheet type sandbodies, Flumy version 3.702

Conditioning statistics:

Parameters	Results
Well Sand Proportion	0.33
Simulation Sand Proportion at well	0.32
Matching at Sand (%)	88.70%
Well Channelized Facies Proportion	0.33
Simulation Channelized Facies Proportion at well	0.36
Matching at Channelized Facies (%)	93.60%

Table 16. Resulting conditioning statistics, three-facies well, large avulsions period, Flumy version 3.702

Analysis of results:

In contrary to the other previous tests, the first OB interval is 100% reproduced because the channel arrival to the well is delayed. So, the lower part of the PB interval is not honored. Further, during the second facies transition (from PB to OB), the channel is blocked at the well due to the "repulsion" effect of the new OB active brick. Concerning the exact conditioning statistics, only 93.60% of Channelized Facies at well are honored, due to the mismatches discussed above. 3% of Channelized Facies are deposited instead of OB.

3.2.2.4 Conclusion

From these tests with three facies, the following points can be summarized:

- Transitions between the data facies result in complex interaction between aggradation and migration, interactions that could not be detected in the one-facies wells.
- Problems concerning OB→ PB transition: the channel is sometimes attracted to the well too quickly and erodes the OB deposited below, or is attracted too slowly and does not honor the bottom of the PB. This suggests that a better equilibrium between the processes of "repulsion" and "attraction" of the channel has to be looked for. This question will be addressed in the new conditioning techniques (Chapter 3.4).
- Problems concerning PB → OB transition: after the change of the Active Brick, the channel may be blocked at the well due to the decrease of erodibility ("repulsion" effect of the new Non-Channelized data brick). In this case, the only way for the channel to leave the well is the avulsion. This problem is noted for modification.
- The top of an already completely honored well should be better "protected" by conditioning techniques if deposited facies at the top should not be replaced.
- The middle PB brick was 100% honored in the majority of the performed tests; on the contrary, in every test we observed an OB proportion lower than expected due either to a replacement of OB by some PB or a deposit of PB thicker than expected. It means that sand deposition is favored by the conditioning algorithm, and Non-Channelized Facies are not sufficiently protected from erosion. In the further modifications this problem will be taken into account.

3.2.3 Multiple wells

We perform two tests to estimate the capacity of the conditioning algorithm to reproduce several wells at the same time. In the first test, the well data are toy data that are not necessarily compatible with the simulation parameters, while in the second test, they are extracted from a non-conditional simulation with given parameters to be used in the conditional simulation.

3.2.3.1 Four synthetic wells

In this test, we created four synthetic wells made of three to four bricks of PB or OB facies. The thickness of each of these facies is in the range of 4 to 7 m (Figure 86). They correspond to a simplified description of a well (sand/no sand).

Conditions of the test:

Parameters	Values
Channel max depth	3 m (channel width = 30 m)
Grid size	4005 m x 3000 m; grid lags: 15m x 15 m
Avulsions - regional - local	 Periodic (600) Periodic (400)
Aggradation - occurrence - thickness	 Poisson (28) Constant (0.1)
Flumy version	3.702

Table 17. Simulation parameters of four synthetic wells test, Flumy version 3.702

Well locations on the simulation domain (aerial view) are shown in the Figure 86.

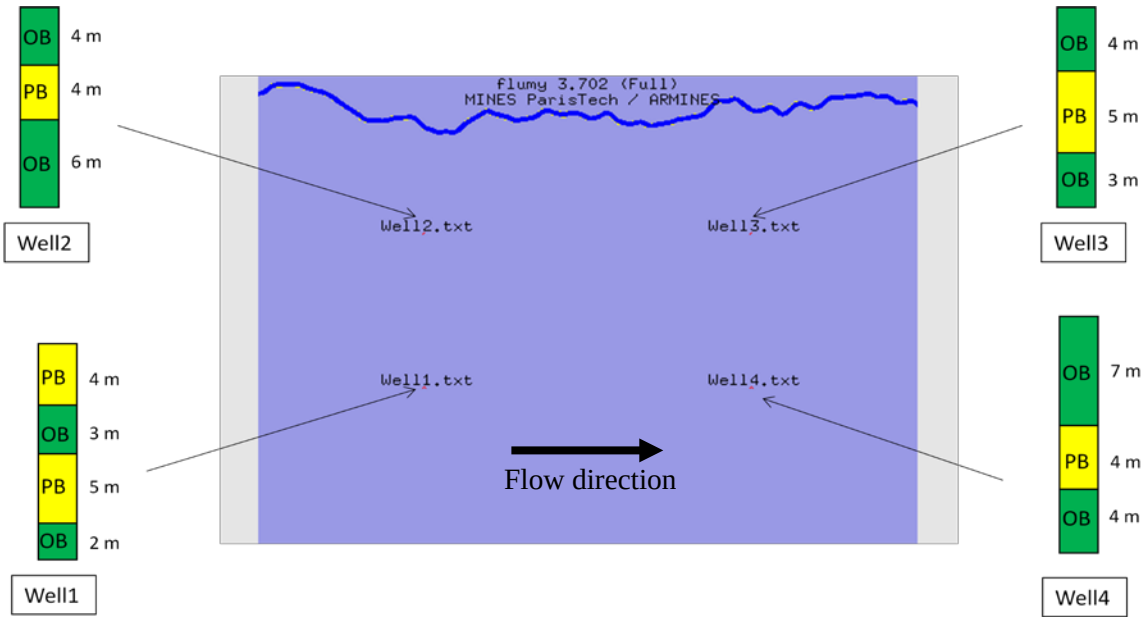

Figure 86. Conditions of four synthetic wells test, Flumy version 3.702

Two pairs of wells are aligned along the flow direction. Computed sand proportion of the four synthetic wells is equal to 36.7 %. The conditional simulation was performed, resulting in a global sand proportion of 21 %.

Resulting reproduction of wells is shown on Figure 87:

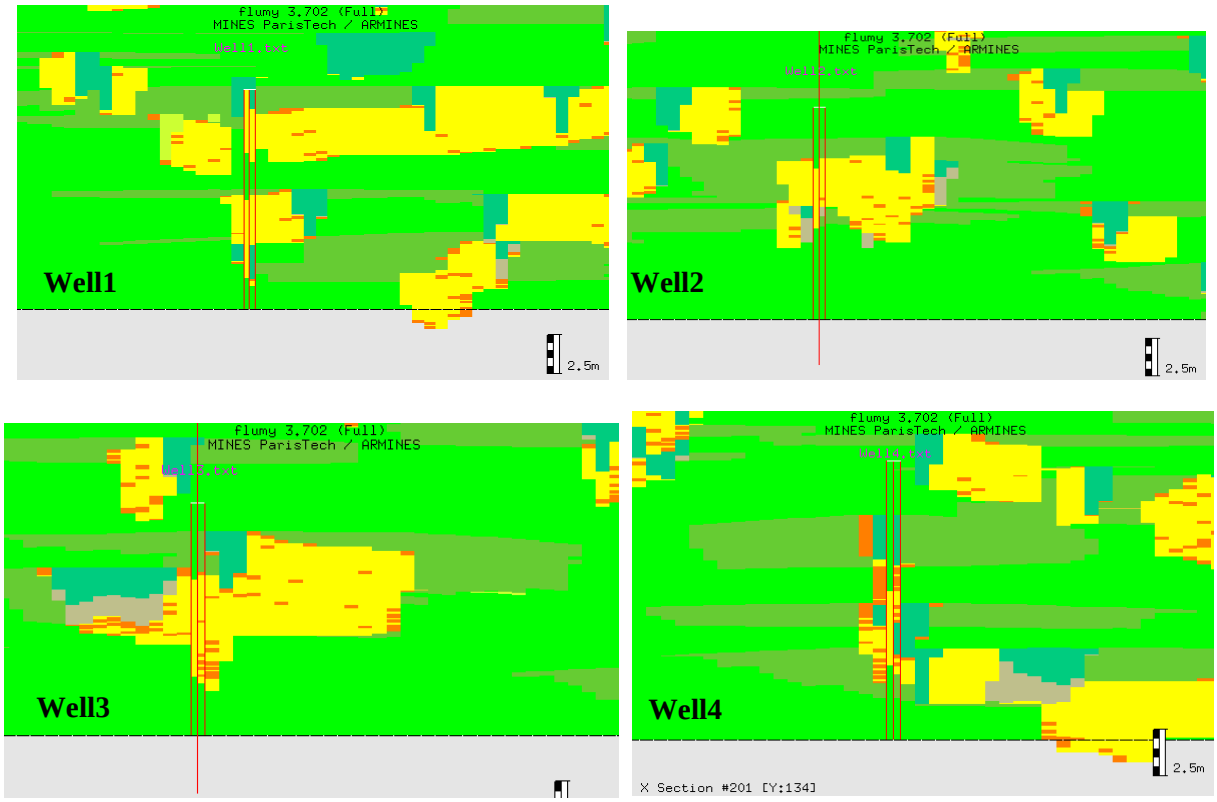

Figure 87. Four synthetic wells reproduction, Flumy version 3.702

As previously observed during the multi-facies well tests, it is difficult to perfectly honor the transition between facies OB/PB: the channel arrives at well either too early (Well1, Well4) or too late (Well2). During the transitions PB/OB the channel may stay blocked at the well until the next avulsion (Well4).

Conditioning statistics:

Parameters	Results
Well Sand Proportion	0.40
Simulation Sand Proportion at well	0.38
Matching at Sand (%)	73.27%
Well Channelized Facies Proportion	0.40
Simulation Channelized Facies Proportion at well	0.52
Matching at Channelized Facies (%)	96.23%

Table 18. Resulting conditioning statistics, four synthetic wells test, Flumy version 3.702

The exact results of the wells reproduction show that, again, the Channelized Facies deposition is favored in the conditioning procedure: instead of 40% of Channelized Facies at the wells, 52% were deposited, with a matching of more than 96%.

A comparison of the cross-sections containing wells from the non-conditional and conditional simulations run with the same input parameters show the influence of conditioning procedure on the sand distribution. The following Figure 88 shows two types of cross-sections: transversal (cross valley) and longitudinal (along the flow):

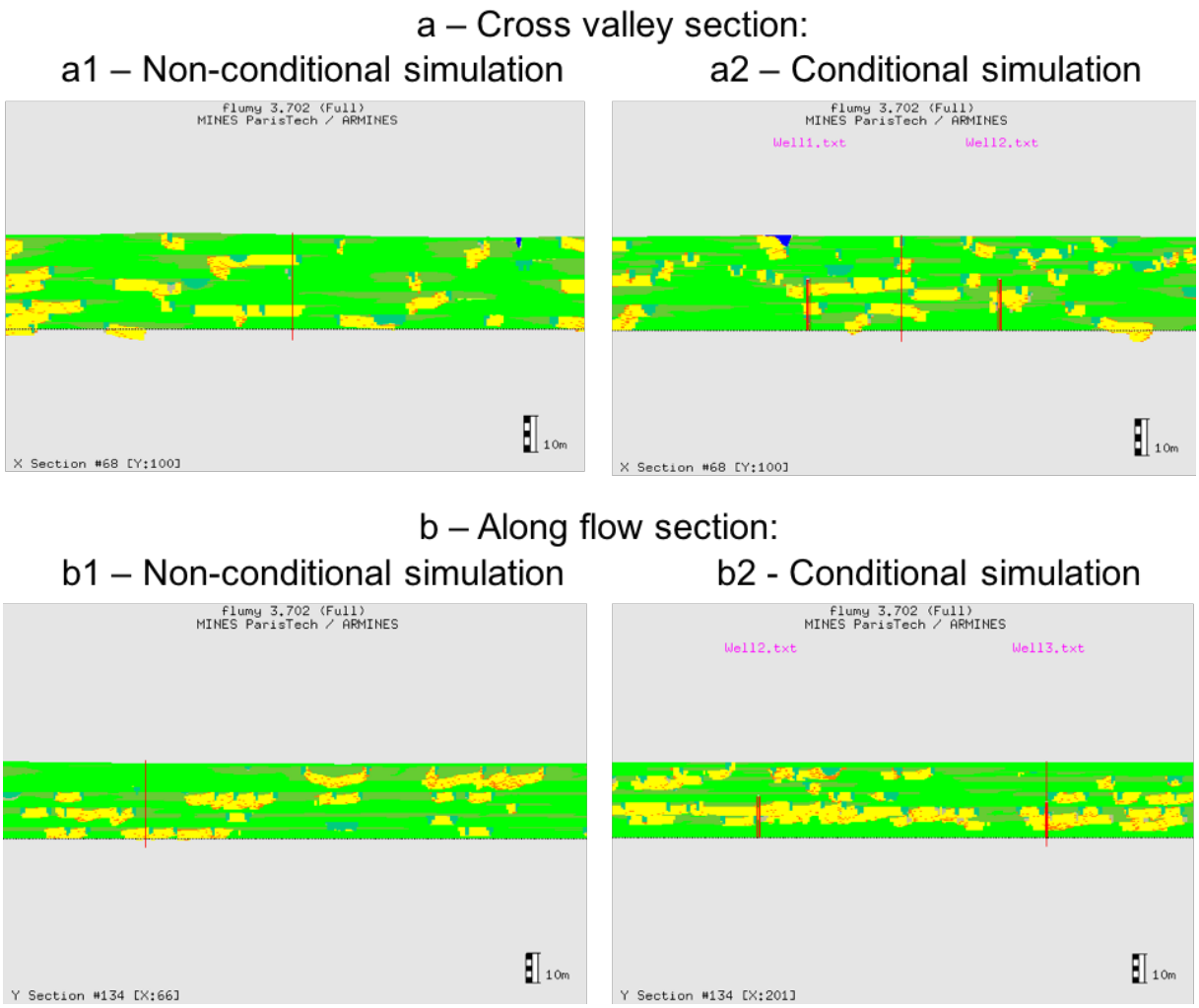

Figure 88. Four synthetic wells test, comparison of cross-valley (a1-a2) and along flow (b1-b2) sections of non-conditional and conditional simulations; Flumy version 3.702

Sand proportion of non-conditional simulation is 20 %, and the one of conditional simulation is 21%.

Observations:

- The global sand proportion is quite similar for the conditional and the non-conditional simulations but there is too much sand deposited at well in the conditional simulation.
- A comparison of cross-sections above shows that the corresponding cross-valley sections of the non-conditional and conditional simulations are quite similar (they may be considered as representing two different realizations of the same model).
- The longitudinal sections present some differences: the sandbodies are elongated upstream and downstream of wells in the conditional simulation while they are fairly well distributed in the non-conditional simulated block.
- The observed sand proportion for both non-conditional and conditional simulations are almost equal but the conditioning procedure tends to increase the sand deposition in the vicinity of the wells along the flow direction and lowers the sand proportion along the intervals where no sand is desired. This issue is to be investigated in the section §3.3.

3.2.3.2 Four simulated wells

The last well exact reproduction test conducted is a simulation conditioned by four extracted wells from a non-conditional simulation. This procedure ensures the consistency between the well data and the conditional simulation parameters.

It is possible with the Flumy software to export vertical wells from a simulation. In order to obtain the extracted wells for this test, the following procedure was performed: four wells with chosen coordinates are extracted from a non-conditional simulation. These wells are used during the conditional simulation which is performed using the same input parameters as the non-conditional simulation. Thus, the simulation parameters are compatible with the well data.

Conditions of test (both non-conditional and conditional simulations):

Parameters	Values
Channel max depth	3 m (channel width = 30 m)
Grid size	4005 m x 3000 m; grid lags: 15m x 15 m
Avulsions - regional - local	 Periodic (600) Periodic (400)
Aggradation - occurrence - thickness	 Poisson (28) Constant (0.1)
Flumy version	3.702

Table 19. Simulation parameters of four extracted wells test, Flumy version 3.702

Wells location on the simulation domain (aerial view) is similar to that used in the previous test, the wells are aligned two by two along flow and cross valley (Figure 89). The extracted wells have a thickness of 20 m.

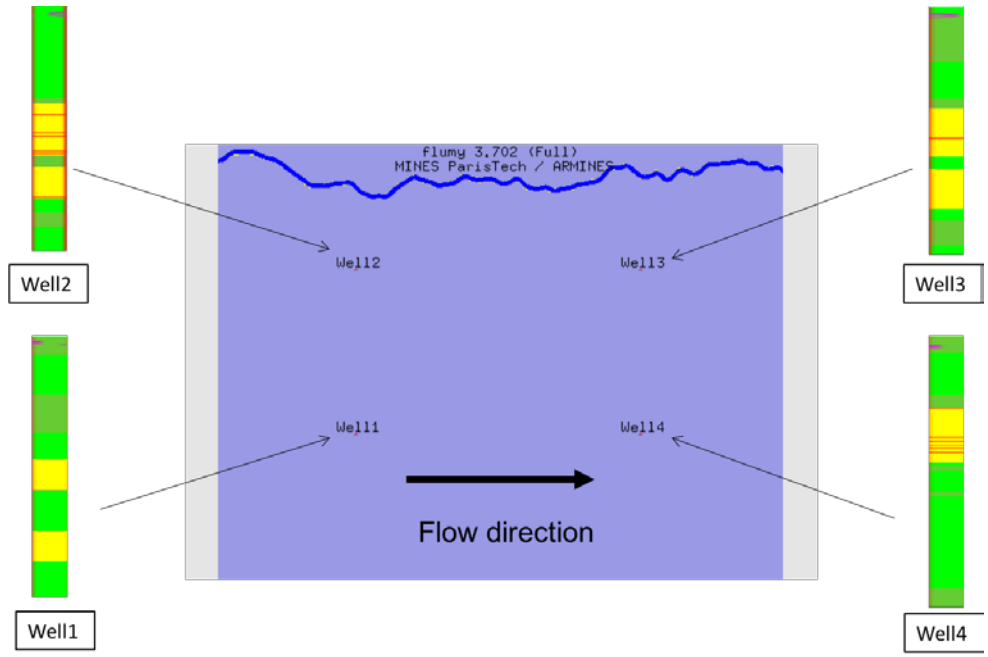

Figure 89. Conditional simulations with four extracted wells, Flumy version 3.702

The non-conditional simulation sand proportion is 20 %; and the one of the four extracted wells is slightly higher – 27.3% (sampling bias). The conditional simulation sand proportion is equal to 20 %.

Resulting reproduction of wells is shown on the next figures:

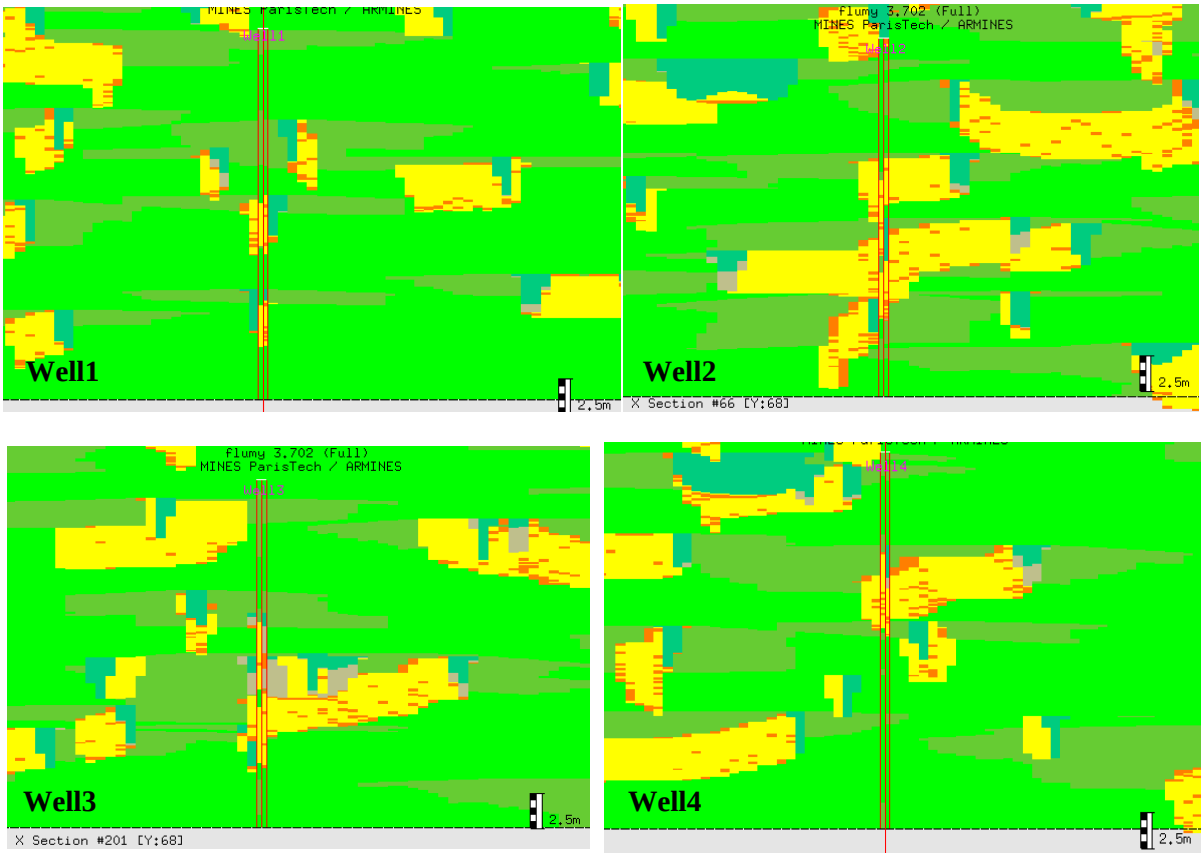

Figure 90. Four extracted wells reproduction, Flumy version 3.702

Conditioning statistics:

Parameters	Values
Well Sand Proportion	0.28
Simulation Sand Proportion at well	0.29
Matching at Sand (%)	79.82%
Well Channelized Facies Proportion	0.28
Simulation Channelized Facies Proportion at well	0.36
Matching at Channelized Facies (%)	96.35%

Table 20. Resulting conditioning statistics, four extracted wells test, Flumy version 3.702

In this test, the facies distribution is better respected than in the previous one. For example, two PB intervals in Well1 are accurately reproduced, and Well4 is reproduced almost exactly. But still, the problems on the transition between different facies inside one well remains: in Well2 the channel leaves the well to honor a small OB interval between two PB deposits, and then moves back to the well with a delay and stays there too long (depositing PB instead of OB above the PB interval). In Well3, the small OB interval between two PB bricks is not honored at all. All these differences between well data and simulated data at well, even if they seem to be small, result in an excessive Channelized Facies deposition: 36% deposited instead of 28% in the wells.

In this test, we can see more precisely the influence of the conditioning procedure on the sand distribution by a direct comparison of the sandbodies distribution between the non-conditional simulation and the conditional one.

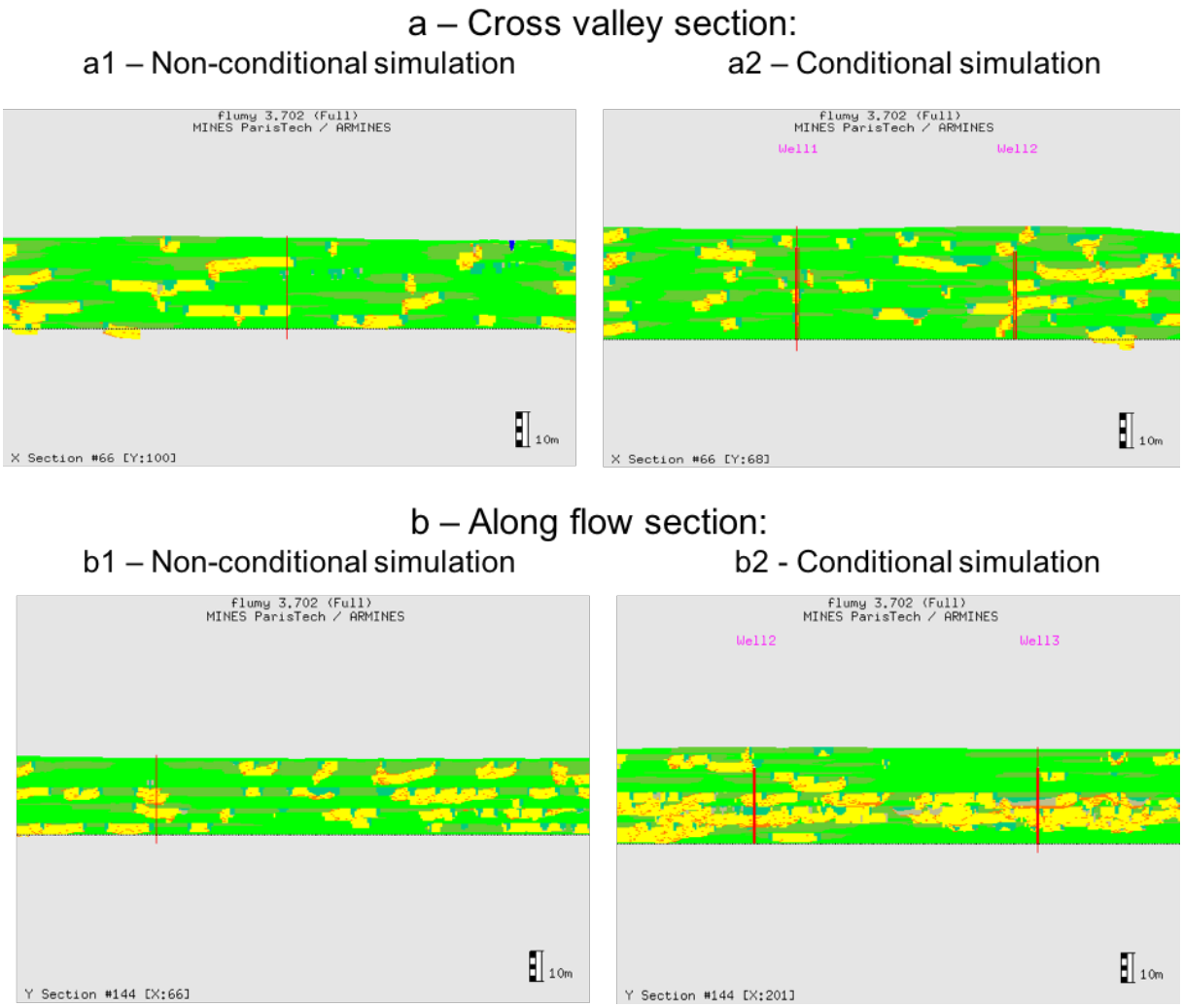

Figure 91. Four synthetic wells test, comparison of cross-valley (a1-a2) and along flow (b1-b2) of non-conditional and non-conditional simulations, Flumy version 3.702

Observations:

- The cross-valley sections do not present a lot of differences. They could be two realizations of one simulation with the same input parameters but different seed values.
- On the contrary, the longitudinal cross-sections of non-conditional and conditional simulations are very different in terms of sandbodies distribution: conditional model is obviously richer in sand than a non-conditional one. Because the resulting sand proportion of both simulations is equal to 20%, we can conclude that a conditional simulation has less uniform sandbodies distribution than the non-conditional one. The channel is too often attracted to the wells aligned along the flow direction, which results in an increasing sand deposition in the wells longitudinal sections. The issue of the spatial sand proportion in conditional simulation is needed to be solved to improve the conditioning procedure.

3.2.4 Conclusions

The tests presented above aim to estimate the exactness of wells reproduction during conditional simulations. Analysis of the results included the visual analysis of well reproduction, as well as the conditioning statistics (exact matching between well and simulation data) and, in the tests of several wells, comparison of cross-sections of non-conditional and conditional simulations with the same input parameters.

Two types of single well tests were performed: one-facies well (OB or PB) and three-facies well (OB - PB - OB bricks). The first tests revealed that the initial conditioning algorithm permits to honor a well composed of only one facies using either “attraction” or “repulsion” technique. Besides of it, one-facies well tests showed that it is more efficient to interpret the data using Non-Channelized and Channelized facies classification, rather than using the initial Flumy classification (OB, LV, PB …) or grain size description (Clay, Levee, Sand).

The tests of three-facies well aimed at checking the potential of the conditioning techniques to successfully reproduce transition between data facies. During the tests, it was detected that the initial conditioning algorithm favors Channelized Facies deposition by attracting the channel either too early (replacing the Non-Channelized facies below the Channelized facies by Channelized facies), or too late (not honoring completely the Channelized facies). Another issue concerns the channel expulsion from a repulsive well: during the PB $\rightarrow$ OB transitions: due to the lowering of the erodibility during the repulsion phase, the channel stays blocked in the well and leaves it only after the next avulsion.

The tests conducted with several wells (synthetic and simulated) were performed in order to, firstly estimate the reproduction of more than one well and, secondly, compare the spatial sand distribution in the non-conditional and conditional simulations using the same input parameters. The conditioning statistics of well reproduction is similar to the three-facies well results (the same problems of transitions between different groups of facies were observed). Moreover, the comparison of longitudinal cross-sections shows the excessive sand deposition along the wells aligned along the flow direction, indicating that the favored sand deposition at wells is also propagated to the area along the flow direction containing the wells.

These questions will be addressed in the section §3.4: Revised conditioning techniques.

3.3 Resulting sand spatial distribution

As suggested from the tests conducted with four wells, the conditioning procedure influences the sand distribution, favoring its accumulation in the well vicinity along the flow direction.

This chapter aims at studying the influence of dynamic conditioning on the spatial sand distribution in Flumy simulations. The results are estimated using the various well locations on the simulation domain relatively to the flow direction.

Tests are conducted keeping the same procedure as for the multi-well conditioning from extracted wells. This ensures the compatibility between well data and simulation parameters. It also provides a non-conditional 3D block to be compared with the conditional one in order to evaluate the influence of the conditioning on the sand distribution.

The tests presented in this part vary from each other by the number of wells (2, 8, 7 and 15 wells) and their location on the simulation domain (along a cross valley line, aligned perpendicular to the flow). The objective is to investigate the "pure" influence of conditioning procedure by comparing the conditional simulations obtained from different sets of parameters.

General test conditions, used both for non-conditional and conditional simulations, are the following:

Parameters	**Values**
Channel max depth	3 m (channel width = 30 m)
Grid size	4005 m x 4500 m x 60m; grid lags: 15m x 15 m Oxy = (524000; 4447500)
Avulsions - regional - local - Sandbodies extension	 Periodic (500) Periodic (360) Standard
Aggradation - occurrence - thickness - Sand proportion	 Poisson (80) Constant (0.1) Medium
Flumy version	4.005

Table 21. General simulation parameters for the tests of spatial sand distribution, Flumy version 4.005

3.3.1 Influence of flow direction

The first tests represent a conditional simulation with 2 extracted wells. The objective is to study if there is a relationship between the spatial sand distribution and the flow direction in the conditional simulation. In this section, the different sand proportions will be given using N_G (Net-to-Gross) notation.

Two sets of non-conditional simulations are performed over the same domain with the simulation parameters given in Table 21 but with different flow directions: simulation 1, flow to the North; simulation 2, flow to the N-NW. Two wells are extracted from each non conditional simulation (Figure 92; Figure 93).

The extracted well statistics are:

- simulation 1 (flow to the North), N_G of extracted wells = 38.6%;
- simulation 2 (flow to the N-NW), N_G of extracted wells = 52.9%.

The difference between two extracted wells sets is explained by a sampling bias. Sand Proportion Maps (SPM), created from non-conditional and conditional simulation blocks, are presented on the next figures:

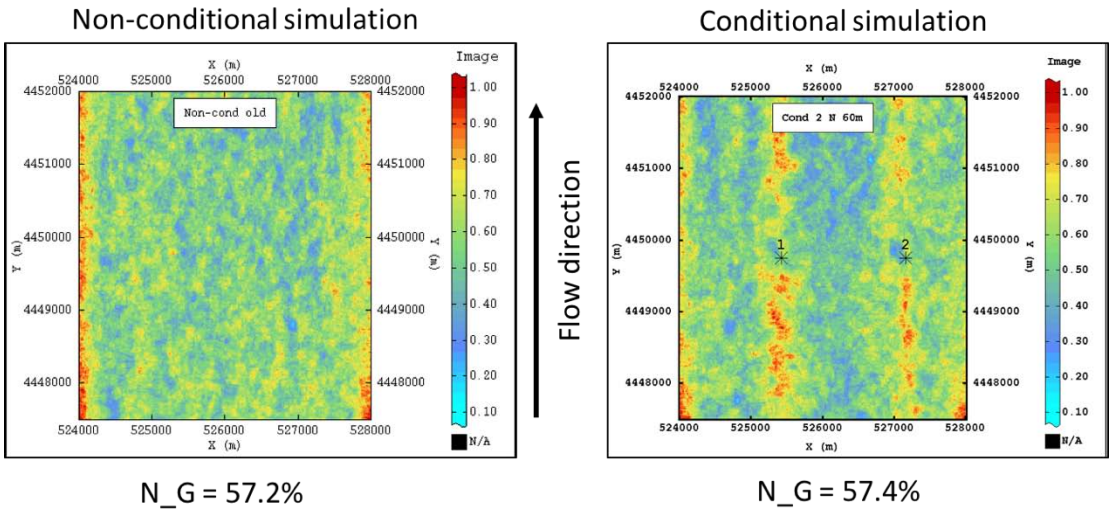

Figure 92. Sand Proportion Maps comparison, 2 wells test, non-conditional (left) and conditional (right) simulations with resulting N_G, Flumy version 4.005

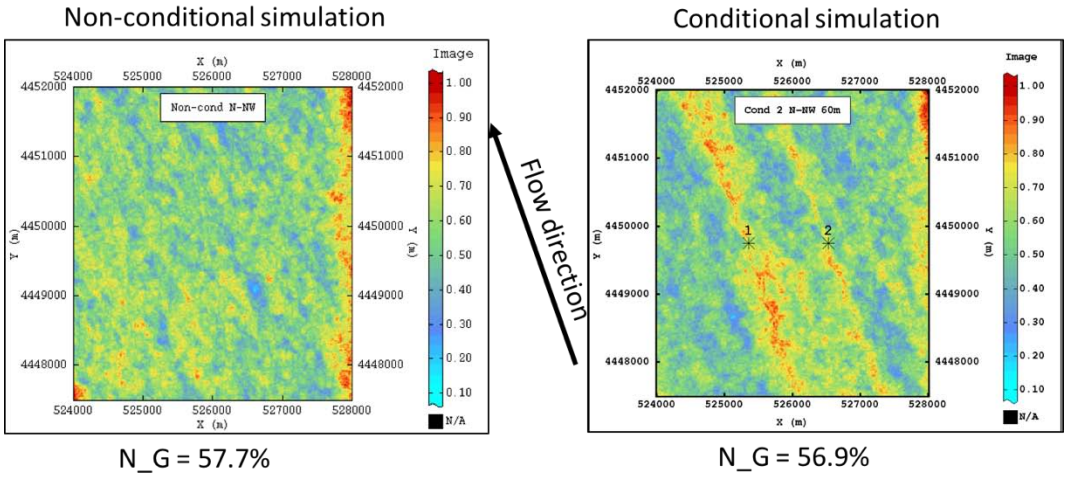

Figure 93. Sand Proportion Maps comparison, 2 wells test, flow direction N-NW, with resulting N_G

Observations:

In case of the North flow direction simulations, non-conditional and conditional simulation N_G are very close: 57.2% and 57.4% respectively. Both models contain the same amount of sand and the differences found on the SPM are truly the change of the model homogeneity by the conditioning processes. On all figures, the more concentrated sand zones are observed in the domain borders. Two more sandy lines are clearly visible on the conditional SPM, they correspond to elongated strips of sand proportion higher than the N_G of the simulation, each well is contained in one of these strips, and the strips length is parallel to the flow line. These results show that the sand deposition is

influenced during conditioning by the flow direction, when it is homogeneously distributed in a non-conditional simulation (except for the border effects).

In the conditional simulation run with a different flow direction (N-NW), while keeping the wells at the same location (Figure 93) the sandy strips are still visible around the wells, and are oriented along the flow direction.

The possible reason for this phenomenon is that Channelized Facies deposition is favored at attractive wells location. Firstly, the favored migration (larger migration rate than the average one) results in larger point bars deposition in the vicinity of the well. Secondly, the forced regional avulsions ensure that new channel paths pass through the attractive wells (pseudo topography containing some valleys parallel to the flow line). A third point to be looked for is that the channel may be blocked at the well during the PB → OB transition (because of the reduced migration rate) which increases the channel lag deposition inside the well.

Conditioning statistics for 2 wells reproduction, flow direction = N, are:

Parameters	**Values**
Well Sand Proportion	0.39
Simulation Sand Proportion at well	0.52
Matching at Sand (%)	69.61%
Well Channelized Facies Proportion	0.56
Simulation Channelized Facies Proportion at well	0.69
Matching at Channelized Facies (%)	99.87%

Table 22. Resulting conditioning statistics, 2 extracted wells test, Flumy version 4.005

Conditioning statistics, flow direction = N-NW:

Parameters	**Values**
Well Sand Proportion	0.53
Simulation Sand Proportion at well	0.51
Matching at Sand (%)	47.67%
Well Channelized Facies Proportion	**0.72**
Simulation Channelized Facies Proportion at well	**0.86**
Matching at Channelized Facies (%)	98.85%

Table 23. Resulting conditioning statistics, 2 extracted wells test, flow direction N-NW, Flumy version 4.005

The conditioning statistics show that the problem of excessive Channelized Facies deposition remains. The simulation Channelized Facies proportion (flow–N: 0.69; flow–N-NW: 0.86) is higher than the data Channelized Facies proportion (flow–N: 0.56; flow–N-NW: 0.72) (Table 22, Table 23).

3.3.2 Case of aligned wells

Another test subject is the influence of the well layout compared to the flow direction. Two different well sets are used for the conditional simulation: one set of wells aligned along the flow direction and one aligned perpendicular to the flow direction.

3.3.2.1 Wells aligned along the flow

The 8 extracted wells are aligned by four, along the flow direction. The objective is to check whether the several wells aligned in the flow direction increase the effect of the “sand lines”.

Conditions of test: 8 extracted wells aligned by four; N_G of extracted wells = 55%; flow direction = N. The resulting Sand Proportion Maps are:

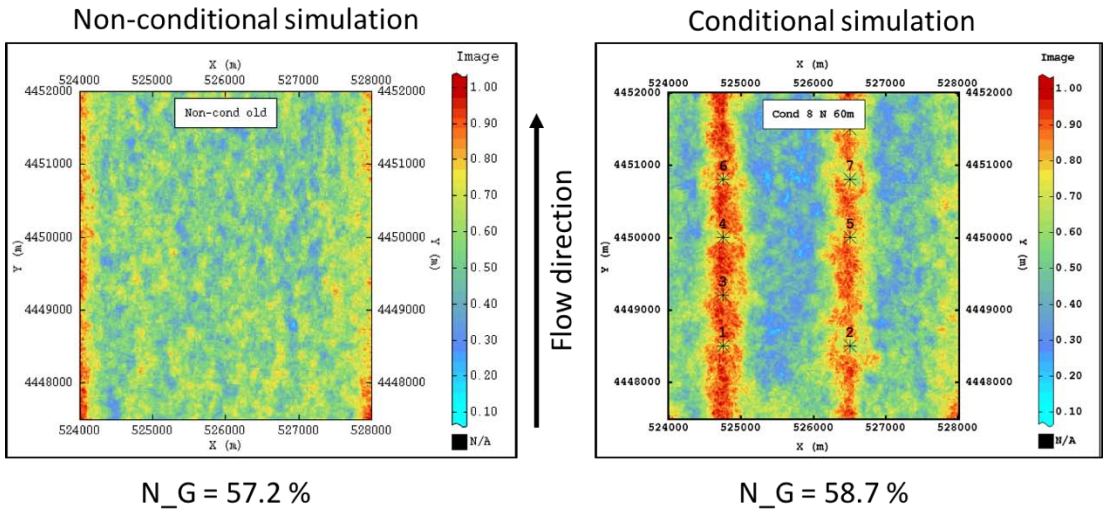

Figure 94. Sand Proportion Maps comparison, 8 wells test, with resulting N_G

Observations: comparing with Figure 94 – left, the SPM of conditional simulation (Figure 94 – right) is much more heterogeneous. The “sand lines” are strongly marked. Several wells aligned in the flow direction result in a more frequent attraction of channel (by migration and avulsions conditioning procedures), which gives such a contrast in the spatial sand distribution.

Conditioning statistics shows an excessive Channelized facies deposition at well (0.80 instead of 0.67 in well data):

Parameters	**Values**
Well Sand Proportion	0.55
Simulation Sand Proportion at well	0.63
Matching at Sand (%)	73.10%
Well Channelized Facies Proportion	**0.67**
Simulation Channelized Facies Proportion at well	**0.80**
Matching at Channelized Facies (%)	97.17%

Table 24. Resulting conditioning statistics, 8 extracted wells test, Flumy version 4.005

3.3.2.2 *Wells aligned perpendicularly to the flow*

The last two tests concern wells aligned perpendicularly to the flow direction, forming a "barrier" for the channel in the middle of the simulation domain.

In field case studies, wells are often drilled with regular mesh. So, it is possible that in some cases the wells are densely aligned cross-valley, forming a line perpendicular to the flow direction. Such a well layout is studied in the last two tests: 7 wells cross-valley, with 500 m distance between them, and 15 wells cross-valley, with 250 m distance. (Reminder: channel depth = 3 m, channel width = 30 m.).

These tests are conducted to check if a denser well cross-valley deposition has an impact on the "Sand Lines" formation and parameters. When regularly distributed, each well may evenly attract and repulse the channel; so, it may result in more homogeneous general sand distribution in the conditional model. Besides of it, these tests permit to check how the channel passes through a "barrier" of wells: a comparison of upstream and downstream distribution will be made.

3.3.2.2.1 7 wells

Conditions of test: N_G of extracted wells = 49%; flow direction = N; distance between wells is 500 m.

The resulting Sand Proportion Maps are:

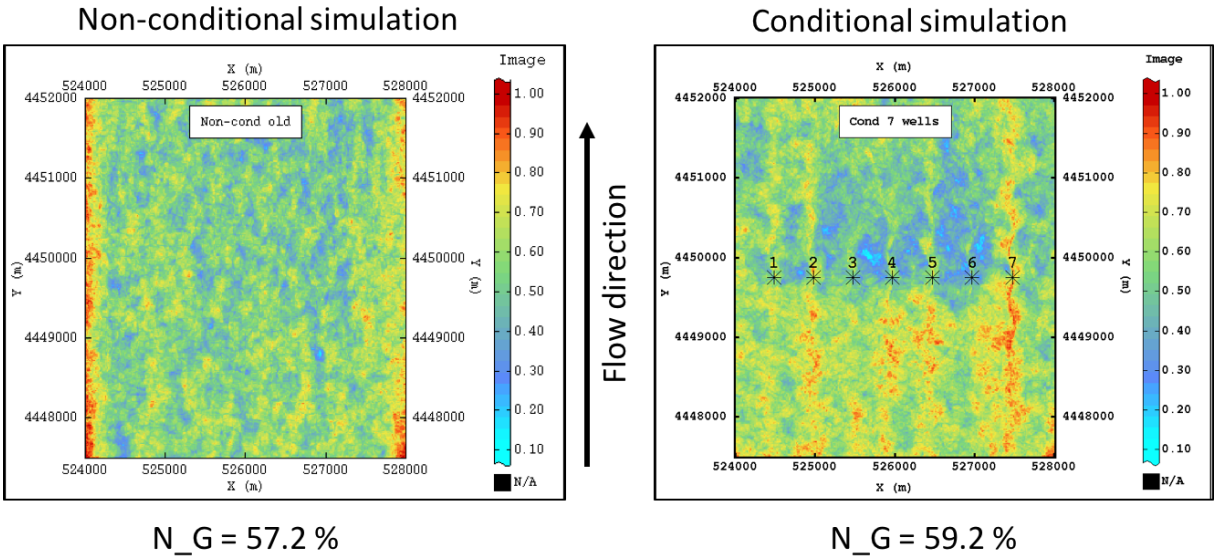

Figure 95. Sand Proportion Maps comparison, 7 wells aligned perpendicularly to the flow direction, with resulting N_G

Observations: firstly, the concentrated "Sand lines" are still represented on the conditional SPM. It should be noted that the wells with a higher concentration of sand engender the more apparent sand lines. In this example, wells 2, 4, 5 and 7 contain nearly 53% of sand, unlike the other wells (1, 3 and 6) which contain 44 to 47% of sand. So, the first hypothesis about sand lines nature is proved: it is an attraction effect of the conditioning process which forces the channel to pass more often by the wells (and sometimes to stay blocked at the well location); the richer the well in sand, the more intense the "sand lines" are.

Secondly, there is a difference between the upstream and downstream sand distribution. The sand proportion in the upstream part of simulation domain (before the wells barrier) is higher than in the

downstream part (after the wells). Possible reason for this phenomenon is that meanders are developing more rapidly upstream from the attractive wells because the conditioning procedure increases the migration rate in the upstream part of the domain. This hypothesis will be studied in details in the next test.

Conditioning statistics: Excessive Channelized Facies deposition is still observed.

Parameters	Values
Well Sand Proportion	0.49
Simulation Sand Proportion at well	0.45
Matching at Sand (%)	54.70%
Well Channelized Facies Proportion	**0.65**
Simulation Channelized Facies Proportion at well	**0.74**
Matching at Channelized Facies (%)	97.78%

Table 25. Resulting conditioning statistics, 7 wells aligned perpendicularly to the flow direction, Flumy version 4.005

3.3.2.2.2 15 wells

The last test performed with the initial conditioning procedure is a more complicated case than the previous one: the 15 extracted wells are aligned cross-valley.

Conditions of test: N_G of extracted wells = 55.3%; flow direction = N; distance between wells is 250 m.

Resulting Sand Proportion Maps are:

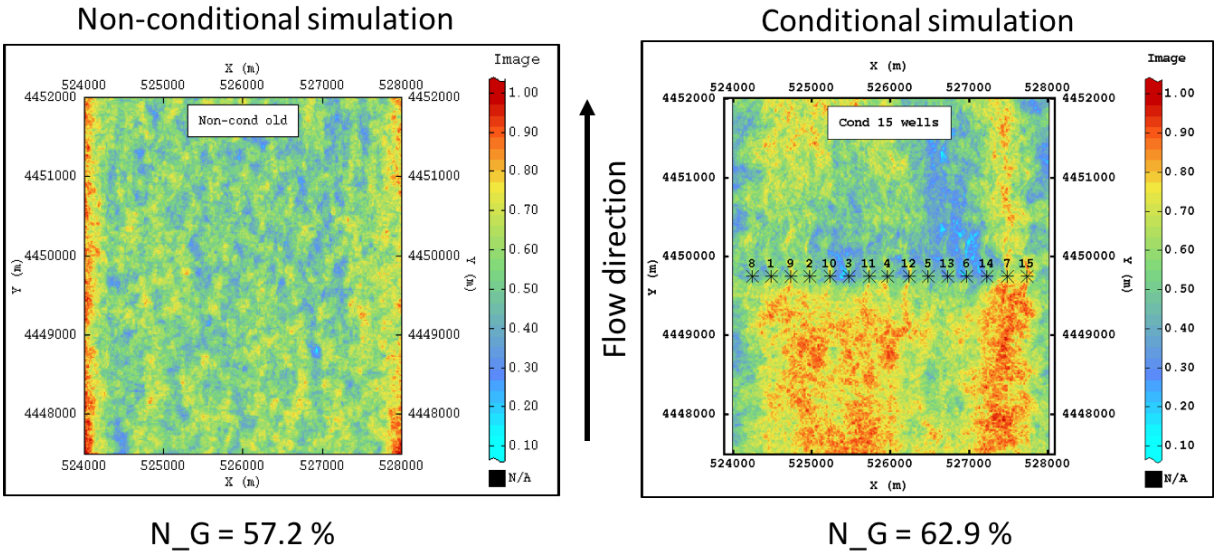

Figure 96. Sand Proportion Maps comparison, 15 wells aligned perpendicularly to the flow direction, with resulting N_G

Observations: In this test, the “sand lines” are transformed into large “sand zones” which, of course, represent a large problem for the conditioning in general: such a difference between non-conditional and conditional simulations (run with the same parameters and the extracted wells perfectly compatible with) is unacceptable. Besides of it, the distance between the wells is not so small related to the channel width: 250 m for a channel width of 30 m. The upstream/downstream sand distribution

is extremely contrasted: nearly 70-90% upstream versus 20-60% downstream. In order to explain the reasons of this problem, the horizontal Z-slices of non-conditional and conditional models are compared (40 m elevation among 60 m thickness in total).

Comparison of horizontal Z-slices (non-conditional and conditional simulations):

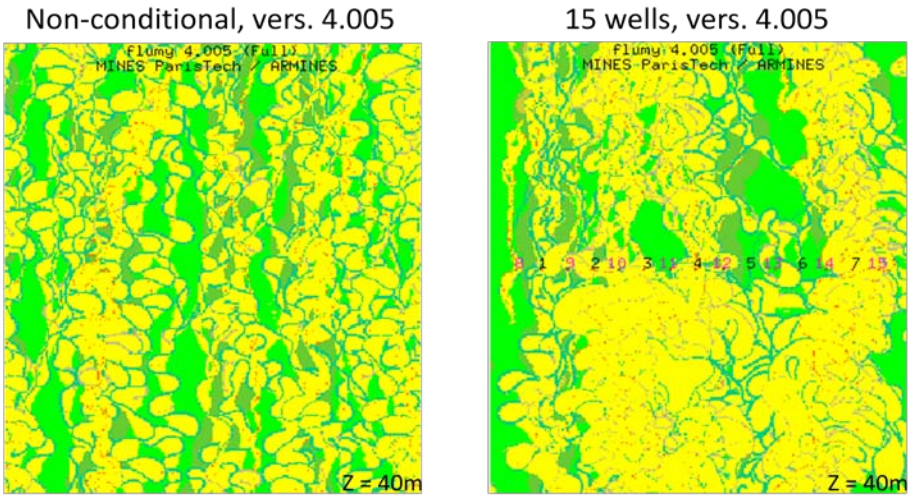

Figure 97. Comparison of horizontal slices of two models: non-conditional, Flumy vers. 4.005 (left) and conditional by 15 aligned wells, Flumy vers. 4.005 (right). Z = 40 m

Observations: it is obvious that in the conditional simulation the meanders upstream from the well line are much more developed than downstream. Possible reasons for this phenomenon is that only the upstream meanders are influenced by the wells during the migration (increase of erodibility for a faster migration, in order to attract the channel to the well) which results in more developed meanders upstream from the well lines.

Conditioning statistics:

Parameters	**Values**
Well Sand Proportion	0.55
Simulation Sand Proportion at well	0.44
Matching at Sand (%)	52.63%
Well Channelized Facies Proportion	**0.69**
Simulation Channelized Facies Proportion at well	**0.78**
Matching at Channelized Facies (%)	97.30%

Table 26. Resulting conditioning statistics, 15 wells aligned perpendicularly to the flow direction, Flumy version 4.005

3.3.3 Conclusions

All the representative tests, performed to estimate the influence of the conditioning on the spatial sand distribution, have been summarized in this section before presenting the general conditioning modifications.

The spatial sand distribution in non-conditional and conditional simulations (with the same input parameters) was analyzed by a comparison of the Sand Proportion Maps of these two simulations. The wells used for the tests were extracted from non-conditional simulations, so they were compatible with the simulation parameters used during the conditional simulation. This permits to avoid the influence of a change of model parameters between the conditional and non-conditional simulations and allows estimating the “pure” impact of the dynamic conditioning.

The first phenomenon to mention is the presence of “sand lines” formed for each well along the simulation domain in the flow direction. Width and sand content of such lines does not depend on the well position relative to the flow direction (aligned along the flow or cross-valley). If several wells are aligned along the flow, the sand lines become more apparent. Besides of it, the wells with a higher sand proportion (in relation to model N_G) tend to create more concentrated sand lines. The reason of this heterogeneity in the conditional simulation is related to a too “efficient” conditioning method for the migration and avulsions processes: the channel is strongly attracted to the well each time Channelized Facies are needed. In order to balance a global sand distribution in a simulation, the conditioning techniques should be “softened”.

Another problem was detected when using several wells, densely aligned cross-valley. In this case the wells look as a “barrier” for the channel, the upstream sand proportion is much higher than the downstream one. Horizontal Z-slices show that the meanders upstream from the wells are far more developed than after. The possible reason of such difference is that only upstream meanders are attracted to the wells during migration conditioning, resulting in much more developed meander loops.

The next part of this chapter contains all the modifications of the conditioning algorithm, made during this work.

3.4 Revised conditioning techniques

Conditioning procedure has been modified in order to solve the problems detected during the previous tests that mainly resulted in larger sand deposits in conditional simulation when compared to the non-conditional with similar parameters. The problems correspond to the following situations:

1. Channel arrives to the well too early or too late (if Channelized Facies are required at well)
2. Excessive Channelized Facies deposition at wells
3. Channel stays blocked at well (PB → OB transition)
4. Sand Lines parallel to the flow at well location over the simulation domain
5. Difference between the upstream and downstream sand distribution with respect to well layout.

All basic concepts of conditioning stay unchanged: well first interpretation, Active Level and Active Brick. Modifications have been performed in three domains: i) the dynamic well interpretation (small changes), ii) completely reviewed Update AL algorithm and iii) the migration, avulsion and aggradation adaptation algorithms.

As it was explained in Chapter 2.3, detailed techniques of conditioning are functions in the software source code. The lain structure of existed functions are not changed; all the modifications concern the internal algorithms of each function. Here is a short reminder of the three main conditioning algorithms:

1. *Active Level update* (for each conditioning well) is called each time the topography is changed at the well. This function was completely changed; the new algorithm will be presented in details in the section §3.4.2.
2. *Migration adaptation* is called at each iteration, before the migration of the channel centerline, and after AL update. The output is a correction of channel migration velocity (attraction or repulsion). This function was slightly modified (additional constraint for channel attraction is added), but main principles remain the same.
3. *Avulsions adaptation* is called before each local or regional avulsion. The output is a correction of the real topography ("pseudo topography"), so that the new channel is tossed at the right locations (according to conditioning). This function was also slightly changed (not only local, but also regional forced avulsions), main principles remain the same.

A forth function has been added to the list:

4. *Aggradation blocking* is called in two cases. First is when waiting a forced avulsion in Avulsions adaptation algorithm. The second case is when the channel is inside a well and its Active Brick is non-erodable (Non-Channelized).

In the following, we develop and illustrate the concepts and the corresponding modifications in the algorithms. Results of the tests are presented in the next section §3.5 due to the complex interactions between the different algorithms (Active Brick, Active Level, migration and avulsion conditioning algorithms) that prevent to perform a validation test for each modification.

3.4.1 Revised treatment of thin lithofacies data

The dynamic well interpretation procedure (details in section §2.2.3), intends to limit the situations where thin deposits could not be honored given the channel size.

The only modification made in this procedure is the integration of neutral facies bricks (Undefined facies, UDF, which has no influence on the conditioning), into the dynamically interpreted data bricks.

The first case concerns the presence of Undefined facies next to a thin Channelized facies and can be represented as following (Figure 98):

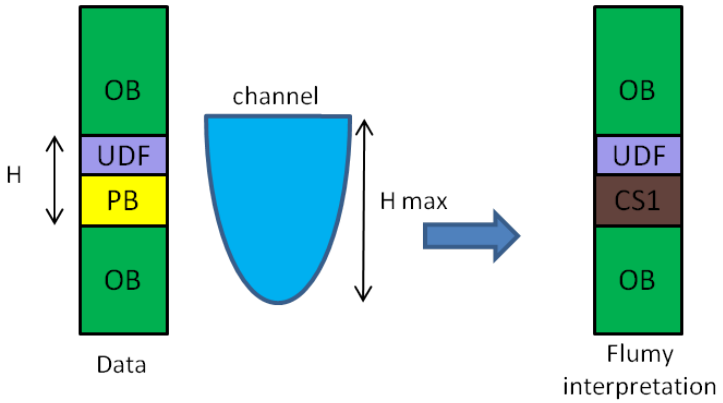

Figure 98. First case of new dynamic well interpretation

Second case, concerns the presence of Undefined facies next to a thin interval of Non-Channelized facies (e.g.; OB, Figure 99), is:

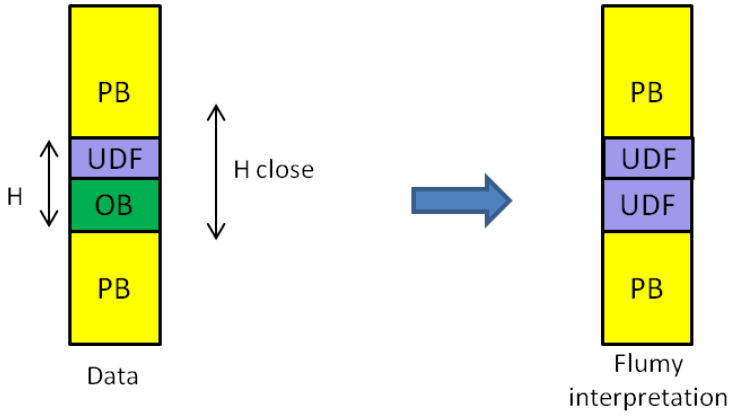

Figure 99. Second case of new dynamic well interpretation

3.4.2 Refactoring of updating Active Level

A new algorithm of AL update is proposed. This procedure has been reviewed and completely modified in its logic. It helps to solve directly the problem (3), and indirectly the problems (2), (4) and (5) listed in the introduction of the section 3.4. More of these problems may be the consequence of the channel blocked at well.

One of the most important new features is the concept of "*Wet Well*": anytime the channel is located inside the well, the well status is changed and well data are treated separately. Besides of Wet Well concept, a large attention is paid to the correctness of the channel arrival time into the well which aims to resolve the problem (1).

The list of the new internal variables used (as before, calculated at the well location) are the following:

botab – active brick bottom elevation;
topab – active brick top elevation;
zb – well bottom elevation;
zt – well top elevation;
zdep – bottom elevation of the last deposit remaining part to be validated;
zdom – top elevation of the last deposit (corresponds to the floodplain elevation at the well);
twat – top water elevation (top elevation of the channel in a *Wet Well*).

Remark: As in the initial *AL Update* function, AL can be updated only upwards. The only possible case for decreasing AL is when eroding data at well by removing some top deposits by an erosion surface (manual operation in Flumy, look at Flumy user guide for more details). The new *Wet well* feature is illustrated below in the case A. All cases have been identified by a new letter.

New *AL Update* algorithm can be described as eight steps. This structure is more generalized than before; it contains not only the new *Wet Well* concept, but also has less separation of algorithm into Erodable / Not-to-be-eroded deposits cases. Neutral facies have been used as more as possible when the data facies correct nature was not relevant.

In a pseudo-code form, new *AL Update* algorithm can be presented as the following:

1. New deposit while the channel is at the well (case A) – quit;
2. New deposit outside the well (case B) – quit;
3. New deposit below Active Level (case C) – quit;
4. New deposit below channel bottom (case D) – continue;
5. New deposit including Active Level (case E) – continue;
6. New deposit at non-erodable Active Level (case F) – go back to 5 or quit;
7. New erodable deposit at erodable Active Level (case G) – go back to 5 or quit;
8. New non-erodable deposit at erodable Active Level (case H) – go back to 5 or quit.

Now, these steps will be considered in more details.

1) New deposit while the channel is at the well (case A)

First case considers all possible *Wet Well* deposits. As the channel in Flumy has a parabolic section shape and occupies several grid cells, the channel at well can correspond to a small part of the channel, not especially the deepest part. Four different channel positions can be considered. It should be also mentioned that in such case new deposit is always below the channel bottom (*zdom* = channel bottom, following the principles of the simulation construction and erosion processes).

Case A1 (Figure 100): the channel is fully below well bottom (both new deposition and top water elevations); in such case, nothing happens, AL is not changed.

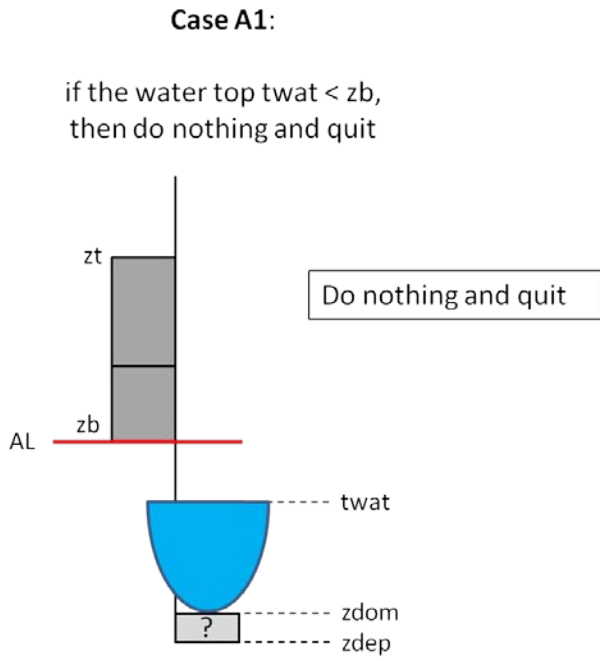

Figure 100. Case A1 in new Update AL algorithm

Case A2 (Figure 101): Water top elevation falls inside the well (between well bottom and top). Two sub-cases are possible in such situation: in Case A2a, AL falls inside the water, between channel bottom and top water. In this case, AL is set to the top water elevation. This AL update will help to avoid channel blocking at the well and also is rather logical – the channel will deposit erodable facies until top water, so it is better to validate it completely as soon as possible.

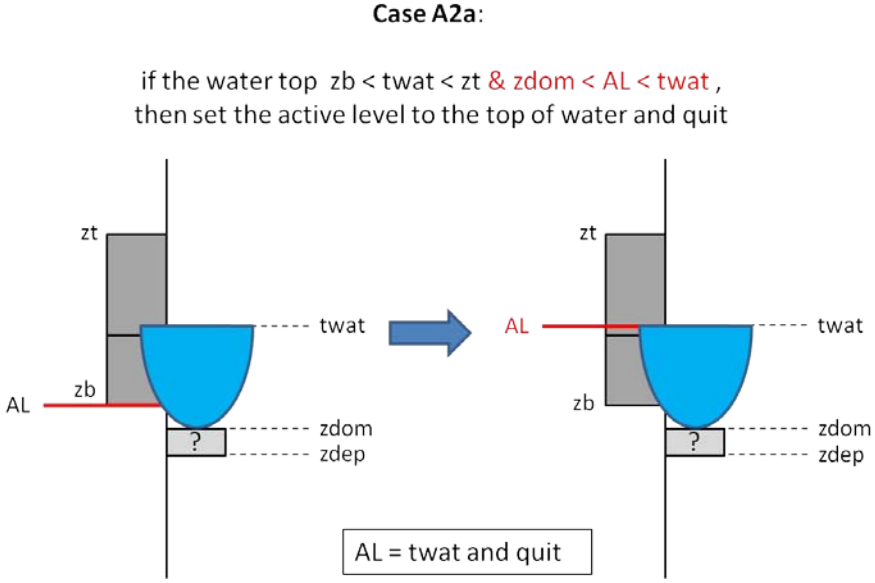

Figure 101. Case A2a in new Update AL algorithm

In Case A2b (Figure 102) AL is not inside the water, but below the bottom of the channel. In this case AL is not changed (firstly, the new deposit below the channel should be validated before).

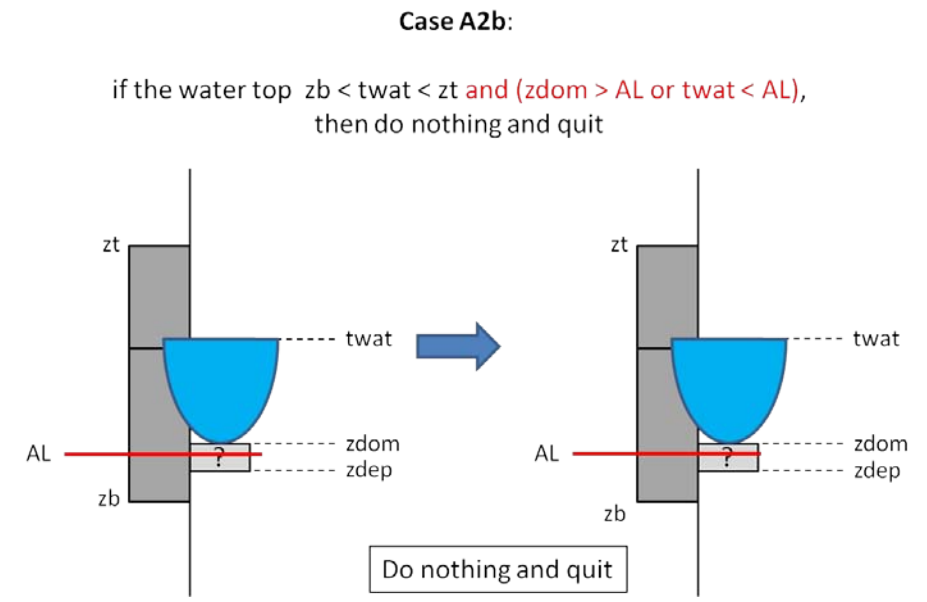

Figure 102. Case A2b in new Update AL algorithm

Case A3 (Figure 103): new deposit is inside the well (between well bottom and top), and top water elevation is above the well top. In this case, AL is set to the well top. Similarly to case A2a, it is better to validate completely the future deposit (to avoid blocking), but this time – until the well top.

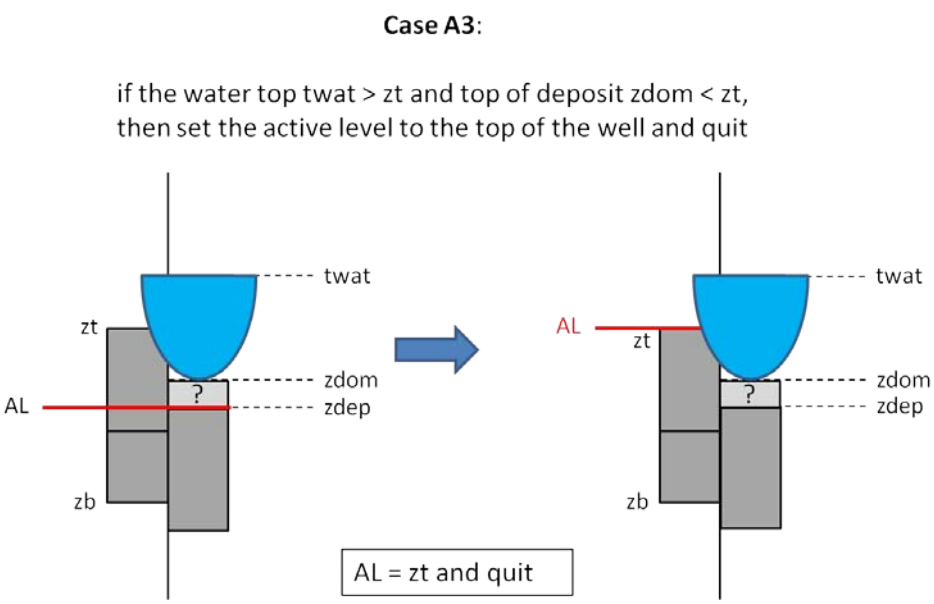

Figure 103. Case A3 in new Update AL algorithm

Case A4 (Figure 104): the channel completely above the well top. AL is not changed in this case.

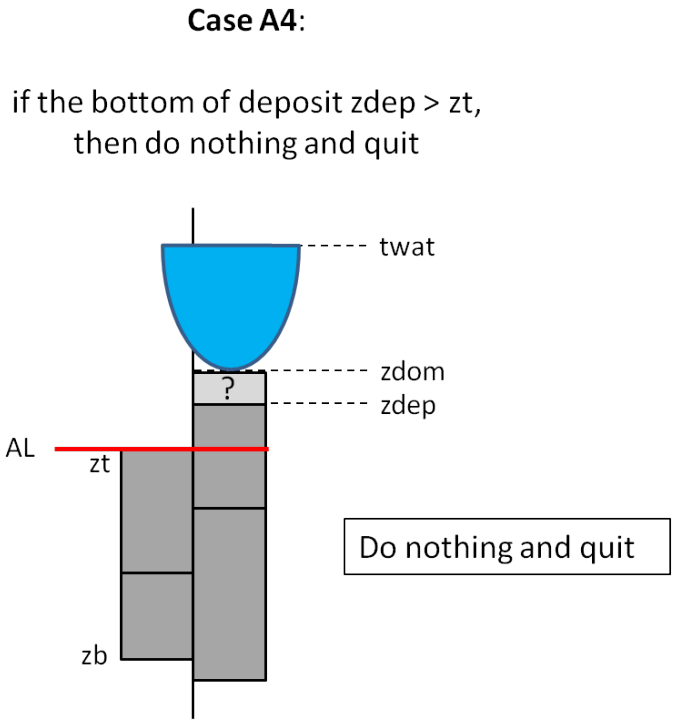

Figure 104. Case A4 in new Update AL algorithm

2) New deposit outside the well (case B)

In these two cases, the channel is somewhere in the domain and the new deposits are entirely below or above the well.

Case B1 (Figure 105): if deposits are entirely below the well bottom, AL is not changed.

Case B1:

if the deposit top zdom < zb,
then do nothing and quit

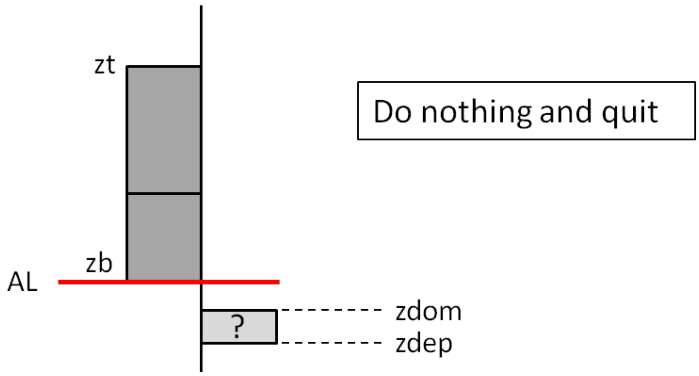

Figure 105. Case B1 in new Update AL algorithm

Case B2 (Figure 106): if deposit is entirely above well top, AL is not changed.

Case B2:

if the deposit bottom zdep > zt,
then do nothing and quit

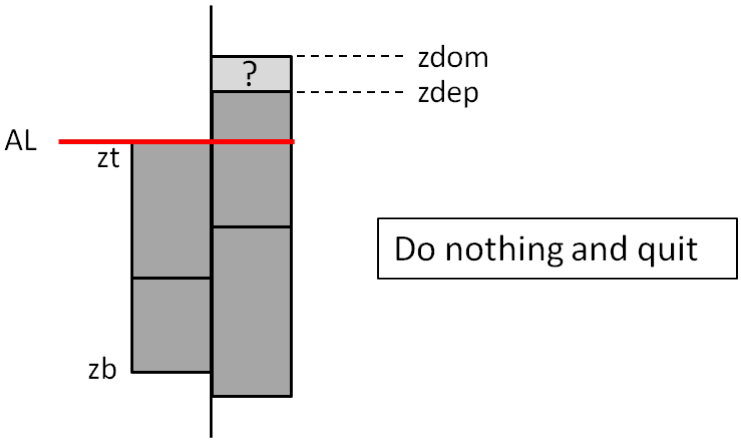

Figure 106. Case B2 in new Update AL algorithm

3) New deposit below Active Level (case C)

If the new deposits are entirely below AL, nothing is changed (AL is never updated down). This case can be useful during manual erosion of the simulation, or after case G3.

Case C:

if the domain elevation zdom < AL, then do nothing and quit

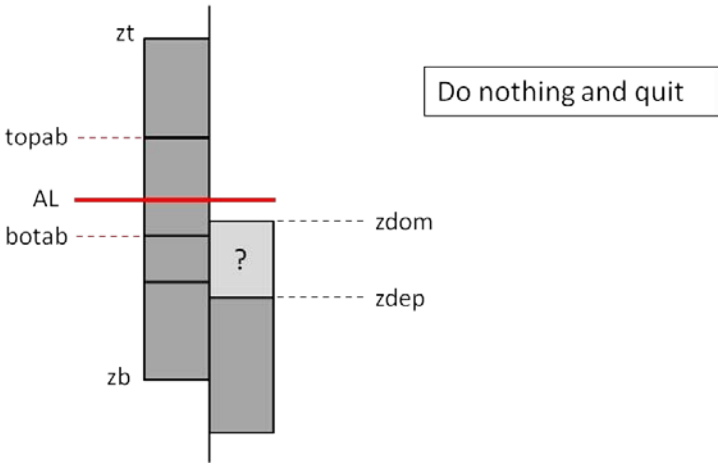

Figure 107. Case C in new Update AL algorithm

4) New deposit below channel bottom (case D)

This case concerns the validation of data that becomes too deep compared to the channel elevation for a re-deposition (even in the case of the channel presence at the well). Now, maximal possible re-deposition thickness is equal to 100% of channel maximum depth (*zmin* = *zdep* - H_{max}, see §3.2.1.2.2). Thus, AL is updated up to zmin and data below zmin are considered honored.

Case D: validation of data that become too deep (100% of channel max depth)
zmin = zdom – Hmax (minimum elevation that can be redeposited)

if the active level is too deep (i.e. AL < zmin), then set the active level to zmin elevation and continue

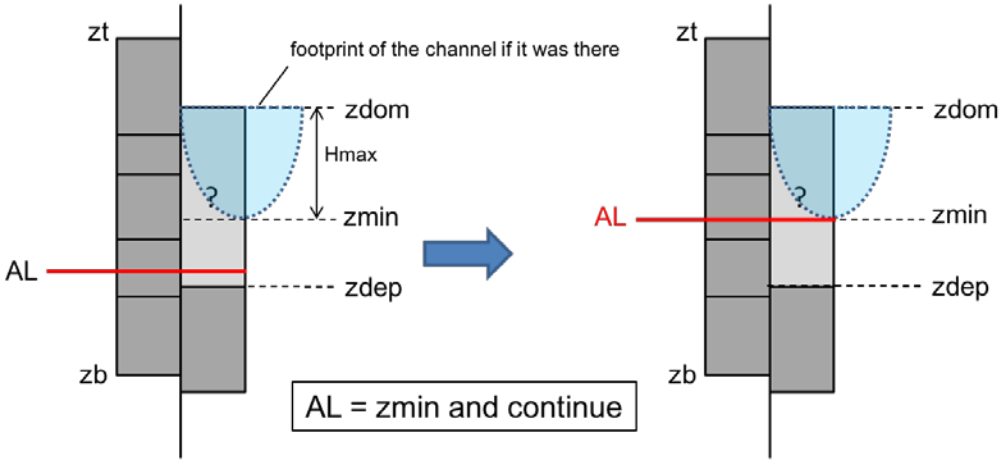

Figure 108. Case D in new Update AL algorithm

5) New deposit including Active Level (case E)

If AL falls inside the new deposits, only deposits part above AL will be considered. After that, the algorithm continues. This case is a preparation for the last three ones, in order to generalize the input AL and *zdep* relations.

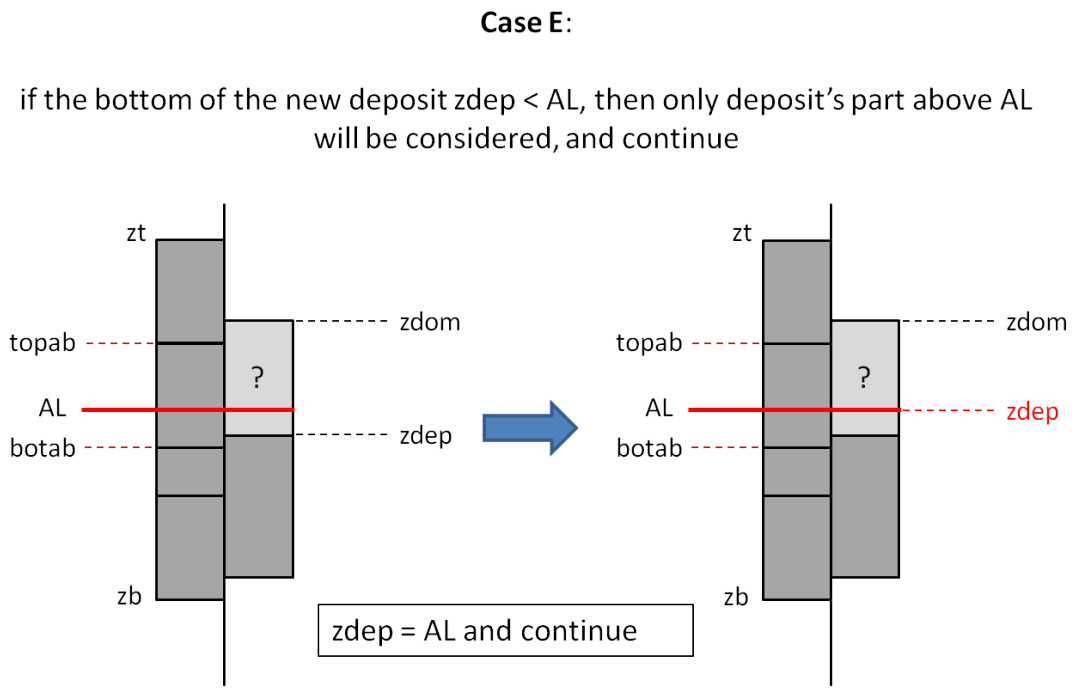

Figure 109. Case E in new Update AL algorithm

Reminder: when starting the last cases F, G and H, the considered deposit bottom (*zdep*) is always equal to the Active Level and above the channel bottom (AL = *zdep* > *zmin*).

6) New deposit at non-erodable or neutral Active Level (case F)

In these two cases, the Active Brick is always non-erodable or neutral and considered deposits can be any facies (even if PB is deposited instead of OB – it can not be replaced).

Case F1 (Figure 110): the top of AB is below the top of the new deposit. In such a case, AL is set to the top of AB and AB is changed (top of previous AB is equal to bottom of new AB). If new deposit is non-erodable, it will protect the deposit against the replacement; if new deposit is erodable (PB), it already cannot be replaced and should be validated.

Then, case E is called in order to set *zdep* equal to the AL.

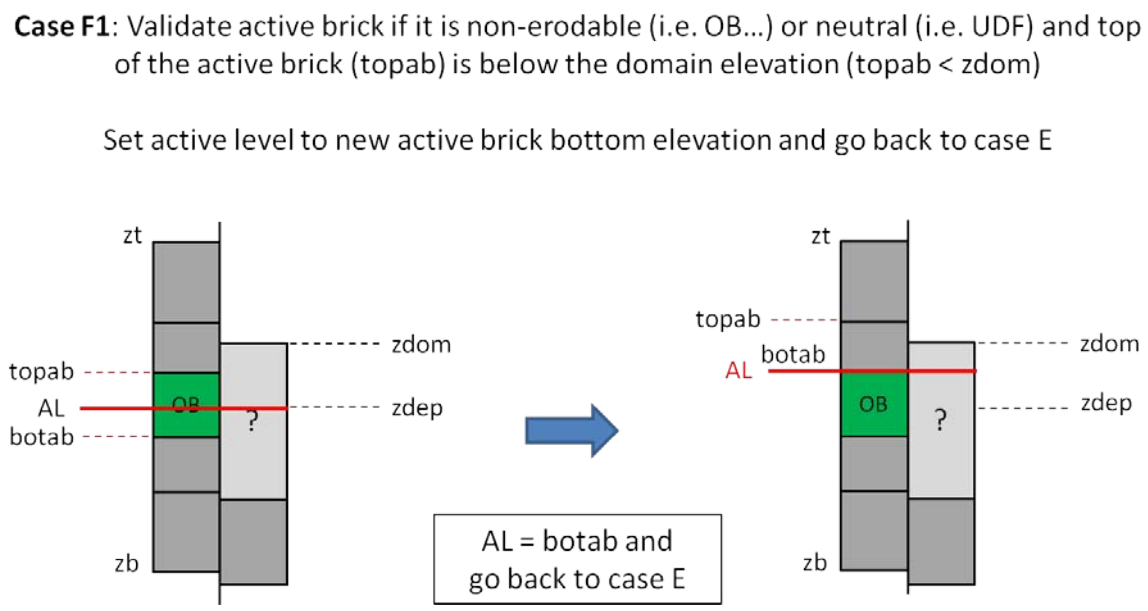

Figure 110. Case F1 in new Update AL algorithm

Case F2 (Figure 111): top of AB (non-erodable or neutral active brick) is above new deposit top: AL is set to *zdom* elevation and algorithm stops.

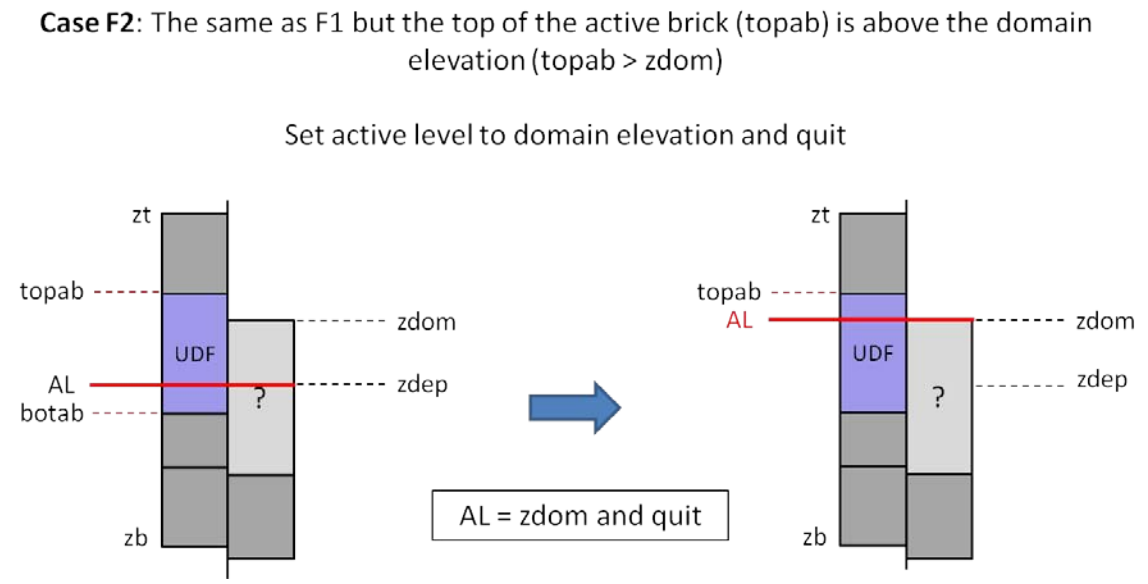

Figure 111. Case F2 in new Update AL algorithm

7) New erodable deposit at erodable Active Level (case G)

This case considers erodable facies in the AB. Since the sandy facies can replace the clay and levee facies, in this case there is a possibility to wait for the "good" deposit (case D was already performed before, so *zmin* is less or equal to AL).

Case G0 (Figure 112): This is a verification of the new deposit consistency. The proportion of non-erodable deposit part is computed. Only if this proportion is more than 80%, the case G continues; else, algorithm stops until a new deposition occurs. So, only erodable deposits are considered here.

Case G0: If active brick is erodable (i.e. PB), check the composition of non-validated deposit: compute the proportion of non-erodable (i.e. OB) deposit part

pob = proportion of non-erodable data between AL and zdom (excluding neutral)

If pob is **greater** that 20% , then do nothing and quit. Else, test the next case G1.

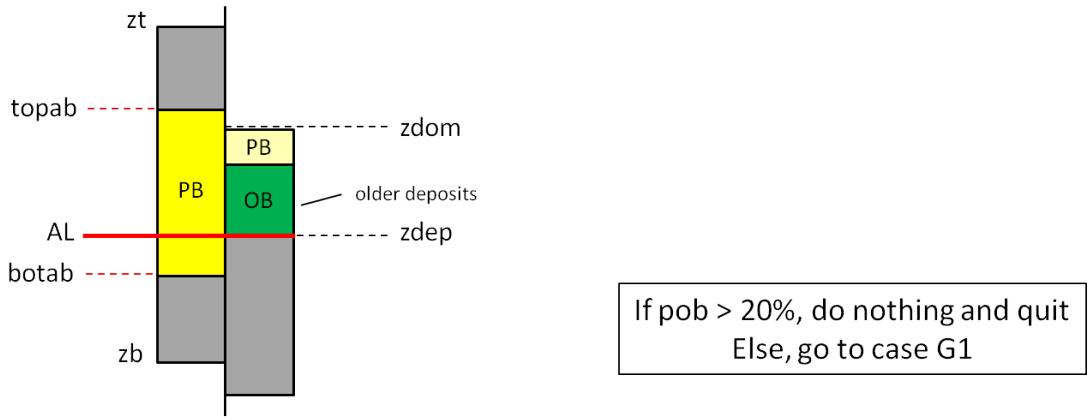

Figure 112. Case G0 in new Update AL algorithm

Case G1 (Figure 113) is similar to the F1: if top of AB is below the new deposit top, AL is set to top AB and Active Brick is changed. It helps to avoid the channel blocking in the well, if the next AB is non-erodable. Then, case E is called in order to update *zdep* variable up to AL.

Case G1: Validate active brick if it is erodable (i.e. PB…), top of active brick is below the domain elevation, and deposited brick is erodable (i.e. PB)

Set active level to new active brick bottom elevation and go back to case E

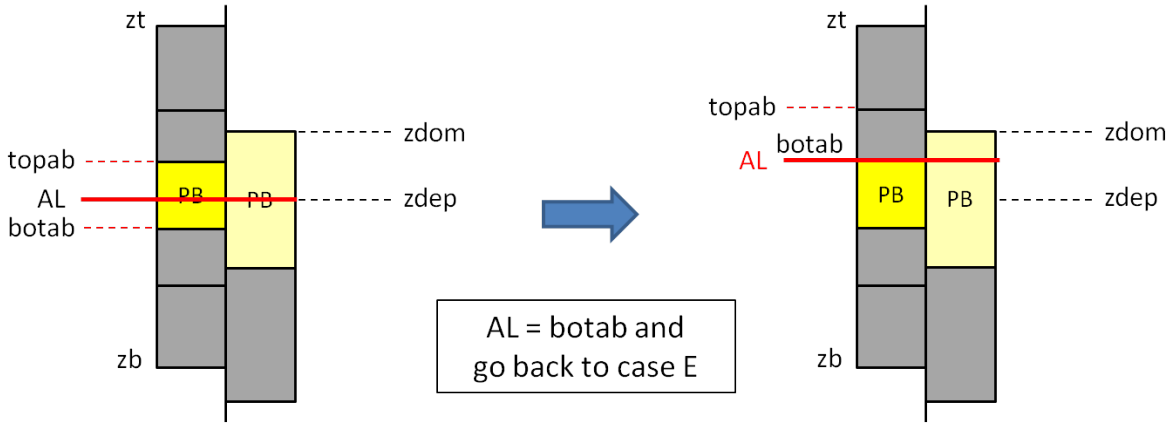

Figure 113. Case G1 in new Update AL algorithm

Case G2 (Figure 114) is similar to F2: if top of AB is above the new deposit top, AL is set to *zdom*. Then, the last case G3 should be tested.

Case G2: The same as G1 but the top of the active brick (topab) is above the domain elevation (topab > zdom)

Set active level to domain elevation and test the next case G3

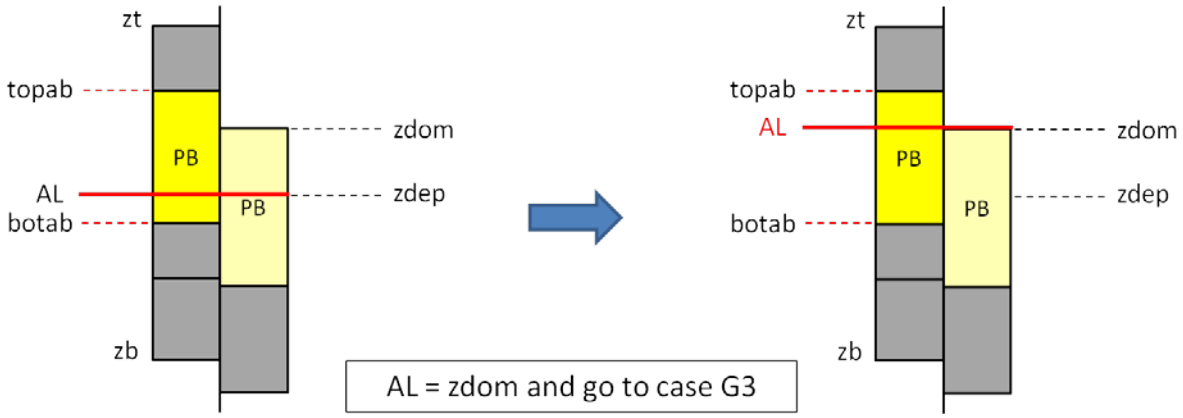

Figure 114. Case G2 in new Update AL algorithm

Case G3 (Figure 115) is a final check: if the remaining gap between AL and top of AB is too small (less than 0.1 m by default), AL is set to top AB. This will help to protect the bottom of the next AB if it is non-erodable.

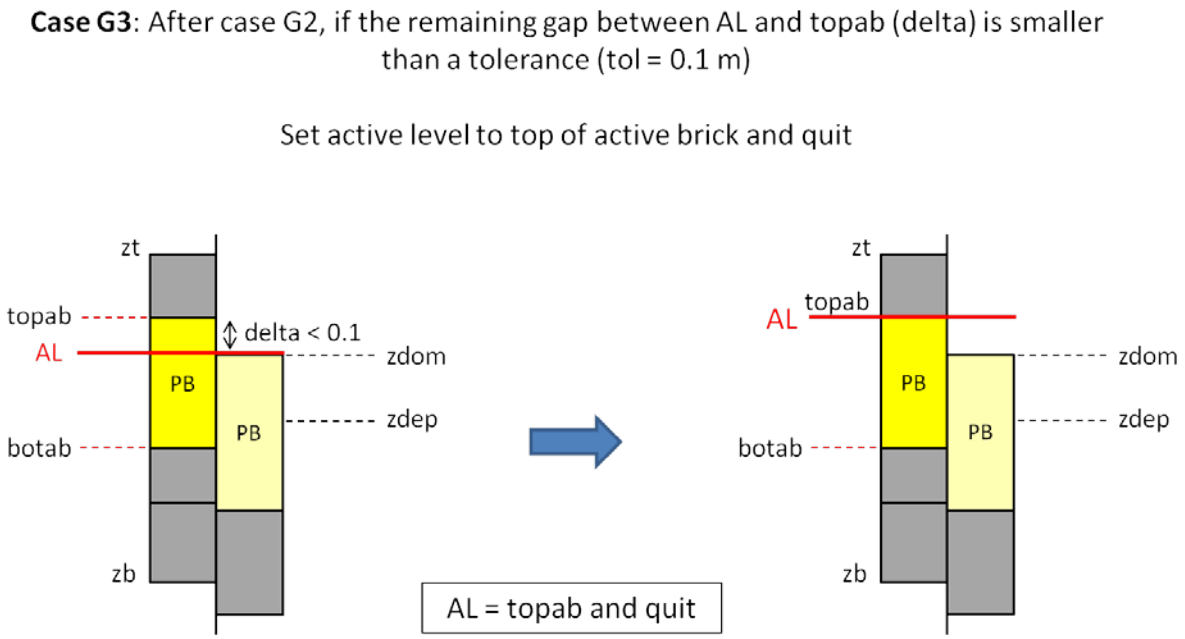

Figure 115. Case G3 in new Update AL algorithm

The last case considers the only remaining deposit possibility: AB is erodable, deposit is non-erodable. In some cases, even such deposits should be validated.

8) New non-erodable deposit at erodable Active Level (case H)

Case H1 (Figure 116) can be applied before case G0: if AB is erodable, new deposit is completely non-erodable or neutral, and top of AB is above the new deposit top – algorithm stops, nothing is changed. There is still a possibility to replace this deposit by an erodable one.

Case H1: If active brick is erodable (i.e. PB…), top of active brick is **above** the domain elevation (zdom), and deposited brick is non-erodable (i.e. OB) or neutral (i.e. UDF)

Then, do nothing and quit

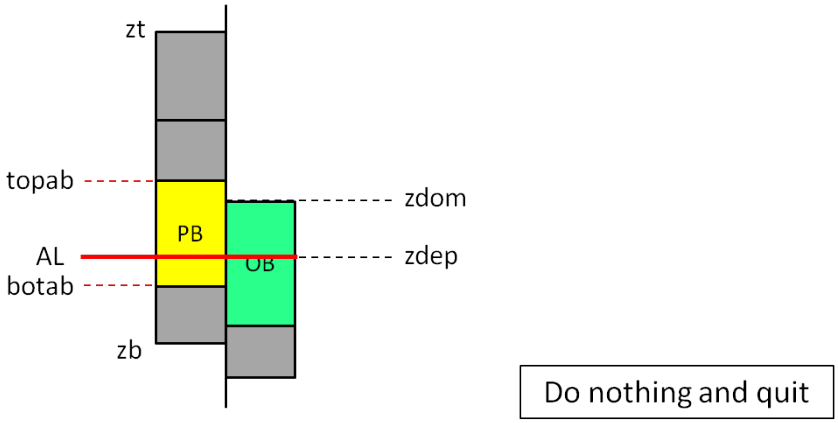

Figure 116. Case H1 in new Update AL algorithm

The next two cases take into account the possible presence of small data bricks (relatively to the channel depth). In such situation the case G can be never called, waiting for the channel arrival at the well. But, if the proportion of OB data bricks is high, non-erodable deposit can be validated, because it is difficult to honor the relatively small sandy bricks without replacing non-erodable deposits at well. In this case the proportion of non-erodable data is computed.

Case H2 (Figure 117) is called if top of AB is below the new deposit top. The proportion of non-erodable data in the well is computed, between AL and new variable *zob*:

$$zob = \min(zdom, \max(tops\ of\ non\text{-}erodable\ bricks))$$

So, if the proportion of non-erodable data between *zob* and AL (excluding neutral) is less than 50%, the algorithm stops and nothing is changed.

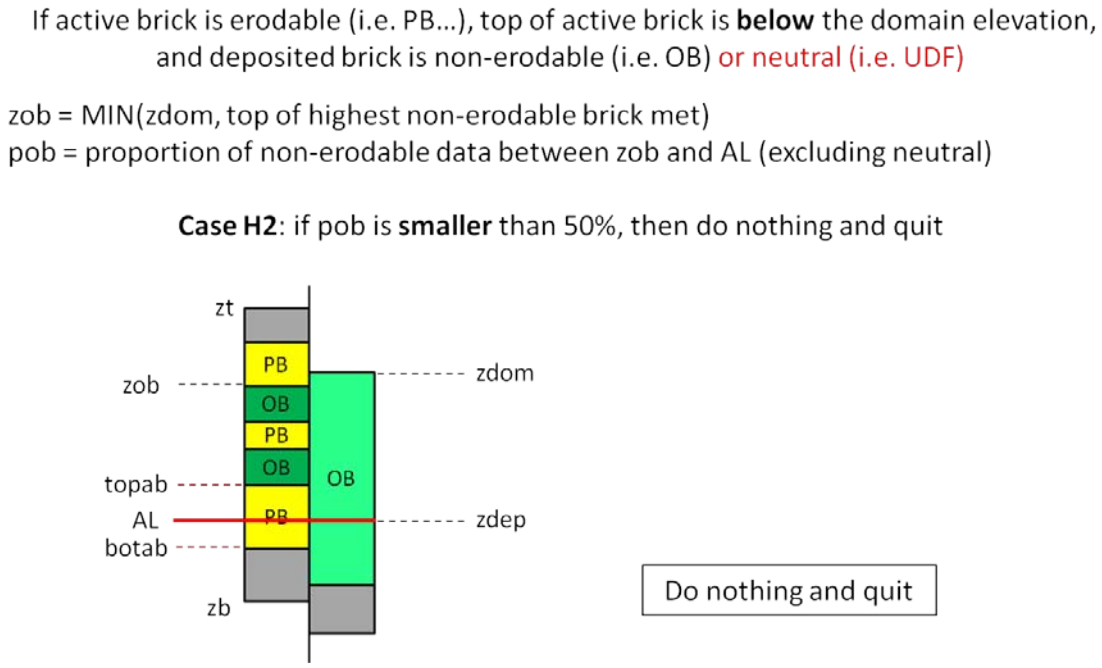

Figure 117. Case H2 in new Update AL algorithm

Case H3 (Figure 118): if this proportion is more than 50%, AL is set to *zdom*:

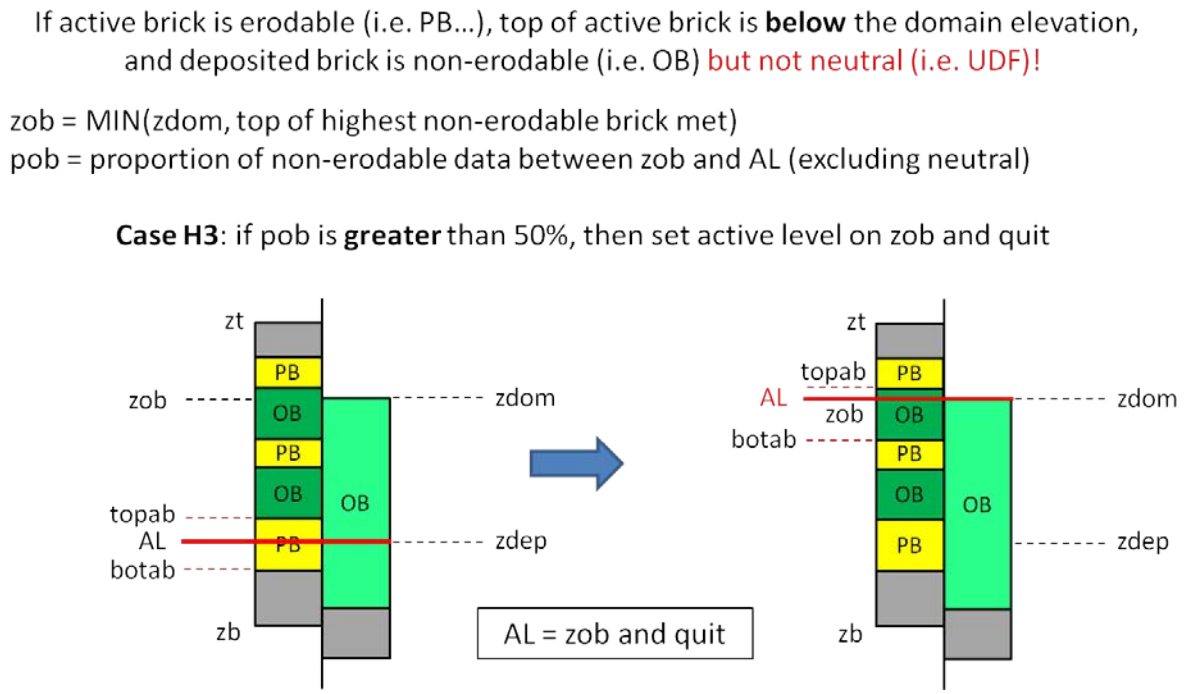

Figure 118. Case H3 in new Update AL algorithm

3.4.3 Improvement of migration adaptation

Some modifications were introduced in the **migration adaptation** procedure. The main steps of the function were not modified. Here is a reminder from section §2.3.2:

- Step 1: Identification of the **closest upstream** channel point to the well**,** according to the Von Mises distance formula,
- Step 2: Computation of the **multiplicative** factor of erodibility correction at the selected channel point either for attraction or repulsion (migration correction),
- Step 3: **Extension** of the correction to the points of the same channel meander – a bend between the two points with the velocity perturbation = 0.

The first modification of migration adaptation function is the reduction of the distance of meander attraction. Now, only meanders close enough to the well location are attracted. The default maximum distance is 15 * *w* (where *w* is the channel width).

This restriction aims at avoiding "useless" meander attraction: if the channel is too far away from the well, there is no way for it to be attracted for depositing Channelized Facies at well before the next avulsion. The initial unlimited distance of attraction resulted in excessive meander development upstream (as seen in the test of 15 wells, Figure 96) without any positive impact on conditioning statistics.

Step 1 of the algorithm is now presented as following: Identification of the **closest upstream** channel point to the well**,** according to the Von Mises distance formula:

a. If the distance between identified upstream point and the well is less than 15 * *w*, then continue with Step 2 and Step 3 described above;
b. If not, quit.

The second modification concerns the *avoidh* coefficient. As mentioned in section §2.3.2, if AB is a Channelized facies and "not-to-be-eroded" facies are present below the AB, the channel should not come to the well location too early (see Figure 64).

The tests showed that initial condition of protection ($h < avoidh$) was not sufficient. Now, this distance has been increased to a "repulsion" zone around the well with a bigger diameter equal to:

$$radius < 1.5 * avoidh,$$

where $radius = h - 0.5 * w$,

h = the distance between the chosen channel point (Step 1) and the well.

This aims at fixing the OB → PB transition problem (1).

The third modification: if the channel is inside a repulsive well ("not-to-be-eroded" active brick), the well becomes "attractive" (migration is favored). The multiplicative factor of the erodibility correction (Step 2) is equal to 2, so that the channel can leave the well by migration and is no more blocked. This aims at fixing the PB → OB transition problem (1).

3.4.4 Improvement of avulsions adaptation

By analogy with the migration corrections, two modifications were made.

The first modification concerns the forced avulsions (section §2.3.3). Initially, if a sand deposition was strongly needed at the well and it was not possible to attract the channel to the well by migration, a local avulsion was forced to toss a new path through the well. Now, we introduced the possibility to trigger a local or a regional avulsion in order to take into account the distance between the channel and the well. We use a threshold similar to that chosen for the migration correction (i.e. 15 * *w*). Thus, the function is performed as following:

If *above_al* > 0.98 or *gap_up* ≤ 0, then:

1) If the distance between the channel and the well is less than 15 * *w*, a forced local avulsion is triggered,
2) If the distance between the channel and the well is more than 15 * *w*, a forced regional avulsion is triggered.

Forced avulsions can not be performed more often than twice within the corresponding avulsion period parameter.

The second modification concerns *avoidh* distance. Initially, in order to protect the "not-to-be-eroded" facies below the "attractive" AB during the new avulsion tracing, a small conical shape of *avoidh* radius was constructed at the well location. Now, the conical shape has a larger diameter:

If $h < 5 * avoidh$, return

$$E_{corr} = -\text{gauss\_cov}\,(hh, 11w),$$

where *hh* – an anisotropic distance between the well and each grid point, $hh = \sqrt{(dx)^2 + 4(dy)^2}$;

dx and *dy* – projections of distance between the well and a grid point on the *Ox* (flow direction) and *Oy* axis respectively.

3.4.5 Blocking aggradation

Now, there exists a function to switch on/off the aggradation process. The aggradation is authorized during the simulation, except for two cases:

1) If the channel is at the well, and AB is "repulsive" (Non-Channelized Facies).
   In this case, the aggradation is blocked until the channel leaves the well. The third correction in migration conditioning (channel at the well → the migration is favored) minimizes the aggradation blocking time.
2) If the forced avulsions are needed but cannot be performed.
   In this case, the aggradation is blocked. As the avulsions forcing is an "extreme" case, which is performed at the last possible moment of sand deposition at the well, the aggradation blocking aims at decreasing an error in the well data reproduction. The aggradation is enabled after the avulsion.

3.4.6 Conclusions

The modifications of the existing conditioning functions are based on the problems detected in well reproduction and spatial sand distribution of conditional models. Most of these problems were related to the presence of the channel at the well and its integration into conditioning techniques.

In the next chapter, the modified conditioning procedure will be tested; old and new results will be compared.

3.5 Impact of the revised conditioning techniques

In this section the conditional simulations performed with the modified conditioning algorithms are presented and discussed with regard to the problems illustrated in the section §3.2 and §3.3.

These tests have been performed with the updated version of Flumy (5.600) when the initial conditioning tests were performed with the versions 3.700 and 3.702. Modifications in Flumy, beside the conditioning algorithms mainly concern computing algorithms, adjustment of internal coefficient, introduction of the local slope algorithm (see PhD thesis, B. Grappe, 2014). An illustration is given below with the Sand Proportion Maps (cf. section§3.1). Output sand proportion in new simulation is slightly higher – 60% of N_G compared to the 57.2% with the 4.005 Flumy version. Sand distribution in both non-conditional simulations stays uniform, without any significant concentration zones.

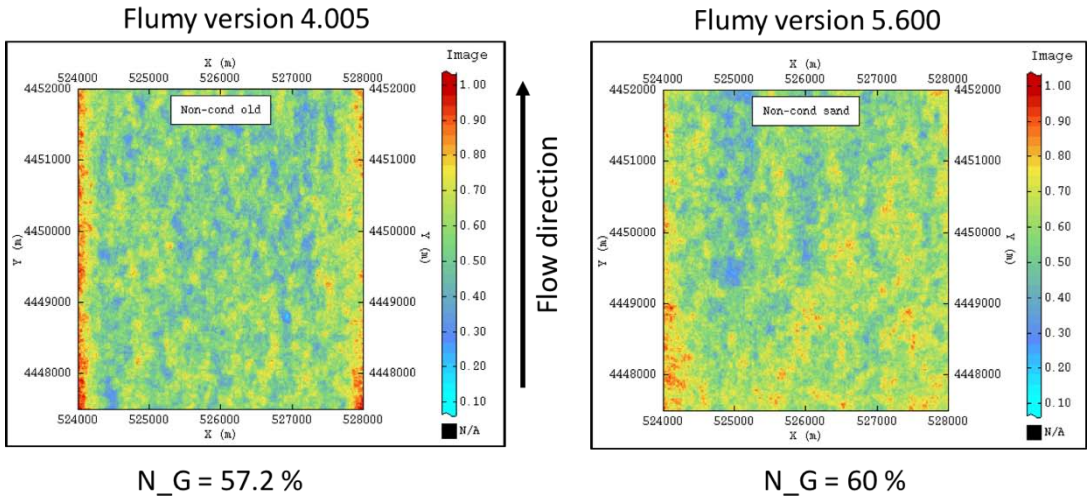

Figure 119. Sand Proportion Maps comparison, non-conditional simulation vers. 4.005 (left) and. 5.600 (right) with resulting N_G (flow to the north)

The impact of new version on conditioning results was also tested. The following Sand Proportion Maps illustrate the conditional simulation presented in section §3.3.2.2.2 (15 aligned wells, vers. 4.005) and the same test performed in vers. 5.600, but with old conditioning algorithm:

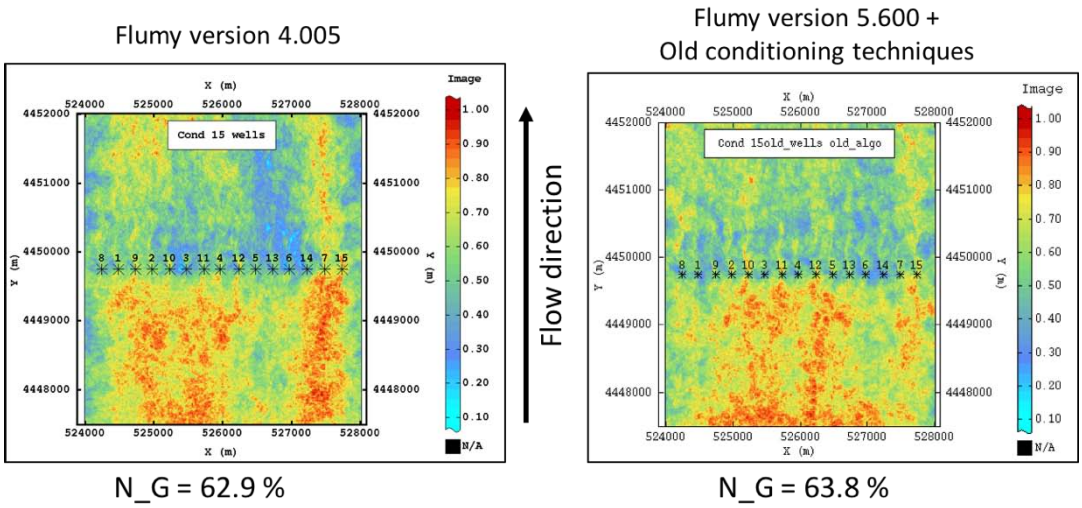

Figure 120. Sand Proportion Maps comparison, 15 extracted wells conditional simulation vers. 4.005 (left) and. 5.600 with old conditioning algorithm (right) with resulting N_G (flow to the North)

Both SPM on Figure 120 show the same problems in spatial sand distribution: a strong contrast between upstream and downstream meanders development. The conditioning statistics proves that new Flumy version alone does not improve the well exact reproduction:

Parameters	**4.005**	**5.600 + conditioning from 4.005**
Well sand Proportion	0.55	
Simulation Sand Proportion at well	0.44	0.60
Matching at Sand (%)	52.63%	80.49%
Well Channelized Facies Proportion	0.69	
Simulation Channelized Facies Proportion at well	0.78	0.76
Matching at Channelized Facies (%)	97.30%	98.72%

Table 27. Resulting conditioning statistics, 15 extracted wells test, Flumy versions 3.702 and 5.600 with old conditioning algorithm

This chapter is organized in the same manner as the one presenting the initial conditioning tests (section §3.2):

- comparison of multi-facies wells reproduction results (old vs. new);
- comparison of spatial sand distribution in non-conditional and conditional simulations (old vs. new).

In order to estimate the efficiency of the new conditioning algorithms, the input conditions of all tests stay the same: simulation parameters; the same synthetic wells are used, and the same technique of wells extraction from non-conditional simulations is performed in the tests with extracted wells.

3.5.1 Reproducing facies at wells

The tests presented in the previous chapter showed that there is a main issue on the reproduction of multi-facies wells, when the one-facies wells (both Channelized and Non-channelized facies classes) are 100% exactly reproduced.

In the following, multi-facies well tests and multi-well conditioning tests will be presented.

3.5.1.1 Multi-facies well

The well used in this test contains a succession of three facies, named in the following facies bricks. From bottom to top, they correspond to 10 m of OB, overlain by brick of 10 m of PB and finally 10 m of OB. Such test permits to estimate the ability of the new conditioning techniques to switch between different facies during the simulation as the initial technique tend to favor the channelized facies resulting in too much sand at well and in the simulation. Previously detected problems were:

- OB → PB transition – the channel arrives to the well location too early (eroding Non-Channelized facies) or too late (the lower part of central PB brick is not honored);
- PB → OB transition – the channel may be blocked inside the well at the top of the central Channelized facies brick (the well becomes “repulsive”, so the channel migration is blocked);
- as a result, Non-Channelized facies bricks were less honored.

3.5.1.1.1 Mean sand proportion

The first test is run using the default simulation parameters, mean sand proportion and standard type of sandbodies (Table 28).

Parameters	Old values	New values
Avulsions: - regional - local - Sandbodies extension	 Periodic (600) Periodic (400) Standard	 Poisson (600) Poisson (400) Standard
Aggradation: - occurrence - thickness - Sand proportion	 Poisson (28) Const (0.1) Poor	 Poisson (28) Normal (0.1 , 0.03) Poor
Flumy version	3.702	5.600

Table 28. Flumy simulation parameters, test of three-facies well, default parameters, Flumy vers. 3.702 and 5.600

Results with the initial conditional algorithms and the new ones are graphically compared (Figure 121) and statistics are also computed (Table 29).

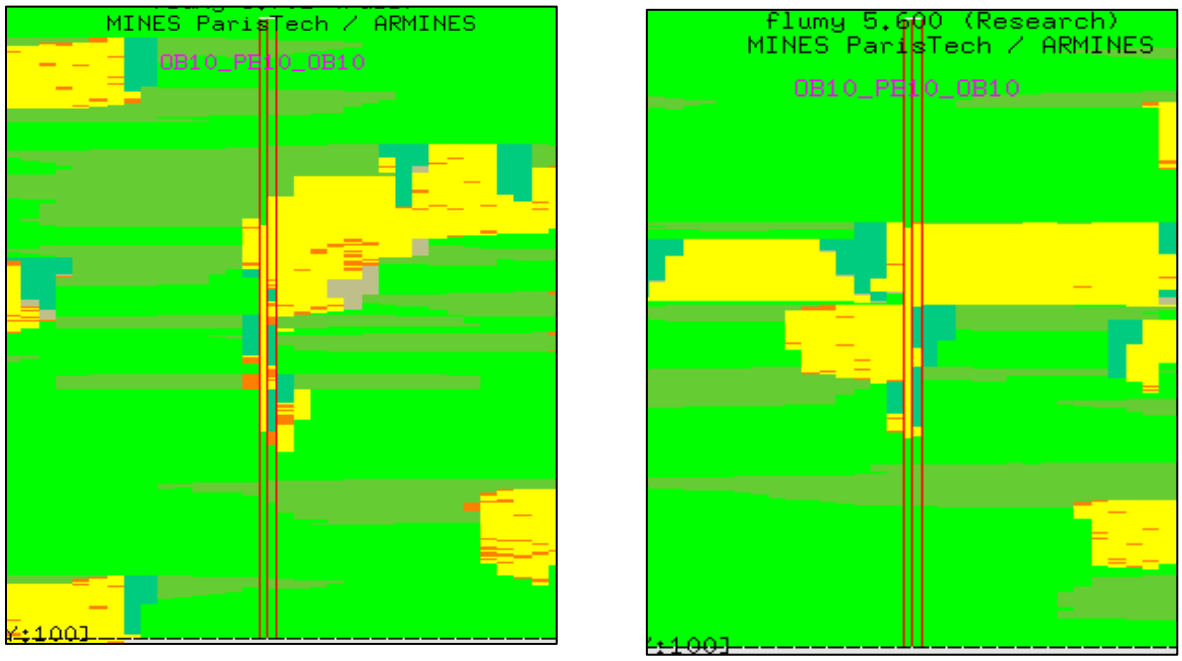

Figure 121. Three-facies well reproduction, default parameters, comparison of Flumy versions 3.702 (left) and 5.600 (right)

Parameters	Old results	New results
Well sand Proportion	0.33	
Simulation Sand Proportion at well	0.25	0.18
Matching at Sand (%)	54.10%	51.70%
Well Channelized Facies Proportion	0.33	
Simulation Channelized Facies Proportion at well	0.40	0.34
Matching at Channelized Facies (%)	100%	99.70%

Table 29. Resulting conditioning statistics, three-facies well, default parameters, Flumy versions 3.702 and 5.600

Analysis of results:

The two problems observed in the initial tests (Figure 121, left):

1 during the reproduction of the first OB brick, the channel arrives to the well too early and deposits Channelized facies in front of the upper part of the first data OB brick;
2 the channel stays too long at the well when the PB brick is honored and deposit Channelized facies in front of the lower part of the second data OB brick.

These two problems are resolved with new conditioning algorithms (Figure 121, right), due to the additional OB "protection" by *avoidh* (first problem) and aggradation blocking when the channel is at the well and AB is "repulsive" (second problem). Conditioning statistics confirms the visual observations: Channelized facies proportion in data is 33%, and only 1% of it was excessively deposited with new conditioning algorithm (instead of 7% with the old test).

3.5.1.1.2 Extremely poor sand proportion

The following simulation parameters are used to produce a simulation with extremely poor sand proportion and standard type of sandbodies.

Parameters	**Old values**	**New values**
Avulsions: - regional - local - Sandbodies extension	 Periodic (600) Periodic (400) Standard	 Poisson (600) Poisson (400) Standard
Aggradation: - occurrence - thickness - Sand proportion	 Poisson (10) Const (0.1) Extremely Poor	 Poisson (10) Normal (0.1 , 0.03) Extremely Poor
Flumy version	3.702	5.600

Table 30. Flumy simulation parameters, test of three-facies well, small N_G, Flumy vers. 3.702 and 5.600

Comparison of old results of well reproduction and new results is illustrated by the visual comparison (Figure 122) and the statistical table (Table 31):

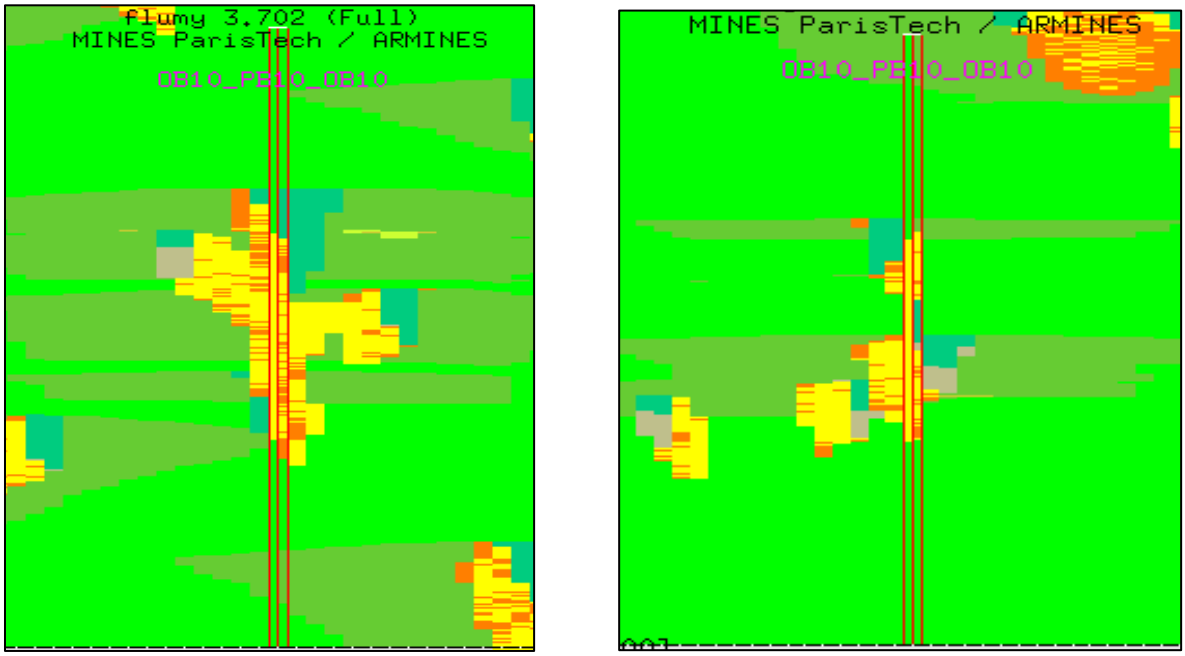

Figure 122. Three-facies well reproduction, small N_G, comparison of Flumy versions 3.702 (left) and 5.600 (right)

Conditioning statistics:

Parameters	Old results	New results
Well sand Proportion	0.33	
Simulation Sand Proportion at well	0.35	0.28
Matching at Sand (%)	97.90%	79.20%
Well Channelized Facies Proportion	0.33	
Simulation Channelized Facies Proportion at well	0.44	0.34
Matching at Channelized Facies (%)	100%	99.20%

Table 31. Resulting conditioning statistics, three-facies well, small N_G, Flumy versions 3.702 and 5.600

Analysis of results:

This test shows the problem of a too early channel arrival to the well (Figure 122, left), already discussed above. Again, this problem was successfully resolved with new conditioning algorithm. Another visible problem in old test is the channel blocked at the well during PB → OB transition: the MP at the lower part of the second OB data brick indicates that the channel stayed blocked until the next avulsion. New test result shows that this problem was fixed: the channel is no more blocked at the well. At the end of the conditional simulation, only 1% of Channelized facies was excessively deposited, instead of 11%.

3.5.1.1.3 Extremely rich sand proportion

The following simulation parameters were used: extremely rich sand proportion, Standard sandbodies extension.

Parameters	Old values	New values
Avulsions: - regional - local - Sandbodies extension	 Periodic (600) Periodic (400) Standard	 Poisson (600) Poisson (400) Standard
Aggradation: - occurrence - thickness - Sand proportion	 Poisson (300) Const (0.1) Extremely Rich	 Poisson (300) Normal (0.1 , 0.03) Extremely Rich
Flumy version	3.702	5.600

Table 32. Flumy simulation parameters, test of three-facies well, large N_G, Flumy vers. 3.702 and 5.600

Comparison of old results of well reproduction (left image) and new results (right image):

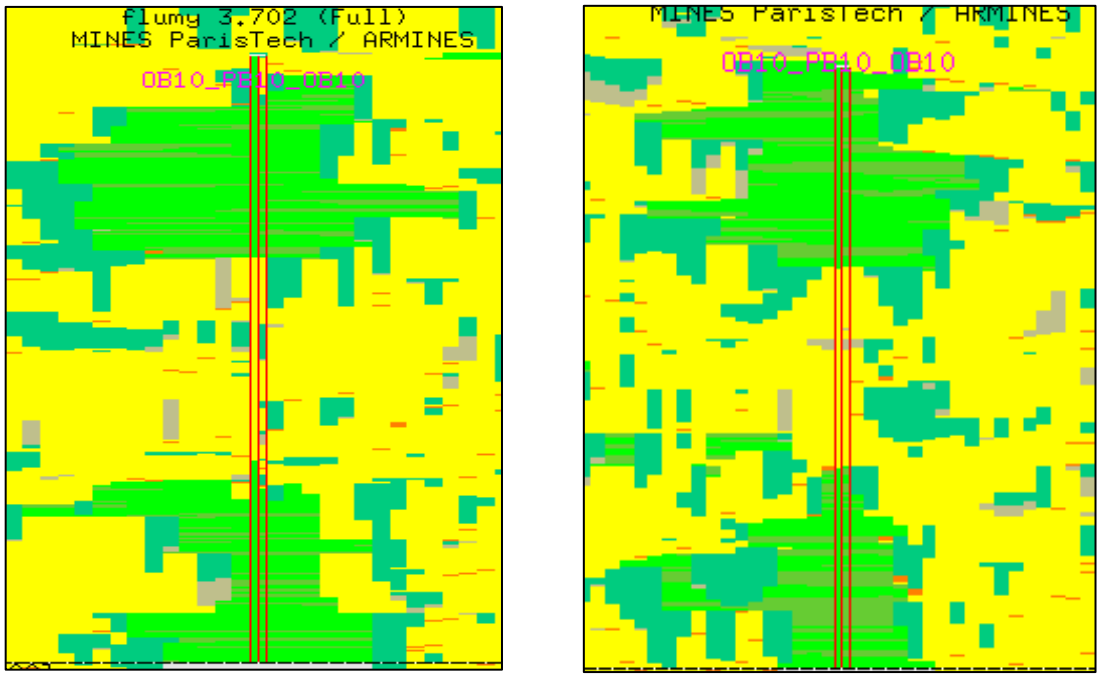

Figure 123. Three-facies well reproduction, large N_G, comparison of Flumy versions 3.702 (left) and 5.600 (right)

Conditioning statistics:

Parameters	Old results	New results
Well sand Proportion	0.33	
Simulation Sand Proportion at well	0.34	0.33
Matching at Sand (%)	76.40%	98.50%
Well Channelized Facies Proportion	0.33	
Simulation Channelized Facies Proportion at well	0.46	0.33
Matching at Channelized Facies (%)	100%	99.10%

Table 33. Resulting conditioning statistics, three-facies well, large N_G, Flumy versions 3.702 and 5.600

Analysis of results:

In this test, again, the channel early arrival to the well was fixed (the upper part of the first OB, Figure 123). Another problem of the initial conditioning algorithm is visualized: completely honored well is not enough “protected”, and the upper part of the second OB was replaced by PB. This problem was successfully fixed by the new conditioning (new *avoidh* value). According to conditioning statistics, the balance between Non-Channelized and Channelized facies reproduction is excellent: exactly 33% of Channelized facies are deposited, instead of 46% in old result.

3.5.1.1.4 Sheet sandbodies

In this test, we evaluate the conditioning algorithm when the sandbody extension is large. The following simulation parameters are used in the last test: Sheet sandbodies extension, Average sand proportion.

Parameters	Old values	New values
Avulsions - regional - local - Sandbodies extension	 Periodic (1100) Periodic (644) Sheet	 Poisson (1100) Poisson (644) Sheet
Aggradation - occurrence - thickness	 Poisson (28) Const (0.1)	 Poisson (28) Normal (0.1 , 0.03)
Flumy version	3.702	5.600

Table 34. Flumy simulation parameters, test of three-facies well, large avulsions period, Flumy vers. 3.702 and 5.600

Comparison of well reproduction in old result (left image) and new result (right image):

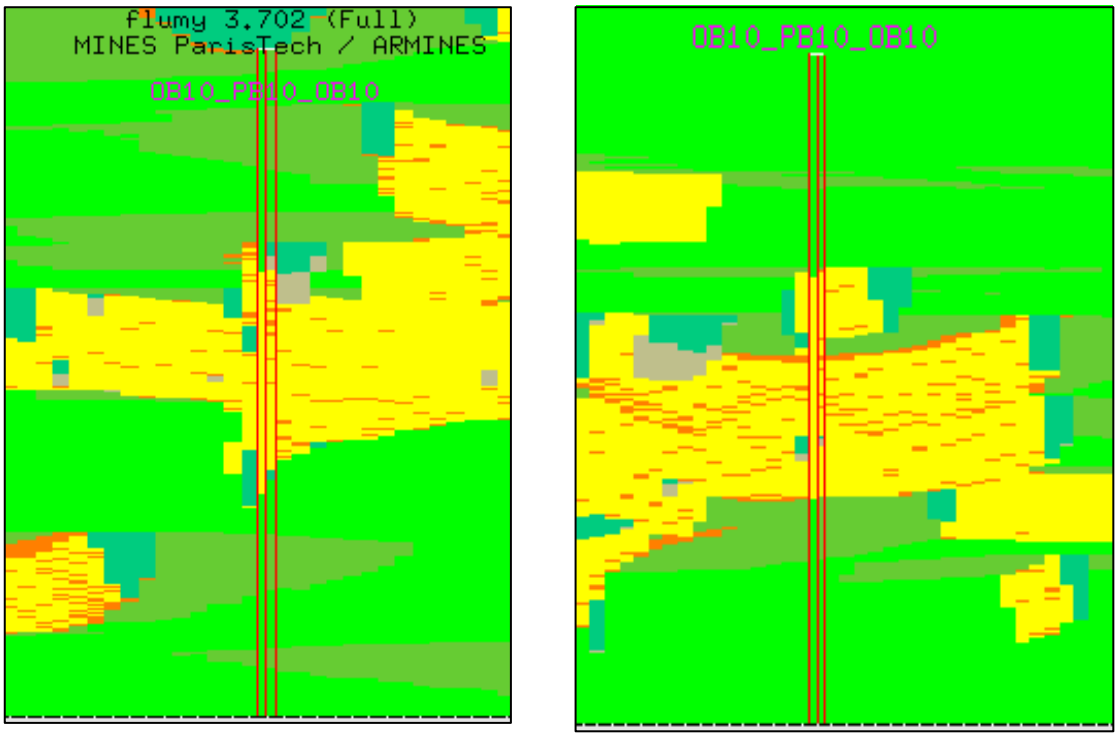

Figure 124. Three-facies well reproduction, large avulsions period, comparison of Flumy versions 3.702 (left) and 5.600 (right)

Conditioning statistics:

Parameters	Old results	New results
Well sand Proportion	0.33	
Simulation Sand Proportion at well	0.32	0.34
Matching at Sand (%)	88.70%	97.00%
Well Channelized Facies Proportion	0.33	
Simulation Channelized Facies Proportion at well	0.36	0.34
Matching at Channelized Facies (%)	93.60%	98.50%

Table 35. Resulting conditioning statistics, three-facies well, large avulsions period, Flumy versions 3.702 and 5.600

Analysis of results:

In the last test, the problem of the channel blocked at the well during PB → OB transition is fixed by the new conditioning algorithms. On Figure 124 (right), it can be noted that the aggradation is blocked at this moment (a sand body at the upper part of PB is a little bit flat), so that the channel may leave the well due to new migration adaptation algorithm (at that moment the well becomes “attractive”, the migration velocity is increased). Besides of it, on Figure 124 (left) the fact that the channel arrived to the well too late during OB → PB transition was fixed by new Update AL algorithm.

3.5.1.1.5 Conclusion

As it was shown on the tests results, the main problems concerning the facies transition using one multi-facies well were identified and addressed as follows:

- Channel arrives to the well too early and provokes unwanted erosion of already deposited Non-Channelized facies – updated *avoidh* coefficient;
- Channel arrives to the well too late, not honoring the lower parts of Channelized facies bricks – new Update AL algorithm;
- Channel blocked at the well during PB → OB transition – aggradation blocking and new migration adaptation algorithm.

3.5.1.2 Multiple wells

In the previous section, two tests were performed in order to estimate the conditioning techniques ability to reproduce several wells in one simulation. Now, the same tests are repeated and the results are compared. The first one uses four synthetic wells for conditioning, not perfectly compatible with the simulation parameters (the same wells as those used in the previous chapter). In the second test, four extracted wells are used for conditioning: they are more compatible with simulation parameters but were extracted from a non-conditional simulation created with old Flumy version (the wells used in the previous chapter, Flumy version 3.702).

3.5.1.2.1 Four synthetic wells

The synthetic wells consist of several data blocks (PB and OB), they correspond to the simplified description of well (sand / no sand).

Conditions of test:

Parameters	Old values	New values
Channel max depth	3 m (channel width = 30 m)	
Grid size	4005 m x 3000 m; grid lags: 15m x 15 m	
Avulsions - regional - local	 Periodic (600) Periodic (400)	 Poisson (600) Poisson (400)
Aggradation - occurrence - thickness	 Poisson (28) Const (0.1)	 Poisson (28) Normal (0.1 , 0.03)
Flumy version	3.702	5.600

Table 36. Simulation parameters of four synthetic wells test, Flumy versions 3.702 and 5.600

Wells disposition on the simulation domain (aerial view) is shown on the Figure 125.

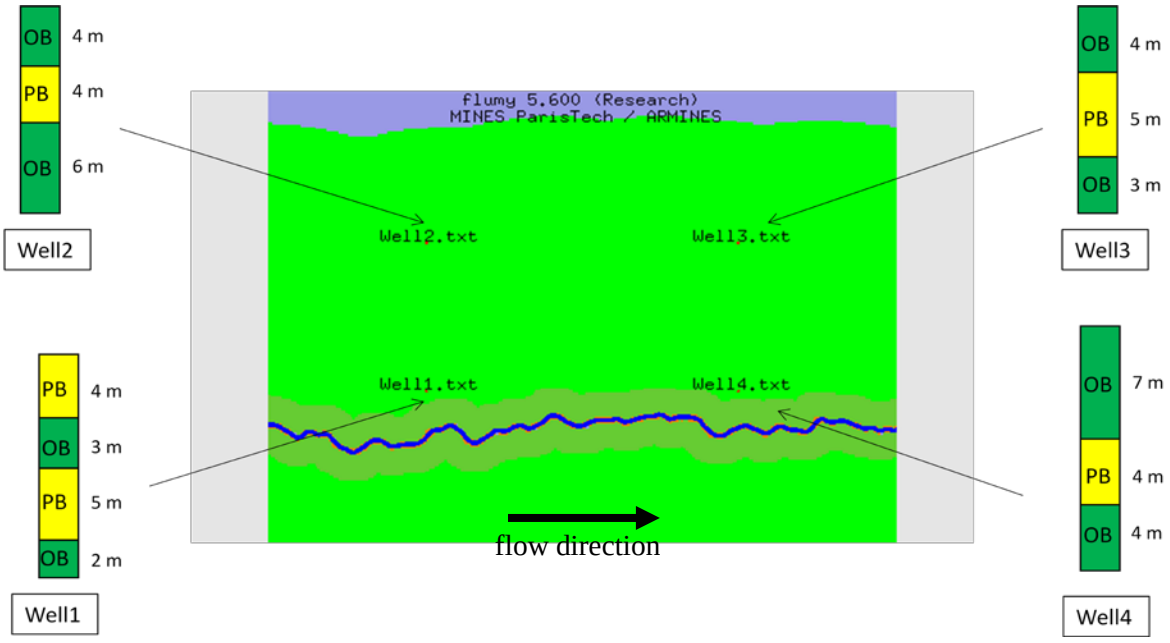

Figure 125. Conditions of four synthetic wells test, Flumy version 5.600

Two pairs of wells are aligned along the flow direction. N_G of four synthetic wells is equal to 36.7%. N_G of the two resulting conditional simulations are 21% for old test (Flumy version 3.702) and 31% for a new test (version 5.600). Such difference (10% of output simulation N_G) was already mentioned above – it comes from the change of the internal Flumy migration process.

Resulting reproduction of four wells is shown at the Figure 126:

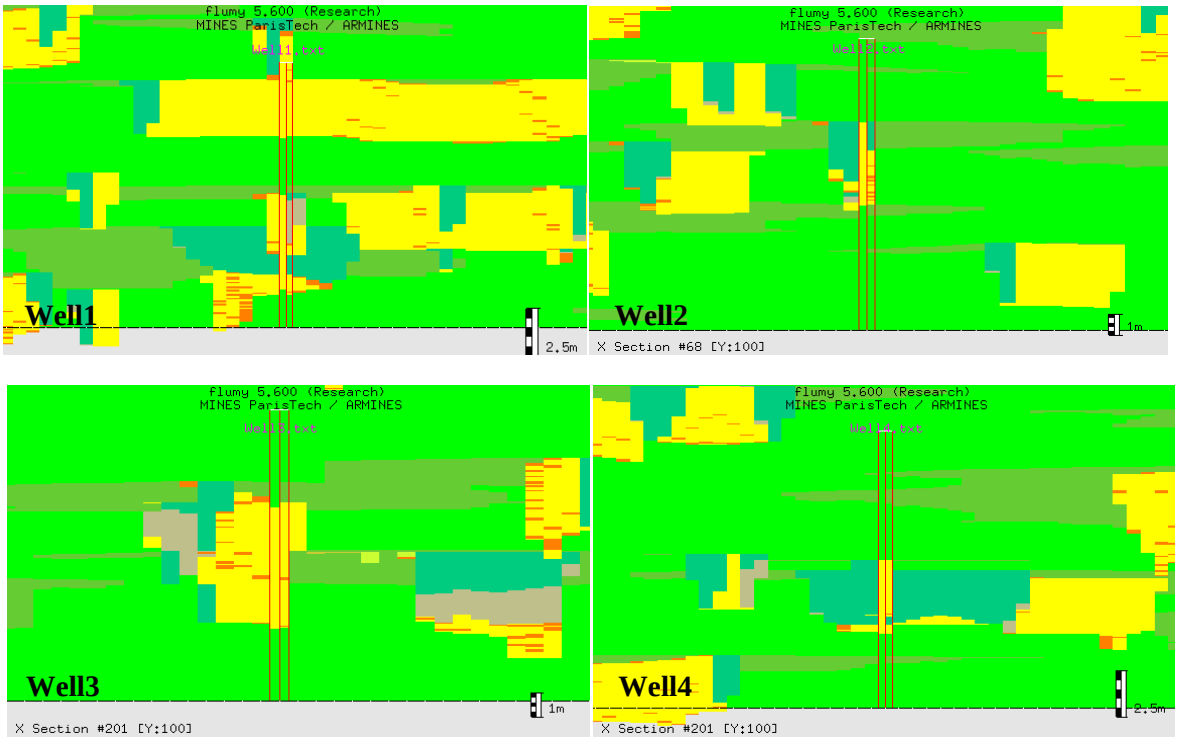

Figure 126. Four synthetic wells reproduction, Flumy version 5.600

Conditioning statistics:

Parameters	Old results	New results
Well sand Proportion	0.40	
Simulation Sand Proportion at well	0.38	0.35
Matching at Sand (%)	73.27%	84.86%
Well Channelized Facies Proportion	0.40	
Simulation Channelized Facies Proportion at well	0.52	0.41
Matching at Channelized Facies (%)	96.23%	99.23%

Table 37. Resulting conditioning statistics, four synthetic wells test, Flumy versions 3.702 and 5.600

Analysis of the wells images and conditioning statistics permits to conclude that the wells are almost perfectly reproduced. Statistics show a higher sand matching and a proportion of channelized facies at well (0.40) close to the Simulation Channelized Facies Proportion at well (0.41) instead of 0.52 in the old conditioning simulation.

The next step is to compare cross-valley and along flow cross-sections containing the wells obtained from the non-conditional simulation, the conditional simulations (old and new algorithms) (Figure 127):

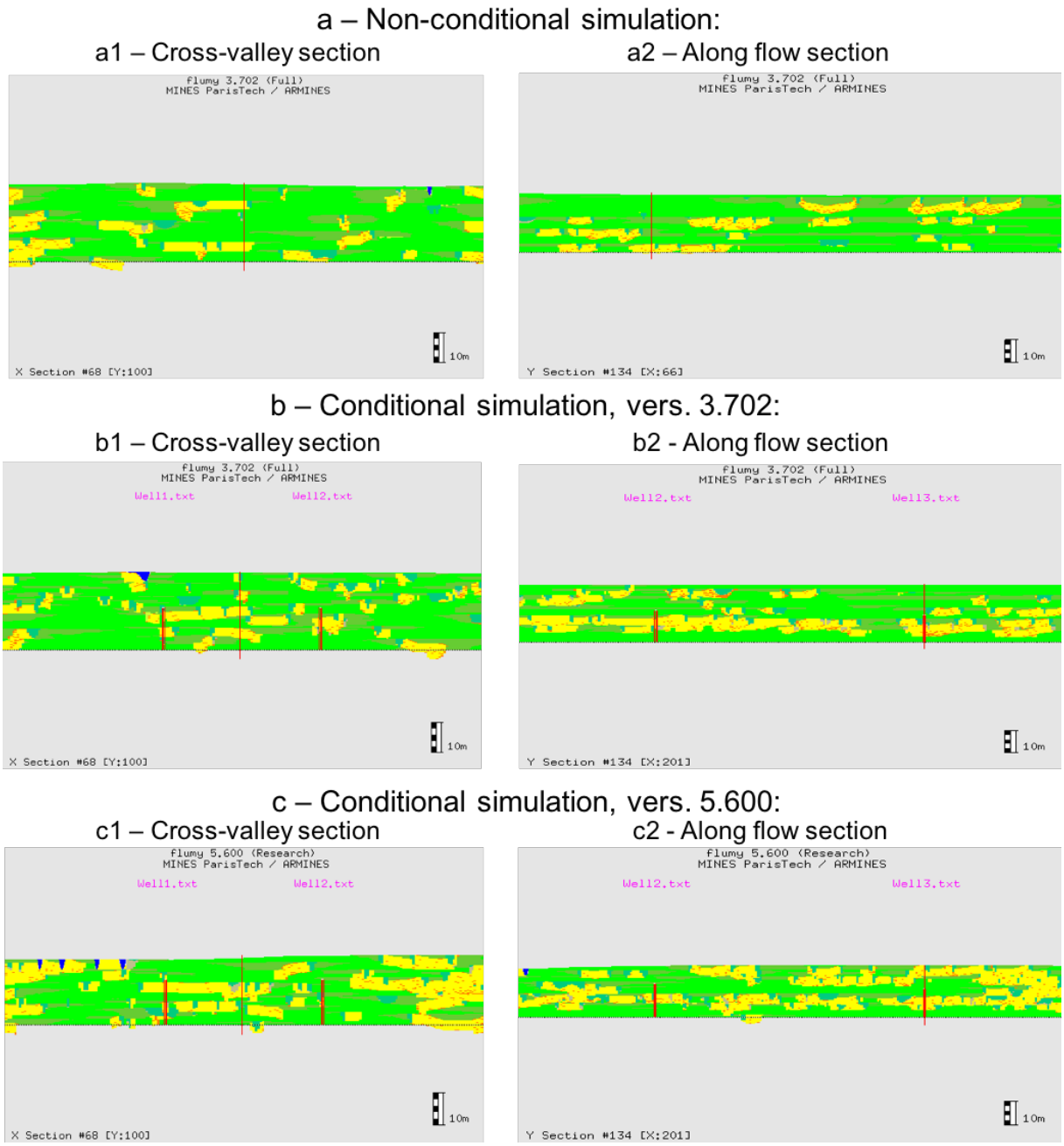

Figure 127. Four synthetic wells test, comparison of simulation cross-sections: non-conditional simulation, vers. 3.702 (a1-a2); conditional simulation, vers. 3.702 (b1-b2); conditional simulation, vers. 5.600 (c1-c2)

Observations:

- The new conditional simulation is visibly richer in sand, but this difference comes from the general simulation N_G: non-conditional simulation N_G = 20%; conditional simulation (vers. 3.702) N_G = 21%, conditional simulation (vers. 5.600) N_G = 31%.
- Both along flow and cross valley sections of new conditional simulation (Figure 127c) contain more sandbodies than old non-conditional simulation (Figure 127b):
    - in cross-valley section these sandbodies are uniformly distributed, so it may represent another, sandier realization of a non-conditional simulation.
    - it is difficult to compare along flow cross-sections (a2-b2) with cross-sections (c2): it is unknown whether increased concentration of sandbodies on (c2) is a result of

conditioning procedure or a result of increased sand proportion in the whole simulation. This issue will be studied with Sand Proportion Maps in the next chapter.

3.5.1.2.2 Four simulated wells

The wells used in this test are the same extracted wells from the section §3.2.3.2: a non-conditional simulation with fixed input parameters (Table 38) is performed, four wells are extracted from it and then used for conditional simulation with the same parameters. But in this case the wells may be not perfectly compatible with the simulation parameters because of the new Flumy version and modified internal migration process.

Conditions of test:

Parameters	Old values	New values
Channel max depth	3 m (channel width = 30 m)	
Grid size	4005 m x 3000 m; grid lags: 15m x 15 m	
Avulsions - regional - local	 Periodic (600) Periodic (400)	 Poisson (600) Poisson (400)
Aggradation - occurrence - thickness	 Poisson (28) Const (0.1)	 Poisson (28) Normal (0.1, 0.03)
Flumy version	3.702	5.600

Table 38. Simulation parameters of four extracted wells test, Flumy versions 3.702 and 5.600

Wells disposition on grid (aerial view):

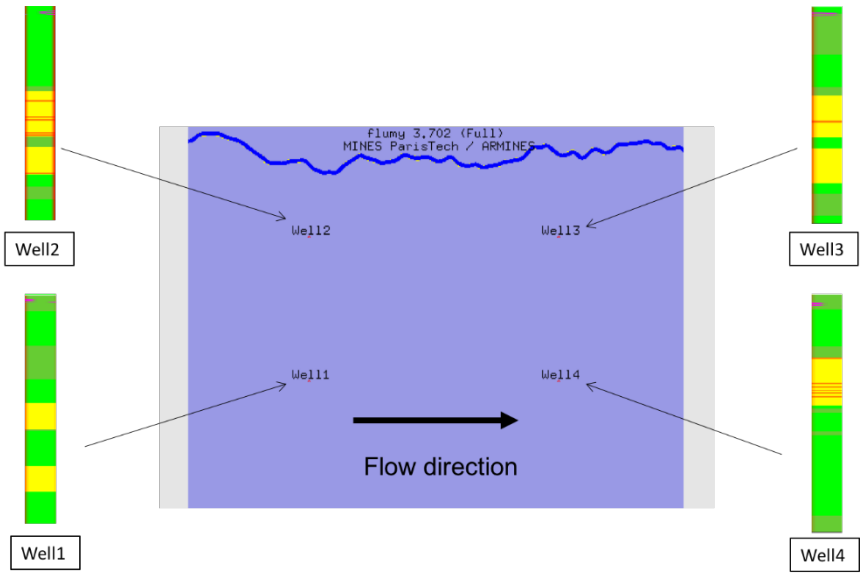

Figure 128. Conditions of four extracted wells test, Flumy version 5.600

Sand proportion of four extracted wells is equal to 27.3%. Old conditional simulation (vers. 3.702) has an output sand proportion of 20%; new conditional simulation (vers. 5.600) – 31%.

Wells reproduction images:

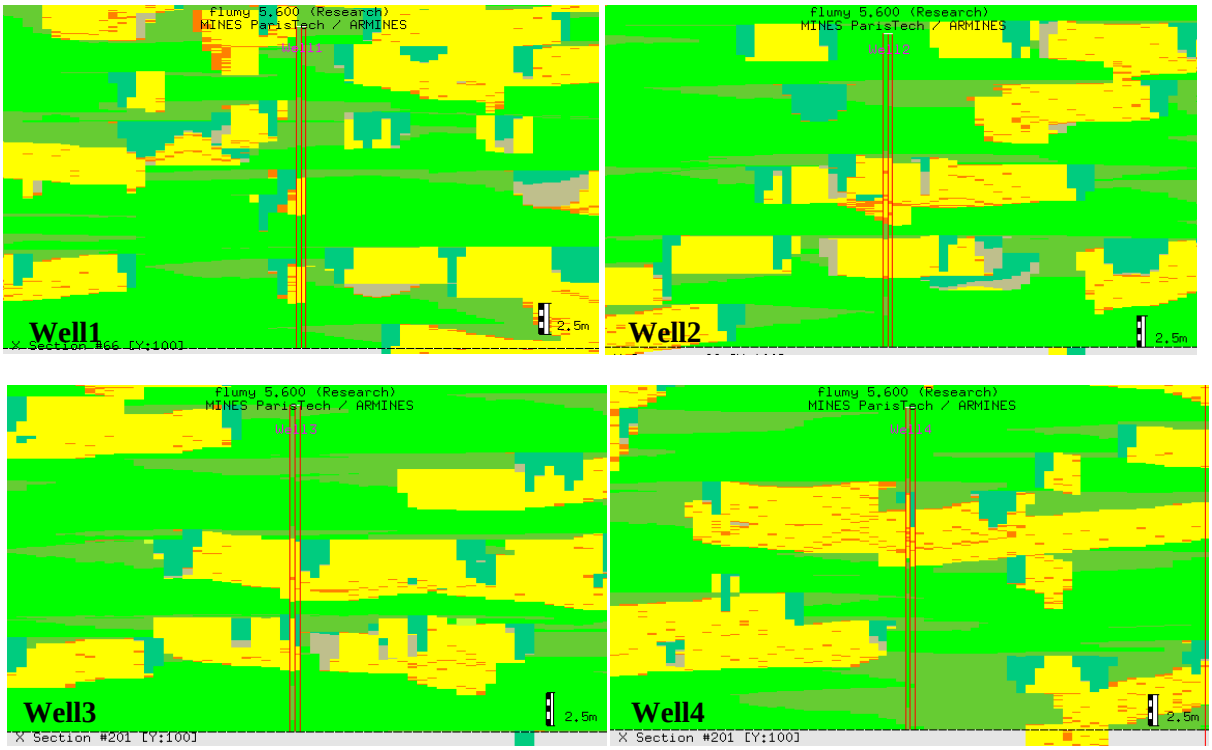

Figure 129. Four extracted wells reproduction, Flumy version 5.600

Conditioning statistics:

Parameters	Old results	New results
Well sand Proportion	0.28	
Simulation Sand Proportion at well	0.28	0.23
Matching at Sand (%)	79.82%	80.79%
Well Channelized Facies Proportion	0.28	
Simulation Channelized Facies Proportion at well	0.36	0.29
Matching at Channelized Facies (%)	96.35%	98.57%

Table 39. Resulting conditioning statistics, four extracted wells test, Flumy versions 3.702 and 5.600

Well images and conditioning statistics show that new conditioning algorithms result in almost perfect well reproduction: only 1% of Channelized lithofacies is deposited excessively (28% in well data, 29% in simulation) with more than 98% of matching. This result is very satisfactory in conditions of several wells and change of Flumy version.

The following simulation cross-sections are compared (Figure 130): non-conditional simulation used for well extraction (vers. 3.702); conditional simulations (vers. 3.702 and 5.600).

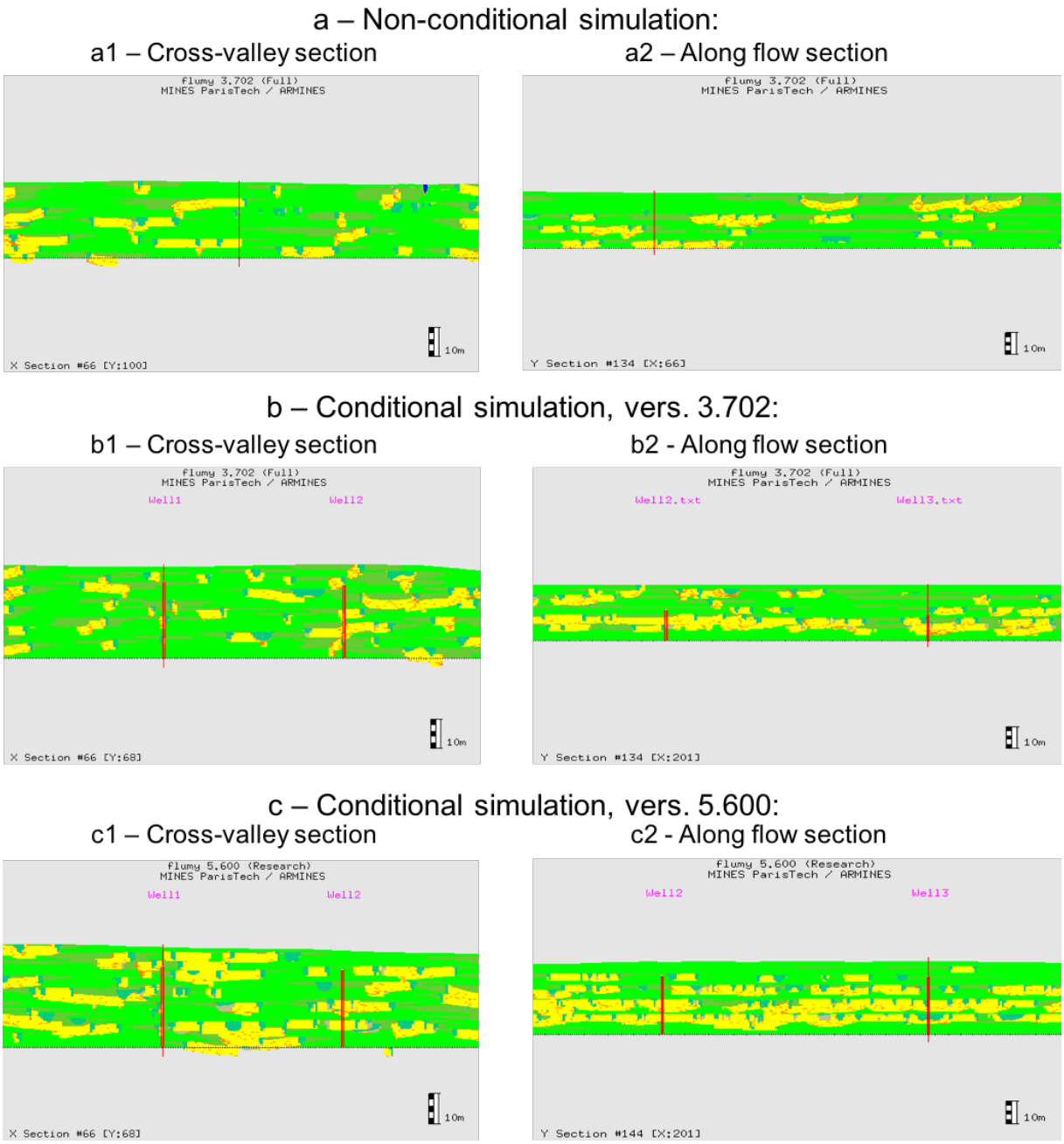

Figure 130. Four extracted wells test, comparison of simulation cross-sections: non-conditional simulation, vers. 3.702 (a1-a2); conditional simulation, vers. 3.702 (b1-b2); conditional simulation, vers. 5.600 (c1-c2)

Observations:

As previously observed, conditional simulations performed with the new Flumy version (Figure 130c) contain more sand (10% more) than the non-conditional and conditional simulations performed with the old versions (Figure 130a,b). In order to make stronger conclusions, Sand Proportion Maps of new conditional simulations should be analyzed.

3.5.1.3 Conclusion

The following conclusions can be made from the tests presented above:

- now, the output simulations generally contain more sand than in old Flumy versions (2-5% more of resulting simulation N_G) with the same input parameters: the conditioning tests were performed before the re-calibration of the internal migration process.
- new conditioning algorithms have a strong impact on conditioning results. They fix all the previously detected main problems in well reproduction: too early or too late channel arrival to the well location; channel blocking at the well during Channelized → Non-Channelized facies transition at the well; excessive Channelized facies deposition at well (replacement of the “not-to-be-eroded” Non-Channelized facies);
- tests performed with several wells confirm the previous conclusion: even if the wells are not perfectly compatible with the simulation parameters, they can be well reproduced during the simulation. Still, it is important to define the simulation parameters compatible with the data in order to create the most realistic simulations;
- comparison of the initial conditioning tests with the new ones is made complicated by Flumy versions change (3.702 and 5.600): simulations with the new Flumy version contain a higher sand proportion than those with the old Flumy version, for the same input simulation parameters (changed internal Flumy processes).

3.5.2 Resulting sand spatial distribution

The tests showing the spatial sand distribution in conditional models are presented. In previous section §3.3, the impact of the well layout vs. the flow direction was evaluated. Summary of the detected problems is:

- Alignment of sandbodies near the wells along the flow, independently on the flow direction. It was caused by an excessive channel "attraction" to the wells (too strong migration/avulsions adaptation by conditioning);
- If the wells are aligned cross valley, the upstream (before the wells) and downstream (after the wells) sand deposition varies significantly: a very high sand proportion is observed in the upstream part of the simulation domain, and a poor sand proportion in downstream part. Such differences were caused by a possible channel blocking at the wells during PB → OB transition, and the fact that only upstream channel meanders were attracted to the well during the migration conditioning algorithm.

In this part, we evaluate the impact of the new algorithms by repeating the tests with new Flumy version that includes the new conditioning algorithms. The input simulation parameters stay the same and are shown in the Table 40.

Parameters	**Old values**	**New values**
Channel max depth	3 m (channel width = 30 m)	
Grid size	4005 m x 4500 m x 60m; grid lags: 15m x 15 m Oxy = (524000; 4447500)	
Avulsions - regional - local	 Periodic (500) Periodic (360)	 Poisson (500) Poisson (360)
Aggradation - occurrence - thickness	 Poisson (80) Constant (0.1)	 Poisson (80) Normal (0.1 , 0.03)
Flumy version	4.005	5.600

Table 40. General simulation parameters for the tests of spatial sand distribution, Flumy versions 4.005 and 5.600

The tests are organized as follow:

- firstly, two non-conditional simulations, created with Flumy versions 4.005 and 5.600 respectively, are analyzed by Sand Proportion Maps;
- secondly, a test of two extracted wells is performed, in order to estimate the spatial sand distribution in conditional simulation depending on well locations;
- finally, tests of several extracted wells aligned along the flow direction and cross-valley are analyzed and discussed.

Four different tests are presented in this section: 2 wells aligned cross-valley, 8 wells aligned four by four along the flow direction, and 7 and 15 wells aligned cross-valley in the middle of simulation domain. The tests results are analyzed by Sand Proportion Maps and conditioning statistics and then compared with the old results from section §3.3. All well data are the same as those used in the tests with the old version (section §3.3 tests) (extracted from non-conditional simulation).

3.5.2.1 *Influence of flow direction*

N_G of extracted wells = 38.6%; flow direction = North. The resulting Sand Proportion Maps of old (left) and new (right) tests are:

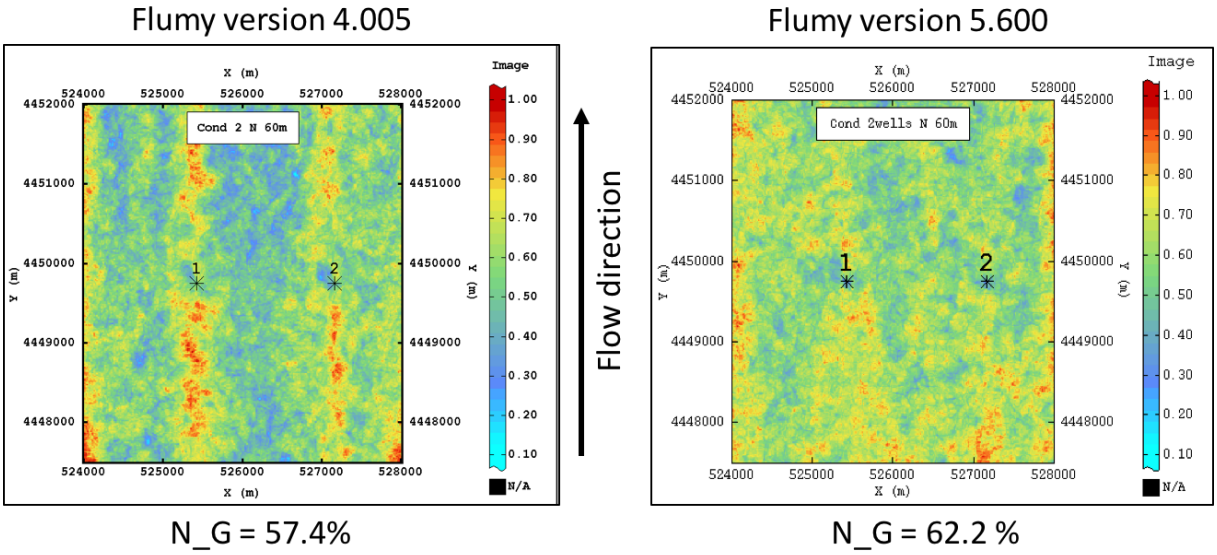

Figure 131. Sand Proportion Maps comparison, 2 wells test, Flumy vers. 4.005 (left) and Flumy vers. 5.600 (right) with resulting N_G

Conditioning statistics:

Parameters	Old results	New results
Well sand Proportion	0.39	
Simulation Sand Proportion at well	0.52	0.44
Matching at Sand (%)	69.61%	76.93%
Well Channelized Facies Proportion	0.56	
Simulation Channelized Facies Proportion at well	0.69	0.58
Matching at Channelized Facies (%)	99.87%	97.79%

Table 41. Resulting conditioning statistics, 2 extracted wells test, Flumy versions 4.005 and 5.600

Observations:

Firstly, the resulting conditional simulation N_G is higher in new test simulation (62.2% almost 5% of difference with conditional simulation run with the old algorithm). As mentioned previously, this results from the algorithms used in the new Flumy version: N_G of the non-conditional simulations are respectively 60% Flumy 5.600, 57.2% Flumy 4.005). This difference in N_G is not considered as the impact of new conditioning procedure.

Secondly, the simulation performed with vers. 5.600 is more uniform in terms of spatial sand distribution. Instead of the two sandy lines along each well location in the flow direction, now there are no significant sand proportion zones in the simulation block. This improvement is a result of new Update AL algorithm, as well as the reduced migration/avulsion adaptation during conditioning.

Finally, conditioning statistics is considerably improved: only 2% of Channelized lithofacies are excessively deposited at well, (instead of 13%) with an accuracy of almost 98% (Table 41).

3.5.2.2 *Wells aligned along the flow*

In this test, wells have been extracted from the non-conditional simulation run with the old Flumy version. Wells are distributed along two lines containing four wells each, and oriented parallel to the flow, flow direction is North. Wells occupy the same location as in the test run with the previous Flumy version (Figure 132). The sand proportion of the extracted wells is 55%. Resulting Sand Proportion Maps for old (left) and new (right) conditional simulations are:

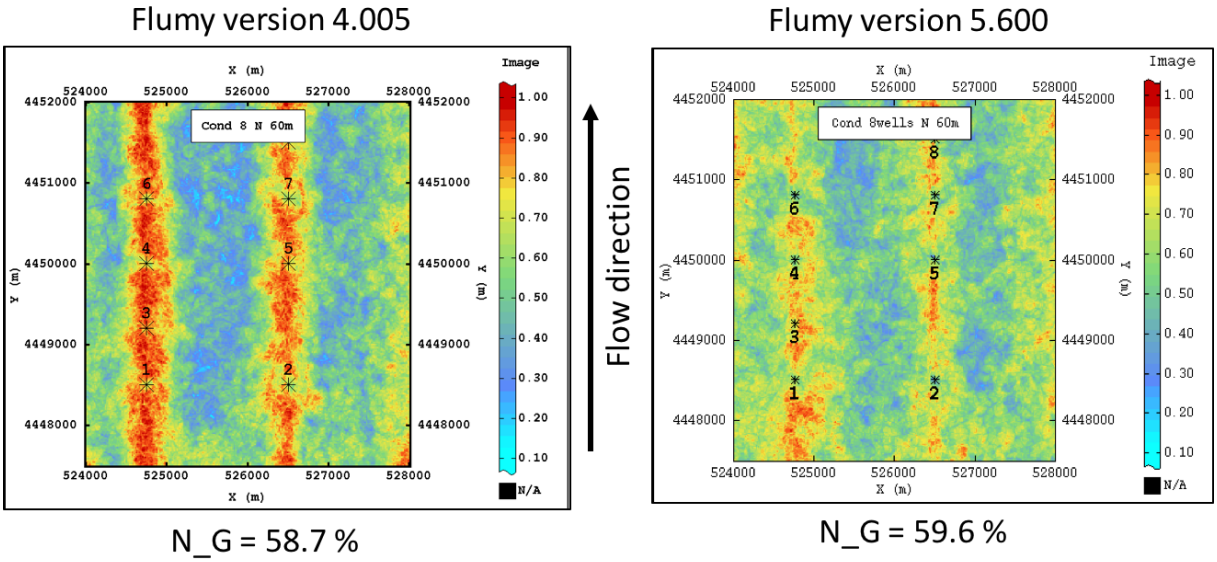

Figure 132. Sand Proportion Maps comparison, 8 wells test, Flumy vers. 4.005 (left) and Flumy vers. 5.600 (right) with resulting N_G

Conditioning statistics:

Parameters	Old results	New results
Well sand Proportion	0.55	
Simulation Sand Proportion at well	0.63	0.55
Matching at Sand (%)	73.10%	78.69%
Well Channelized Facies Proportion	0.67	
Simulation Channelized Facies Proportion at well	0.80	0.69
Matching at Channelized Facies (%)	97.17%	97.14%

Table 42. Resulting conditioning statistics, 8 extracted wells test, Flumy versions 4.005 and 5.600

Observations:

Resulting simulation N_G (59.6%) is very comparable to the N_G of the non-conditional simulation (Flumy 5.600 (60%) when a small difference was observed with the old algorithm (58.7% instead of 57.2%)).

As it is showed on the Figure 132 (right), the sand lines along the well locations are still visible but the gradient between the low sand proportion and the high ones is smoother, resulting in less abrupt transitions between the sand-rich and sand poor areas. The maximum sand proportion has also been lowered from 100% near the wells to less than 85%. High proportion areas are narrower and shorter along flow resulting in discontinuous “sand lines” of lower sand proportion. It can be concluded that the new conditioning algorithm improves the conditional simulation results.

Conditioning statistics shows that the wells reproduction is strongly improved by the new conditioning algorithms: only 2% of Channelized facies are deposited excessively (instead of 13% in old test) with an accuracy of more than 97%.

3.5.2.3 Wells aligned perpendicular to the flow

In the previous section §3.3), this setting showed an inability of the algorithm to deal with such well distribution. An excessive sand proportion was observed, upstream from the wells and along lines parallel to the flow, at well location. It was due to an excessive channel meander development in the upstream grid part, induced by the attraction migration algorithm.

The wells used in new tests are exactly the same wells as those used previously – extracted from non-conditional simulation, Flumy vers. 4.005. Two tests are run with different numbers of wells (7 and 15), aligned in the middle part of grid along a cross-valley line.

3.5.2.3.1 7 wells

In this simulation, distance between the wells is equal to 500 m. Sand proportion in the 7 extracted wells is equal to 49%; simulation flow direction is North.

Resulting Sand Proportion Maps of old conditional simulation (left) and new one (right) are:

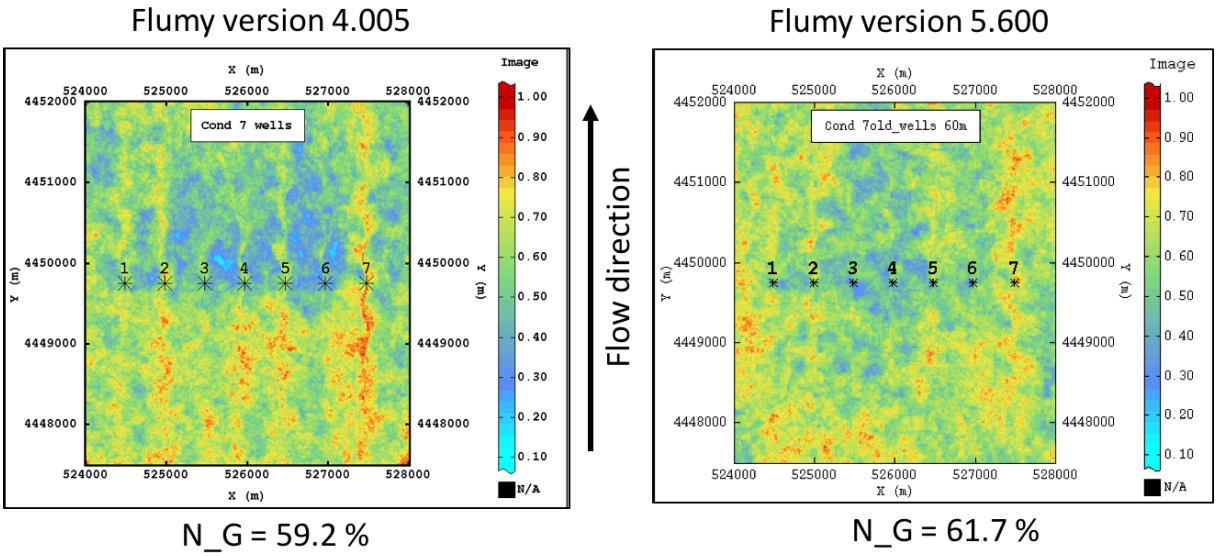

Figure 133. Sand Proportion Maps comparison, 7 wells aligned perpendicularly to the flow direction, Flumy vers. 4.005 (left) and Flumy vers. 5.600 (right) with resulting N_G

Conditioning statistics:

Parameters	**Old results**	**New results**
Well sand Proportion	0.48	
Simulation Sand Proportion at well	0.45	0.53
Matching at Sand (%)	54.70%	74.49%
Well Channelized Facies Proportion	0.65	
Simulation Channelized Facies Proportion at well	0.74	0.68
Matching at Channelized Facies (%)	97.78%	97.96%

Table 43. Resulting conditioning statistics, 7 wells aligned perpendicularly to the flow direction, Flumy versions 4.005 and 5.600

Observations:

Resulting output sand proportions in the two simulations are comparable: 59.2% vs. 61.7% and close to the N_G of the non-conditional simulations (57.2% vs 60% for the old and new version).

Analysis of the two Sand Proportion Maps shows that the new simulation is more uniform in terms of sand spatial distribution although several zones with a higher sand proportion are still visible (sand line downstream of well 7) (Figure 133). Nevertheless, sand distribution between the upstream/downstream parts of the domain are much more similar. It should also be noted that the middle part of the domain (the area containing the wells around 200 m upstream and downstream from the wells) contains less sand that its surroundings. This phenomena, as well as the reasons of improvements, will be discussed with the results of the next test run (15 wells aligned perpendicular to the flow).

Conditioning statistics table show that modified conditioning algorithms improve the exact well reproduction: 3% of Channelized facies are deposited excessively at the wells (instead of 9% in the old test), with an accuracy of almost 98%.

3.5.2.3.2 15 wells

In this simulation, distance between the wells is equal to 250 m. Sand proportion in the 15 extracted wells is equal to 55.3%; simulation flow direction is North. The resulting Sand Proportion Maps of old simulation (left) and new simulation (right) with corresponding simulation N_G are:

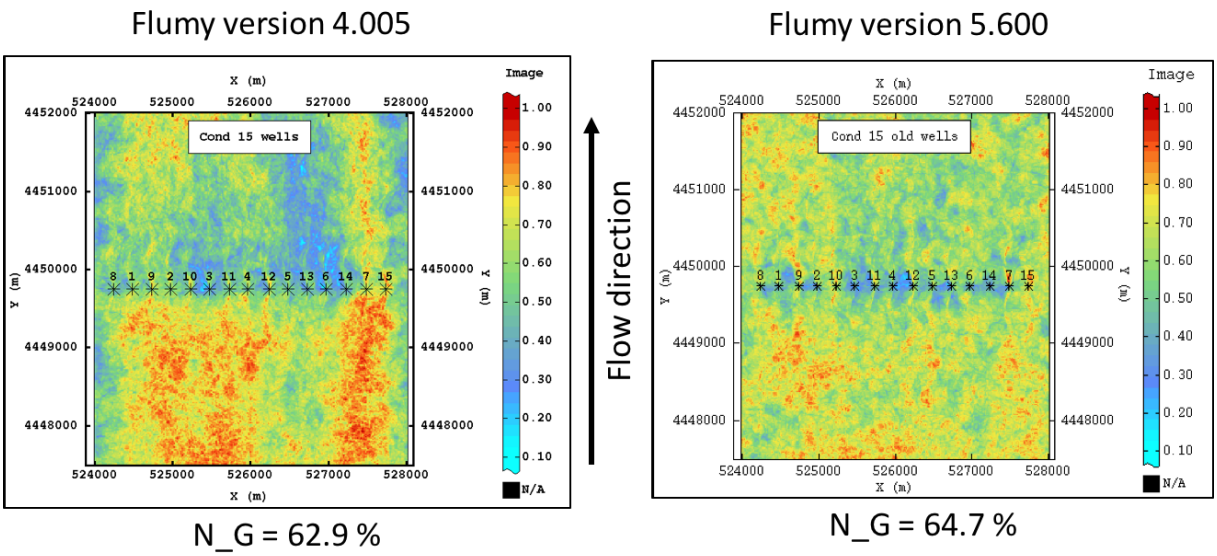

Figure 134. Sand Proportion Maps comparison, 15 wells aligned perpendicularly to the flow direction, Flumy vers. 4.005 (left) and Flumy vers. 5.600 (right) with resulting N_G

Conditioning statistics:

Parameters	**Old results**	**New results**
Well sand Proportion	0.55	
Simulation Sand Proportion at well	0.44	0.57
Matching at Sand (%)	52.63%	79.22%
Well Channelized Facies Proportion	0.69	
Simulation Channelized Facies Proportion at well	0.78	0.70
Matching at Channelized Facies (%)	97.30%	97.39%

Table 44. Resulting conditioning statistics, 15 wells aligned perpendicularly to the flow direction, Flumy versions 4.005 and 5.600

Observations:

The new conditional simulation is slightly richer in sand (64.7%) than the non-conditional one (60%) for the 5.600 version simulations.

Sand Proportion Maps show that new simulation is much more uniform in sand distribution than the old one: especially in the upstream/downstream parts of the grid parts, no more excessive sand proportion is observed upstream of the wells. Nevertheless, we observe, as in the previous simulation with 7 wells, an area that roughly extended 200 m upstream and downstream from the wellsthat contains less sand than its surroundings. This is discussed in the next paragraph. Conditioning statistics confirms that wells exact reproduction is also improved: 1% of Channelized facies is deposited excessively (instead of 9% in old test), with an accuracy of more than 97%.

To discuss the mechanisms that conduct to the area with a lower sand proportion in the zone of the wells, we compare the horizontal slices taken at the same elevation for the conditional simulation run with the old algorithm (Figure 135, left) and the new one (Figure 135, right).

Comparison of horizontal Z-slices (versions 4.005 and 5.600):

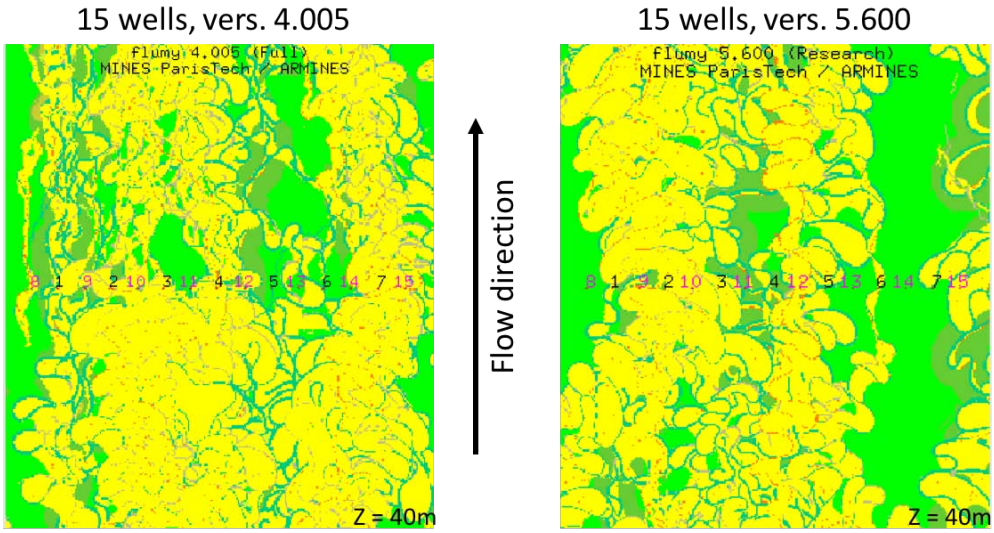

Figure 135. Comparison of horizontal slices of two simulations: conditional by 15 aligned wells, Flumy vers. 4.005 (left) and conditional by 15 aligned wells, Flumy vers. 5.600 (right). Z = 40m

The horizontal slices show that in the new simulation (Figure 135 – right), sandbodies are equally developed upstream and downstream from the wells. The issue of the excessive upstream meander development, observed with the old conditioning (Figure 135 – left) was fixed with the new algorithm. Thus, the low N_G in the vicinity of the wells may be due to a combined effect of the "repulsion" algorithm and the small distance between the wells. That is, the channel migration is slowed/blocked in a small vicinity of well locations every time a well is "repulsive", which results in non-sufficient sandbodies development between the wells. This hypothesis is studied in more details in the next section.

3.5.3 Identified issue in the vicinity of wells

The previous tests run with several wells showed that in any studied case, the new conditioning algorithms tend to produce low sand proportion in the vicinity of the well location despite an excellent sand matching at well.

To address this question, we build a Vertical Proportion Matrix of the simulation (VPM) that gives the lithofacies proportion in chosen simulation sub-domains. For this study, the simulation domain is divided along the Oy axis (along the flow direction), with spacing equals to four grid cells (60 m). A Vertical Proportion Curve (VPC) is then computed within each sub-domain. Thus, for a given Oy set of consecutive values, each VPC aggregates all cells of Ox axis (one VPC for 300 cells). The Vertical Proportion Matrix permits to visualize the difference in sand proportion between all cross-valley sub-domains. In particular, the difference between the central section that contains the wells toward the rest of the simulation block (Figure 136).

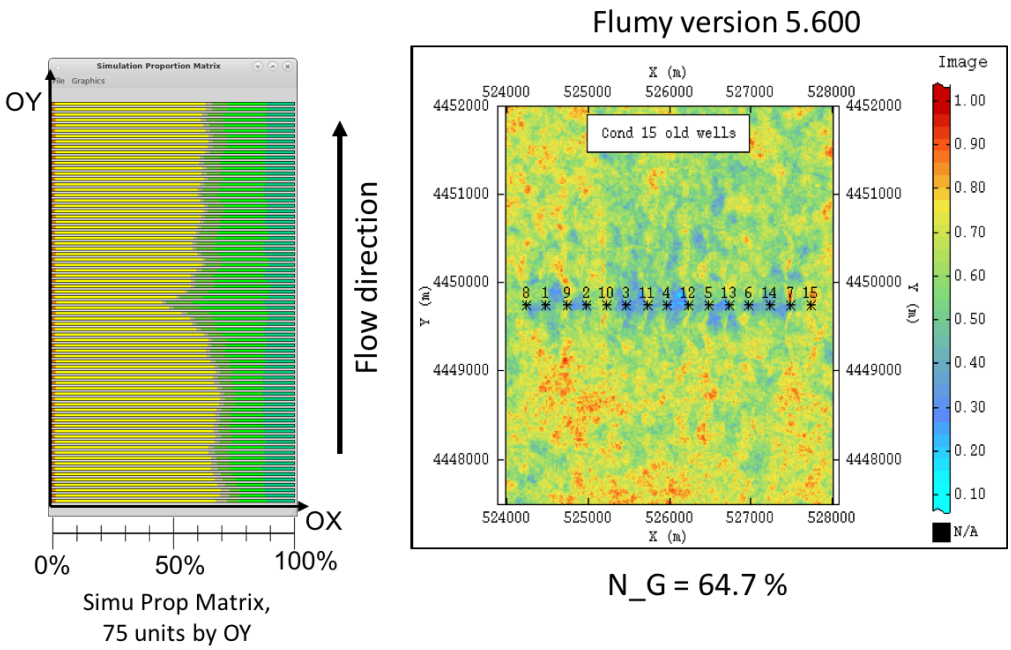

Figure 136. Illustration of remaining problem, test of 15 wells aligned perpendicularly to the flow direction: wells vertical cross-section contains less sand than the whole simulation

Observations:

The VPM shows that the sand proportion in the sub-domain containing the wells is the lowest one (50 %) while the mean value is around 64% upstream of the wells and 61% downstream. Transition in sand proportion between the well sub-domain and the rest of the domain occurs in around 100 m. It should be noted that the simulated sand proportion at wells corresponds to that of the input wells, and that sand matching at well is good (79.2%) and channelized facies even better (97.4%).

The hypothesis to explain such difference might be related to the "repulsion" effect during conditioning: the channel migration is slowed/blocked in a small vicinity of well locations when a well is "repulsive", which results in limited sand body extension between the wells. In order to test this hypothesis, two additional tests were performed with different levels of "repulsion" in conditioning algorithm:

- test 1: Conditioning algorithm without "repulsion" for Non-Channelized facies reproduction (OB and LV);
- test 2: Conditioning algorithm without "repulsion" at all (no *avoidh* to protect already deposited OB and LV).

3.5.3.1 Sand distribution vs repulsion algorithm in the well vicinity

The scenario with 15 extracted wells was chosen as an example for result analysis as it is the test with the closest wells.

The comparison of Sand Proportion Maps and Vertical Proportion Matrix obtained with the Flumy version 5.600 (new migration algorithm and full new conditioning algorithm) are presented with those obtained with tests 1 and 2 on Figure 137:

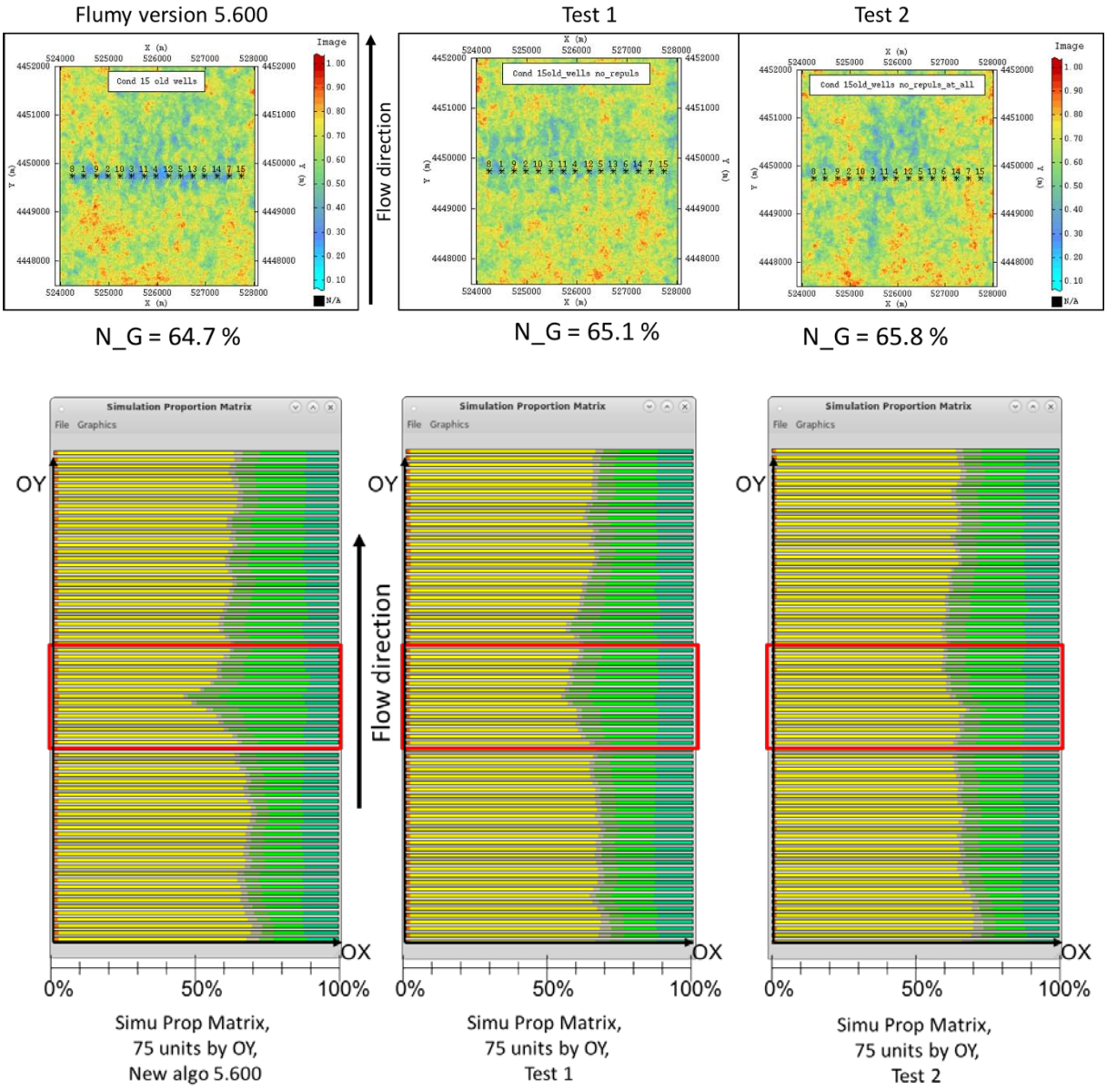

Figure 137. Comparison of Sand Proportion Matrices (above) and Simulation Proportion Matrices (below), 15 wells aligned perpendicularly to the flow direction. From left to right: original test, vers. 5.600; test without migration repulsion for OB/LV reproduction, vers. 5.600; test without migration repulsion at all, vers. 5.600

Observations:

Test 1 SPM shows more uniform sand distribution as indicated by the VPM (Figure 137 – middle). The well sub-domain is slightly poorer in sand (55%) than the rest of simulation (around 65.5%). Simulation sand content is not impacted (N_G = 65.1%).

Test 2 simulation is slightly, but not significantly, richer in sand (65.8%) and the well sub-domain is no longer characterized by a smaller content in sand (Figure 137 – right).

These tests illustrate the impact of the repulsion algorithm that is needed for reproducing the facies succession at well, but that induces a lowering of the N_G in the vicinity of the wells.

3.5.3.2 Uniform sand distribution during conditioning

We also evaluate the influence of the repulsion algorithm on the spatial distribution of sandbodies on three cross-sections perpendicular to the flow: one upstream from the wells, one along the wells line and a third one downstream from the wells.

The cross-valley sections are compared for the simulations run with the Flumy version 5.600, test 1 and Test 2. The resulting images are presented on Figure 138:

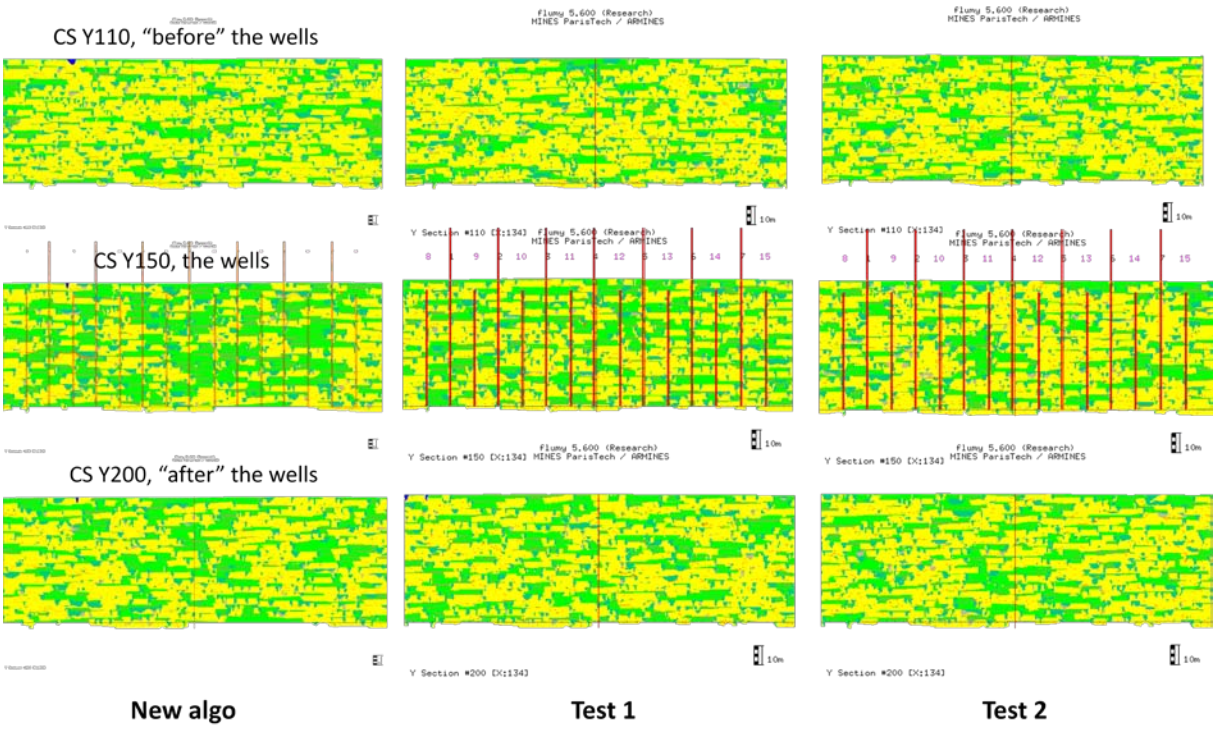

Figure 138. Comparison of vertical model cross-sections before the wells, containing the wells and after the wells, for three models: original vers. 5.600, vers. 5.600 without migration repulsion for OB/LV reproduction and vers. 5.600 without migration repulsion at all

Observations: upstream and downstream cross-sections of the three tests may represent different realizations of one simulation – no visual differences in sandbodies distribution and extension were detected. The well cross-section is quite different between the three simulations. With the Flumy version 5.600, fined grained deposits are dominant in the areas in-between the wells. These areas become sandier during tests 1 and 2 as a result of the cancelling of “repulsion” algorithms of conditioning (Figure 138 from left to right).

Although sand is more uniformly distributed in cross-sections, the reduction of the repulsion algorithm induces also more Channelized facies at well (+10% during test 1 and + 17% during test 2), resulting in less Non-Channelized facies honored (Table 45).

Conditioning statistics:

Parameters	**5.600**	**Test 1**	**Test 2**
Well sand Proportion	0.55		
Simulation Sand Proportion at well	0.57	0.63	0.72
Matching at Sand (%)	79.22%	77.48%	81.66%
Well Channelized Facies Proportion	**0.69**		
Simulation Channelized Facies Proportion at well	**0.70**	**0.80**	**0.87**
Matching at Channelized Facies (%)	97.39%	98.37%	99.05%

Table 45. Resulting conditioning statistics, 15 wells aligned perpendicularly to the flow direction, Flumy versions 5.600, 5.600 without migration repulsion for OB/LV reproduction and 5.600 without migration repulsion at all

3.5.3.3 Conclusion

We tested an extreme case with a high well density on a relatively small surface where the effects of the "repulsion" algorithm on the conditioning results are more visible than in the case of some few dispersed wells.

The main conclusion of the analysis of the impact of the repulsion algorithm on the conditioning results is that there is a competition between the exactness of the conditioning at well and the uniform distribution of sand in cross-sections. Nevertheless, the "repulsion" techniques stay the main tool for Non-Channelized facies exact deposition, and its cancellation makes the conditioning statistics significantly worse.

3.5.4 Conclusion

In this section, the impact of new conditioning techniques was estimated. The tests concerning the wells exact reproduction and spatial sand distribution in conditional models were performed; new results were compared with the results of initial conditioning techniques. Improvement of the migration algorithm in Flumy also contributed to the quality of the conditioning results as it reduces the lateral migration of the meanders, resulting in sandbodies of smaller lateral extension.

The tests dedicated to the evaluation of well data honoring showed that new algorithms significantly improve the results. The following previously detected problems are fixed:

1. excessive Channelized facies deposition – now, this error can reach 1 - 3 percentage points at maximum, which is treated as a satisfactory result for dynamic conditioning;
2. complicated transitions between opposite conditioning techniques (PB "attraction" $\rightarrow$ OB "repulsion" and conversely) – new algorithms make this transition more efficient: the channel is no more blocked at the well and deposited "not-to-be-eroded" facies are better protected.

The tests concerning the spatial sand distribution in conditional simulations also demonstrated the improvements of results:

- the phenomenon of increased sandbodies alignment along the wells in the flow direction is less represented: such sand lines are still visible in the test of 8 wells aligned by 4, but it is a consequence of "attraction" of new channel paths during avulsions;
- difference of upstream/downstream sand proportion in the tests of wells aligned perpendicular to the flow direction is strongly equilibrated: new tests result in more uniform conditional simulations;
- question of non-sufficient sand deposition in small wells vicinity was additionally studied: it is an effect of "repulsion" of channel during conditioning. But without "repulsion" the conditioning becomes less effective, so this consequence could be considered acceptable.

3.6 Conclusions

The tests conducted on specific sets of wells contained different facies associations (one facies, several facies) and located following different patterns (one well, wells aligned along flow, perpendicular to flow) enabled us to identify some problems during the conditioning procedure:

1. Channel arrives to the well too early or too late (if Channelized Facies are needed);
2. Excessive Channelized Facies deposition at wells;
3. Channel stays blocked at the well (PB → OB transition);
4. Sand Lines parallel to the flow at well location over the simulation domain;
5. Difference between the upstream and downstream sand distribution with respect to well location.

Based on the problems that have been identified, we modified and proposed some new conditioning techniques:

1. New algorithm of AL update:
    - Concept of Wet Well optimally takes into account the channel presence at the well;
    - Wet Well automatically becomes “attractive”, so the channel is never blocked at the well;
2. New migration adaptation: only meander close to the well may be connected for an “attraction” (erodibility correction to make migration faster):
    - Default maximum distance between a well and a meander for connection is equal to 15*w, where w is the channel width;
3. New avulsions adaptation: local avulsions are forced only if channel is close to the well (distance between closest channel meander and the well is less than 15*w). Else, regional avulsion is forced;
4. Aggradation may be blocked:
    - If the channel is inside the well and Active Brick is repulsive;
    - In expectation of a forced avulsion.

The new conditioning techniques improve the facies reproduction at well and the spatial sand distribution in conditional simulations and respect the simulation sand proportion:

1. Excessive Channelized facies deposition is significantly decreased;
2. Transitions between the lithofacies of different classes are better honored;
3. Spatial sand distribution in conditional simulation is more uniform.

4 Automatic Determination of Sedimentary Units from Well Data

Résumé français: Les réservoirs naturels montrent souvent une hétérogénéité verticale liée à la superposition d'unités stratigraphiques possédant des caractéristiques différentes. En modélisation de réservoirs, la détermination de ces unités doit être faite préalablement à la simulation de réservoir, de façon à pouvoir définir les valeurs de paramètres les plus appropriées pour chacune des unités. La détermination de ces unités à partir de données de puits n'est cependant pas toujours évidente. Dans ce chapitre, une méthode géostatistique hiérarchique de classification automatique est proposée pour aider au choix de telles unités, en exploitant l'hétérogénéité verticale présente sur la fraction sableuse de la courbe de proportion verticale globale des puits. La méthode, testée sur des exemples synthétiques et sur un cas réel, conduit à des résultats intéressants. Le chapitre est présenté sous la forme d'un papier soumis à Mathematical Geosciences.

Natural reservoirs are often characterized by a vertical heterogeneity. It may result of the stacking of several stratigraphic units, easy to identify when bounded by specific discontinuities (angular unconformity, erosion surface ...). Such stratigraphic successions are the result of the depositional conditions that governed the strata architecture and the sand ratio in response to the controlling factors that are the sea level, climate and tectonics.

Such sedimentary units should be determined before the reservoir simulations, in order to define the optimal parameters for each unit and obtain the most realistic simulations. When bounded by specific discontinuities, the lower and upper surfaces of these sedimentary units are easily mapped from 2 to 3D seismic data or identified on cores.

In this chapter, we develop a new method to identify sedimentary units from well data when no specific discontinuity has been identified during core analysis or on seismic data. These sedimentary units may correspond to subtle changes in aggradation rate or geometry of the sandbodies within a larger stratigraphic unit defined by specific discontinuities. Being able to identify such changes is of prime importance in conditional process-based simulations which aims at simulating the architecture of the sedimentary units.

The method is based on the Geostatistical Hierarchical Clustering (GHC, Romary et al., 2017) to which we added a stratigraphic criterion. The method is tested on VPC from synthetic wells composed of a of known number of stratigraphic units and is evaluated on a field case where the clustering results are compared to the field interpretation.

The chapter is presented in a form of an article submitted to *Mathematical Geosciences* journal.

Automatic Determination of Sedimentary Units from Well Data

Anna Bubnova[1], Fabien Ors[1], Jacques Rivoirard[1], Isabelle Cojan[1]

[1] *MINES ParisTech, PSL University, Centre de Géosciences,*

35 rue Saint-Honoré, 77300 Fontainebleau, France

Corresponding author: fabien.ors@mines-paristech.fr

Abstract

For honoring well data in reservoir models, it is recommended to ensure the maximal compatibility between the model parameters and the data. The issue of identifying the stratigraphic units within a reservoir is of prime importance because it allows splitting the reservoir simulation into several units with specific parameters, thus reducing the vertical non stationarity. A new method is proposed for a semi-automatic determination of the sedimentary units from well logging using a customized geostatistical hierarchical clustering algorithm. A new linkage criteria derived from the Ward criteria (cluster minimum variance) is proposed to ensure that the dissimilarities increase monotonically. The sand lithofacies proportion calculated from the well vertical proportion curve is taken as input data. At each step of the procedure, the algorithm merges the two consecutive most similar sand lithofacies units. Finally, the method proposes a number of units corresponding to the first most dissimilar step. The user can investigate a larger number of units by looking at the clusters with lower levels of dissimilarities. The method is validated using two synthetic cases built for a fluvial meandering reservoir. Results show that the units are identified at a lower level of dissimilarity when the conditions are less favorable (few wells, low sand contrasts between units). Finally the method is successfully applied to a field study by defining cluster units comparable to the field ones and suggesting a limit between units defined by paleosols rather than lacustrine levels.

Keywords:

geostatistical hierarchical clustering, reservoir model, stratigraphic unit, vertical proportion curve, well data, fluvial system

---

4.1 Introduction

Construction of sub-surface models of natural reservoirs is a large multidisciplinary activity used for resources estimation and production, or for environmental studies. It consists in creating three-dimensional numerical reservoir models, with a defined grid and mesh, informed with rock types facies and/or petrophysical characteristics (porosity, permeability). In the case of heterogeneous reservoirs, different models, for instance different realizations of stochastic models, can be developed. Such models are used for instance for estimating the reservoir quality and determining the associated model uncertainty by performing flow simulations through the generated block. The more detailed the model (realism, heterogeneity, stratigraphic architecture), the better are the decisions concerning the exploitation of the reservoir (well location, production strategy).

Typical workflow of a reservoir model construction is: (i) collect and analyze the available data (well or seismic data); (ii) determine stratigraphic units (reservoir architecture); (iii) define facies rock types properties as used in models (e.g.: pixel-based models, object-based model or process-based models); (iv) add petrophysical characteristics (porosity, permeability…) to the lithofacies; (v) create multiple realizations with the same dataset, that are further used for reservoir decision making and flow simulations (Pyrcz and Deutsch, 2014).

There exists now a large variety of reservoir model types: sequential simulations (Pyrcz and Deutsch, 2014), truncated plurigaussian simulations (Armstrong et al., 2011; Galli et al., 1994b; Le Loc'h and Galli, 1999), MPS simulations (Mariethoz and Caers, 2015b), object-based boolean models (Chilès and Delfiner, 2012b; Lantuejoul, 2002), another object-based model (Parquer et al., 2017b), or even process-based (or process-mimicking) models (Lopez, 2003c; Lopez et al., 2008b; Pyrcz and Deutsch, 2014). All types of reservoir models need a set of input parameters. In order to create realistic models, reservoir data (wells and seismic) combined with field data from outcropping analogs or modern systems are used for determining the input parameters optimal values, then, for conditioning to reservoir data during modeling.

Two main types of data are usually available during a reservoir study: seismic block and well data (e.g. well logging and coring). Seismic block provides information about the reservoir architecture and tectonic deformations. Stratigraphic resolution of a seismic block is at best 6.5 m, necessitating more detailed investigations to precisely locate the stratigraphic unit surfaces. Well logs give local information about stratigraphy, depositional facies including grain size and petrophysical characteristics (Doveton, 1986, 1994; Luthi, 2001).

During well log analysis, stratigraphic surfaces can be identified. They correspond to bio- or chemo-stratigraphic key horizons, and sequence stratigraphy key surfaces (maximum flooding condensed interval, or erosional surface, resulting in a strong contrast between clay and sand for instance). Beside these, some faults can be seen from the well logging. Such markers are further well-to-well correlated, which results in several stratigraphic and faults surface determination. Nowadays, the procedure of marker picking and well-to-well correlation could be performed automatically. Several techniques exist: multi-dimensional functions of differences (Lapkovsky et al., 2015), dynamic programming and mismatch matrix between two logs (Mirowski et al., 2005), wavelet tessellation applied to gamma ray logs (Hill et al., 2015; Wilde et al., 2017). Luthi and Bryant (1997) propose a back-propagation neural network, which can be trained to recognize geological markers in wells. Edwards et al. (2017) introduce another training-based method of stratigraphic well correlation, based on topological

relations between wells and calculation of well stratigraphic column (conversion of well log data into stratigraphic piles and their subsequent correlation).

An easy tool for a visualization of vertical facies heterogeneity is the Vertical Proportion Curves (VPC) (Armstrong et al., 2011; Ravenne et al., 2002). Such curves display the vertical variability of lithofacies proportions in wells, and give first information about the reservoir structure. The VPC construction consists in dividing all data into a chosen number of vertical intervals or levels and then displaying the proportion of lithofacies within each interval (the elevation is reported along the vertical axis). The Figure 139 shows an example of a VPC computed from 20 synthetic wells extracted from a Flumy® simulation (MINES ParisTech, ARMINES, 2016) with 50 meters thickness divided into a hundred 50 cm thick intervals. See §4.3.2 section for more details about Flumy model.

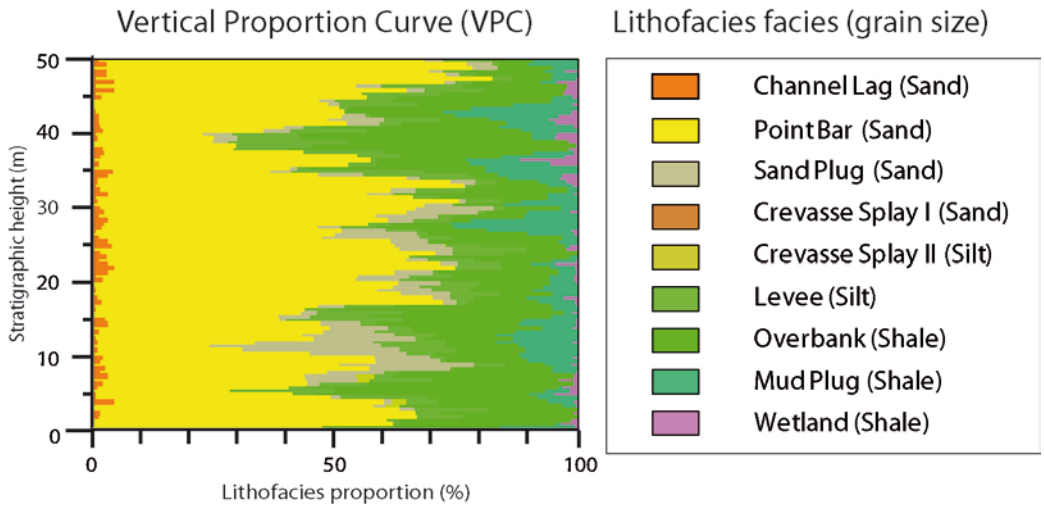

Figure 139. Example of a Vertical Proportion Curve (VPC) with its lithofacies color scale. Image from Flumy®

A strong contrast in the vertical sand distribution indicates the possible presence of separate sedimentary sequences (controlled by tectonic, climate fluctuation or sea level variation) leading to distinct reservoir units within the considered stratigraphic interval. Grouping consecutive VPC levels with similar sand proportion results in a reservoir sedimentary architecture made of distinct units.

Starting from the idea of classifying and grouping the most similar data (here the homogeneous parts of the reservoir in terms of sand proportion), one popular method to be recalled is the clustering. Currently, it is applied to a wide range of data, including geology (Berkhin, 2006). Clustering technique can be seen as a method of numerical unsupervised learning which automatically forms clusters from data presenting some kind of hidden patterns (then reducing the “human factor”). In reservoir or ore deposit data analysis, clustering is generally used for samples classification, but with various types of input data and for different aims. For instance, it can be useful for sorting data measurements and defining rich/poor reservoir regions (Allard and Guillot, 2000), for data interpretation into lithofacies classes determined from well logs (Ferraretti et al., 2012), for well logs conversion into architectural elements (Allen and Pranter, 2016). Romary and collaborators (Romary et al., 2015) introduced the concept of Geostatistical Hierarchical Clustering (GHC), which is an adaptation of the multivariate classical hierarchical clustering method to regionalized data.

The main purpose of this paper is to present a new automatic method for determining sub-horizontal sedimentary units by developing a simplified version of the Geostatistical Hierarchical Clustering

(GHC) applied to sand vertical distribution coming from well data. First, the GHC algorithm is presented, as well as its adaptation to well data using well Vertical Proportion Curves (VPC). Then the material used for datasets is presented: eight sections (considered as pseudo-wells) coming from a fossil meandering fluvial succession located in Spain (Loranca basin) and the Flumy model used to build two synthetic datasets by computing VPC from a limited number of wells extracted from Flumy simulations. Then the results obtained when applying the proposed method to these three datasets are presented. Finally, the method is discussed with respect to its potential for an automatic stratigraphic units detection from limited data.

4.2 Method

4.2.1 Hierarchical clustering overview

Clustering is an unsupervised learning technique which consists in grouping similar data elements into clusters. Only clustering techniques which assign each data element to only one cluster will be considered here. Among those algorithms, some of them (the partitioning clustering algorithms) need to have a prior knowledge of the dataset, as the number of resulting clusters is requested at the beginning. Some others, called hierarchical clustering, use an ascending agglomerative approach for aggregating elements step by step into clusters. Such algorithms, combined to a spatial connectivity constraint, ensure that elements owning to the same cluster are spatially close (Romary et al., 2015). This neighborhood capability is the reason why this last technique will be considered in this paper.

In hierarchical clustering, the initial data element dissimilarity (generally called “distance”) is calculated from one or several element properties. At the beginning of the algorithm, each element is classified as a single cluster. Then, at each iteration, the two most similar clusters are merged forming a new cluster, and the distances from the other clusters to the new one are updated. The algorithm stops when all the elements are classified into one cluster. This procedure is strictly consistent (only one new cluster is formed at each step, and the data elements are never mixed), so it is possible to draw an exact scheme describing the order of mergers and the measure of their dissimilarity. Moreover, some dissimilarities update techniques ensure that dissimilarities are monotonically increasing, resulting in merging clusters that also have monotonically increasing dissimilarities. The Figure 140 illustrates a dendrogram of such a synthetic hierarchical clustering example as well as its variant, the associated cluster dissimilarity graph. The dendrogram (Figure 140a) is to be read from bottom to top. Each vertical segment represents a cluster and the horizontal segment joining the tops of two such segments corresponds to their merging into a new cluster. The elevation of this horizontal segment corresponds to the dissimilarity between the two merged clusters. At each step the two most similar clusters are merged, and their dissimilarity is displayed step by step on the cluster dissimilarity graph (Figure 140b).

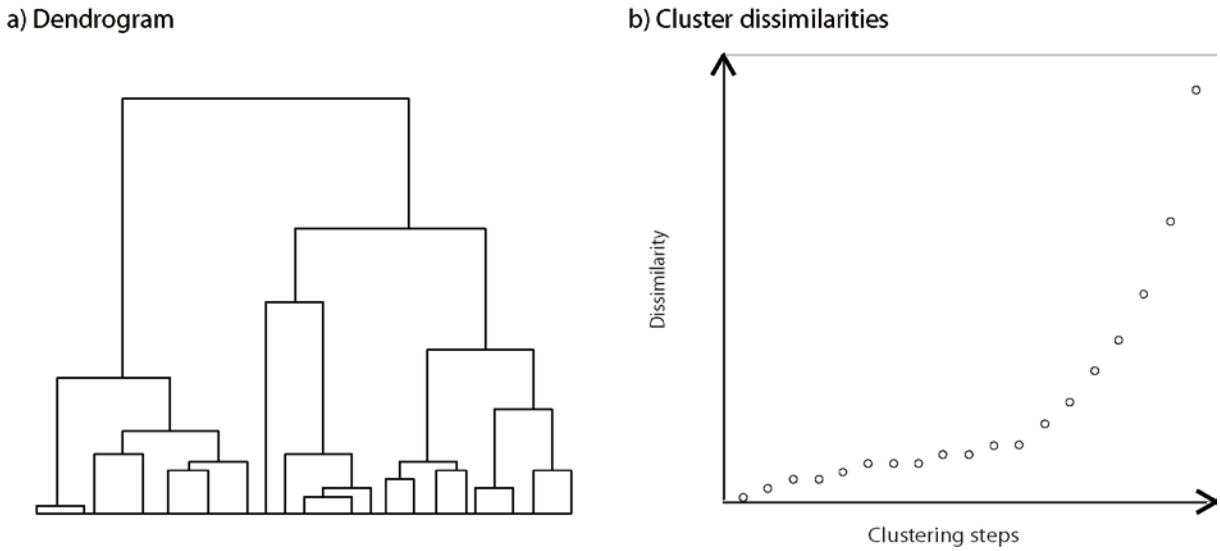

Figure 140. Example of (a) a dendrogram and (b) its variant, a graph of cluster dissimilarities

Three components should be defined for performing a hierarchical clustering:

1) The input variables used for calculating the initial element dissimilarities. Variables may be multidimensional (Fouedjio, 2016; Parks, 1966), continuous or categorical (Romary et al., 2015).
2) The initial element dissimilarity formula (distance calculation). It is computed at the first step of the algorithm – see Eq. (1).
3) The linkage criterion which defines the technique for updating intercluster distance (if clusters contain more than one element). It is computed at each step of the algorithm – see Eq. (2).

Romary and collaborators define the general initial distance formula between two elements x_i and x_j (represented by their p variables) by:

$$\boldsymbol{d}(\boldsymbol{x_i}, \boldsymbol{x_j}) = \sum_{\boldsymbol{k=1}}^{\boldsymbol{p}} \sum_{\boldsymbol{l=1}}^{\boldsymbol{p}} \boldsymbol{\omega_{k,l}} \boldsymbol{d}^{(\boldsymbol{k,l})} \left(\boldsymbol{x_i^{(k)}}, \boldsymbol{x_j^{(l)}} \right) \quad (1)$$

where:

- p is the number of input variables
- $x_i^{(k)}$ is the value of the variable k for the element x_i
- $d^{(k,l)}(x_i^{(k)}, x_j^{(l)})$ is the coupled distance between the value $x_i^{(k)}$ and the value $x_j^{(l)}$
- $\omega_{k,l}$ is the weight to be applied to the coupled distance $d^{(k,l)}(x_i^{(k)}, x_j^{(l)})$

Therefore, this general distance calculation is a weighted sum of coupled distances.

The Lance and Williams formula (Lance and Williams, 1967) is a unique recurrence formula which permits to update the intercluster distance when merging two clusters. This generic formula handles a large family of linkage criteria, including maximum, minimum and average distances or minimum variance (respectively named “complete”, “single”, “average” and “Ward’s” linkage criteria, see Milligan (1979) for details on the criteria). The recurrence formula is computed as:

$$d_{k(ij)} = \alpha_i d_{ki} + \alpha_j d_{kj} + \beta d_{ij} + \gamma \left| d_{ki} - d_{kj} \right| \quad (2)$$

where:

- $d_{k(ij)}$ is the updated distance between a cluster k and the new cluster *(ij)* created by merging clusters i and j,
- d_{ij}, for instance, is the distance between clusters i and j,
- α_i, α_j, β and γ are parameters calculated once at startup, then at every step according to the required linkage criterion.

Under conditions:

$$\alpha_i + \alpha_j + \beta \geq 1, \alpha_i, \alpha_j \text{ and } \gamma \geq 0 \quad (3)$$

The recurrence formula ensures that dissimilarities are monotonically increasing, resulting in merging clusters that present increasing dissimilarities.

4.2.2 Geostatistical Hierarchical Clustering (GHC)

The method proposed in this paper is based on the Geostatistical Hierarchical Clustering (GHC, (Romary et al., 2015). The spatial aspect of the dataset is usually taken care of by adding the coordinates as input variables for the initial distance calculation. Romary and collaborators have preferred adding in the GHC, a connectivity constraint for merging two clusters. Hence, in GHC, a forth component is necessary: the connectivity graph given through a connectivity matrix.

The general form of the connectivity matrix C is:

$$C = \begin{pmatrix} c_{11} & \dots & c_{1n} \\ \vdots & \ddots & \vdots \\ c_{n1} & \dots & c_{nn} \end{pmatrix} \quad (4)$$

where:

- $c_{ij} = \begin{cases} 1, \text{ if elements } i \text{ and } j \text{ are connected,} \\ 0, \text{ otherwise.} \end{cases}$

The GHC procedure can be presented in the following algorithmic form:

1/ Compute the initial distances between all the elements (1 element = 1 cluster),
2/ Find the two connected clusters with the minimal distance and merge them,
3/ Update the distances between the new cluster and all other clusters using the recurrence formula for the chosen linkage criterion,
4/ Repeat steps 2/ to 4/ until all the elements belong to one cluster (or until clusters cannot be merged anymore because they are not connected).

Note that, because of the constraint on connectivity, clusters to be merged at a given iteration are not necessarily the most similar, as they must be connected. It follows that having increasing dissimilarities when merging clusters is not guaranteed whatever the linkage criterion, even if the dissimilarity update is monotonically increasing.

4.2.3 Adaptation of the GHC to well data

Well data can vary from continuous information (well logging) to discontinuous one (lithofacies). In the present paper, we chose to describe the vertical facies heterogeneity from its sand proportion, which is of primary importance in reservoir studies and flow simulations. Considering VPC, each element i, indexed upwards, contains only one variable: the sand proportion ($sand_i$). Hence the initial cluster distance between x_i and x_j is a simple square difference (the unique weight ω of the Eq. (1) is equal to 1):

$$d(x_i, x_j) = (sand_i - sand_j)^2 \quad (5)$$

In order to split the wells VPC into contiguous intervals (without intrication), the connectivity constraint is added so that only contiguous clusters can be compared and merged:

$$c_{ij} = \begin{cases} 1, \text{ if } i = j+1 \text{ or } j = i+1, \\ 0, \text{ otherwise.} \end{cases} \quad (6)$$

The linkage criterion that showed the best results (smoothing evolution and increasing monotonic property of dissimilarities with a large contrast between the few last merger dissimilarities and all the first steps) is a variant of the Ward's criterion (minimum variance). For the Ward's criterion, the coefficients used in the Lance and Williams formula (Milligan, 1979) are:

$$\propto_i = \frac{n_i + n_k}{n_i + n_j + n_k} \qquad \propto_j = \frac{n_j + n_k}{n_i + n_j + n_k} \qquad \beta = \frac{-n_k}{n_i + n_j + n_k} \qquad \gamma = 0 \qquad (7)$$

where for instance n_i refers to the number of elements in cluster i. It is easy to see that these coefficients satisfy the conditions (3) ensuring the monotonic increasing of dissimilarity updates.

Unfortunately, by adding the connectivity constraint, the monotonic increasing property of dissimilarities of mergers is no longer guaranteed whatever the linkage criterion. This desirable property has been obtained in practice (but may not be always the case as it is not proved mathematically) by modifying Ward's criterion into the criterion we call "Ward+". This is obtained by inverting the sign of β in Eq. (7):

$$\propto_i = \frac{n_i + n_k}{n_i + n_j + n_k} \qquad \propto_j = \frac{n_j + n_k}{n_i + n_j + n_k} \qquad \beta = \frac{n_k}{n_i + n_j + n_k} \qquad \gamma = 0 \qquad (8)$$

This modification also satisfies conditions (3) and results in reinforcing the monotonic increasing of dissimilarity updates.

An advantage of the hierarchical clustering is that each step of the algorithm is recorded. it is possible to visualize the whole procedure evolution, but also to select the number of most dissimilar clusters by "cutting" the dendrogram. This is facilitated using the new Ward+ criterion since the last dissimilarity steps tend to be much larger than the previous ones, as shown in Figure 141. In the following, the adaptation of the GHC is named GHC_{ward+}.

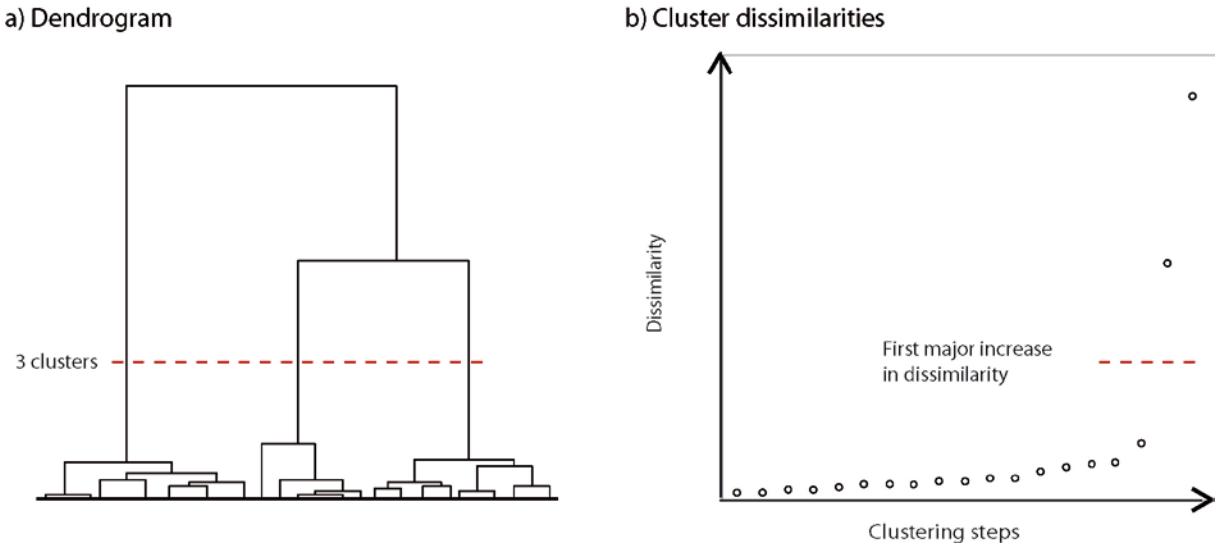

Figure 141. Example of (a) a dendrogram and (b) its graph of cluster dissimilarities using the Ward+ linkage criterion

4.3 Material

4.3.1 The Loranca meandering succession

The continental succession of the Loranca basin (Figure 142) has been extensively studied because of its excellent outcropping conditions that allow detailed studies (Daams et al., 1996; Diaz-Molina et al., 1985; Martinius, 2000). The Lower-Miocene deposits of the Loranca formation are dominated by meandering fluvial deposits in the Huete area, corresponding to the distal part of the system (Figure 142a). The excellent quality of its outcrops provides a unique opportunity to describe all facies associated to a 95 m thick fluvial meandering succession (Figure 142b, Figure 142c) (Cojan et al., 2009, 2006; Martinius, 2000).

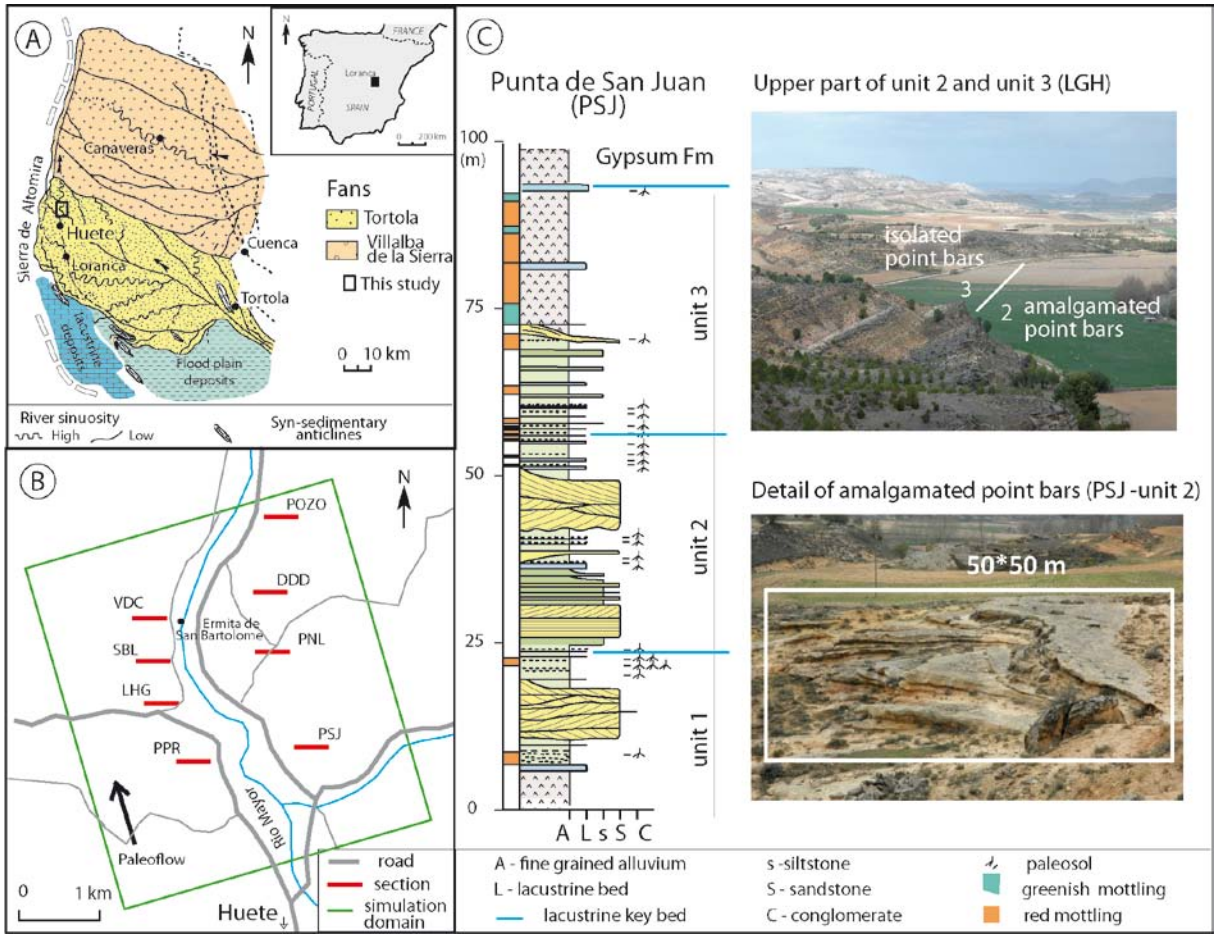

Figure 142. Loranca basin: (a) location of the study area in the Tortola fan and (b) location of the measured sections along the Rio Mayor valley sides with (c) an illustration of the architecture of isolated and amalgamated sand bodies

Paleohydrological reconstruction of the fluvial system indicates a mean bankfull channel depth of 3 ±0.5 m that does not vary significantly along the considered stratigraphic interval (Cojan et al., 2006; Diaz-Molina et al., 1985; Weill et al., 2013). The meandering system developed mature meander bends as indicated by the extension of the point bar migration sets and the frequent oxbow deposits attesting for meander neck cut-offs. The paleo-flow direction towards the NW remained stable along the studied interval.

The clustering tests were conducted on eight sections measured along the left and right banks of the Rio Major, a few kilometers north of the town of Huete. These are distributed over a domain of 4 × 4.5 km² (Figure 142b). Sections are measured in the field with a precision of 0.10 m. Sections are correlated thanks to lacustrine deposits and flattened for removing subsequent tectonic deformation.

The sandy facies correspond to point bar sets with pebble-size channel lags, and crevasse splay deposits. Silty facies are always associated to crevasse splays or levees and fine-grained material corresponds to overbank alluvium and shallow lake deposits (mainly carbonate and organic material) (Figure 142c).

4.3.2 The Flumy model

Flumy® (MINES ParisTech, ARMINES, 2016) is a stochastic process-based model that allows reproducing complex architectures of meandering fluvial deposits (such as the Loranca succession – see§4.3.1) and results in three-dimensional block models informed with facies and associated grain size (Lopez, 2003c; Lopez et al., 2008b). It provides realistic reservoir models by mimicking the meandering system processes and deposits: i) the channel migration which generates sandy point bars deposits at meander inner banks, and mud or sand plugs into abandoned loops (following channel cut-off); (ii) the aggradation which generates channel lag pebbles, silty levee deposits close to the channel and overbank alluvium further away in the floodplain; iii) the levee breaches that results in crevasse splay deposits and the avulsions which lead to a new channel path and an abandoned channel filled of sand or mud plugs.

After choosing the simulation domain size and resolution, the Flumy model is controlled by a small number of key parameters such as the channel geometry (bankfull depth and width, paleo-flow direction, mean wavelength) and the external events ones (aggradation intensity and period, avulsion periods). The avulsion periods and the migration rate govern the meander lateral development and connectivity of the resulting sand bodies, whereas the channel size parameters and the aggradation rate govern the resulting sand proportion.

While building the block model by depositing sediments, it is possible to interrupt the reservoir simulation and update the parameters. Then, by resuming the simulation, a new unit is stacked above the previous one with different sand proportion and lateral sand bodies extension. Vertical Proportion Curves can be computed from the whole simulated three-dimensional block or from a given number of extracted vertical wells (see Figure 139).

4.4 Results

The GHC_{ward+} method is evaluated using data from three case studies of some meandering fluvial successions: two synthetic test cases (see below) and the Loranca field case (see §4.3.1).

The two synthetic cases correspond to multi-unit three-dimensional blocks, built using Flumy software (see §4.3.2). They are simulated using a domain size (4 × 4.5 km²), a channel mean bankfull depth of 3 m and a paleo-flow direction toward the NW comparable to that of the Loranca field study.

Each synthetic simulation is obtained by stacking several units with distinct thickness and sand proportions (3 stratigraphic units for the first synthetic case, and 5 units for the second one). Periods of avulsion, levee breaches and overbank events are chosen to obtain the desired sand proportion for each simulated unit (see Figure 144 and Figure 145).

In the following, sandy (point bar, sand plug and crevasse splay) and pebbly facies (channel lags) are grouped into the "sand lithofacies" to be considered for the clustering process. VPC from synthetic cases are calculated for the sand lithofacies proportion (at a 1 m thick interval) along the entire simulated sedimentary succession, either from the whole three-dimensional block (named "Reference VPC) or from a given number of wells extracted from the three-dimensional block (named "Well VPC"). The location of the synthetic wells is depicted in Figure 143. In the first synthetic case, the wells are regularly distributed over the simulation domain (Figure 143a). In the second synthetic case, the location of the 8 wells (Figure 143b) is the same as that of the field sections from the Loranca basin (Figure 142b).

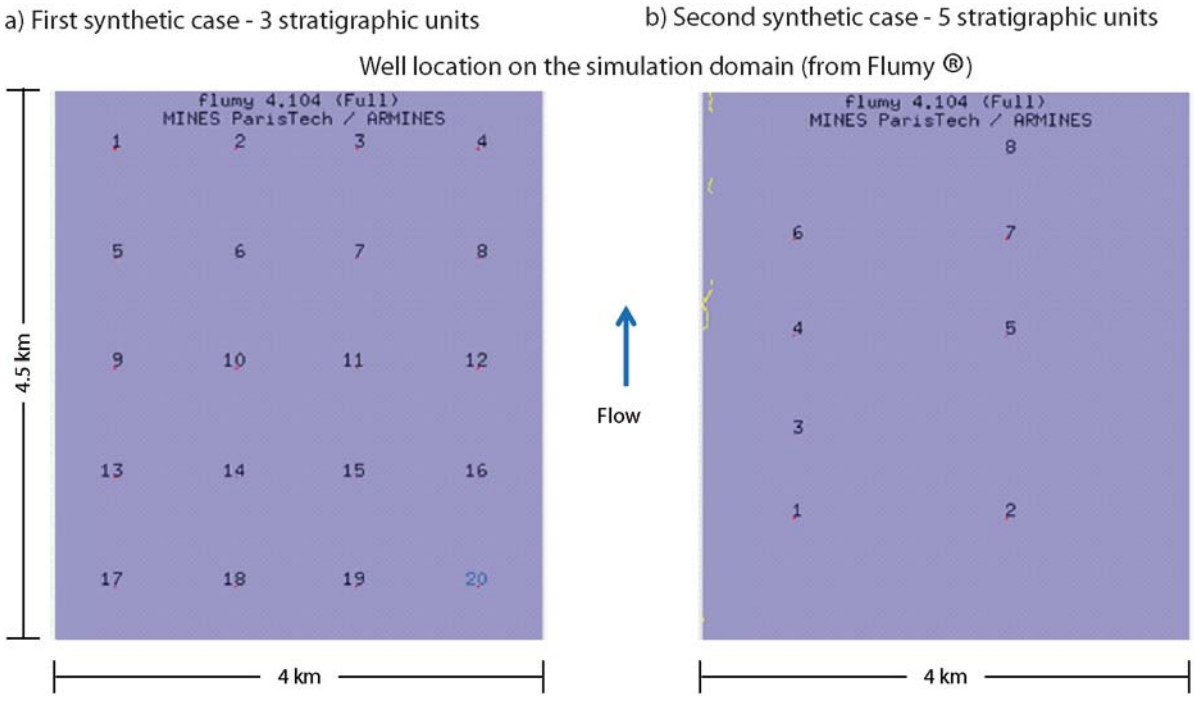

Figure 143. Location of wells for (a) the first synthetic case (20 wells), and (b) the second synthetic case (8 wells)

The two synthetic cases allow testing the GHC_{ward+} method in different conditions. They permit to compare the units determined by the method from a limited number of wells to the original units. Data from the Loranca field sections are treated the same as would be wells extracted from a simulation.

The GHC_{ward+} algorithm is applied considering the sand lithofacies proportion every 1 m along the VPC, e.g. the same interval thickness as for the synthetic simulations. The resulting units can then be compared to the units determined by the geologists.

4.4.1 First synthetic case: contrasted units

The first synthetic three-dimensional block of 85 m thickness, is composed of a succession of three units, of contrasted thickness and sand proportion (unit 1 – 35 m, 60%; unit 2 – 15 m, 45%; unit 3 – 35 m, 65%).

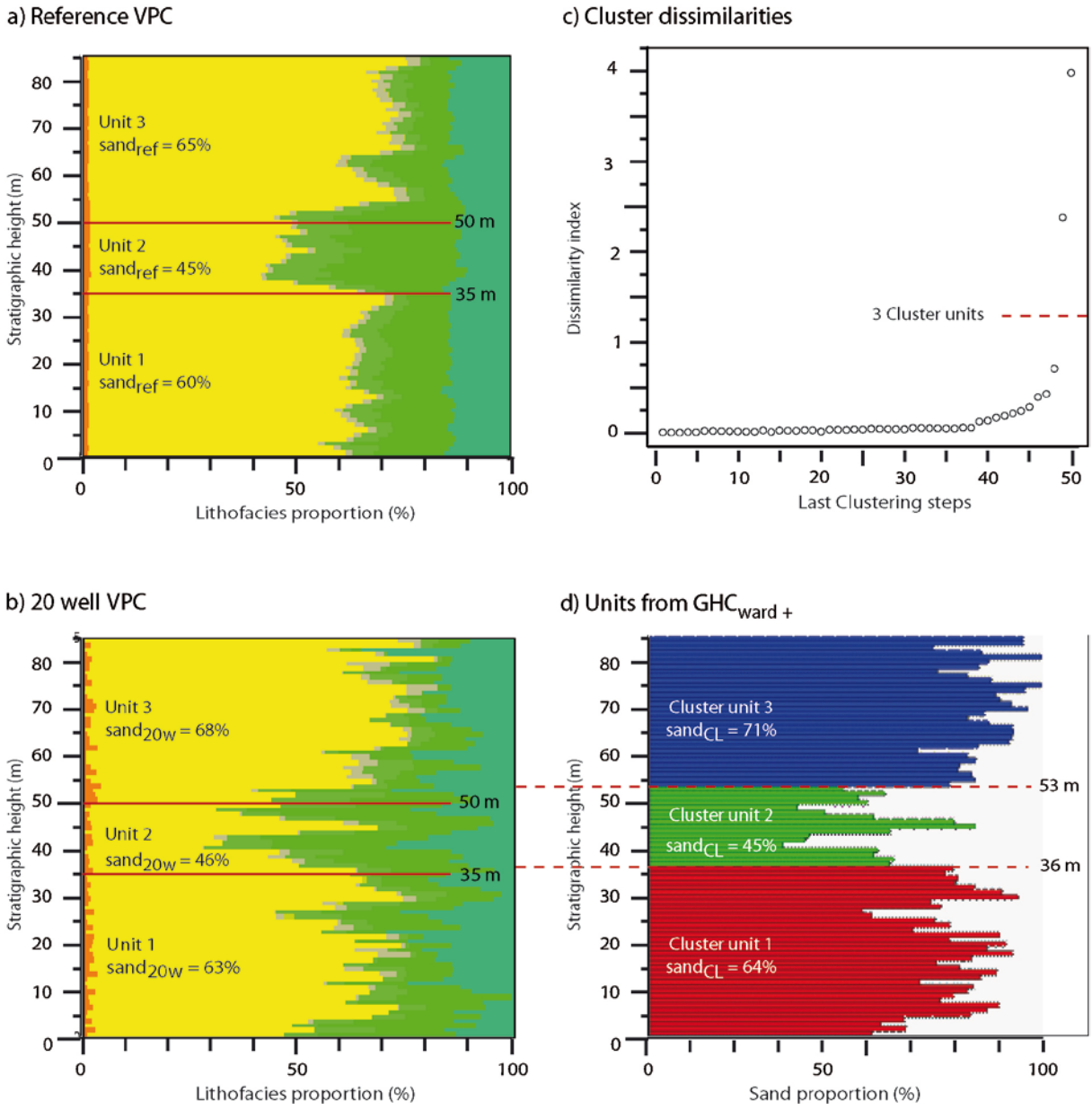

Figure 144. First synthetic test with 3 contrasted units. (a) Reference VPC, red solid lines represent initial units limits. (b) VPC of 20 extracted wells. (c) Cluster dissimilarities graph. (d) The last three clusters proposed by our method.

The initial units are easily identified on the reference VPC, in particular, the sharp drop or increase in sand proportion which defines the unit limits, and the contrasted sand proportion from one unit to the other one (Figure 144a). The initial units are less detectable in the extracted well VPC (Figure 144b).

Units and limits between units are difficult to locate because the sand proportion is more variable than in the reference VPC. Application of the GHC_{ward+} to the VPC built from 20 wells shows a big step in the cluster dissimilarities graph for the two last mergers (Figure 144c), suggesting a cut of the dendrogram before these two last steps (Figure 144c, red dotted lines). The proposed unit limits are at elevations of 36 m and 53 m, very close to the reference VPC (35 m and 50 m). The sand proportions of the proposed units are slightly more contrasted than the sand proportions on wells data within the original units.

The first conclusion is that the proposed method succeeds in recognizing the three contrasted initial units quite accurately.

4.4.2 Second synthetic case: less contrasted units

The second synthetic three-dimensional block of 80 m thickness corresponds to a succession of 5 units showing less contrast in thickness and sand proportion between units (unit 1 – 20 m, 50%; unit 2 – 10 m, 40%; unit 3 – 20 m, 35%; unit 4 – 15 m, 45%; unit 5 – 15 m, 55%). Eight wells situated in the same location than Loranca sections within the simulation domain were extracted.

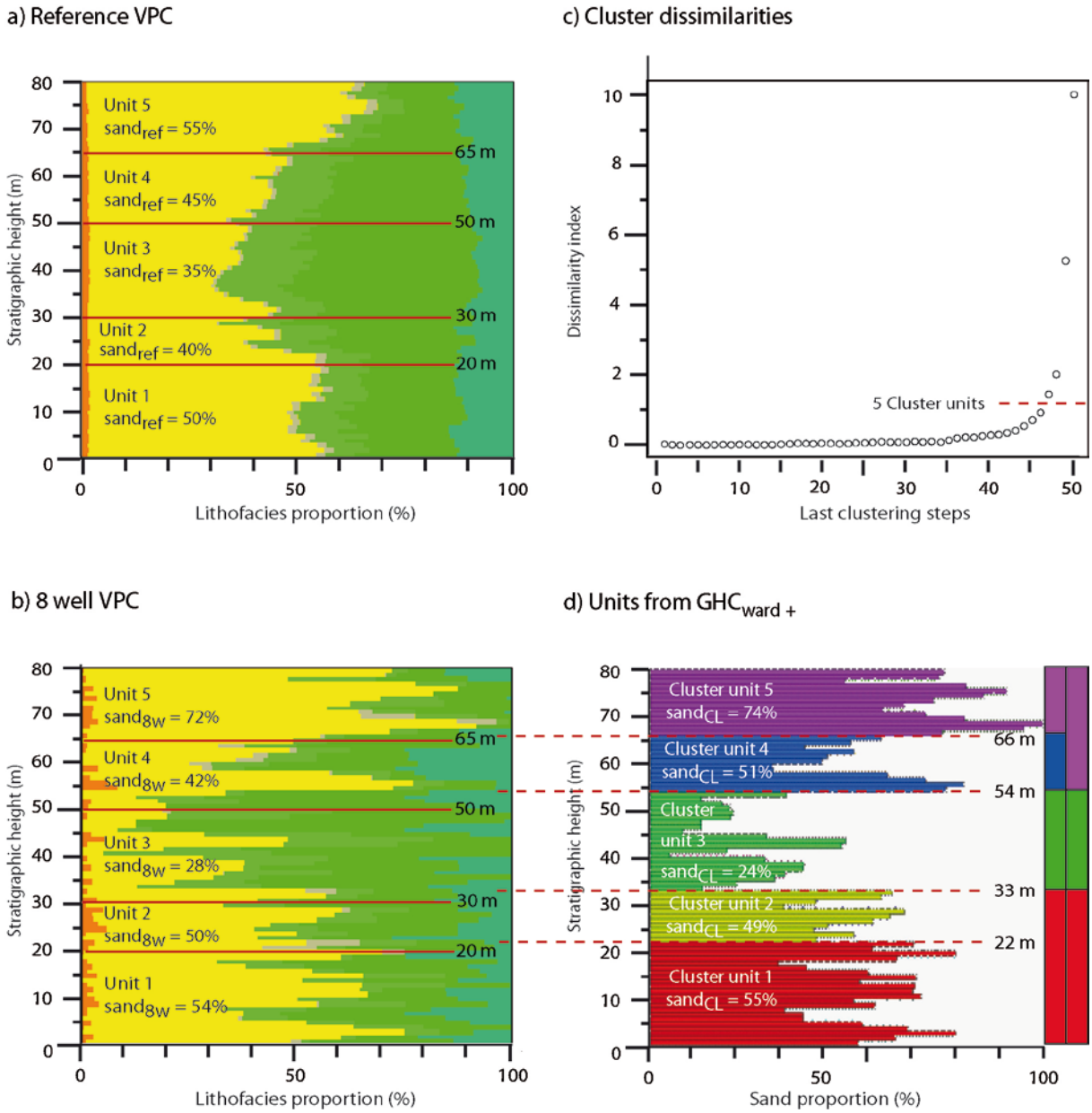

Figure 145. Second synthetic test with 5 less contrasted units. (a) Reference VPC, red solid lines represent initial units limits. (b) VPC of 8 extracted wells. (c) Cluster dissimilarities graph. (d) The last five clusters proposed by our method

The initial units are not clearly visible in the reference VPC (Figure 145a) which shows trends more than contrasts between units. It is even more difficult to detect the initial units when looking at the extracted wells VPC (Figure 145b) which displays numerous fluctuations of large amplitude at a scale of several meters. By analyzing the cluster dissimilarity graph (Figure 145c), the first large step in dissimilarity is observed before the two last mergers. This would lead to obtain three clusters: the bottom one composed of the red and yellow units (Figure 145d), the middle one of the green unit, and the top one comprising the blue and purple units (Figure 145d). By "cutting" the dendrogram before the four last mergers, the last five most dissimilar clusters are visualized (Figure 145d). These clusters almost correspond to the initial units. The resulting elevations of the different units are close to the original ones, and the resulting sand proportions are also close to the sand proportions on well data within the original units. The contrast between the sand proportions of the different units is in fact slightly enhanced (for instance the highest sand proportion is 74% instead of 72% and the lowest is

24% instead of 28%). This is due to the fact that the elevations resulting from clustering appear to be close to the original ones but are determined to favor the contrasts. Note that testing a different way to "cut" the dendrogram does not require running the algorithm another time. The hierarchical story and the interval frontiers remain the same.

The second conclusion is that even when it is difficult to identify sedimentary units in the well VPC, the proposed method gives to the user the choice in the number of units composing the reservoir architecture, and provides consistent stratigraphic elevations. With a low number of wells and a complex stratigraphic architecture, the number of units may have to be looked for at levels of dissimilarity which are not the largest ones.

4.4.3 Loranca case study

The eight measured sections have been divided by the geologists into three units defined from the relationship between the channelized sandy deposits giving different sand proportions. The lower unit comprises some stacked point bars isolated in thick overbank alluvium, with fairly low sand proportion (~16%). The middle one is composed of amalgamated, partly truncated point bar deposits resulting in an interval with a higher sand proportion (~44%). The upper unit is made of isolated point bars disseminated within shale to clay rich overbank alluvium, with an intermediate sand proportion (~27%) (Figure 146a).

As above mentioned, sections are correlated based on lacustrine deposits that are taken as horizontal surfaces in the floodplain. Similarly, the stratigraphic units are defined using the lacustrine beds that showed a good lateral extension. Nevertheless, in the case of the limit between units 2 and 3, unit correlation between sections is performed within an interval with numerous lacustrine beds, which may have induced some uncertainty in the exact correlated bed when physical correlation was made difficult by vegetation cover.

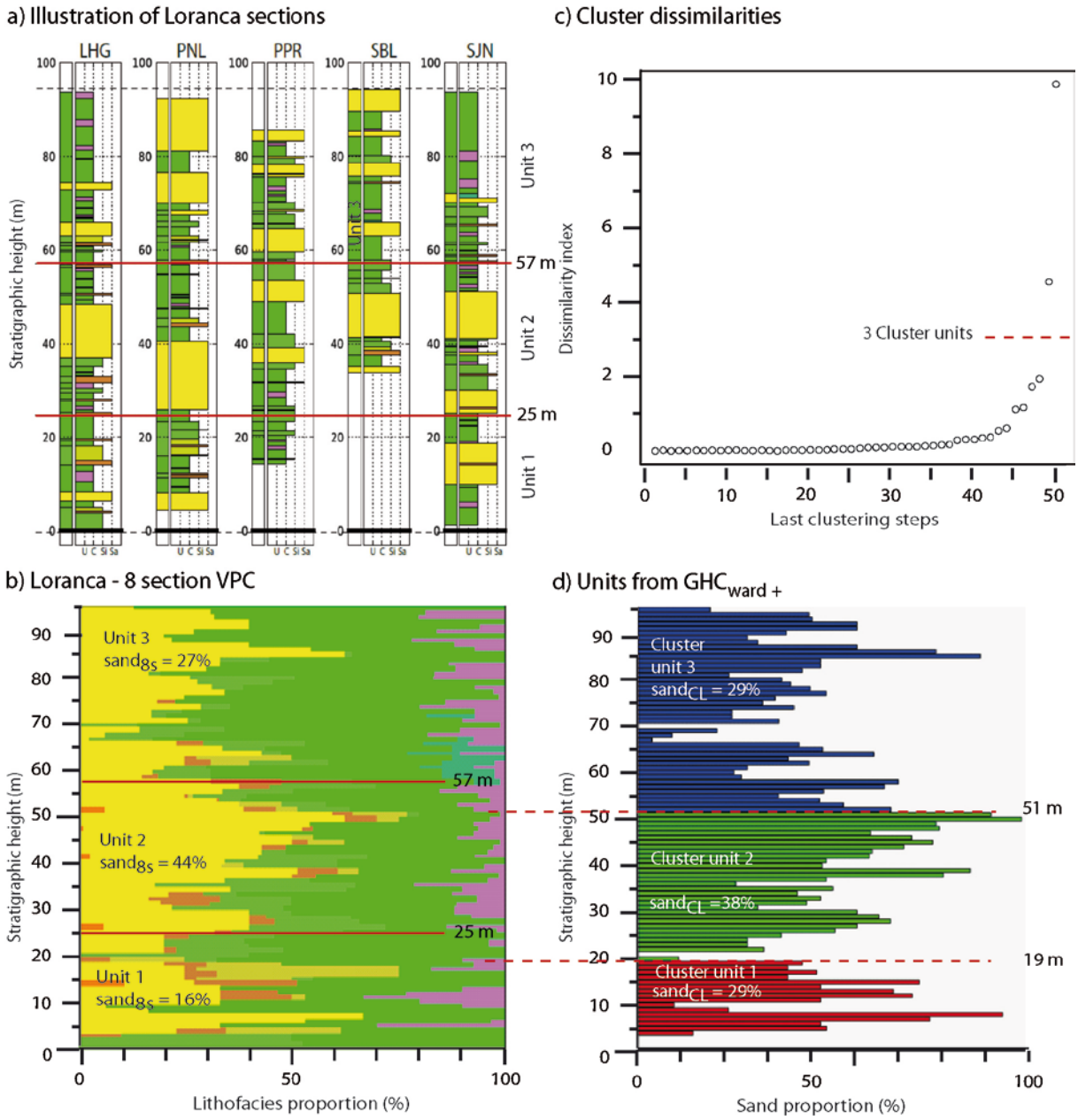

Figure 146. Application to a real dataset: Loranca basin. (a) 5 sections out of the 8 available, red solid lines represent units limits proposed by geologists. (b) VPC of the 8 Loranca wells. (c) Cluster dissimilarities graph. (d) The last three clusters proposed by our method

The 8 sections VPC (Figure 146b) shows large variations in the sand proportion along the studied interval and within each of the field units. It is not possible to identify the field units from the 8 sections VPC.

Application of the GHC_{ward+} algorithm shows a large step in the cluster dissimilarity (Figure 146c) before the two last points, indicating that the sedimentary succession could be split in three units. The limits between the stratigraphic intervals that are proposed by the GHC_{ward+} (Figure 146d) are 6 m below those proposed from the field study. The shift in the unit limits results in a higher sand proportion for the lower unit (29% instead of 16%) and close proportions for the other units (unit 2 – 38% instead of 44%; unit 4 – 29% instead of 27%).

By comparison with the facies succession, the limit proposed by the GHC_{ward+} algorithm corresponds to the first lacustrine bed associated to paleosols in the upper part of unit 1 or unit 2. Thus, the GHC_{ward+} algorithm identifies the hiatus associated to pedogenesis in the lowland of the floodplain as a significant limit during sedimentation. One can conclude that the proposed methodology permits to give a first guess of the reservoir sedimentary structure even when having few wells data and important vertical variability of the sand proportion; it may also help in identifying limits in environments where facies lateral continuity is limited, such as in fluvial systems.

4.5 Conclusions and perspectives

In this paper, a new tool for determining automatically sedimentary units from the well data is presented. The proposed methodology is based on the Geostatistical Hierarchical Clustering (GHC) algorithm applied to the wells global Vertical Proportion Curve (VPC). The main idea is to merge iteratively elementary VPC levels into a decreasing number of units using a modified Ward criterion (GHC_{ward+}). The objective is to obtain several contrasted sedimentary units (last clusters), that are the most homogeneous in term of sand proportion.

It is shown that this methodology gives quite good results by using synthetic data, even when it is difficult to recognize the initial units from the well VPC. The results on a field case (Loranca – Spain) are also very interesting as they confirm the field correlation and refine the choice of the key levels for the stratigraphic units, in this case unit limits are placed on pedogenic horizons associated to lacustrine beds.

The choice of the optimal number of units is currently manual and is done by detecting the first merge which shows a large gap of dissimilarity among the last steps. However this is not always straightforward, and when the number of wells is very limited, the desired number of units may have to be looked for at levels of dissimilarity which are not the largest. Future work is to be done to cut the dendrogram automatically in order to directly propose some best reservoir splitting.

Another future work could be to test the influence of well density on the choice of the dissimilarity level used to propose the units. The extension to more variables (i.e. grain size or gradients) for calculating initial dissimilarities is another important perspective.

As mentioned above, well data must be flattened before performing the clustering analysis. This new tool may also be used in order to help the user in choosing the optimal reference plane, by testing several flattening hypothesis and selecting the best contrasted clustering results.

Finally, an important perspective would be to enhance the method for handling sedimentary units delimitated by three-dimensional surfaces by using a VPC for each well and merging elements in all directions. This improvement would in particular permit to detect sedimentary units that do not extend onto the whole field.

Acknowledgements

This method has been implemented as a well analysis tool into the Flumy software within the scope of the Flumy Research Program. The authors are grateful to ENGIE (Neptune Energy) and ENI partners, for support and fruitful discussions.

5 Conclusions and perspectives

Résumé français: Deux sujets bien distincts ont été traités dans ce travail: le conditionnement de Flumy aux données de puits d'une part, la détermination des unités stratigraphiques par un algorithme de classification automatique appliqué aux données de puits d'autre part.

Les tests ont révélé que les principes généraux du conditionnement dynamique aux données de puits sont plutôt efficaces, mais que les algorithmes pouvaient conduire à des situations indésirables et devaient être améliorés. Le conditionnement dynamique est basé sur un principe d'attraction aux données de sable et de "répulsion" aux données d'argile. De façon générale cependant, il y avait un déséquilibre être les processus d'attraction, dominants, et ceux de répulsion, déséquilibre responsable d'un dépôt excessif de sable à l'endroit des puits comme à leur amont. Une attention spéciale a due être portée aux problèmes posés par la transition entre lithofaciès chenalisés et non chenalisés le long des puits, en particulier lorsque le chenal est présent sur le puits. La révision des algorithmes, notamment concernant la mise à jour du niveau dit actif en chaque puits, a permis une amélioration significative des résultats. L'obtention d'un conditionnement à 100% parait plus du ressort d'un "post-processing" permettant d'effacer les écarts entre données et simulation à l'endroit des puits et dans leur voisinage. Des pistes de conditionnement par des voies statistiques, plutôt que par des modifications portant sur les processus physiques, sont envisageables moyennant une puissance de calcul démultipliée.

La détermination des unités stratigraphiques est une étape préalable à la simulation de réservoirs. L'adaptation d'un outil de classification automatique hiérarchique géostatistique à la courbe de proportion verticale des puits fournit une aide à l'utilisateur pour l'identification des unités. Le développement d'un critère d'optimalité pourrait rendre la détermination des unités entièrement automatique. Actuellement l'outil exploite la courbe de proportion verticale globale du sable calculée sur les puits. Il pourrait être étendu à plus de variables. Une autre perspective pourrait être la détermination d'unités délimitées par des surfaces autre que des plans horizontaux.

5.1 General Discussion

Various types of models are used for the creation of natural reservoir numerical analogues. Flumy is a process-based model, with three main processes included into simulation: migration, aggradation and avulsions. Two types of conditioning to field data are possible, in order to create more realistic simulations: seismic data conditioning (soft) and well data conditioning (hard). This thesis discusses only conditioning to wells. Two main questions were considered during the work.

The first one concerns a procedure of conditioning and was presented in Chapters 2 and 3. Conditioning to wells in Flumy is a dynamic procedure – no trial / error, the well data are reproduced during the simulation. Well data are interpreted according to a lithofacies classification which divides the data lithofacies into three main classes: Channelized, Levee and Fine-Grained lithofacies. This classification is further used to adapt the main Flumy simulation processes for well reproduction. To do this, special conditioning techniques are applied: “repulsion” / “attraction” of the channel to the well location (increase / decrease of migration velocity in the direction of wells); adapted tossing of new channel paths in the appropriate locations by creating a “pseudo topography”; aggradation blocking in extreme cases.

Choice of simulation parameters which are consistent with the well data is an important issue of conditioning procedure: the more compatible the parameters are with the data, the less the conditioning is violent for the original Flumy simulation process. Now, a simulation can be run with three main input parameters: N_G (sand expected proportion in simulation), H_{MAX} (maximal channel depth) and I_{SBX} (sandbodies extension coefficient). In this case, the other parameters can be approximately defined by the Nexus tool, which is based on heuristic formulas. There exists a method of H_{MAX} definition from the well data. Determination of I_{SBX} is quite an issue as a computation of horizontal parameter from vertical data. Definition of N_G from the wells is a simple task of sand proportion computation, but only if the modelled reservoir is vertically homogeneous in sand.

In the case when several stratigraphic layers are presented in reservoir, it should be modelled as a sequence of units with different simulation parameters. In Chapter 4, a new method of determination of such units from the well data is proposed. This method permits to evaluate a vertical heterogeneity of sand present in wells, and to define the horizontal units which are internally more homogeneous in terms of sand proportion. The user can visualize the difference in a chosen number of units and define the optimal units for simulation. The method is based on Geostatistical Hierarchical Clustering; as one of unsupervised learning methods, clustering returns results which can be better than a simple visual analysis.

The following two sections contain the more detailed conclusions that can be made on the two main points.

5.1.1 Improved dynamic conditioning to well data

The review of various techniques, presented at the beginning of Chapter 2, shows the main hypothesis of well data conditioning: the sand deposits at well are associated with the channel presence at well; the non-sand deposits, in opposite, are associated with the channel path far from the well. In Flumy, the similar principle is used, but with a more realistic approach – the channel by itself is not equal to sand, but it stays the source of sand deposits: Points Bars, constructed during the channel migration; Crevasse Splays, constructed during levee breaches.

Conditioning to well data already existed in Flumy, before this thesis work. The first objective was therefore to evaluate its efficiency on various types of simulation scenarios (including simplistic cases). The most significant results of these tests were presented in Chapter 3.2 – 3.3. The initial conditioning procedure was analyzed using two scales: local (percentage of exact matching between data and simulation at well location) and regional (comparison of sand distribution in non-conditional and conditional simulation blocks with the same input parameters). The tests revealed that the main conditioning principles were rather efficient but not perfect, and could be improved. A list of problems to be fixed was noted, as a reference for the future modifications (Chapter 3.4). A special attention was paid to the transition between Non-Channelized and Channelized lithofacies in one well (switch between opposite conditioning techniques), and uniformity of sand distribution in conditional simulation blocks.

The modifications of the conditioning procedure were then performed and tested (Chapter 3.4 – 3.5). The main concepts stayed the same; the biggest change made is a completely reviewed Update AL algorithm. It deals more accurately with the channel at well (*Wet Well*), which helps to equilibrate “repulsion” / “attraction” techniques. Other conditioning algorithms were corrected, in order to reduce the previously observed undesirable impacts of conditioning: migration and avulsion adaptation became less violent, and aggradation blocking was restored. Improvement of results at both scales, local and regional, was proven and illustrated using the same tests as for Initial Conditioning evaluation (it permits to visualize the “net” differences in results).

With the new techniques, the proportion of excessively deposited Channelized facies is equal to 0-2 percentage points (compared with 3-13 presented in Initial conditioning tests), and the spatial sand distribution in conditional simulation blocks is visibly more uniform. One undesirable impact of conditioning, which can still be observed, is an insufficient (compared to the rest of simulation block) sand deposition in a small vicinity of wells. It is a result of the “repulsion” for Non-Channelized facies deposition and protection; cancelling this option makes the simulation even more uniform, but decreases significantly the exactness of well reproduction.

5.1.2 Determination of optimal simulation units

Geostatistical Hierarchical Clustering (GHC) applied to wells global VPC is proposed for the determination of simulation units. It permits to cut the wells into several more homogeneous (in terms of sand proportion) horizontal units. The main idea is to merge iteratively elementary VPC levels, obtaining at the end several contrasted sedimentary units (last clusters), that are the most homogeneous in term of sand proportion.

For a successful application of GHC to rather simple data (only vertical elevation coordinate and sand concentration value are needed), the internal clustering functions should have been accurately defined: a distance (initial distance between all the elements) and a linkage criterion (which is used for updating the distance between newly merged clusters, during the procedure). After a large series of synthetic tests, a simple function of distance was chosen: a squared difference of sand proportion values in two elementary VPC units. As a linkage criterion, Ward's minimum variance criterion was taken, with a slight modification ("Ward+" in Chapter 4) which favors a monotonically increasing dissimilarity of clusters merge. These clustering options resulted in the most efficient automatic determination of simulation units from extracted wells global VPC.

The method was also tested on the real case study data (8 wells from Loranca, Spain). The obtained results confirm the field correlation defined by geological expertise and refine the choice of the key levels for the stratigraphic units (the limits of units are placed on pedogenic horizons associated to lacustrine beds).

GHC is now integrated into Flumy as a new well analysis tool.

5.2 Perspectives

5.2.1 Improving the conditioning to well data

As it was shown in Chapter 3, it is hardly possible to perform a 100% matching at well reproduction during dynamic conditioning, even with new conditioning techniques. Some simple wells, e.g. a single-facies well, can be perfectly reproduced, but it is a rare case for real data. However, a further forcing of dynamic conditioning techniques for 100% well reproduction may result in a decrease of the conditional simulation realism.

It can be noted that the deposits simulated on a cell by Flumy are in fact computed for the center of the cell, and that in the reality the wells have no reason to be located exactly at the center of their grid cells. Moreover, the simulation on a cell is implicitly considered as representative of that cell – a support larger than its center point. Hence a 100% conditioning is not always justified. However, it may be desirable.

Since Flumy conditioning, while not being 100%, is close to this, a solution consists in a post-processing treatment. A very simple post-processing (which has been implemented in Isatis software) consists in:

- Interpretation of the lithofacies in terms of thresholds of a grain size variable;
- Detection of mismatches in well reproduction, between data and simulation;
- Computation of the correction to be applied on the grain size values simulated at well data location
- Interpolation of this grain size correction, vanishing up to a small neighborhood of wells (by default, elliptic);
- Inverse interpretation of grain size variable into lithofacies.

Hence the mismatches observed at wells are corrected both at wells and in their vicinity. One possible improvement of this method consists in the transformation of grain size into a Gaussian variable, and in the use of a conditional kriging for the interpolation step. This idea is close to considering that the lithofacies can be locally derived from the thresholding of a Gaussian field. A combination of Flumy simulation with a Truncated Gaussian or Pluri-gaussian simulation could perhaps be envisaged.

Dynamic conditioning to well data is a hard way of conditioning, as it requires to get into the processes. A completely different way may be used, thanks to the increasing power of computers: the Sequential Monte Carlo methods (SMC). This would consist in constructing simultaneously a number of Flumy simulations, and iteratively in time, reinforcing the representation of the simulations that are the most consistent with data. Although this is not a solution for a 100% conditioning, it is flexible, does not distort the processes, and does not require looking into these.

5.2.2 Improving the determination of simulation units

As it was said in Chapter 4, now the choice of the number of optimal simulation units is manual and can for instance be performed by detecting the first merge which shows a large gap of dissimilarity among the last steps. A first improvement that can be done is an automatic cut of the dendrogram, in order to directly propose some best reservoir splitting. The extension to more variables (i.e. grain size or gradients of global VPC) for calculating initial dissimilarities is another perspective.

Besides of it, an important perspective would be to extend the method to the determination of non-horizontal sedimentary units (defined by 3D surfaces) by using a VPC for each well and merging elements in both vertical and horizontal directions, for instance. This improvement would in particular permit to detect sedimentary units that do not extend laterally onto the whole field.

5.2.3 Further considerations

Here we have focused on the two main topics of our work: the conditioning of Flumy on well data, and the determination of simulation units. But at the end, let us just mention that there are a number of directions worth being investigated when developing a forward model like Flumy. These are notably:

- the definition and improvement of processes, as well as their extension to other contexts (e.g., from fluvial to turbiditic, deltaic, terminal lobes...);
- the choice of parameters from bibliography and analogues, the inference of key parameters from data, the development and calibration of formulas that facilitate the choice of the other ones;
- the conditioning on data, including different types of data.

References

Allard, D., Guillot, G., 2000. Clustering geostatistical data, in: Proceedings of the Sixth Geostatistical Conference.

Allen, D.B., Pranter, M.J., 2016. Geologically constrained electrofacies classification of fluvial deposits: An example from the Cretaceous Mesaverde Group, Uinta and Piceance Basins. AAPG Bulletin 100, 1775–1801. https://doi.org/10.1306/05131614229

Armstrong, M., 2011. Plurigaussian simulations in geosciences. Springer, Berlin New York.

Armstrong, M., Galli, A., Beucher, H., Loc'h, G., Renard, D., Doligez, B., Eschard, R., Geffroy, F., 2011. Plurigaussian Simulations in Geosciences. Springer Berlin Heidelberg, Berlin, Heidelberg. https://doi.org/10.1007/978-3-642-19607-2

Berkhin, P., 2006. A survey of clustering data mining techniques, in: Grouping Multidimensional Data. Springer, pp. 25–71.

Bridge, J.S., 2003. Rivers and floodplains: forms, processes, and sedimentary record. Blackwell Pub, Oxford, UK ; Malden, MA, USA.

Brierley, A., Watkins, J., Murray, A., 1997. Interannual variability in krill abundance at South Georgia. Marine Ecology Progress Series 150, 87–98. https://doi.org/10.3354/meps150087

Castro, J.M., Jackson, P.L., 2001. Bankfull Discharge Recurrence Intervals and Regional Hydraulic Geometry Relationships: Patterns in the Pacific Northwest, Usa1. JAWRA Journal of the American Water Resources Association 37, 1249–1262. https://doi.org/10.1111/j.1752-1688.2001.tb03636.x

Chilès, J.-P., Delfiner, P., 2012a. Geostatistics: modeling spatial uncertainty, 2. ed. ed, Wiley series in probability and statistics. Wiley, Hoboken, NJ.

Chilès, J.-P., Delfiner, P., 2012b. Geostatistics: modeling spatial uncertainty, 2. ed. ed, Wiley series in probability and statistics. Wiley, Hoboken, NJ.

Clevis, Q., Tucker, G.E., Lancaster, S.T., Desitter, A., Gasparini, N., Lock, G., 2006. A simple algorithm for the mapping of TIN data onto a static grid: Applied to the stratigraphic simulation of river meander deposits. Computers & Geosciences 32, 749–766. https://doi.org/10.1016/j.cageo.2005.05.012

Cojan, I., Fouché, O., Lopéz, S., Rivoirard, J., 2005. Process-based Reservoir Modelling in the Example of Meandering Channel, in: Leuangthong, O., Deutsch, C.V. (Eds.), Geostatistics Banff 2004. Springer Netherlands, Dordrecht, pp. 611–619. https://doi.org/10.1007/978-1-4020-3610-1_62

Cojan, I., Geffroy, F., Laratte, S., Rigollet, C., 2006. Process-based and stochastic modeling of fluvial meandering system. From model to field case study: example of the Loranca Miocene succession (Spain). Presented at the 17 th International Sedimentological Congress, IAS, Fukuoka, Japan, p. 222.

Cojan, I., Ors, F., Rivoirard, J., Weill, P., 2012. Inferring process-based models from well data -- an innovative method dedicated to meandering systems. Presented at the 34th International Geological Congress - Abstracts Unearthing our Past and Future -- Resourcing Tomorrow, p. 1829.

Cojan, I., Rivoirard, J., Renard, D., 2009. From outcrop to process-based reservoir modelling of fluvial meandering systems. The key issue of parameter choice. Presented at the From River to Rock Record, p. 21.

Cojan, I., Rivoirard, J., Weill, P., Ors, F., 2013. Inferring sandbody parameters from well data. An innovative method dedicated to process-based modelling of fluvial meandering systems. Presented at the ICFS.

Daams, R., Díaz-Molina, M., Mas, R., 1996. Uncertainties in the stratigraphic analysis of fluvial deposits from the Loranca Basin, central Spain. Sedimentary Geology, Approaches to Sequence Stratigraphy 102, 187–209. https://doi.org/10.1016/0037-0738(95)00062-3

Diaz-Molina, M., Bustillo, A., Capote, R., Lopez-Martinez, N., 1985. Wet fluvial fans of the Loranca Basin (Central Spain), channel models and distal bioturbated gypsum with chert. 6th European Regional Meeting, Lerida, Spain 37.

Doveton, J., 1986. Log analysis of subsurface geology: Concepts and computer methods. Wiley, New York.

Doveton, J.H., 1994. Geologic Log Interpretation. SEPM (Society for Sedimentary Geology).

Edwards, J., Lallier, F., Caumon, G., Carpentier, C., 2017. Uncertainty management in stratigraphic well correlation and stratigraphic architectures: A training-based method. Computers & Geosciences 111. https://doi.org/10.1016/j.cageo.2017.10.008

Ferraretti, D., Gamberoni, G., Lamma, E., 2012. I2AM: a Semi-Automatic System for Data Interpretation in Petroleum Geology., in: PAI. pp. 14–20.

Fouedjio, F., 2016. A hierarchical clustering method for multivariate geostatistical data. Spatial Statistics 18, 333–351. https://doi.org/10.1016/j.spasta.2016.07.003

Friedkin, J.F., Commission, M.R., 1945. A Laboratory Study of the Meandering of Alluvial Rivers. Waterways Experiment Station.

Galli, A., Beucher, H., Loc'h, G.L., Doligez, B., Group, H., 1994. The Pros and Cons of the Truncated Gaussian Method, in: Geostatistical Simulations, Quantitative Geology and Geostatistics. Springer, Dordrecht, pp. 217–233. https://doi.org/10.1007/978-94-015-8267-4_18

Hastings, W.K., 1970. Monte Carlo Sampling Methods Using Markov Chains and Their Applications. Biometrika 57, 97–109. https://doi.org/10.2307/2334940

Hauge, R., Holden, L., Syversveen, A.R., 2007. Well Conditioning in Object Models. Mathematical Geology 39, 383–398. https://doi.org/10.1007/s11004-007-9102-z

Hill, E., Robertson, J., Uvarova, Y., 2015. Multiscale hierarchical domaining and compression of drill hole data. Computers & Geosciences. https://doi.org/10.1016/j.cageo.2015.03.005

Howard, A.D., Knutson, T.R., 1984. Sufficient conditions for river meandering: A simulation approach. Water Resources Research 20, 1659–1667. https://doi.org/10.1029/WR020i011p01659

Ikeda, S., Parker, G. (Eds.), 1989. River Meandering, Water Resources Monograph. American Geophysical Union, Washington, D. C. https://doi.org/10.1029/WM012

Ikeda, S., Parker, G., Sawai, K., 1981. Bend theory of river meanders. Part 1. Linear development. Journal of Fluid Mechanics 112, 363–377. https://doi.org/10.1017/S0022112081000451

Johannesson, H., Parker, G., 2013. Linear Theory of River Meanders, in: River Meandering. American Geophysical Union (AGU), pp. 181–213. https://doi.org/10.1029/WM012p0181

Lance, G.N., Williams, W.T., 1967. A general theory of classificatory sorting strategies: 1. Hierarchical systems. The computer journal 9, 373–380.

Lantuejoul, C., 2002. Geostatistical Simulation: Models and Algorithms. Springer-Verlag, Berlin Heidelberg.

Lapkovsky, V.V., Istomin, A.V., Kontorovich, V.A., Berdov, V.A., 2015. Correlation of well logs as a multidimensional optimization problem. Russian Geology and Geophysics 56, 487–492. https://doi.org/10.1016/j.rgg.2015.02.009

Le Loc'h, G., Beucher, H., Galli, A., Doligez, B., 1994. Improvement In The Truncated Gaussian Method: Combining Several Gaussian Functions. Presented at the ECMOR IV - 4th European Conference on the Mathematics of Oil Recovery, Røros, Norway. https://doi.org/10.3997/2214-4609.201411149

Le Loc'h, G., Galli, A., 1999. Truncated plurigaussian method: Theoretical and practical points of view. Geostatistics Wollongong '96 1, 211–222.

Lemay, M., Cojan, I., Ors, F., Rivoirard, J., 2016. Potential of FLUMY, a Meandering Fluvial Process-based Model, to Simulate Submarine Channels. Presented at the Second Conference on Forward Modelling of Sedimentary Systems. https://doi.org/10.3997/2214-4609.201600383

Leopold, L.B., Wolman, M.G., 1960. RIVER MEANDERS. GSA Bulletin 71, 769–793. https://doi.org/10.1130/0016-7606(1960)71[769:RM]2.0.CO;2

Leopold, L.B., Wolman, M.G., 1957. River channel patterns: Braided, meandering, and straight (USGS Numbered Series No. 282- B), Professional Paper. U.S. Government Printing Office, Washington, D.C.

Lopez, S., 2003. Modélisation de réservoirs chenalisés méandriformes une approche génétique et stochastique (PhD thesis). École Nationale Supérieure des Mines de Paris.

Lopez, S., Cojan, I., Rivoirard, J., Galli, A., 2008. Process-Based Stochastic Modelling: Meandering Channelized Reservoirs, in: Analogue and Numerical Modelling of Sedimentary Systems: From Understanding to Prediction. Wiley-Blackwell, pp. 139–144. https://doi.org/10.1002/9781444303131.ch5

Lopez, S., Galli, A., Cojan, I., 2001. Fluvial Meandering channelized reservoirs: a stochastic & process-based approach. Presented at the IAMG Annual Meeting, Cancun, Mexico.

Luthi, S., 2001. Geological Well Logs: Their Use in Reservoir Modeling. Springer-Verlag, Berlin Heidelberg.

Luthi, S.M., Bryant, I.D., 1997. Well-log correlation using a back-propagation neural network. Mathematical geology 29, 413–425.

Mariethoz, G., Caers, J., 2015. Multiple-point geostatistics: stochastic modeling with training images. John Wiley & Sons Inc, Chichester, West Sussex, UK ; Hoboken, NJ, USA.

Mariethoz, G., Comunian, A., Irarrázaval, Í., Renard, P., 2014. Conditional simulation of realistic meandering channels using 1D multiple-point simulations.

Martinius, A.W., 2000. Labyrinthine Facies Architecture of the Tortola Fluvial System and Controls on Deposition (Late Oligocene-Early Miocene, Loranca Basin, Spain). Journal of Sedimentary Research 70, 850–867. https://doi.org/10.1306/2DC4093D-0E47-11D7-8643000102C1865D

Milligan, G.W., 1979. Ultrametric hierarchical clustering algorithms. Psychometrika 44, 343–346. https://doi.org/10.1007/BF02294699

Mirowski, P., Herron, M., Fluckiger, S., Seleznev, N., McCormick, D., 2005. New Software for Well-to-Well Correlation of Spectroscopy Logs. Presented at the AAPG International Conference, Paris, France.

Mulvihill, C.I., Baldigo, B.P., 2007. Regionalized equations for bankfull-discharge and channel characteristics of streams in New York State—Hydrologic Region 3 east of the Hudson River (USGS Numbered Series No. 2007–5227), Scientific Investigations Report. U.S. Geological Survey, Reston, VA.

Oliver, D.S., 2002. Conditioning channel meanders to well observations. Mathematical geology 34, 185–201.

Parks, J.M., 1966. Cluster Analysis Applied to Multivariate Geologic Problems. The Journal of Geology 74, 703–715. https://doi.org/10.1086/627205

Parquer, M., Collon, P., Caumon, G., 2017. Reconstruction of Channelized Systems Through a Conditioned Reverse Migration Method. Mathematical Geosciences. https://doi.org/10.1007/s11004-017-9700-3

Perucca, E., Camporeale, C., Ridolfi, L., 2007. Significance of riparian vegetation dynamics on meandering river morphodynamics. WATER RESOURCES RESEARCH 43, W03430-1. https://doi.org/10.1029/2006WR005234

Piegl, L., Tiller, W., 1997. The NURBS Book, Monographs in Visual Communication. Springer Berlin Heidelberg, Berlin, Heidelberg. https://doi.org/10.1007/978-3-642-59223-2

Pyrcz, M.J., Deutsch, C.V., 2014. Geostatistical reservoir modeling, Second edition. ed. Oxford University Press.

Pyrcz, M.J., Deutsch, C.V., 2005. Conditioning event-based fluvial models, in: Geostatistics Banff 2004. Springer, pp. 135–144.

Ravenne, C., Galli, A., Doligez, B., Beucher, H., Eschard, R., 2002. Quantification of Facies Relationships Via Proportion Curves, in: Geostatistics Rio 2000, Quantitative Geology and Geostatistics. Springer, Dordrecht, pp. 19–39. https://doi.org/10.1007/978-94-017-1701-4_3

Reading, H.G., 1978. Sedimentary environments and facies. New York: Elsevier : sole distributors in U.S.A. and Canada, Elsevier North-Holland.

Rivoirard, J., Cojan, I., Renard, D., Geffroy, F., 2008. Advances in quantification of process-based models for meandering channelized reservoirs. VIII International Geostatistics Congress, GEOSTATS 2008.

Romary, T., Ors, F., Rivoirard, J., Deraisme, J., 2015. Unsupervised classification of multivariate geostatistical data: Two algorithms. Computers & Geosciences 85, 96–103.

Sun, T., Meakin, P., Jøssang, T., 2001. A computer model for meandering rivers with multiple bed load sediment sizes: 2. Computer simulations. Water Resources Research 37, 2243–2258. https://doi.org/10.1029/2000WR900397

Sweet, W.V., Geratz, J.W., 2003. Bankfull Hydraulic Geometry Relationships and Recurrence Intervals for North Carolina's Coastal Plain1. JAWRA Journal of the American Water Resources Association 39, 861–871. https://doi.org/10.1111/j.1752-1688.2003.tb04411.x

Wang, J., Wang, X., Ren, C., 2009. 2D conditional simulation of channels on wells using a random walk approach. Computers & Geosciences 35, 429–437. https://doi.org/10.1016/j.cageo.2008.07.001

Weill, P., Cojan, I., Ors, F., Rivoirard, J., Beucher, H., 2013. Process-based modelling of a meandering fluvial reservoir: FLUMY and the Miocene Loranca Basin. Presented at the ICFS.

Wilde, A., Hill, E.J., Schmid, S., Taylor, W.R., 2017. Wavelet Tessellation and its Application to Downhole Gamma Data from the Manyingee & Bigrlyi Sandstone-Hosted Uranium Deposits.

Williams, G.P., 1978. Bank-full discharge of rivers. Water Resources Research 14, 1141–1154. https://doi.org/10.1029/WR014i006p01141

Softwares:

1) Flumy®
   Process-based channelized reservoir models
   Copyright © MINES ParisTech / ARMINES
   Free download from http://cg.ensmp.fr/flumy
2) Paradigm®
   E&P Subsurface Software Solutions
   © 2018 Emerson Paradigm Holding LLC. All rights reserved.
   http://www.pdgm.com
3) Petrel®
   E&P Software Platform
   © 2018 Schlumberger Limited. All rights reserved.
   https://www.software.slb.com/products/petrel
4) Isatis®
   Geostatistical Software Solution
   © 2018 Geovariances. All rights reserved.
   https://www.geovariances.com/en/software/isatis-geostatistics-software

RÉSUMÉ

Les modèles génétiques de réservoirs sont construits par la simulation des principaux processus de sédimentation dans le temps. En particulier, les modèles tridimensionnels de systèmes chenalisés méandriformes peuvent être construits à partir de trois processus principaux : la migration du chenal, l'aggradation du système et les avulsions, comme c'est réalisé dans le logiciel Flumy pour les environnements fluviatiles. Pour une utilisation opérationnelle, par exemple la simulation d'écoulements, ces simulations doivent être conditionnées aux données d'exploration disponibles (diagraphie de puits, sismique, …). Le travail présenté ici, basé largement sur des développements antérieurs, se concentre sur le conditionnement du modèle Flumy aux données de puits.

Deux questions principales ont été examinées au cours de cette thèse. La première concerne la reproduction des données connues aux emplacements des puits. Cela se fait actuellement par une procédure de "conditionnement dynamique" qui consiste à adapter les processus du modèle pendant le déroulement de la simulation. Par exemple, le dépôt de sable aux emplacements de puits est favorisé, lorsque cela est souhaité, par une adaptation des processus de migration ou d'avulsion. Cependant, la manière dont les processus sont adaptés peut générer des effets indésirables et réduire le réalisme du modèle. Une étude approfondie a été réalisée afin d'identifier et d'analyser les impacts indésirables du conditionnement dynamique. Les impacts ont été observés à la fois à l'emplacement des puits et dans tout le modèle de blocs. Des développements ont été réalisés pour améliorer les algorithmes existants.

La deuxième question concerne la détermination des paramètres d'entrée du modèle, qui doivent être cohérents avec les données de puits. Un outil spécial est intégré à Flumy - le "Non-Expert User Calculator" (Nexus) - qui permet de définir les paramètres de simulation à partir de trois paramètres clés : la proportion de sable, la profondeur maximale du chenal et l'extension latérale des corps sableux. Cependant, les réservoirs naturels comprennent souvent plusieurs unités stratigraphiques ayant leurs propres caractéristiques géologiques. L'identification de telles unités dans le domaine étudié est d'une importance primordiale avant de lancer une simulation conditionnelle avec des paramètres cohérents pour chaque unité. Une nouvelle méthode de détermination des unités stratigraphiques optimales à partir des données de puits est proposée. Elle est basée sur la Classification géostatistique hiérarchique appliquée à la courbe de proportion verticale (VPC) globale des puits. Les unités stratigraphiques ont pu être détectées à partir d'exemples de données synthétiques et de données de terrain, même lorsque la VPC globale des puits n'était pas visuellement représentative.

MOTS CLÉS

Classification hiérarchique, géostatistique, modèles génétiques, réservoirs, simulations conditionnelles

ABSTRACT

Process-based reservoir models are generated by the simulation of the main sedimentation processes in time. In particular, three-dimensional models of meandering channelized systems can be constructed from three main processes: migration of the channel, aggradation of the system and avulsions, as it is performed in Flumy software for fluvial environments. For an operational use, for instance flow simulation, these simulations need to be conditioned to available exploration data (well logging, seismic, …). The work presented here, largely based on previous developments, focuses on the conditioning of the Flumy model to well data.

Two main questions have been considered during this thesis. The major one concerns the reproduction of known data at well locations. This is currently done by a "dynamic conditioning" procedure which consists in adapting the model processes while the simulation is running. For instance, the deposition of sand at well locations is favoured, when desired, by an adaptation of migration or avulsion processes. However, the way the processes are adapted may generate undesirable effects and could reduce the model realism. A thorough study has been conducted in order to identify and analyze undesirable impacts of the dynamic conditioning. Such impacts were observed to be present both at the location of wells and throughout the block model. Developments have been made in order to improve the existing algorithms.

The second question is related to the determination of the input model parameters, which should be consistent with the well data. A special tool is integrated in Flumy – the Non Expert User calculator (Nexus) – which permits to define the simulation parameters set from three key parameters: the sand proportion, the channel maximum depth and the sandbodies lateral extension. However, natural reservoirs often consist in several stratigraphic units with their own geological characteristics. The identification of such units within the studied domain is of prime importance before running a conditional simulation, with consistent parameters for each unit. A new method for determining optimal stratigraphic units from well data is proposed. It is based on the Hierarchical Geostatistical Clustering applied to the well global Vertical Proportion Curve (VPC). Stratigraphic units could be detected from synthetic and field data cases, even when the global well VPC was not

KEYWORDS

Hierarchical Clustering, Geostatistics, Process-based models, reservoirs, conditional simulations